A MASS SPECTROMETRIC STUDY OF LOW ENERGY REARRANGEMENT REACTIONS IN OXYGEN CONTAINING IONS

BY

DENNIS DONG-KYUN SUH, M.SC

A Thesis

Submitted to the School of Graduate Studies

in Partial Fulfilment of the Requirements

for the Degree

Doctor of Philosophy

McMaster University

DOCTOR OF PHILOSOPHY (1995) McMASTER UNIVERSITY

(Chemistry) Hamilton, Ontario

TITLE: A Mass Spectrometric Study of Low Energy Rearrangement Reactions in Oxygen Containing Ions

AUTHOR: Dennis Dong-Kyun Suh

SUPERVISOR: Professor J.K. Terlouw

NUMBER OF PAGES: xiv, 272

A MASS SPECTROMETRIC STUDY OF LOW ENERGY REARRANGEMENT REACTIONS IN OXYGEN CONTAINING IONS

To my mom and dad

ABSTRACT

Low energy rearrangement reactions in selected oxygen-containing ions have been studied by means of mass spectrometry-based techniques (metastable ion (MI), collision-induced dissociation (CID), neutralization-reionization (NR) mass spectrometry as well as multiple collision experiments (MS^n)) in conjuntion with *ab initio* molecular orbital calculations.

The atom connectivity in the product ions has been investigated in detail by tandem mass spectrometry-based experiments on ^2H-, ^{13}C- and ^{18}O-labelled isotopologues of some oxygen-containing ions. The thermochemical data (i.e. heat of formation (ΔH_f) values) of the oxygen-containing ions have been obtained either experimentally from the appropriate measurement of ionization energy (IE), appearance energy (AE) and/or proton affinity (PA) or computationally.

It has been proposed that the C-H••O bonded counterparts of the O••H••O bonded species may, despite their lower thermodynamic stability, play an even more important role in the decay of oxygen-containing radical cations of the type $HOCH(R_1)C(=O)R_2^{\bullet+}$. A case in point is ionized acetol (R_1=H,R_2=CH_3), methyl glycolate (R_1=H,R_2=OCH_3), methyl lactate (R_1=CH_3,R_2=OCH_3) and acetoin (R_1=R_2=CH_3). These species all dissociate by loss of $R_1CO^{\bullet}$ by double hydrogen transfer (DHT). It is further proposed, from *ab initio* calculations, that the C-H••O bonded intermediate $R_1C(H)=O\cdots H\text{-}C(=O)R_2^{\bullet+}$, **I**, does not lose $R_1CO^{\bullet}$ via a hydrogen *atom* shift from neutral $R_1C(H)=O$ to ionized $H\text{-}C(=O)R_2^{\bullet+}$.

Instead, charge transfer takes place in **I** so that the neutral $R_1C(H)=O$ becomes charged and thus it can rotate and donate a *proton* to $H\text{-}C(=O)R_2$, after which dissociation follows.

Keto-enol tautomerism in the dilute gas-phase has been studied in the unimolecular reactions of ionized ethyl glycolate, $HOCH_2CO_2C_2H_5^{\bullet+}$, **II**, and its enol isomer, $HOCH=C(OH)OC_2H_5^{\bullet+}$, **III**. It has been shown that the metastable ionized keto isomer **II** undergoes unidirectional isomerization to the enol ion **III**, via two consecutive 1,5-hydrogen shifts, from which C_2H_4 is lost to give the ionized trihydroxy-ethylene, $(HO)_2C=CH(OH)^{\bullet+}$. NR experiments show that neutral trihydroxyethylene in the gas-phase is a remarkably stable species, which does not tautomerize to the keto isomer glycolic acid, $HOCH_2CO_2H$.

Some members of the important homologous series of oxonium ions, $C_nH_{2n+1}O^+$, have been extensively investigated by ^2H- and ^{13}C-labelling experiments especially at low internal energies. Their intriguing unimolecular chemistry has been interpreted by means of mechanisms in which distonic ions and ion/neutral complexes play crucial roles in the hydrogen transfer and skeletal isomerization steps.

Finally, part of the $C_3H_5O_2^+$ potential energy surface was investigated by *ab initio* molecular orbital calculations and by mass spectrometry-based experiments to ascertain whether the carbonyl-protonated β-propiolactone ions $\overline{CH_2CH_2OCOH^+}$, **IV**, can interconvert in the dilute gas-phase with protonated acrylic acid, $CH_2=CHC(OH)_2^+$, **V**, as suggested in a thermolysis study. It is shown that metastable ions **IV** do not communicate with ions **V** and the observed equilibrium **IV** $\rightleftarrows$ **V** in solution is due to an intermolecular process. Also, ions **IV** do not undergo cycloreversions to $HOCO^+ + C_2H_4$ and to $CH_2=COH^+ + CH_2O$, but rather they spontaneously dissociate $CH_3CHOH^+ + CO$, $CH_3CO^+ + CH_2O$, $CH_2=CHCO^+ + H_2O$ and $C_2H_5^+ + CO_2$. The product ions of these dissociation reactions are characterized by multiple collision experiments and mechanisms for their formation are proposed. Analysis of appropriate isodesmic

reactions indicate that the α-COOH group in 1-carboxyethylium ions, $CH_3CHCOOH^+$, behaves as a hydrogen atom and therefore this group cannot be said to destabilize the adjacent positive charge.

List of Publications

1. Isomerization and Dissociation Processes of Protonated β-Propiolactone and Related $C_3H_5O_2^+$ Isomers: a Combined Experimental and Theoretical Study; D. Suh, C.A. Kingsmill, P.J.A. Ruttink, P.C. Burgers and J.K. Terlouw; *Org. Mass Spectrom.*, **28**, 1270 (1993).
2. Hydrogen-Bridged Ions $[CH_3C{=}O{\cdots}H{\cdots}O{=}CH_2]^{\bullet+}$, $[CH_2C(H){=}O{\cdots}H{\cdots}O{=}CH_2]^{\bullet+}$, and $[CH_3C(H){=}O{\cdots}H{\cdots}O{=}CH]^{\bullet+}$ and Ion-Dipole Complex $[CH_3C(=O){\cdots}O(H)CH_2]^{\bullet+}$: Their Role in the Dissociation Chemistry of Ionized Acetol, $CH_3C(=O)CH_2OH^{\bullet+}$; M. George, C.A. Kingsmill, D. Suh, J.K. Terlouw and J.L. Holmes; *J. Am. Chem. Soc.*, **116**, 7807 (1994).
3. C-H•••O and O•••H•••O Bonded Intermediates in the Dissociation of Low Energy Methyl Glycolate Radical Cations; D. Suh, C.A. Kingsmill, P.J.A. Ruttink, P.C. Burgers and J.K. Terlouw; *Int. J. Mass Spectrom. Ion Processes*, **146/147**, 305 (1995).
4. Low Energy Acetoin Ions $CH_3C(=O)C(H)(OH)CH_3^{\bullet+}$ Decompose to $CH_3CO^{\bullet}$ and CH_3CHOH^+ via a Remarkable "Hidden Rearrangement"; D. Suh, P.C. Burgers and J.K. Terlouw; *Int. J. Mass Spectrom. Ion Processes*, **144**, L1(1995).
5. The Unimolecular Chemistry of the Enol of Ionized Methyl Glycolate: Formation of the Hydrogen Bridged Radical Cation $[CH_3O(H){\cdots}H{\cdots}O{=}CH]^{\bullet+}$; D. Suh, P.C. Burgers and J.K. Terlouw; *Rapid Commun. Mass Spectrom.*, **9**, 862 (1995).
6. The Chemistry of Ionized Ethyl Glycolate, $HOCH_2CO_2C_2H_5^{\bullet+}$, and Its Enol Isomer, $HOCH{=}C(OH)OC_2H_5^{\bullet+}$. Formation of Ionized and Neutral Trihydroxyethylene; D. Suh, J.T. Francis, P.C. Burgers, R.D. Bowen and J.K. Terlouw; *Eur. Mass Spectrom* (1996) accepted.
7. Reactions of Ionized Dibutyl Ether; R.D. Bowen, D. Suh and J.K. Terlouw; *Org. Mass Spectrom.*, **29**, 791 (1994).
8. Mechanism of Propene and Water Elimination from the Oxonium Ion $CH_3CH{=}O^+CH_2CH_2CH_3$; R.D. Bowen, D. Suh and J.K. Terlouw; *J. Chem. Soc. Perkin Trans. 2*, 119 (1995).
9. The Mechanism of Alkene Elimination from the Oxonium Ions $(CH_3CH_2)_2C{=}OH^+$, $CH_3CH_2CH_2(CH_3)C{=}OH^+$ and $(CH_3CH_2CH_2)_2C{=}OH^+$; R.D. Bowen, D. Suh and J.K. Terlouw; *Eur. Mass Spectrom.*, **1**, 33 (1995).

10. Unimolecular Reactions of Isolated Organic Ions: the Chemistry of the Unsaturated Oxonium Ions $CH_2=CHC(CH_3)=OCH_3^+$, $CH_2=(CH_3)CCH=OCH_3^+$ and $CH_3CH=CHCH=OCH_3^+$; R.D. Bowen, D. Suh and J.K. Terlouw; *Int. J. Mass Spectrom. Ion Processes* (1995) submitted.
11. On the Generation and Identification of Various Dialkoxycarbenes in the Rarefied Gas Phase of the Mass Spectrometer; D. Suh, D. Pole, J. Warkentin and J.K. Terlouw; *Can. J. Chem.*, (1996) accepted.

ACKNOWLEDGEMENTS

This thesis represents more than the compilation from scientific research I have worked for four years. It embodies the encouragement, influence, and support from many people, each of whom have played an important role which ultimately made the outcome of thesis possible.

First of all, I would like to express my gratitude to my supervisor, Prof. J.K. Terlouw, for his patient assistance and excellent guidance throughout the course of this work. I would like to thank Dr P.C. Burgers and Dr R.D. Bowen for their valuable discussions and critical comments given in this work, and Prof. J. Warkentin and Prof. N.H. Werstiuk for their valuable assistance with synthetic problems.

Thanks are extended to : Prof. P.J.A. Ruttink, Dr C.A. Kingsmill and Dr J.T. Francis for their expertise in *ab initio* MO calculations performed in this thesis; Dr R.D. Smith and Mr. F.A. Ramelan for their assistance in the use and maintenance of the ZAB-R mass spectrometer; Dr G.A. McGibbon and Mr. T (Y.C.) Wong for their assistance with the ZAB-R and their friendship.

I would like to thank Rev. Y.R. Kim and the members of the Korean United Church in Hamilton for their encouragement and moral support throughout the completion of this work.

Finally, I would like to thank my dad and family for everything that they have given me through my life. I am very sad that my mom, who passed away when I was in 1st year in Mac, could not witness the completion of this thesis, an event to which she looked forward so much.

TABLE OF CONTENTS

LIST OF FIGURES

LIST OF ABBREVIATIONS

AE	=	appearance energy
CA	=	collisional activation
CE	=	charge exchange
CID	=	collision-induced dissociation
CIDI	=	collision-induced dissociative ionization
CR	=	charge-reversal
CS	=	charge-stripping
EI	=	electron ionization
ESA	=	electrostatic analyser
eV	=	electron Volt (1 eV = 23.061 kcal/mol or 96.487 kJ/mol)
ffr	=	field-free region
ΔH_f	=	enthalpy of formation
HF	=	Hartree-Fock
IE	=	ionization energy
k	=	rate constant
KER	=	kinetic energy release
MI	=	metastable ion
MO	=	molecular orbital
MP	=	Moller-Plesset (perturbation theory)
MS	=	mass spectrometry
NDMA	=	N,N-dimethylaniline
m/z	=	mass to charge ratio
NR	=	neutralization-reionization
PA	=	proton affinity
q	=	charge
r,R	=	radius
SCF	=	self-consistent field
T	=	kinetic energy release (value)
PEPICO	=	photoelectron photoion coincidence
TS	=	transition state
ZAB-R	=	BEE three-sector mass spectrometer
ZPVE	=	zero-point vibration energy

CHAPTER 1

INTRODUCTION

Positive ions produced by electron impact ionization of a neutral molecule were first observed by Goldstein [1] in 1866 and it was J.J. Thomson [2] in 1913 who thoroughly characterized these ions using the first mass spectrograph. Later, Aston [3] and Dempster [4] reported the first precision measurements of ionic masses and abundances, which are known as a mass spectrum. Thomson's mass spectrograph was developed into modern sector mass spectrometers when A.O. Nier and co-workers [5] introduced the sector magnetic analyzer which in turn led them to the design of the first double-focussing mass spectrometer of high resolution [6].

Electron impact ionization is the oldest and still the most common method of producing positive ions from a neutral precusor molecule. The ionization is caused by an electron impinging on a molecule in the ionization chamber. Electrons produced from a hot filament which is held at a negative potential of 5-100 V with respect to the ionization chamber are accelerated through a small hole into the chamber. Their kinetic energy is determined by the potential difference between the filament and the ionization chamber. Mostly, 70 eV electron energies are used. Electrons which have passed through the chamber and exited through a small hole on the opposite side are collected by the "trap" or anode. The trap current or emission current can be used to control the filament current and thus, a constant rate of ion production is maintained. A small magnetic field is applied along the path of the electron beam to constrain it into a narrow helical path (see Figure 1.1). When 70 eV electrons interact with gas-phase neutral molecules, some of these molecules (ca. 1 in 1000) lose an electron and become positively charged molecular ions.

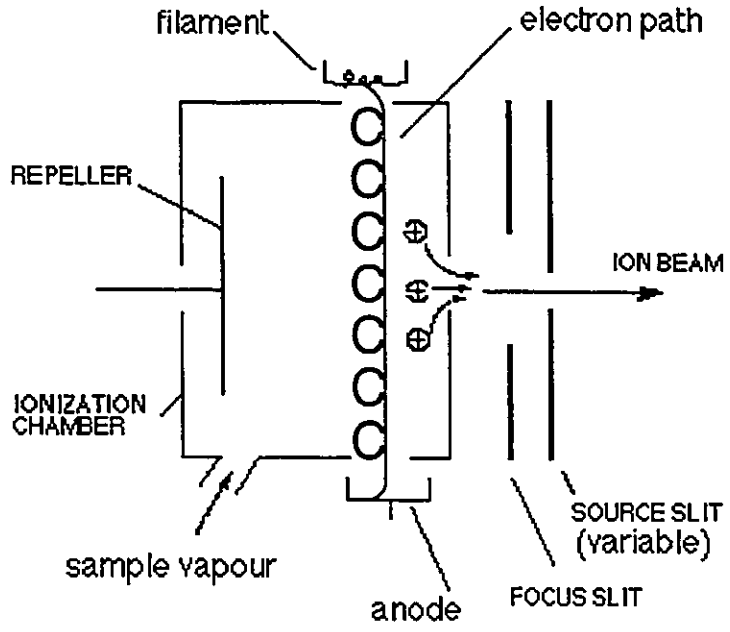

Figure 1.1 Ion source for EI mass spectrometry.

The positive ions thus formed are extracted through the ion exit slit by a small potential applied to the repeller electrode and are accelerated through a large voltage (V = 3000 - 8000 V) towards a source slit which is at ground potential. The potential drop for the ions is equal to the kinetic energy gained by ions. The beam of ions which posses a kinetic energy equal to the accelerating voltage is termed the "main beam".

The VG Analytical ZAB-R instrument used in this work is a double focussing mass spectrometer having reversed Nier-Johnson geometry in which the magnetic sector (B) precedes the electrostatic analyzer (ESA) (see Figure 1.2). Thus, for an ion to reach the collector slit and be recorded, it must first traverse through the magnetic sector (B), the momentum analyzer.

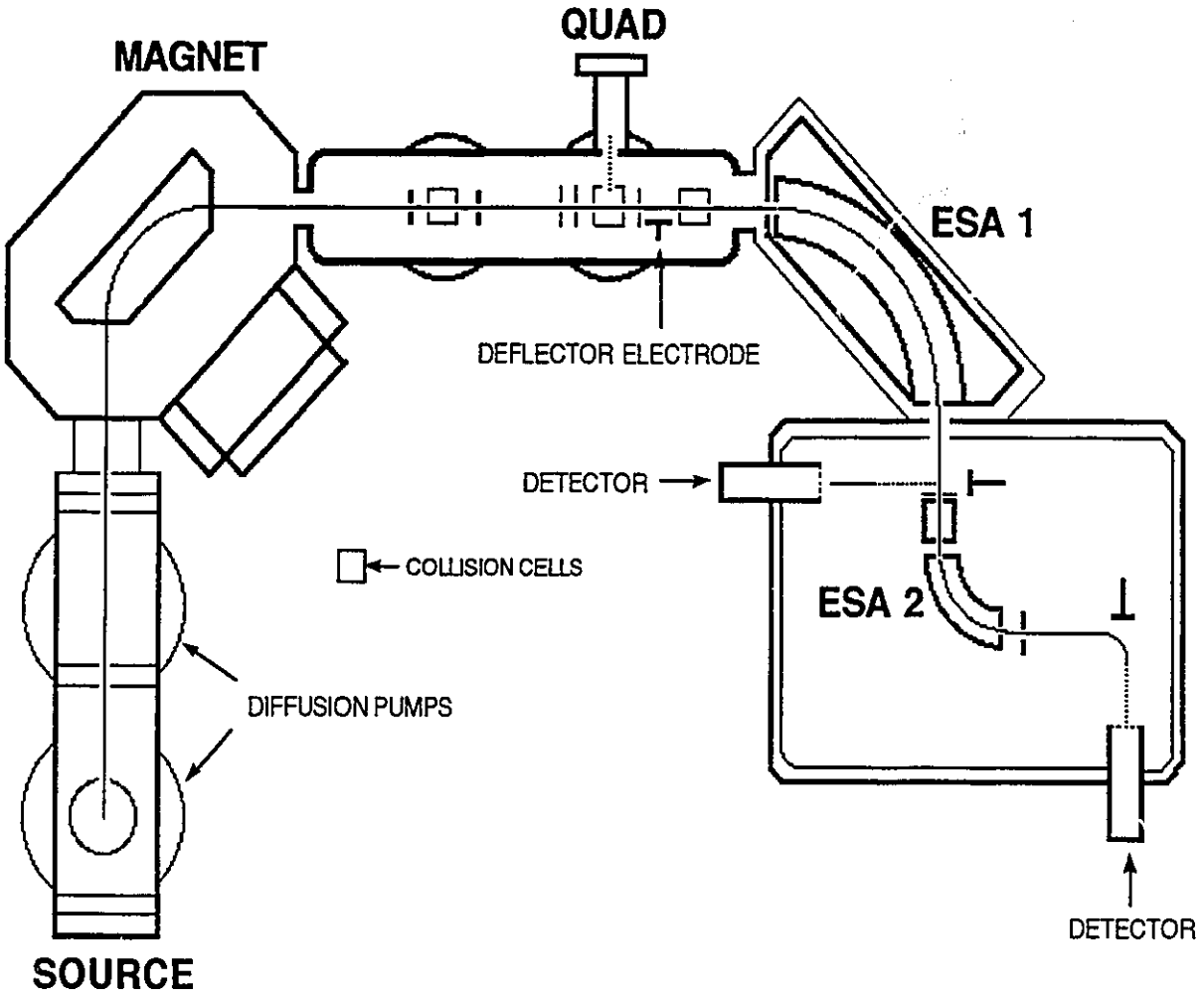

Figure1.2 Schematic drawing of the VG Analytical ZAB-R.

Since the kinetic energy of an ion is equal to the potential difference, we have

$$z \cdot eV = 1/2 \cdot m\upsilon^2 \qquad \text{(Eq. 1.1)}$$

where e is the charge on an electron, z is the number of such charges on the ion, V is the accelerating voltage, m is the mass of the ion and υ is the velocity of the ion.

An ion of mass m, charge ze and velocity υ injected into a magnetic flux B will follow a circular path of radius given by

$$r = (m\upsilon)/(z \cdot e \cdot B) \qquad \text{(Eq. 1.2)}$$

From eq. 1.1, we have

$$\upsilon = [(2 \cdot z \cdot eV)/m]^{1/2} \quad \text{(Eq. 1.3)}$$

$$m \cdot \upsilon = (2 \cdot m \cdot z \cdot eV)^{1/2} \quad \text{(Eq. 1.4)}$$

From eq. 1.2, we have

$$m \cdot \upsilon = z \cdot e \cdot B \cdot r \quad \text{(Eq. 1.5)}$$

Combining equations 1.4 and 1.5, we have

$$(2 \cdot m \cdot z \cdot eV)^{1/2} = z \cdot e \cdot B \cdot r \quad \text{(Eq. 1.6)}$$

$$2 \cdot m \cdot z \cdot eV = z^2 \cdot e^2 \cdot B^2 \cdot r^2 \quad \text{(Eq. 1.7)}$$

$$2 \cdot m \cdot V = z \cdot e \cdot B^2 \cdot r^2 \quad \text{(Eq. 1.8)}$$

$$m/z = (e \cdot B^2 \cdot r^2)/(2 \cdot V) \quad \text{(Eq. 1.9)}$$

Thus, ions of different mass-to-charge (m/z) ratio can be transmitted by varying the magnetic field (B) at a fixed accelerating voltage (V). The strength of the magnetic field is adjusted by varying the flow of the current through the coils of the electromagnet.

After being analyzed according to their momentum by the magnetic sector, the ions now enter an electric-sector analyzer (ESA) which acts as an energy filter. The ions can only be transmitted by the ESA when the electrostatic force (E_{ESA}) acting on them balances the centrifugal force ($m \cdot \upsilon^2 / R$). Thus, the radius of curvature (R) of the ion path in the ESA is dependent on its energy, not its mass.

$$m \cdot \upsilon^2 / R = z \cdot e \cdot E_{ESA} \quad \text{(Eq. 1.10)}$$

$$R = (m \cdot \upsilon^2)/(z \cdot e \cdot E_{ESA}) \quad \text{(Eq. 1.11)}$$

From eq. 1.1, we have

$$m \cdot \upsilon^2 = 2 \cdot z \cdot eV \quad \text{(Eq. 1.12)}$$

Substituting eq. 1.12 into 1.11, we have

$$R = (2 \cdot z \cdot eV)/(z \cdot e \cdot E_{ESA}) \quad \text{(Eq. 1.13)}$$

$$R = 2 \cdot V / E_{ESA} \quad \text{(Eq. 1.14)}$$

The mass of the ion (m) and the number of charges on the ion (z) do not appear in the equation 1.14. Thus, at a constant E_{ESA}, ions are focussed by the ESA according to their kinetic energies. A normal mass spectrum in the ZAB-R is thus obtained by scanning the magnetic field (B) when the E_{ESA} is adjusted so that V/E_{ESA} satisfies equation 1.14.

1.1 Quasi-Equilibrium Theory (QET)

The removal of an electron from a neutral molecule, M, generating its radical cation, $M^{\bullet+}$, occurs when energy-rich electrons (typically 70 eV) interact with the molecule. However, only *ca.* 10 eV of energy is needed to ionize most of the organic molecules. This means that at the instant of ionization a part of the excess energy of the electron is transferred into the internal energy of the molecule. Typically, *ca.* 0-10 eV of energy is transferred to the molecule. The extent to which the molecular ion ($M^{\bullet+}$) undergoes unimolecular dissociation depends on its internal energy content, hence its lifetime. Typically ions spend *ca.* 10^{-6} s in the ion source before acceleration. Thus, ions having lifetime greater than 10^{-5} s are detected as stable molecular ions whereas those having lifetime less than 10^{-7} s are referred to as unstable ions which decompose in the source. Ions having lifetime in the range between 10^{-7} and 10^{-5} s are defined as metastable ions which decompose in the field-free regions (ffr) in the mass spectrometer. The ionization process occurs within 10^{-16} s which is about two orders of magnitude faster than a vibration within a molecule (10^{-13} to 10^{-14} s). It can thus be described by the Franck-Condon principle, which states that the configuration and momenta of the nuclei do not alter during electronic transitions [7].

The Quasi-Equilibrium Theory (QET) [8] states the following criteria: i) the rate of unimolecular dissociation of the initial molecular ion is slow compared with that of its formation and excitation; ii) the unimolecular dissociation of the molecular ion occurs

only after the initial excitation energy is redistributed over all degrees of freedom; iii) ions generated in a mass spectrometer represent a series of isolated, competing and consecutive unimolecuar reactions.

To discuss a mass spectrum in a semi-quantitative way, it is useful to consider a simplified version of the QET which expresses the rate of unimolecuar dissociation (k) of an ion by the following equation:

$$k = \upsilon[(E - E_0)/E]^{N-1} \qquad \text{(Eq. 1.15)}$$

where υ is a frequency factor, E is the excess internal energy of the ion, E_0 is the activation energy and N is the number of oscillators in the ion.

From the rate equation 1.15, it can be seen that the rate of decomposition is proportional to $(E - E_0)^{N-1}$, i.e. the amount of energy transferred during ionization. Thus, the greater the excess internal energy of the ion, the faster it decomposes. The rate equation 1.15 can also be applied to predict the relative intensity ratios of fragment ions in the mass spectrum. The k(E) curves for two competing reactions, one is a simple direct bond cleavage and the other is a rerrangement process, are shown in Fig. 1.3

Here, the two k(E) curves intersect above the metastable region as indicated. An important observation from the above k(E) curves is that the relative fragment ion intensities reflect the activation energies at low internal energies and at long ion lifetimes. Thus, reactions with lower activation energy and tighter transition state (rearrangement) are important among low energy (metastable) ions.

1.2 Methods for Ion Structure Elucidation

The most challenging problem in the study of gas-phase ion chemistry is undoubtedly the determination of ion structures. With the advent of multi-sector mass

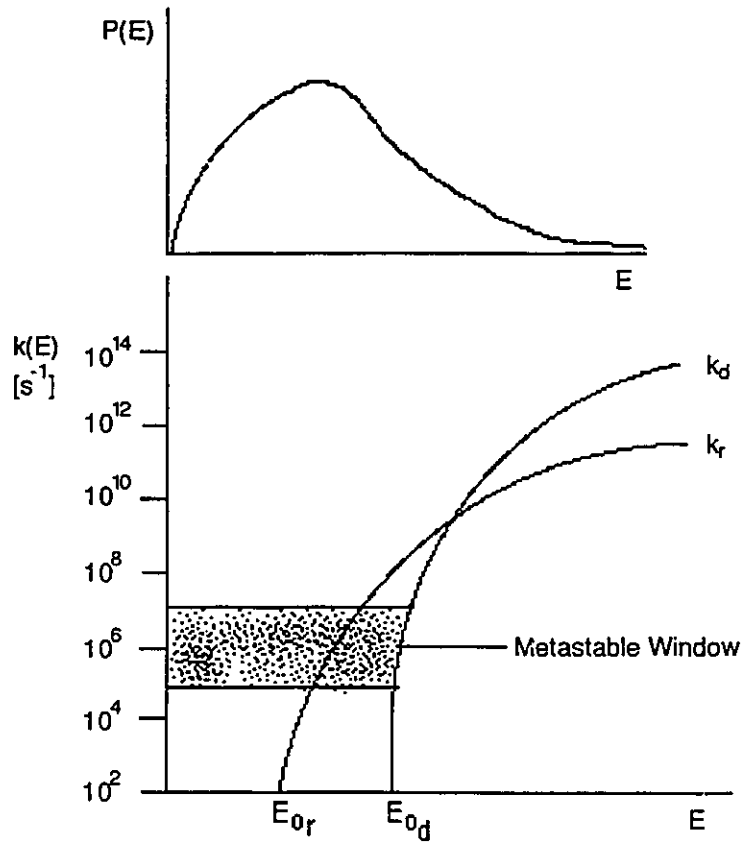

Figure 1.3 k(E) curves for competing rearrangement (r) and direct bond cleavage (d) reactions. The upper part of the figure shows an arbitrary internal energy distribution function.

spectrometers, the elucidation of ion structures has become amenable. The mass spectrometer provides an environment suitable for the study of isolated gas-phase ions whose properties can be directly compared with the results of *ab initio* molecular orbital calculations.

All experimental methods for ion structure assignment can only yield information on the constitution (i.e. connectivity of atoms) of an ion. The configuration (e.g. bond lengths, bond angles and charge distribution) of an ion can be obtained from sufficiently high level *ab initio* molecular orbital calculations.

The techniques described below are an assessment of the important experimental methods in gas-phase ion chemistry whose correct interpretation in

conjunction with *ab initio* molecular orbital calculations can lead to the elucidation of ion structures. In general, one method alone cannot suffice for an ion structure assignment, but combinations of techniques can provide a powerful tool for the determination of ion structures in the gas-phase.

1.2.1 Ion and Neutral Thermochemistry

Ion structures and reaction mechanisms are central to the study of organic ions in the gas-phase. They can be inferred from reliable heats of formation, of both ionic and neutral species, obtained either experimentally or by use of *ab initio* calculations. Heat of formation (ΔH_f) values for ions and neutral species can be provided by appropriate measurements of ionization and/or appearance energies (IE and AE, respectively).

For the reaction $AB^{\bullet+} \rightarrow A^+ + B^{\bullet}$, the ionization and appearance energies (measured experimentally by techniques such as electron ionization using an "electron monochromator" [9], photoelectron spectroscopy (PES) [10] or photoelectron-photoion coincidence (PEPICO) spectroscopy [11]) are defined as a minimum energy required to ionize a molecule (AB) and to cause the appearance of fragment ion (A^+), respectively. They are related to heats of formation (ΔH_f) as shown in equation 1.16 and 1.17:

$$IE = \Delta H_f (AB^{\bullet+}) - \Delta H_f (AB) \qquad \text{(Eq. 1.16)}$$

$$AE = \Delta H_f (A^+) + \Delta H_f (B^{\bullet}) - \Delta H_f (AB) + \varepsilon_{excess} \qquad \text{(Eq. 1.17)}$$

If the above reaction has a significant kinetic shift (i.e. the extra amount of energy needed to observe a signal on the μs time-scale of the experiment) or reverse

activation energy barrier, heats of formation values for ions and neutral species obtained from the appearance energy method represent an upper limit for their heats of formation. In addition heats of formation values for even-electron ions are available in some cases from proton affinities (PA) as determined from gas phase ion/molecule equilibria studies in an ion-cyclotron resonance (ICR) spectrometer [12], flow tube [13] or a high pressure mass spectrometer [14], i.e. for the reaction $AB + H^+ \rightarrow ABH^+$,

$$PA = \Delta H_f (AB) + \Delta H_f (H^+) - \Delta H_f (ABH^+) \qquad \text{(Eq. 1.18)}$$

In 1988, Lias et. al [15] accomplished their monumental task of producing a comprehensive compilation of thermochemical data, derived from IE, AE as well as PA measurements, in "Gas-Phase Ion and Neutral Thermochemistry". It covers ΔH_f values for not only positive and negative ions but also their corresponding neutral species. However, there still remains a lack of reliable data for ions and neutral molecules such that it becomes necessary to use the "additivity" scheme [16], isodesmic substitution [17] or even to devise new or provisional additivity terms of one's own [18] to derive ΔH_f values.

Another approach to determine ΔH_f values for both ions and neutral molecules involves the use of *ab initio* molecular orbital theory calculations [19]. One important aspect of the theoretical approach is that it can be applied as readily to reactive species, such as ylid ions, distonic ions, hydrogen-bridged ions and ion-dipole complexes as to molecular ions of conventional structure. Additionally, the *ab initio* calculations refer to isolated species in the gas-phase, and thus they are immediately relevant to many of the experiments dealing with gas-phase ions.

One way to estimate heats of formation of a set of isomeric ions is as follows: *ab initio* calculations at the appropriate level of theory can provide accurate *relative*

energies for the isomers, and if the heat of formation of one (or more) of the isomers is available from well characterized experiments then ΔH_f values for the other species can confidently be assigned.

Another approach is to use two new levels of theory introduced by Pople and co-workers [20], known as G1 and G2 theory (G = Gaussian). They were designed with the aim of being able to reproduce known thermochemical data to a prescribed accuracy of *ca.* 2 kcal/mol (10 kJ/mol or 0.1 eV) and to be applicable with similar accuracy to species where the experimental values have not been as well established.

G1 theory is a composite procedure with geometry optimization at the MP2(FULL)/6-31G* level and relative energies are obtained (effectively) through QCISD(T)/6-311+G(2df,p), together with isogyric (i.e. processes which leave the number of unpaired electrons unchanged) and zero-point vibrational energy corrections. G2 theory is an improvement over G1 theory by eliminating an additivity approximation used in G1 theory and employing a larger ultimate basis set, leading to results (effectively) at the QCISD(T)/6-311+G(3df,2p) level, again with isogyric and zero-point vibrational energy corrections. For ions of larger size, the G2(MP2) method utilizes a more computationally economical approach which sacrifices little in accuracy [21].

Finally, it is worthwhile to mention that although the use of semi-empirical methods such as MNDO, MINDO/3 and AM1 for the estimation of heats of formation values is especially useful for larger systems not (yet) amenable to high-level *ab initio* calculations, one should be cautious about applying such procedures to organic ions and neutrals for which experimental values are not available or uncertain [22].

1.2.2 Unimolecular Dissociations

Soon after the discovery of "metastable ions" by Hipple and Condon [23], they [24] provided the correct explanation for the observation of peak broadening relative to product ions in a normal mass spectrum as being due to the conversion of internal energy of fragmenting ions into translational energy of the products. Since then, metastable ion studies became one of the major sources of information about the structures and reactivities of gas-phase ions [25].

Metastable ions are those ions that are sufficiently stable to leave the ion source but undergo unimolecular decomposition before reaching the detector. Thus, metastable peaks can arise from ions that decompose unimolecularly within the field free regions of a mass spectrometer of reversed (or conventional) geometry. The major advantage of the reversed geometry for studying metastable ions is that any mass-selected ion can be transmitted into the second field free region (ffr) and its subsequent decompositions can then be investigated by scanning the electric sector. This technique is called mass-analyzed ion kinetic energy spectroscopy (MIKES) or metastable ion (MI) spectrum.

The MI spectrum samples ions which have a narrow range of internal energies (*ca.* < 2 eV above threshold) and fragment over a small time interval (typically 1-2 μs). One major aspect of MI studies is concerned with ion structure, provided that it is the reacting configuration of the ion, i.e. the ion structure which, existing in a potential well, leads directly to the transition state without further rearrangement. The observation of metastable ions enables one to deduce the reaction pathways because metastable ion transitions allow a precursor ion to be linked to a daughter ion by a chemical degradation reaction. It is noteworthy that MI spectra may sometimes suffer from artifact signals, which may be mistaken as normal signals [26]. The origin of these

interference signals in the MI spectra in the second ffr has been attributed to unimolecular decomposition reactions in the first ffr or in the accelerating region of the ion source. These artifact signals, which are easily recognized by their narrow peak width, can only occur in the MI spectra of ions having lower mass than that of the molecular ion.

The first approach to deduce ion structures used metastable peak intensity ratios. This approach was used by Shannon and McLafferty [27] in 1966 following a similar study by Rosenstock and co-workers [28]. The method is based on the assumption that the relative ratio of metastable peak intensities is not affected by the internal energy distribution of the fragmenting ions. Thus, one may confidently conclude that if two ions have the same structure, then their MI spectra are identical, whereas the opposite conclusion is not always true. Conversely, characteristically different MI spectra point to different structures.

The analysis of metastable peak shapes under high energy resolution (i.e. the main beam width at half height is $\leqslant$ 5 eV for ions having 8000 eV translational energy) provides more valuable information on ion structures than that of the relative abundance of metastable peaks. From a detailed examination of peak shape, composite metastable peaks may be detected (e.g. a Gaussian-shaped peak superimposed onto a dish-shaped peak) [25]. The presence of a composite metastable peak in a decomposition reaction of the molecular ion indicates that two competing fragmentation mechanisms exist. If it occurs upon decomposition of fragment ions, it means that either the fragment ion is formed via two reaction channels leading to two non-interconverting isomeric precursor ions or that a pair of isomeric daughter ions are formed from a single precursor ion structure. This method can also yield information on the kinetic energy release (KER, T) values upon unimolecuar decomposition.

As illustrated in Figure 1.4, the KER has two main sources: the non-fixed energy, $\varepsilon^{\ddagger}$, of the activated complex leading to $T^{\ddagger}$ and the activation energy for the reverse reaction, $\varepsilon_0{}^r$, leading to T^e [25]. Its value can be determined from the width of the MI peak at half height for the reaction $m_1{}^+ \rightarrow m_2{}^+ + m_3$ as shown in eq. 1.19:

$$T_{1/2} = [m_1{}^2 / (16 \cdot m_2 \cdot m_3)] \cdot V_{acc.} \cdot (\Delta E/E)^2 \qquad \text{(Eq. 1.19)}$$

where $V_{acc.}$ is the accelerating voltage, E is the main beam energy and ΔE is the energy width of the MI peak at half height.

Through comparative analysis, identical KER values point to identical structures and vice versa.

1.2.3 Collision-Induced Dissociations

Collision-induced dissociation (CID) or collision-activated dissociation (CAD) of ions in a field-free region (ffr) of the mass spectrometer has emerged as a powerful technique for probing ion structures and the mechanisms of their formation and decomposition [29].

The first signals due to collision-induced dissociation were discovered by the first mass spectroscopist, J.J. Thomson [2], in 1913, although it was Aston [3] who correctly identified the process. Thus, these peaks were referred to as 'Aston bands'. The pioneering work of McLafferty [30-32] and Jennings [33] developed the CID as a tool for distinguishing isomeric ion structures while Cooks and co-workers [34] systematically explored the potential of this technique for direct analysis of mixtures of organic compounds.

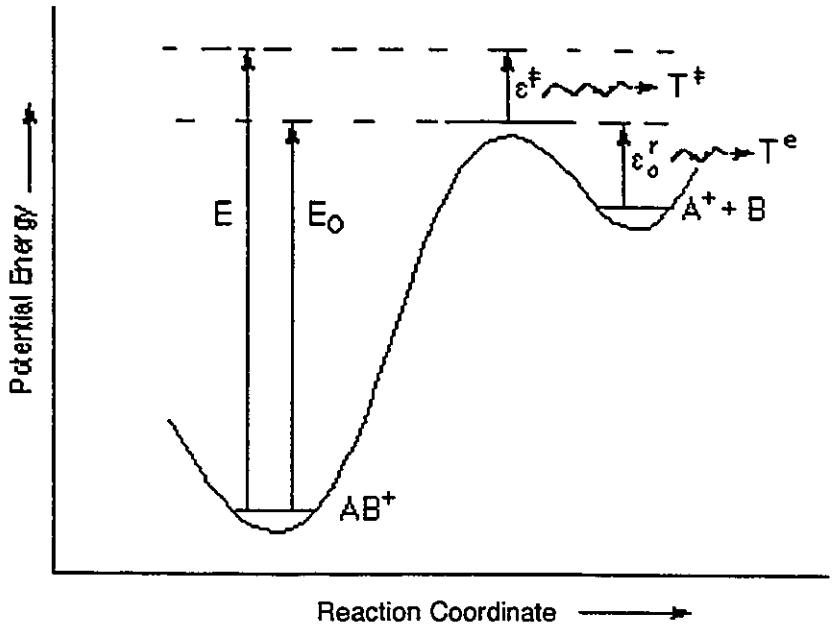

Figure 1.4 Contribution of the non-fixed energy, $\varepsilon^{\ddagger}$, in the transition state and the reverse activation energy, ε_o^r, leading to the observed KER.

Collisions of polyatomic ions (M_1^+) having keV translational energy with stationary neutral target gas atoms or molecules (G) can result in non-dissociative inelastic processes in which a fraction of the ions' translational energy is converted into internal energy leading to subsequent fragmentation [29]. A collision-induced dissociation of this kind is believed to proceed via two-step processes, viz., collisional activation (eq. 1.20) followed by unimolecular fragmentation of the internally excited ion (eq. 1.21):

$$M_1^+ + G \rightarrow (M_1^+)^* \qquad \text{(Eq. 1.20)}$$

$$(M_1^+)^* \rightarrow M_2^+ + M_3 \qquad \text{(Eq. 1.21)}$$

The whole group of the collision-induced products of a given primary ion is known as the collision-induced dissociation (CID) or collisional-activation (CA) spectrum of this

ion. The validity of the two-step model is based on the concept that the collision time (< 10^{-15} s) is shorter by at least an order of magnitude than the vibrational period of the fastest molecular vibrations (10^{-14} s). This results in two separate processes: collisional activation followed by unimolecular decomposition. During this period of time delay, the internal energy of ion is redistributed among various internal degrees of freedom. The mode of energy deposition in collision and the extent of internal energy redistribution before unimolecular decomposition form the central mechanistic studies in CID of polyatomic ions [29].

The unimolecular dissociation of collisionally activated ions can be described within the framework of the quasi-equilibrium theory (QET) or Rice-Rampsperger-Kassel-Marcus (RRKM/QET) theory [35]. In support of this mechanism, the relative fragment ion intensities in 70 eV electron-impact (EI) spectra are very similar to those obtained in CID spectra of the same molecular ions with 8-10 keV ions [32c,33]. In addition, the overall time-scales (*ca.* 10^{-6} s) for dissociation in CID and EI mass spectrometry are comparable.

To apply CID techniques in studies in gas-phase ion chemistry (i.e. the elucidation of ion structure and reaction mechanisms), it is desirable for the CID process to obtain maximum fragment ion currents as well as to favour dissociation reactions with high critical energy, such as direct bond cleavages. The efficiency for collision-induced dissociation, i.e. the extent to which the reaction can be driven, can be defined as shown in eq. 1.22:

$$\text{CID(efficiency)} = [\sigma_{CID} / (\sigma_{CID} + \sigma_L)] \cdot T \qquad \text{(Eq. 1.22)}$$

where σ_{CID} is the cross-section for collision-induced dissociation, σ_L is the cross-section for ion loss due to elastic scattering, charge-stripping, charge inversion

and charge exchange, and T is the relative transmission of daughter ions to precursor ions.

The cross-sections for charge stripping and charge inversion processes are relatively small as compared to other processes, such as scattering and neutralization. Thus, in order to optimize σ_{CID}, the competing ion-removal processes (in particular scattering and neutralization) must be minimized. It has been established from a number of studies [36] that helium has proven to be the collision gas of choice for high-energy CID mainly due to the small ion-loss cross-sections.

Massey's adiabatic criterion [37] allows us to predict, at least approximately, the maximum energy (ΔE_{max}) transferred during an inelastic high-energy collision, i.e. the probability for the maximum energy transfer occurs when:

$$a / \upsilon = h / \Delta E_{max} \qquad \text{(Eq. 1.23)}$$

where a is an interaction distance of the order of atomic dimensions, υ is the ion velocity and h is Planck's constant. Substitution of the ion velocity υ in eq. 1.23 by the kinetic energy, $E = (1/2) \cdot m \cdot \upsilon^2$, gives

$$\Delta E_{max} = (h / a) \cdot (2 \cdot E / m)^{1/2} \qquad \text{(Eq. 1.24)}$$

where m is the mass of the ion.

Thus, for a given interaction distance, a, ΔE_{max} is directly proportional to the square root of ion's kinetic energy, E, and inversely proportional to the square root of its mass, m.

It was shown by McLafferty and co-workers [38] that as the ion's kinetic energy increases, not only the yield of CID fragments increases but also the relative intensity

ratios between these fragments change. A direct consequence of an increase in the mean energy transferred during high-energy collisions is that the intensity of fragments having higher critical energies increases more than that of fragments with lower critical energies. Similar observations are found at high collision gas pressures [39] due to multiple collisions. However, it should be noted that at extremely high collision gas pressures, structure-characteristic fragment ions might disappear from the CID mass spectra due to multiple collisions. Thus, it was found by Holmes [40] that a main beam reduction of ca. 30-40% is optimal for maximum sensitivity and a reduction of <10% is necessary if only single collision processes are desirable.

It was observed from a number of studies [41] that even though the relative intensity ratio of the CID processes with high critical energy is independent of the internal energy of the precursor ion, there is a significant dependence of the relative abundance of CID reactions with low critical energy (i.e. MI decompositions) on the precursor ion internal energy. Since the CID spectrum is largely independent of the excitation energy, i.e. on the energy distribution before the collision, the relative intensity ratio of fragment ions in the spectrum reflects exclusively the structure of the precursor ion. Thus, the structures of two ions are identical if their CID spectra are superimposable, and vice versa. This comparative CID experiment requires knowledge of the structure of one of the ions.

1.2.4 Charge Transfer Reactions

The collision of ions (m_1^+) having high translational energy with stationary neutral target gas atoms or molecules (G) leads to collision-induced decompositions as discussed above in conjunction with a variety of charge transfer reactions, such as charge stripping from a positive ion (eq. 1.25), charge inversion of positive (eq. 1.26) or negative (eq. 1.27) ions and charge exchange (eq. 1.28):

$$m_1^+ + G \rightarrow m_1^{2+} + G + e^- \quad \text{(Eq. 1.25)}$$

$$m_1^+ + G \rightarrow m_1^- + G^{2+} \quad \text{(Eq. 1.26)}$$

$$m_1^- + G \rightarrow m_1^+ + G + 2e^- \quad \text{(Eq. 1.27)}$$

$$m_1^{2+} + G \rightarrow m_1^+ + G^+ \quad \text{(Eq. 1.28)}$$

To study a given charge exchange reaction for all primary ions formed in the ffr of a reversed double-focussing mass spectrometer, the electric sector voltage E must be: i) reduced to one-half of its original value for the observation of charge-stripping reactions (eq. 1.25); ii) doubled for the observation of charge exchange reactions (eq. 1.28); or iii) its polarity must be changed for charge inversion processes (eqs. 1.26 and 1.27).

Although the first charge-stripping (CS) reactions of positive organic ions in normal EI mass spectra were observed by Jennings and Seibl [42], it was Cooks and co-workers [43] who explored the potential of this method systematically. CS mass spectrometry [44] allows one not only to observe stable dications in the gas-phase, but also to determine the energetics of their formation by kinetic energy loss measurements. The most efficient target gases for the CS process are found to be oxygen and nitrogen [45].

As shown above, collision-induced dissociation of organic ions provides an invaluable tool for the assignment of unique structures to ions. A problem with this method is that one cannot distinguish between isomeric ions whose interconversion barriers are considerably lower than decomposition. The failure of CID proposed by Cooks and co-workers [46] was due to the fact that the average collision energy deposited in the ion upon CID was small (ca. 1-2 eV) compare to the depths of the potential wells corresponding to the isomeric ion structures. In other words, the number of non-decomposing ions having energies above the interconversion barrier

is larger than the number of stable ions. Thus, the CID samples predominantly those non-decomposing ions having energies close to the threshold which may have isomerized to a large extent. To circumvent this problem, it is necessary to sample ions from deep in the potential wells (i.e. non-isomerized ions). A CS reaction requires energy deposition of ca. 20 eV and it has been shown [47] that CS and dissociative charge-stripping (DCS) spectra have been successfully used to assign ion structures where CID failed.

When a singly charged positive ion having high (keV) translational energy collides with a neutral target gas, a charge inversion (CI) may take place by capturing two electrons from the target gas (eq. 1.26). The main use of CI spectra is to determine double-ionizaton potentials of the target molecule. Its advantage over CS spectra is that the dication need not to be stable because the energetics of formation of a doubly charged ion is obtained from the translational energy of the transmitted negative ion [48].

Alternatively, charge inversion may also take place when negative ions are fired into a neutral target gas by stripping two electrons from an anion (eq. 1.27). The charge-stripping of two electrons from polyatomic negative ions to form positive ions followed by dissociation was first systematically explored by Bowie and Blumenthal [49]. The decomposition of the resulting positive ion (the +E spectrum derived from the negative ion) can be used to provide a structural fingerprint for that positive ion since the relative intensity of peaks in the +E spectrum is independent of the internal energy of the precursor ion [50]. The main advantage of +E spectra is that positive ions of unusual structure can be produced by inverting the charge of negative ions if the corresponding anion is stable. More importantly, peaks due to simple bond cleavage reactions (high-energy processes) are generally abundant in the +E spectra, whereas

those arising from rearrangements (low-energy processes) are either of small abundance or absent. Thus, +E spectra can be used as a powerful tool for distinguishing isomeric ion structures [51].

In a charge exchange reaction (eq. 1.28), the originally doubly charged ions enter the electric sector with twice the translational energy but the same charge as the other ions. Thus, they can readily be studied by setting the electric sector voltage at 2E and the complete spectra of these doubly charged ions are termed as "2E spectra". These charge exchange reactions were first studied extensively by Lindholm [52]. The extent of ionization of the target depends upon the difference in recombination energy of the reagent ions ($RE(m_1^+)$) and ionization energy of the target (IE(G)). The cross-section for a charge exchange reaction increases as the difference between the two energies (i.e. $RE(m_1^+)$ - IE(G)) becomes small, i.e. when resonant charge exchange process occurs.

The charge separation fragmentation of doubly charged ions has been used for structure elucidation because the intercharge distance in the transition state can be calculated from the total coulombic energy gained on separating the charges, which is related to the kinetic energy (i.e. $T = e^2 / r$, where r is intercharge distance in the transition state) [53].

1.2.5 Double Collision Experiments (MS/MS/MS)

With the advent of multi-sector mass spectrometers equipped with multiple collision cells, it becomes possible to perform a variety of double collision experiments [54], in which mass-selected fragment ions (generated metastably or collisionally-induced) undergo sequential collisions with stationary neutral targets in different field-free regions of a mass spectrometer (see Figure 1.5). This powerful method, which is one of the key techniques used in the reactions described in this thesis,

allows one to probe the structure of fragment ions where unambiguous structure assignment is difficult to make on the basis of a single experiment. Through comparative CID studies, it is possible to deduce the structure of the parent ion from which the fragment ions originated. This requires knowledge of the structure of one of the fragment ions. The major limitation of this method is that the mass-selected fragment ions must have sufficient intensity in order to observe their daughter ions because the sensitivity decreases by a factor of *ca*. 100 from MS to MS/MS experiments performed in sector instruments.

1.2.6 Mass Spectrometry of Fast Neutrals

1.2.6.1 Neutralization-Reionization Mass Spectrometry (NRMS)

In the mid sixties Lavertu and co-workers [55], Devienne [56] and Gray and Tomlinson [57] discovered that beams of fast (e.g. 4-10 keV), mass-selected *ions* can undergo charge transfer (electron transfer) reaction upon collision with a neutral, stationary target gas to form beams of *neutral* molecules. This opened up a new field to probe the gas-phase chemistry of neutral species by means of mass spectrometric techniques. Later, Porter and co-workers [58] exploited the neutralized ion beam technique for the investigation of a great many small neutral species with fascinating unorthodox binding properties [59]. However, the potential of this method was not widely recognized until the technique of neutralization-reionization mass spectrometry (NRMS) was rediscovered by several research groups [60]. This technique allows the "tailored synthesis" of a variety of highly reactive, short-lived neutral species, which cannot be prepared or studied in solution or in a matrix because of intermolecular processes [61].

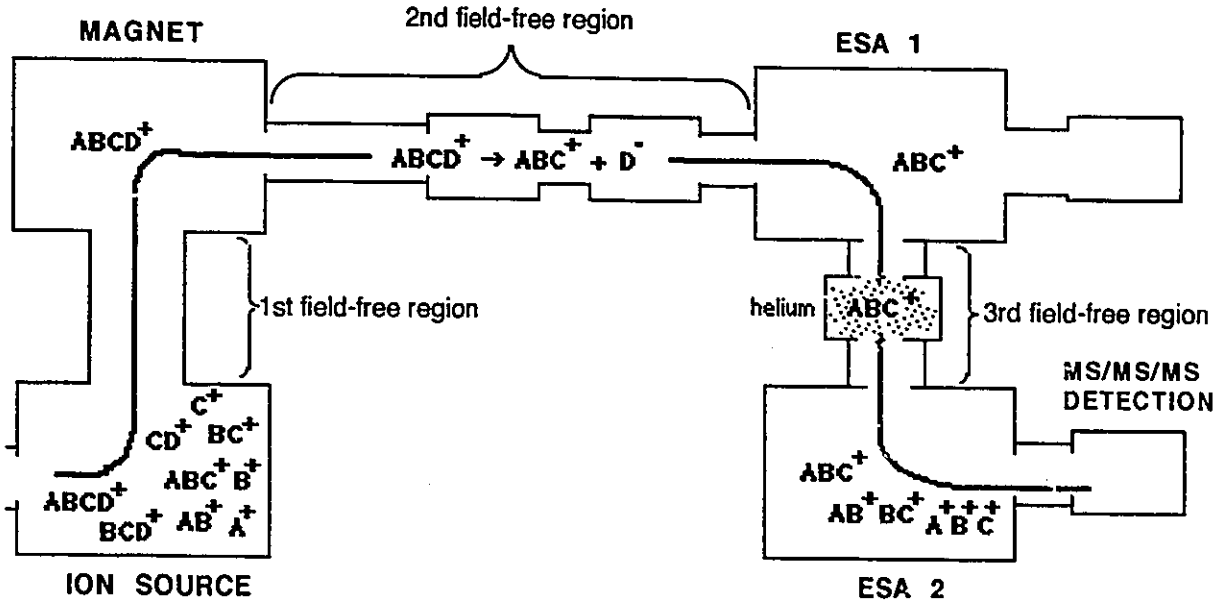

Figure 1.5 Schematic diagram illustrating a MS/MS/MS experiment. Here, a metastably generated ABC^+ ion undergoes collision-induced dissociation with He in the 3rd ffr and its dissociation products are detected by scanning the 2nd electrostatic analyzer. For a real life example involving one more step see Chapter 5, Figure 5.3.

A typical neutralization-reionization experiment is illustrated in the following:

Cell 1 (Neutralization)

$$G_1 + ABCD^+ \rightarrow G_1^{+\cdot} + ABCD \quad \text{(Eq. 1.29)}$$

$$\downarrow \rightarrow ACBD \quad \text{(Eq. 1.30)}$$

$$G_1 + ABCD^+ \rightarrow G_1^{+} + ABCD^* \rightarrow ABC^{\bullet} + D^{\bullet} \quad \text{(Eq. 1.31)}$$

$$G_1 + ABCD^+ \rightarrow G_1 + (ABCD^{+})^* \rightarrow ABC^{\bullet} + D^{+} \quad \text{(Eq. 1.32)}$$

$$\rightarrow ABC^{+} + D^{\bullet}$$

$$ABCD^+ \rightarrow ABC^{\bullet} + D^{+} \quad \text{(Eq. 1.33)}$$

$$\rightarrow ABC^{+} + D^{\bullet}$$

Cell 2 (Reionization)

G_2 + ABCD, ACBD $\rightarrow$ G_2 + e^- + $ABCD^+$ $\rightarrow$ AB^+ (Eq. 1.34)

$\rightarrow$ G_2 + e^- + $ACBD^+$ $\rightarrow$ AC^+ (Eq. 1.35)

G_2 + $ABC^\bullet$, $D^\bullet$ $\rightarrow$ G_2 + e^- + ABC^+, D^+ (Eq. 1.36)

A beam of mass-selected cations (or anions), whose structure is established using one of the accepted methods [62], possessing typically 8 keV translational energy, enters a collision gas chamber 1 (cell 1) where it collides with a neutral target gas, G_1, [63] under near single-collision conditions. A small fraction of these ions then undergoes neutralization via one-electron reduction (or oxidation) (equations 1.29 and 1.30, respectively) leading to a mixed beam of (ground and/or excited) neutral and ionic molecules. "Purification" of the beam is accomplished by removing all ionic species which have not been neutralized and (minor fraction of) their ionic dissociation products (equations 1.32 and 1.33) by a charged deflector electrode. After ca. 1 μs, these neutrals may have survived unchanged (eq. 1.29), isomerized (eq. 1.30) or dissociated (eq. 1.31). A beam of fast neutrals can also be prepared via collision-induced (or unimolecular) dissociation of a precursor ion (equations 1.32 and 1.33, respectively). The "purified" neutral beam then enters a second collision gas chamber (cell 2) where it collides with a second target gas, G_2, and a fraction of these neutrals is reionized.

Reionization of the neutrals by removal of one or more electrons [60c,64] to form cations is done with a target gas such at O_2 or NO, whereas addition of an electron to form anions is accomplished with a target such as Hg, C_6H_6 or Xe [65]. The reionized beam is then analyzed by using an additional sector or can be subjected to further collision experiments.

Positively as well as negatively charged species can be studied by NRMS, and depending on the original charge state of the ions and their reionized species, the

experiments can be denoted as $^{+}NR^{+}$, $^{+}NR^{-}$, $^{-}NR^{+}$, $^{-}NR^{-}$; where, for example, $^{+}NR^{+}$ denotes that primary positive ions are neutralized and reionized to positive ions.

The presence of a survivor ion, $ABCD^{+}$ (or $ABCD^{-}$) in a NR mass spectrum signifies that the neutral species must correspond to a bound state on the μs time scale of the experiment. On the other hand, the absence of a survivor ion does not necessarily mean that the corresponding neutral species cannot be generated as a stable species but it may only indicate that the neutral species is not stable under the given experimental conditions. For example, the absence of a recovery signal in the NR spectra of ethyl fluoride radical cations, $CH_3CH_2F^{\bullet+}$ [66], was attributed to the wholly vertical process of collision-induced ionization failing to regenerate stable $CH_3CH_2F^{\bullet+}$ ions from stable CH_3CH_2F molecules. The survivor ion intensity (I_{SV}) from its stable precursor ion (I_O) depends on four factors as shown by the equation 1.37:

$$I_{SV} = \alpha_N f_N \alpha_R f_R \cdot I_O \qquad \text{(Eq. 1.37)}$$

where α_N and α_R, respectively, are the neutralization and reionization efficiencies, and f_N and f_R are the respective fractions of non-dissociating neutrals and reionized ions [NR 6-b,c]. In a typical NR experiment, a high sensitivity is often required because the combined neutralization and reionization efficiencies is very low (*ca.* 0.1 to 0.001% of the main beam intensity (I_O)).

The nature and mechanism of the electron-transfer reactions (eq. 1.29) in a NR experiment are considered to be a vertical transitions due to the short interaction time in the neutralization process (ca. 10^{-15} s). Its efficiency depends upon two factors: i) the difference between the ionization energy (IE) of the target (G_1) and the recombination energy (RE) for the electron capture by $ABCD^{+}$ and ii) the geometry difference between the precursor ion $ABCD^{+}$ and its neutral counterpart ABCD; if this difference is small, then a stable neutral ABCD will result from resonant electron transfer conditions (i.e. $IE(G_1) = RE(ABCD^{+})$). For an ion and the corresponding

neutral molecule having substantially different equilibrium geometries in their ground electronic states, the electron transfer process results in vibrational excitation of the neutral molecule through Franck-Condon principle which can lead to dissociations [67].

A major problem in the interpretation of NR mass spectra concerns the structural homogeneity of the precursor ions as well as possible isomerization of the neutrals prior to reionization. Knowledge from thermochemistry and *ab initio* molecular orbital calculations renders insight into the height of dissociation and the isomerization barriers in both the precursor ion and its neutral counterpart. In addition, the connectivity of the reionized species can also be elucidated by subjecting them to an additional collision-induced dissociation (NR-CID), provided that the survivor ion intensity is sufficient enough to perform such an experiment. If the CID spectrum of the source-generated ion is identical to the NR-CID, this unequivocally proves that the primary ion flux is "pure" because NR efficiencies of survivor ions of neighbouring mass or even among isomeric and isobaric ions can easily differ by two orders of magnitude.

The efficiency of, and the energy transferred in, the neutralization process can be reflected in the neutralization target mass spectrum (NTMS) [68] which shows the spectrum of ionized target molecules (G_1) and their charged fragments resulting from the neutralization reaction. For example, NTMS of $(CH_3)_3N$ (TMA) resulting from neutralization of $^+CH_2OH$ by TMA shows an intense molecular ion at m/z 59 and very little fragmentation. This reflects that the energy deposited during the charge exchange reaction is very small indicating an efficient neutralization process.

One major advantage of NRMS over EI/MS is that it can provide structural information of the neutral species which is not available in normal EI mass spectra; for the latter, ionic species are considered. The lowest bond dissociation energies of neutrals can be substantially different from those of the corresponding ions; e.g. the

weakest bonds in neutral and ionized methanol are H_3C--OH and H--$CH_2OH^{\bullet+}$, respectively. In addition, neutral molecules are less prone to undergo isomerizations than ions, so that neutral fragmentations can be more characteristic of the neutral structure and thus lead to isomer differentiation [60].

For both ions and neutrals, a method for favouring dissociation over isomerization is to increase the internal energy of the reacting species. The internal energy of the neutral species can be increased by exothermic electron transfer [58] or collision-induced dissociation [60f]. Alternatively, angle-resolved NRMS [69] can be employed to collect neutral products of higher activation energy reactions at an increased scattering angle of the neutralization event. These techniques, however, do not decouple neutral and ion dissociations. Variable-time NRMS [70], on the other hand, can be used to distinguish the dissociations of a neutral from those of its ion following collisional reionization. This method employs variable time-scales for neutral and ion dissociations to obtain the time-dependent changes in the survivor and product ion yields. These, after kinetic analysis, can be related to the rate constants for both neutral and ion dissociations. These rate constants then illustrate, quantitatively, the importance of neutral and ion dissociations in NRMS.

Although NRMS has been used to assist in establishing ion structures in the gas-phase (see Chapters 2, 5, 6, 7 and 10), its main use has been for the generation and identification of numerous elusive and/or hitherto unknown radicals and molecules [60]. As a example, this powerful technique in conjunction with *ab initio* MO calculations was recently employed to demonstrate that nitrileimine (HCNNH), which for a long time was thought to be a reactive intermediate [71], is a stable molecule in the gas-phase [72].

1.2.6.2 Collision-Induced Dissociative Ionization (CIDI) Spectra of Neutral Species N in the Unimolecular Dissociation of Metastable Ions $m_1^+ \rightarrow m_2^+ + N$.

The CIDI technique is used for the investigation of the structure of the neutral species N generated in the unimolecular (metastable) dissociation of ions m_1^+, $m_1^+ \rightarrow m_2^+ + N$. This technique has received very little attention until an ion beam deflection method was developed [72].

A typical CIDI experiment is performed with the instrumental setup for NRMS but without using a neutral target gas, G_1, in the collision gas chamber 1 (cell 1). A small fraction of a beam of mass-selected cations (or anions) undergoes unimolecular dissociation in the second field-free region (ffr) of a double-focussing mass spectrometer of reversed geometry. All ions, i.e. m_1^+ and the ionic dissociation products m_2^+, are then deflected out of the flight path by a deflector electrode so that only the metastably generated neutrals enter the collision gas chamber 2 (cell 2) where they are ionized by collision with a target gas, G_2. A fraction of the ionized neutrals then undergoes collision-induced dissociation and the CIDI mass spectrum obtained therefrom can be used to identify the structure of the neutral N (see Chapter 3). The collision-induced ionization efficiency of fast neutrals was shown to increase with increasing translational energy and to decrease with increasing internal energy [63,73]. The latter may arise from the greater probability of unimolecular dissociation of the neutral molecules.

1.3 Unconventional Ion Structures

Many unimolecular dissociation reactions of organic radical cations do not occur directly from the ionized intact precursor molecule, but rather involve more or less

extensive isomerization to stable and/or reactive intermediates, such as distonic ions, ion-neutral complexes and hydrogen-bridged species, as a key step of the fragmentation mechanism. These stable and/or reactive intermediates having unconventional structures play a crucial role in the studies of unimolecular reaction mechanisms of gas-phase ions [74] and form the central theme of this thesis.

1.3.1 Distonic Ions

The term "distonic", derived from the Latin "distans" meaning "separate", was introduced by Radom and co-workers [75] to describe the general class of radical cations in which the charge and radical sites are adjacent to each other (i.e. α-distonic ion or ylidion) or separated by at least one heavy atom. The $CH_2OH_2^{\bullet+}$ ion was the first ylidion which was identified experimentally [76] and computationally [77] to be more stable species than the conventional isomer $CH_3OH^{\bullet+}$. Thus, distonic ions are those radical cations that formally arise from the ionization of zwitterions (or ylides) or biradicals. Since these neutral species are very reactive or unstable (e.g. $CH_2OH_2^{\bullet+}$ vs. CH_2OH_2), distonic ions cannot be formed by direct ionization. Instead they can be formed via isomerization, ion-molecule reactions, rearrangement-fragmentation, ring-opening or ring-cleavage reactions [74a,i]. Now, distonic ions are a well-defined class of stable [78] and common radical cations with characteristic properties. They play a major role in unimolecular fragmentation mechanisms since many radical cations isomerize to distonic ions prior to fragmentation, which in turn undergo unimolecular fragmentation to generate new distonic product ions. In addition, many unimolecular rearrangement processes involve distonic ions as key intermediates in the dissociations of many organic compounds and their reactions involve both the radical and charged moieties.

Many "puzzling" reactions observed for organic radical cations can readily be rationalized by a sequence of rearrangements of distonic ions which involve a migration of the charged moiety to a radical site followed by a shift of its ionized part to the new radical site [79].

1.3.2 Ion-Neutral Complexes

In many unimolecular reactions of organic radical cations in the gas-phase, an elongation of a covalent bond often does not lead directly to complete separation of molecular fragments. Instead, the charged and neutral moieties remain held together by electrostatic interactions (i.e. ion-dipole and/or ion-induced dipole forces) for a sufficiently long time in order for them to allow a new reaction channel which is less energy-demanding than the direct dissociation. These unconventional radical cations are classified as ion-neutral complexes (INCs) [74d-g,i,80]. The characteristic feature of these INCs is that one (or both) of the partners can freely rotate with respect to one another, thus allowing reactions which are impossible for the covalently bound precursor molecules due to geometrical restrictions [81]. These INCs can be viewed as analogous to solvolysis reactions in solution, which involve the formation of ion pairs [80].

The role of INCs as intermediates in umimolecular dissociations was first proposed by Bowen and co-workers [82] in 1978. The reactivity of these INCs depends on three factors: i) the stabilization energy (SE) of the INC; ii) the kinetic energy released on isomerization of the incipient cation; and iii) the enthalpy change for proton transfer between the charged and neutral components. Thus, the extent of chemistry of these INCs depends on the relative magnitudes of these factors. The stabilization energy (SE) can be estimated using the following equation (eq. 1.38):

$$SE = (q \cdot \mu \cdot \cos\Theta) / r^2 \qquad \text{(Eq. 1.38)}$$

where q is the charge on the ion, μ is the dipole moment, Θ is the angle between the point dipole and the charge to dipole axis and r is the distance between the point charge and point dipole.

In general, the stabilization energies in INCs are in the range 50 - 80 kJ/mol containing a neutral component having a dipole moment μ = 1.5 - 2.5 D. These stabilization energies are sufficient for INCs to allow new reaction channels to be observed: i) isomerization of a cation; ii) hydrogen transfer; or iii) the components may rotate with respect to each other and recombine to yield a new isomer from which subsequent decompositions may occur. Thus, INC-mediated mechanisms can provide a means to the understanding of many unusual unimolecular reactions which would otherwise be inexplicable.

1.3.3 Hydrogen-bridged Radical Cations

Since Morton's proposal [83] that intramolecular hydrogen bonding in a neutral molecule can persist in the molecular ion upon ionization in the gas-phase, hydrogen-bridged radical cations have been increasingly proposed as key intermediates in many unimolecular dissociation of oxygen-containing radical cations. Unlike even-electron proton-bound molecule pairs $[M_1 \cdots H \cdots M_2]^+$ [83,84], hydrogen-bridged radical cations $[M \cdots H \cdots R]^{\bullet +}$, the odd-electron counterparts, are not extensively studied. The principle reason is that the latter ions cannot be generated by ion-molecule reactions under chemical ionization conditions whereas the stable proton-bound dimers can easily be produced under such conditions and are a well studied class of ions. Thus, alternative methods, such as dissociative ionization and/or unimolecular rearrangement of precursor molecules, must be devised to generate

those odd-electron ions. However, these methods can lead to more subtle problems because existing experimental methods (e.g. MI, CID or NR) alone are often not sufficient to unequivocally distinguish between those isomers which are expected to give closely similar characteristics. In such cases, high-level *ab initio* molecular orbital calculations can give invaluable insight into the isomerization barriers as well as their relative energies [85c]. For example, Terlouw et al. [86] showed that the $C_2H_6O_2^{\bullet+}$ ions generated by dissociative ionization of 1,4-butanediol, $HOCH_2CH_2CH_2CH_2OH^{\bullet+}$, were proposed to have structure [vinyl alcohol/water]$^{\bullet+}$. However, the experiments could not distinguish between the hydrogen-bridged species, CH_2=C(H)-O···H···$OH_2^{\bullet+}$, and the distonic isomers H_2O^+-$CH_2CH^{\bullet}$-OH and $^{\bullet}CH_2CH(OH)^+OH_2$. High-level *ab initio* calculations [87], on the other hand, revealed that the O••H••O hydrogen-bridged ion is the most stable isomer and is stable with respect to dissociation into $CH_2CHOH^{\bullet+}$ and H_2O. In a second example, Heinrich and co-workers [88] provided an elegant explanation, using high-level *ab initio* molecular orbital calculations, for the loss of $^{\bullet}CH_2OH$ from ionized metastable methyl acetate involving an O···H···O hydrogen-bridged radical cation, $[CH_3C(=O)\cdots H\cdots O=CH_2]^{\bullet+}$, as a key intermediate.

Even though O••H••O hydrogen-bridged radical cations are more attractive intermediates than their C-H••O counterparts because of their higher thermodynamic stability, the latter ions are being increasingly postulated as key intermediates in the study of low energy rearrangement reactions in oxygen containing ions [89].

As mentioned previously, the elucidation of ion structures forms a central theme in the study of gas-phase ion chemistry. This thesis is not an exception to this theme. It is focussed on the effort to gain some insight into the chemistry of organic ions in the gas-phase, particularly oxygen containing ions whose thermochemistry is well developed. Tandem mass spectrometry based techniques (e.g. MI, CID, or NR etc.) in conjuction with high-level *ab initio* molecular orbital calculations can provide a

powerful tool for the determination of stable ions with unexpected structure (e.g. distonic ions, ion-neutral complexes, or hydrogen-bridged ions) in the gas-phase. However, this requires collaboration between people with different specialisms, who are able not only to analyze the problem, but also to critically interpret the results. The present thesis is based on such a teamwork with Dr. C.A. Kingsmill and the theoretical chemist Prof. P.J.A. Ruttink who performed the *ab initio* calculations. Collaborative work with Prof. J.L. Holmes led to the work described in Chapter 2, whereas Dr. P.C. Burgers provided valuable contributions to the Chapters 3 through 6.

Chapters 2 through 4 focus on the role of C-H•••O hydrogen-bridged radical cations and ion-neutral complexes in the unimolecular decomposition of ionized acetol, $CH_3C(=O)CH_2OH^{\bullet+}$, methyl glycolate, $HOCH_2C(=O)OCH_3^{\bullet+}$, methyl lactate, $HOCH(CH_3)C(=O)OCH_3^{\bullet+}$, and acetoin, $CH_3C(=O)C(H)(CH_3)OH^{\bullet+}$ using tandem mass spectrometry based experiments on D-, ^{13}C- and ^{18}O-labelled isotopologues in combination with *ab initio* molecular orbital calculations.

In Chapters 5 and 6, the keto-enol tautomeric equilibrium of ionized methyl and ethyl glycolate in the gas-phase was investigated by a variety of tandem mass spectrometry based techniques using D-, ^{13}C- and ^{18}O-labelled precursor molecules. In particular, the unimolecular chemistry of the enol form of ionized methyl and ethyl glycolate, $HOCH=C(OH)(OR)$ (R = CH_3 and CH_2CH_3, respectively), was discussed. In addition, the long sought hydrogen-bridged radical cation, $[H\text{-}C{=}O\cdots H\cdots O(H)\text{-}CH_3]^{\bullet+}$, which plays a key role in the dissociation chemistry of low energy ethylene glycol ions was identified by multiple collision experiments.

In Chapter 7, the unimolecular chemistry of ionized di-*n*-butyl ether was investigated with respect to that of ionized *n*-butyl *sec*-butyl and di-*sec*-butyl ethers.

In Chapter 8, an ion-neutral complex-mediated mechanism is proposed for propene and water loss from the oxonium ion $CH_3CH{=}O^+CH_2CH_2CH_3$. This mechanism is supported by the site-selectivity in the hydrogen transfer step(s) which result in propene and water loss from the oxonium ion.

Chapter 9 gives a detailed study of alkene elimination from the metastable oxonium ions $(CH_3CH_2)_2C{=}OH^+$, $CH_3CH_2CH_2(CH_3)C{=}OH^+$, and $(CH_3CH_2CH_2)_2C{=}OH^+$ by means of ^{13}C-labelling experiments. Chapters 7 through 9 reflect projects initiated by Dr. R.D. Bowen (Bradford University).

In Chapter 10, a combined experimental and theoretical information was used to investigate part of the $C_3H_5O_2^+$ potential energy surface as well as to ascertain whether carbonyl-protonated b-propiolactone ions, $CH_2CH_2OCOH^+$, can interconvert with protonated acrylic acid, $CH_2{=}CHC(OH)_2^+$, as claimed in a recent thermolysis study.

References

1 E. Goldstein, *Berl. Ber.*, **39**, 691 (1886).

2 J.J. Thomson, Rays of Positive Electricity and Their Application to Chemical Analysis, Longmans, Green, London (1913).

3 F.W. Aston, *Proc. Cambridge Philos. Soc.*, **38**, 307 (1919).

4 A.J. Dempster, *Phys. Rev.*, **11**, 316 (1918).

5 A.O. Nier, *Phys. Rev.*, **50**, 212 (1940).

6 a) A.O. Nier, T.R. Roberts and E.G. Franklin, *Phys. Rev.*, **75**, 346 (1949); b) A. O. Nier and T.R. Roberts, *Phys. Tev.*, **81**, 507 (1951); c) T.L. Collins, A.O. Nier and W.H. Johnson, *Phys. Rev.*, **84**, 717 (1951).

7 a) J. Franck, *Trans. Faraday Soc.*, **21**, 536 (1926); b) E.U. Condon, *Am. J. Phys.*, **15**, 365 (1947).

8 M.M. Rosenstock, M.B. Wallenstein, A.L. Wahrhaftig and H. Eyring, *Proc. Natl. Acad. Sci. (U.S.A.)*, **38**, 667 (1952).

9 K. Maeda, G.P. Semeluk and F.P. Lossing, *Int. J. Mass Spectrom. Ion Phys.*, **1**, 395 (1968).

10 D.W. Turner, C. Baker, A.D. Baker and C.R. Brundle, Molecular Photoelectron Spectroscopy, Wiley-Interscience, New York (1970).

11 J. Dannacher, *Org. Mass Spectrom.*, **19**, 253 (1984).

12 J.L. Beauchamp, *Ann. Rev. Phys. Chem.*, **22**, 527 (1971).

13 E.E. Furguson, Ion Molecule Reactions, Ed., J.L. Franklin, Chapter 8, Plenum Press, New York (1972).

14 P. Kebarle, Ion Molecule Reactions, Ed., J.L. Franklin, Chapter 7, Plenum Press, New York (1972).

15 S.G. Lias, J.E. Bartmess, J.F. Liebman, J.L. Holmes, R.D. Levin and W.G. Mallard, *J. Phys. Chem. Ref. Data*, **17**, supplement 1 (1988).

16 a) S.W. Bensen, F.R. Cruickshank, D.M. Golden, G.R. Haugen, H.E. O'Neal, A.S. Rodgers, R. Shaw and R. Walsh, *Chem. Rev.*, **69**, 279 (1969); b) S.W. Bensen, Thermochemical Kinetics, Wiley-Interscience, New York, NY (1976); c) J.B. Pedley, R.D. Naylor and S.P. Kirby, Thermochemical Data of Organic Compounds, 2nd edn., Chapman and Hall, London (1986).

17 a) V.V. Takhistov and D.A. Ponomarev, *Org. Mass Spectrom.*, **29**, 395 (1994); b) D.J. McAdoo, *J. Mass Spectrom.*, **30**, 388 (1995).

18 a) J.L. Holmes and F.P. Lossing, *Org. Mass Spectrom.*, **26**, 537 (1991); b) Y.R. Luo and P.D. Pacey, *J. Phys. Chem.*, **95**, 9471 (1991); c) Y.R. Luo and P.D. Pacey, *Int. J. Mass Spectrom. Ion Processes*, **108**, 221 (1991); d) Y.R. Luo and S.W. Bensen, *Acc. Chem. Res.*, **25**, 375 (1992); e) Y.R. Luo, Y. An and J.L. Holmes, *Org. Mass Spectrom.*, **29**, 579 (1994).

19 W.J. Hehre, L. Radom, P.v.R. Schleyer and J.A. Pople, Ab Initio Molecular Orbital Theory, Wiley, New York (1986).

20 a) J.A. Pople, M. Head-Gordon, D. Fox, K. Raghavachari and L.A. Curtiss, *J. Chem. Phys.*, **90**, 5622 (1989); b) L.A. Curtiss, C. Jones, G.W. Trucks, K. Raghavachari and J.A. Pople, *J. Chem. Phys.*, **93**, 2357 (1990); c) L.A. Curtiss, K. Raghavachari, G.W. Trucks and J.A. Pople, *J. Chem. Phys.*, **94**, 7221 (1991).

21 L.A. Curtiss, K. Raghavachari and J.A. Pople, *J. Chem. Phys.*, **98**, 1293 (1993).

22 a) H. Halim, N. Heinrich, W. Koch, J. Schmidt and G. Frenking, *J. Comp. Chem.*, **7**, 93 (1986); b) M.S. Dewar and K.M. Dieter, *J. Am. Chem. Soc.*, **108**, 8075 (1986); c) J.J. Dannenberg and L.K. Vinson, *J. Phys. Chem.*, **92**, 5635 (1988).

23 J.A. Hipple and E.V. Condon, *Phys. Rev.*, **68**, 54 (1945).

24 J.A. Hipple, R.E. Fox and E.V. Condon, *Phys. Rev.*, **69**, 347 (1946).

25 R.G. Cooks, J.H. Beynon, R.H. Caprioli and G.R. Lester, Metastable Ions, Elsevier, Amsterdam (1973).

26 a) W. Heerma, M.M. Sarneel and J.K. Terlouw, *Org. Mass Spectrom.*, **16**, 325 (1981); b) A. Fraefel and J. Seibl, *Mass Spectrom. Rev.*, **4**, 151 (1985).

27 T.W. Shannon and F.W. McLafferty, *J. Am. Chem. Soc.*, **88**, 5021 (1967).

28 H.M. Rosenstock, V.H. Dibeler and F.N. Harllee, *J. Chem. Phys.*, **40**, 591 (1964).

29 a)F.W. McLafferty, P.F. Bente III, R. Kornfeld, S.-C. Tsai and I. Howe, *J. Am. Soc. Mass Spectrom.*, **30**, 797 (1973); b) K. Levsen and H. Schwarz, *Angew. Chem. Int. Ed. Engl.*, **15**, 509 (1976); c) K. Levsen, Fundamental Aspects of Organic Mass Spectrometry, Verlag Chemie, Weinheim (1978); d) J. Los and T.R. Govers, Collision Spectroscopy, R.G. Cooks Ed., Chapter 6, Plenum, New York (1978); e) K. Levsen and H. Schwarz, *Mass Spectrom. Rev.*, **2**, 77 (1983); f) R.A. Yost and D.D. Fetterolf, *Mass Spectrom. Rev.*, **2**, 1 (1983); g) J. Bordas-Nagy and K.R. Jennings, *Int. J. Mass Spectrom. Ion Processes*, **100**, 105 (1990); h) A.K. Shukla and J.H. Futrell, *Mass Spectrom. Rev.*, **12**, 211 (1993).

30 W.F. Haddon and F.W. McLafferty, *J. Am. Chem. Soc.*, **90**, 4745 (1968).

31 W.F. Haddon and F.W. McLafferty, *Anal. Chem.*, **41**, 31 (1969).

32 F.W. McLafferty, R. Kornfeld, W.F. Haddon, K. Levsen, I. Sakai, P.F. Bente III, S.-C. Tsai and H.D.R. Schuddemage, *J. Am. Chem. Soc.*, **95**, 3886 (1973).

33 K.R. Jennings, *Int. J. Mass Spectrom. Ion Phys.*, **1**, 227 (1968).

34 a) R.W. Kondrat and R.G. Cooks, *Anal. Chem.*, **50**, A81 (1978); b) K.L. Busch and R.G. Cooks, Tandem Mass Spectrometry, F.W. McLafferty, Ed., Wiley, New York (1983).

35 a) R.A. Marcus, O.K. Rice, *J. Phys. Colloid. Chem.*, **55**, 894 (1951); b) H.M. Rosenstock, M.B. Wallenstein, A.L. Wahrhaftig and H. Eyring, *Proc. Natl. Acad. Sci. USA*, **38**, 667 (1952).

36 a) M.S. Kim and F.W. McLafferty, *J. Am. Chem. Soc.*, **100**, 3279 (1978); b) J.A. Laramee, D. Cameron and R.G. Cooks, *J. Am. Chem. Soc.*, **103**, 12 (1981); c) S.R. Horning, M. Vincenti and R.G. Cooks, *J. Am. Chem. Soc.*, **112**, 119 (1990); d) A.J. Alexander, P. Thibault and R.K. Boyd, *J. Am. Chem. Soc.*, **112**, 2484 (1990); e) S.A. McLuckey, *J. Am. Soc. Mass Spectrom.*, **3**, 599 (1992).

37 H.S. Massey, *Rep. Prog. Phys.*, **12**, 249 (1949).

38 F.W. McLafferty, P.F. Bente III, R. Kornfeld, S.-C. Tsai and I. Howe, *J. Am. Chem. Soc.*, **95**, 2120 (1973).

39 a) F.W. McLafferty and H.D.R. Schuddemage, *J. Am. Chem. Soc.*, **91**, 1886 (1969), b) C.E.D. Ouwerkerk, S.A. McLuckey, P.G. Kistemaker and A.J.H. Boerboom, *Int. J. Mass Spectrom. Ion Processes*, **56**, 11 (1984).

40 J.L. Holmes, *Org. Mass Spectrom.*, **20**, 169 (1985).

41 a) K. Levsen and H.D. Beckey, *Org. Mass Spectrom.*, **9**, 570 (1974); b) F.W. McLafferty, A. Hirota, M.P. Barbalas and P.F. Pegues, *Int. J. Mass Spectrom. Ion Phys.*, **35**, 299 (1980).

42 a) K.R. Jennings, *Int. J. Mass Spectrom. Ion Phys.*, **1**, 227 (1968); b) J. Seibl, *Org. Mass Spectrom.*, **2**, 1033 (1969).

43 a) R.G. Cooks, J.H. Beynon and T. Ast, *J. Am. Chem. Soc.*, **94**, 1004 (1972); b) T. Ast, J.H. Beynon and R.G. Cooks, *J. Am. Chem. Soc.*, **94**, 6611 (1972); c) R.G. Cooks, T. Ast and J.H. Beynon, *Int. J. Mass Spectrom. Ion Phys.*, **11**, 490 (1973); d) D.L. Kemp, J.H. Beynon and R.G. Cooks, *Org. Mass Spectrom.*, **11**, 857 (1976).

44 a) W. Koch, F. Maquin, D. Stahl and H. Schwarz, *Chimia*, **39**, 376 (1985); b) T. Ast, *Adv. Mass Spectrom.*, **8A**, 555 (1980); c) K. Lammertsma, P.v.R. Schleyer and H. Schwarz, *Angew. Chem. Int. Ed. Engl.*, **28**, 1321 (1989); d) S. Beaudet, A. Ruf and D. Stahl, *Int. J. Mass Spectrom. Ion Processes*, **114**, 61 (1992).

45 T. Ast, C.J. Proctor, C.J. Porter and J.H. Beynon, *Int. J. Mass Spectrom. Ion Phys.*, **40**, 111 (1981).

46 R.G. Cooks, J.H. Beynon and J.F. Litton, *Org. Mass Spectrom.*, **10**, 503 (1975).

47 a) D.L. Miller and M.L. Gross, *Org. Mass Spectrom.*, **18**, 239 (1983); b) E.E. Kingston, J.H. Beynon, T. Ast, R. Flammang and A. Maquestiau, *Org. Mass Spectrom.*, **20**, 546 (1985); c) J.M. Curtis, A.G. Brenton, J.H. Beynon and R.K. Boyd, *Org. Mass Spectrom.*, **22**, 779 (1987).

48 a) B. Leyh and H. Wankenne, *Int. J. Mass Spectrom. Ion Processes*, **107**, 453 (1991); b) W.J. Griffiths, F.M. Harris, S.R. Andrews and D.E. Parry, *Int. J. Mass Spectrom. Ion Processes*, **112**, 45 (1992); c) M.L. Langford, F.M. Harris, C.J. Reid, J.A. Ballantine and D.E. Parry, *Int. J. Mass Spectrom. Ion Processes*, **112**, 285 (1992); d) F.M. Harris, *Int. J. Mass Spectrom. Ion Processes*, **120**, 1 (1992).

49 J.H. Bowie and T. Blumenthal, *J. Am. Chem. Soc.*, **97**, 2959 (1975).

50 M.M. Bursey, *Mass Spectrom. Rev.*, **9**, 555 (1990).

51 a) J.A. Benbow, J.H. Bowie and G. Klass, *Org. Mass Spectrom.*, **12**, 432 (1977); b) J.H. Bowie and J.A. Benbow, *Org. Mass Spectrom.*, **13**, 103 (1978); c) B.L.M. van Baar, N. Heinrich, W. Koch, R. Postma, J.K. Terlouw and H. Schwarz, *Angew. Chem. Int. Ed. Engl.*, **26**, 140 (1987); d) M. Tkaczyk and A.G. Harrison, *Org. Mass Spectrom.*, **27**, 585 (1992); e) S. Dua, J.C. Sheldon and J.H. Bowie, *Rapid Commun. Mass Spectrom.*, **8**, 533 (1994).

52 E. Lindholm, *Proc. Phys. Soc. London*, **A66**, 1068 (1953).

53 a) T. Ast, J.H. Beynon and R.G. Cooks, *Org. Mass Spectrom.*, **6**, 749 (1972); b) T. Ast, *Adv. Mass Spectrom.*, **8**, 555 (1980).

54 S. Villeneuve and P.C. Burgers, *Org. Mass Spectrom.*, **21**, 733 (1986).

55 R. Lavertu, M. Catte, A. Pentenero and P.C.R. LeGoff, *Seances Acad. Sci. Ser. C.*, **263**, 1099 (1966).

56 F.M. Devienne, *Entropie*, **24**, 35 (1968).

57 a) J. Gray and R.H. Tomlinson, *Chem. Phys. Lett.*, **3**, 523 (1969); b) J. Gray and R.H. Tomlinson, *Chem. Phys. Lett.*, **4**, 251 (1969).

58 G.I. Gellene and R.F. Porter, *Acc. Chem. Res.*, **16**, 200 (1983).

59 a) G.I. Gellene, D.A. Cleary and R.F. Porter, *J. Chem. Phys.*, **77**, 3471 (1982); b) G.I. Gellene and R.F. Porter, *J. Chem. Phys.*, **79**, 5975 (1983); c) G.I. Gellene and R.F. Porter, *J. Phys. Chem.*, **88**, 6680 (1984); d) G.I. Gellene and R.F. Porter, *J. Chem. Phys.*, **81**, 5570 (1984); e) S.-J. Jeon, A.B. Raksit, G.I. Gellene and R.F. Porter, *J. Am. Chem. Soc.*, **107**, 4129 (1985); f) A.B. Raksit, S.-J. Jeon and R.F. Porter, *J. Phys. Chem.*, **90**, 2298 (1986).

60 a) A.G. Harrison, R.S. Mercer, E.J. Reiner and A.B. Young, *Int. J. Mass Spectrom. Ion Processes*, **74**, 13 (1986); b) P.O. Danis, R. Feng and F.W. McLafferty, *Anal. Chem.*, **58**, 348 (1986); c) P.O. Danis, R. Feng and F.W. McLafferty, *Anal. Chem.*, **58**, 355 (1986); d) J.K. Terlouw and H. Schwarz, *Angew. Chem. Int. Ed. Engl.*, **26**, 805 (1987); e) C. Wesdemiotis and F.W. McLafferty, *Chem. Rev.*, **87**, 485 (1987); f) R. Feng, C. Wesdemiotis, M.A. Baldwin and F.W. McLafferty, *Int. J. Mass Spectrom. Ion Processes*, **86**, 95 (1988); g) J.L. Holmes, *Mass Spectrom. Rev.*, **8**, 513 (1989); h) F.W. McLafferty, *Science*, **247**, 925 (1990); i) F. Turecek, *Org. Mass Spectrom.*, **27**, 1087 (1992); j) F.W. McLafferty, *Int. J. Mass Spectrom. Ion Processes*, **118/119**, 221 (1992); k) M.J. Polce, M.M. Cordero and C. Wesdemiotis, *Int. J. Mass Spectrom. Ion Processes*, **113**, 35 (1992); l) M.-Y. Zhang and F.W. McLafferty, *J. Am. Soc. Mass Spectrom.*, **3**, 108 (1992); m) D.V. Zagorevskii and J.L. Holmes, *Mass Spectrom. Rev.*, **13**, 133 (1994); n) S. Beranova and C. Wesdemiotis, *J. Am. Soc. Mass Spectrom.*, **5**, 1093 (1994); o) N. Goldberg and H. Schwarz, *Acc. Chem. Res.*, **27**, 347 (1994).

61 C. Wentrup, Reactive Molecules: The Neutral Reactive Intermediate in Organic Chemistry, Wiley, New York (1984).

62 a) J.L. Holmes, *Org. Mass Spectrom.*, **20**, 169 (1985); b) K. Levsen, Fundamental Aspects of Organic Mass Spectrometry, Verlag Chemie, Weinheim (1978).

63 C.E.C.A. Hop, Ph. D. Thesis, University of Utrecht (1989).

64 C. Wesdemiotis, R. Feng, P.O. Danis, E.R. Williams and F.W. McLafferty, *J. Am. Chem. Soc.*, **108**, 5847 (1986).

65 a) R. Feng, C. Wesdemiotis and F.W. McLafferty, *J. Am. Chem. Soc.*, **109**, 6521 (1987); b) C. Wesdemiotis and R. Feng, *Org. Mass Spectrom.*, **23**, 416 (1986); c) A.W. McMahon, S.K. Chowdhury and A.G. Harrison, *Org. Mass Spectrom.*, **24**, 620 (1989).

66 C.E.C.A. Hop, J.L. Holmes, F.P. Lossing and J.K. Terlouw, *Int. J. Mass Spectrom. Ion Processes*, **83**, 285 (1988).

67 a) F. Turecek, M. Gu and C.E.C.A. Hop, *J. Phys. Chem.*, **99**, 2278 (1995); b) S.A. Shaffer and F. Turecek, *J. Am. Chem. Soc.*, **116**, 8647 (1994); c) M. Sirois, M. George and J.L. Holmes, *Org. Mass Spectrom.*, **29**, 11 (1994); d) M.G.H. Boogaarts, P.C. Hinnen and G. Meijer, *Chem. Phys. Lett.*, **223**, 537 (1994); e) S.A. Shaffer, F. Turecek and R.L. Cerny, *J. Am. Chem. Soc.*, **115**, 12117 (1993); f) M. Gu and F. Turecek, *J. Am. Chem. Soc.*, **114**, 7146 (1992); g) J.C. Lorquet, B. Leyh-Nihant and F.W. McLafferty, *Int. J. Mass Spectrom. Ion Processes*, **100**, 465 (1990).

68 T. Wong, J.K. Terlouw, T. Weiske and H. Schwarz, *Int. J. Mass Spectrom. Ion Processes*, **113**, R23 (1992).

69 A. Fura, F. Turecek and F.W. McLafferty, *J. Am. Soc. Mass Spectrom.*, **2**, 492 (1991).

70 a) D.W. Kuhns and F. Turecek, *Org. Mass Spectrom.*, **30**, 463 (1994); b) D.W. Kuhns, T.B. Tran, S.A. Shaffer and F. Turecek, *J. Phys. Chem.*, **98**, 4845 (1994).

71 G. Bertrand and C. Wentrup, *Angew. Chem. Int. Ed. Engl.*, **33**, 527 (1994).

72 N. Goldberg, A. Fiedler and H. Schwarz, *Helv. Chim. Acta*, **77**, 2354 (1994).

73 a) J.L. Holmes and A.A. Mommers, *Org. Mass Spectrom.*, **19**, 460 (1984); b) D. Harnish and J.L. Holmes, *Org. Mass Spectrom.*, **29**, 213 (1994).

74 a) S. Hammerum, *Mass Spectrom. Rev.*, **7**, 123 (1988); b) K.M. Stirk, L.K. Kiminkinen and H.I. Kenttamaa, *Chem. Rev.*, **92**, 1649 (1992); c) H.-F. Grutzmacher, *Int. J. Mass Spectrom. Ion Processes*, **118/119**, 825 (1992); d) R.D. Bowen, *Acc. Chem. Res.*, **24**, 364 (1991); e) T.H. Morton, *Org. Mass Spectrom.*, **27**, 353 (1992); f) P. Longevialle, *Mass Spectrom. Rev.*, **11**, 157 (1992); g) R.D. Bowen, *Org. Mass Spectrom.*, **28**, 1577 (1993); h) H.I. Kenttamaa, *Org. Mass Spectrom.*, **29**, 1 (1994); i) J.S. Splitter and F. Turecek, Applications of Mass Spectrometry to Organic Stereochemistry, VCH, New York (1994).

75 L. Radom, W.J. Bouma, R.H. Nobes and B.F. Yates, *Pure Appl. Chem.*, **56**, 1831 (1984).

76 a) J.L. Holmes, F.P. Lossing, J.K. Terlouw and P.C. Burgers, *J. Am. Chem. Soc.*, **104**, 2931 (1982); b) W.J. Bouma, J.K. MacLead and L. Radom, *J. Am. Chem. Soc.*, **104**, 2930 (1982).

77 W.J. Bouma, R.H. Nobes and L. Radom, *J. Am. Chem. Soc.*, **104**, 2929 (1982).

78 a) B.F. Yates, W.J. Bouma and L. Radom, *J. Am. Chem. Soc.*, **106**, 5805 (1984); b) L. Radom, W.J. Bouma and B.F. Yates, *Tetrahedron*, **42**, 6225 (1986).

79 a) D.J. McAdoo, C.E. Hudson, M. Skyiepal, E. Broido and L.L. Griffin, *J. Am. Chem. Soc.*, **109**, 7648 (1987); b) G. Bouchoux, F. Bidault, F. Djazi, B. Nicod and J. Tortajada, *Org. Mass Spectrom.*, **22**, 748 (1987).

80 D.J. McAdoo, *Mass Spectrom. Rev.*, **7**, 363 (1988).

81 P. Longevialle, G. Bouchoux and Y. Hoppilliard, *Org. Mass Spectrom.*, **25**, 527 (1990).

82 a) R.D. Bowen, B.J. Stapleton and D.H. Williams, *J. Chem. Soc. Chem. Commun.*, 24 (1978); b) D.H. Williams, B.J. Stapleton and R.D. Bowen, *Tetrahedron Lett.*, 2919 (1978).

83 T.H. Morton, *Tetrahedron*, **38**, 3195 (1982).

84 M.T. Bowers, Gas-Phase Ion Chemistry, Academic Press, New York, Vol. 1 (1979).

85 a) P.C. Burgers, J.K. Terlouw, Specialist Periodical Reports: Mass Spectrometry, M.E. Rose, Ed., The Royal Society of Chemistry, London, Vol. 10, Chapter 2 (1989); b) E. Uggerud, *Mass Spectrom. Rev.*, **11**, 389 (1992); c) R. Postma, Ph.D. Thesis, University of Utrecht (1987).

86 J.K. Terlouw, W. Heerma, P.C. Burgers and J.L. Holmes, *Can. J. Chem.*, **62**, 289 (1984).

87 R. Postma, S.P. van Helden, J.H. van Lenthe, P.J.A. Ruttink, J.K. Terlouw and J.L. Holmes,*Org. Mass Spectrom.*, **23**, 503 (1988).

88 N. Heinrich, J. Schmidt, H. Schwarz and Y. Apeloig, *J. Am. Chem. Soc.*, **109**, 1317 (1987).

89 a) M. George, C.A. Kingsmill, D. Suh, J.K. Terlouw and J.L. Holmes, *J. Am. Chem. Soc.*, **116**, 7807 (1994); b) D. Suh, C.A. Kingsmill, P.J.A. Ruttink, P.C. Burgers and J.K. Terlouw, *Int. J. Mass Spectrom. Ion Processes*, in press (1995); c) D. Suh, P.C. Burgers and J.K. Terlouw, *Int. J. Mass Spectrom. Ion Processes*, **144**, L1 (1995); d) D. Suh, P.C. Burgers and J.K. Terlouw, *Rapid Commun. Mass Spectrom.*, **9**, 862 (1995).

CHAPTER 2

Hydrogen-Bridged Ions, $[CH_3C{=}O\cdots H\cdots O{=}CH_2]^{\bullet+}$, $[CH_2{=}C(H)O\cdots H\cdots O{=}CH_2]^{\bullet+}$, and $[CH_3C(H)O\cdots H\cdots O{=}CH]^{\bullet+}$ and Ion-Dipole Complex $[CH_3C(=O)^{+}\cdots O(H)CH_2^{\bullet}]$: Their Role in the Dissociation Chemistry of Ionized Acetol, $CH_3C(=O)CH_2OH^{\bullet+}$

Introduction

Structural isomerization in gas-phase ions has received steadily increasing attention during the past 15 years. By using the combined information from mass spectrometric techniques and *ab initio* molecular orbital theory calculations [1], the gas-phase chemistry of a number of stable ions of unexpected structure has been unraveled. These include ylide, distonic, and hydrogen-bridged radical cations such as $CH_2OH_2^{\bullet+}$, $CH_2CH_2OH_2^{\bullet+}$ and $[CH_2{=}CHO\cdots H\cdots OH_2]^{\bullet+}$, respectively. The latter ions appear to be remarkably stable, but in contrast to their more familiar even-electron

The work presented here has been published under the above title:

M. George , Carol A.Kingsmill, Dennis Suh, Johan K. Terlouw and John L. Holmes, *J. Am. Chem. Soc.*, **116**, 7807 (1994).

counterparts (e.g. proton bound dimers [1d] such as $[CH_3CH{=}O{\cdots}H{\cdots}OH_2]^+$), their generation and identification is less straightforward [1b]. One system that has been carefully explored by experiment and by theory involves the potential energy surface for the isomeric $C_3H_6O_2^{\bullet+}$ ions related to ionized methyl acetate [1a,b]. Interest in this system was sparked by the observation that a majority of low-energy molecular ions of methyl acetate lost $^{\bullet}CH_2OH$ rather than $CH_3O^{\bullet}$ in the formation of the acetyl cation, CH_3CO^+. The key experiment was the collision-induced dissociative ionization of the free-radical products from metastable methyl acetate molecular ions [2].

Heinrich et al., in an ab initio computational study [3], provided an elegant explanation which involved *inter alia* the reaction sequence :

$CH_3C(=O)OCH_3^{\bullet+}$ **1** $\rightarrow CH_3C^+(OH)OCH_2^{\bullet}$ **2** $\rightarrow [CH_3C{=}O{\cdots}H{\cdots}O{=}CH_2]^{\bullet+}$ **3a** $\rightarrow CH_3C{\equiv}O^+ + {}^{\bullet}CH_2OH$

It should be noted, however, that the key intermediate **3a**, an -O···H···O- hydrogen-bridged radical cation [1,4], although of similar stability to the molecular ion, was found to be generated at an energy which results in its spontaneous dissociation. This is because the isomerization barrier for **2→3a** lies above the summed product enthalpies. Thus ion **3**, derived from ionized methyl acetate, represents a transient species, i.e., is probably experimentally inaccessible via this system because it may survive for no more than a few vibrations. Analysis by Rice-Rampsperger-Kassel-Marcus (RRKM) theory [5] of the time dependence of the loss of $^{\bullet}CH_2OH$ from metastable **1** seems to indicate that indeed only the distonic ion **2** may be involved as an observable intermediate. Nevertheless, there must be at least a transition state that is fairly distinct from **2**, presumably resembling **3a**, in its geometry.

The hydrogen-bridged ion **3a** conceivably can be generated from ionized acetol (1-hydroxy-propan-2-one), **4**, *viz.*

$$CH_3C(=O)CH_2OH^{\bullet+}\ \mathbf{4} \rightarrow [CH_3C{=}O{\cdots}H{\cdots}O{=}CH_2]^{\bullet+}\ \mathbf{3a}$$

via a mechanism similar to that which is proposed to initiate the loss of $HCO^{\bullet}$ from ionized ethylene glycol [6]. The above reaction was considered some years ago [2] but no supporting experimental evidence could be provided. However, recently, Kenttämaa and co-workers [7a,b] have described an ion-molecule study of the reactivity of ionized acetol, **4**, using the technique of FT-ICR [7c]. It was proposed that long lived **4** ions have partially isomerized to **3a** and that some of the latter rearrange to $[CH_3C(H){=}O{\cdots}H{\cdots}O{=}CH]^{\bullet+}$, **5a**, a second -O···H···O- bridged species.

$$CH_3C(=O)CH_2OH^{\bullet+}\ \mathbf{4} \rightarrow [CH_3C{=}O{\cdots}H{\cdots}O{=}CH_2]^{\bullet+}\ \mathbf{3a} \rightarrow [CH_3C(H){=}O{\cdots}H{\cdots}O{=}CH]^{\bullet+}\ \mathbf{5a}$$

This reaction sequence has been entertained involving ion **5a** to rationalize the experimental observation that *metastable* ions **4** predominantly produce CH_3CHOH^+ ions by loss of $HCO^{\bullet}$ (>95%) in a reaction characterized by a very small kinetic energy release, $T_{0.5}$ = 3 meV [2], 2.0 meV (this work). However, on the basis of energy measurements described hereunder, this attractive scheme requires that isomerization barriers lie less than 10 kcal mol^{-1} above ΔH_f^o (**4**). *Ab initio* calculations have shown that the barrier heights involved in the chemistry of O···H···O bridged ions are often considerably higher [8] and indeed a preliminary *ab initio* calculation for the transition state **4** → **3a** was not encouraging. This work describes multiple collision experiments on deuterium labelled acetol ions, energy measurements and *ab initio* computational

results. It will be shown that the simple sequence **4** → **3a** → **5a** → $CH_3CHOH^+ + HC{=}O^\bullet$ is at odds with the deuterium labelling experiments. Similarly, the independently generated and characterised O•••H•••O bridged isomer $[CH_2{=}CHO{\cdots}H{\cdots}O{=}CH_2]^{\bullet+}$, **6**, is not involved in the dissociation chemistry of **4**. A pathway to CH_3CHOH^+ which satisfies all of the experimental observations and which is supported by *ab initio* calculations involves dissociation via a series of ion-dipole complexes, as will be described below.

Results and Discussion

Ionized acetol has two dissociation reactions of low energy requirement, as shown in Scheme 2.1:

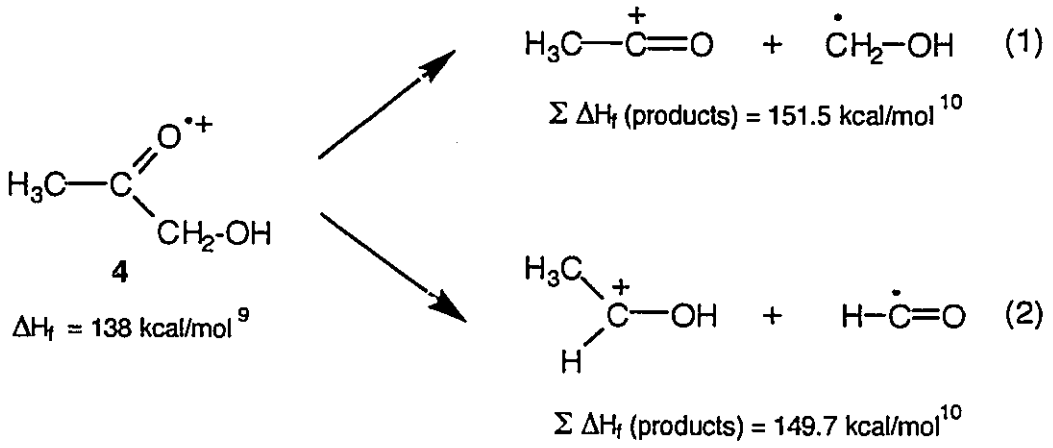

Scheme 2.1

Both reactions take place close to their thermochemical thresholds [9]. Reaction (1) may represent a simple bond cleavage and, not surprisingly, this process dominates the normal mass spectrum. The collision induced dissociation (CID) mass spectrum of

the stable (long lived, i.e., lifetimes > 10^{-5} s) mass selected acetol ions was also dominated by this process (minor peaks at m/z 29, 31, and 42 were also present, 4, 7 and 6 % of m/z 43, respectively), thus showing that these ions have either retained their structure or rearranged into species from which the same fragments readily can be generated, e.g. the hydrogen-bridged ion $[CH_3C{=}O{\cdots}H{\cdots}O{=}CH_2]^{\bullet+}$, **3a**. The optimized geometries of $(acetol)^{\bullet+}$ isomers and some transition states are shown in Figure 2.1.

The neutralization-reionization (NR) mass spectrum of long lived acetol ions, see Figure 2.2a, is again dominated by m/z 43, in keeping with the above [11]. The recovered molecular ion is very weak, only *ca.* 1% of the base peak, m/z 43. Note that the energy requirement for methyl acetate ions to yield $CH_3CO^+ + {}^{\bullet}CH_2OH$ is closely similar to that for acetol ions (14 vs 13 kcal /mol respectively), but the former exhibits a much more intense recovery ion (8 %) relative to the same base peak, m/z 43. The much lower acetol ion recovery signal can be reconciled with facile rearrangement into an ion such as **3a** (see above) which upon neutralization should wholly dissociate to $CH_3CO^{\bullet} + {}^{\bullet}CH_2OH$ and/or a significant distortion of the molecule, post-ionization.

Thus, whereas the CID and NR mass spectra provide no clear evidence for the presence of rearranged species, the metastable ion (MI) mass spectrum is dominated by reaction (2), (see Introduction), a process requiring rearrangement of the acetol ion. Reaction (1) contributes the remaining 5% of the MI mass spectrum [12]. The effect on the MI mass spectrum of slowly admitting collision gas is to cause a major increase in m/z 43, while m/z 45 is essentially unaffected, showing that the ion which leads to the $C_2H_5O^+$ product is present only in very low abundance among stable acetol ions. The MI and CID mass spectra of ionized CH_3COCH_2OD displayed no unexpected features: m/z 43 remained base peak in the normal and CID mass spectra, and m/z 45 in the MI

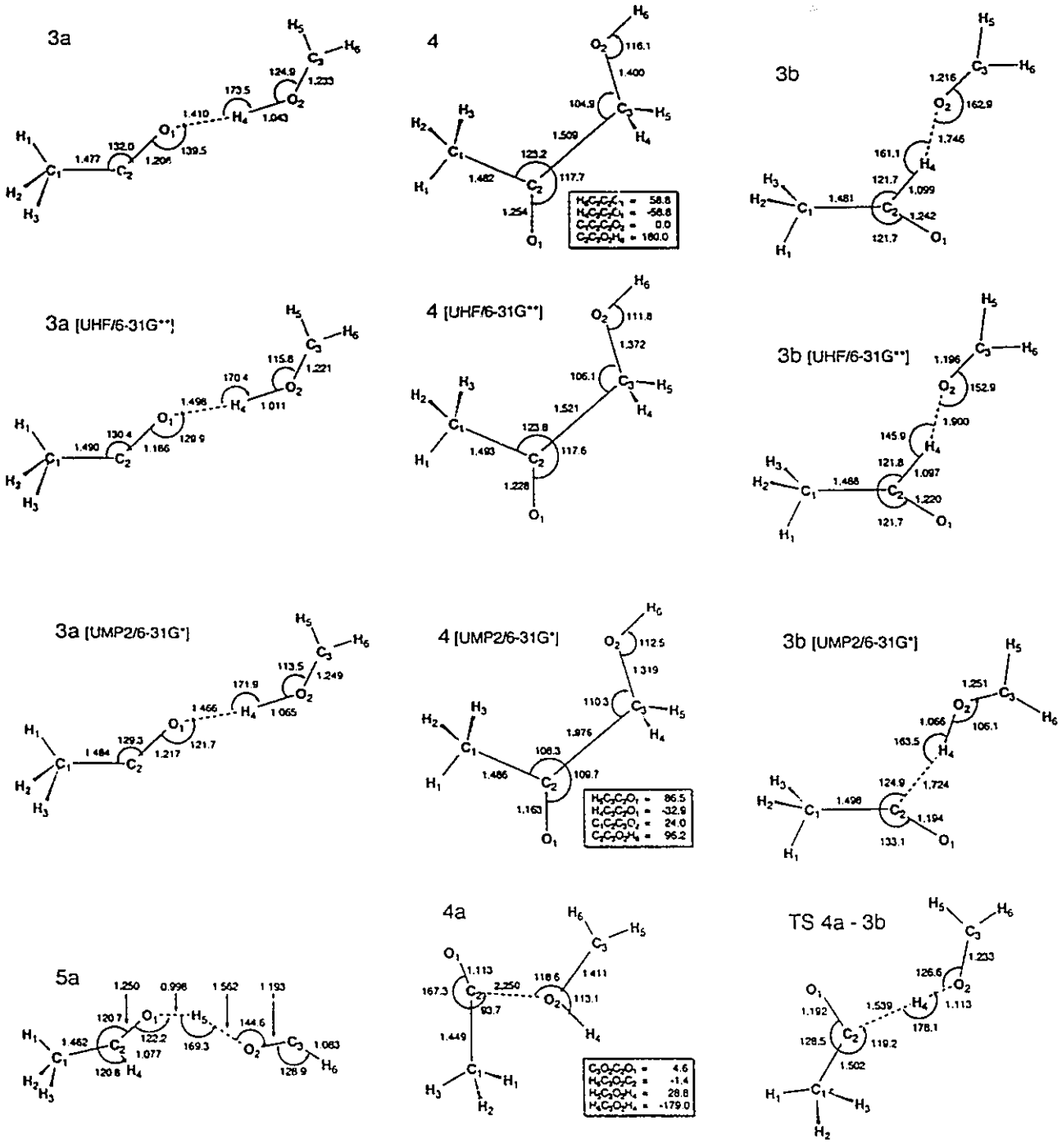

Figure 2.1. Optimized geometries of (acetol)$^{\bullet+}$ isomers and some transition states. Bond lengths in anstroms, bond angles in degrees.

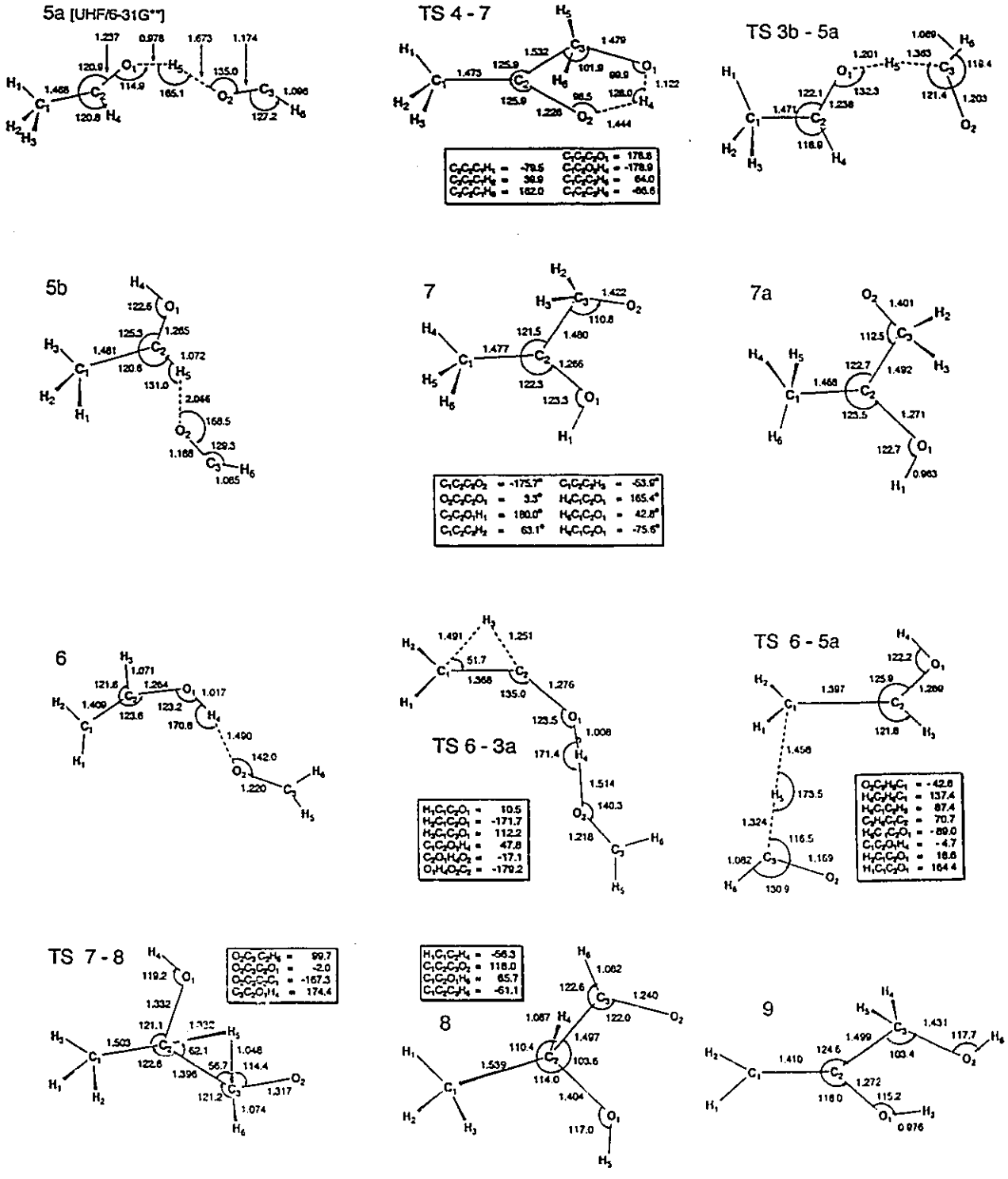

Figure 2.1. Continued.

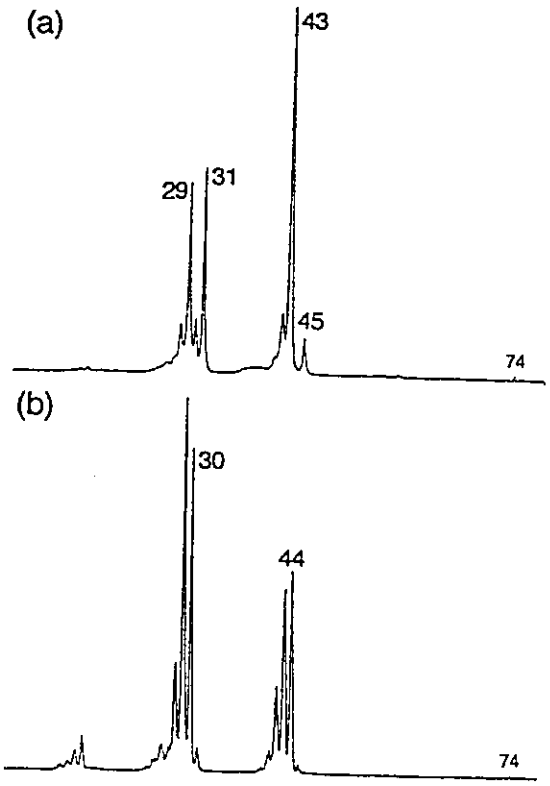

Figure 2.2. NR mass spectra of (a) $CH_3C(=O)CH_2OH^{\bullet+}$ (**4**) and (b) $[CH_2=CH\text{-}O\cdots H\cdots O=CH_2]^{\bullet+}$ (**6**).

mass spectrum was cleanly shifted to m/z 46 and m/z 31 to m/z 32. The absence of H/D mixing prior to the principal dissociation to $[CH_3CO]^+$ rules out involvement with any long-lived ion structures associated with the ionized methyl acetate hypersurface, where H/D loss of positional identity approaches the statistical limit among metastable ions [1a].

In the recent FT-ICR study [7a], the reactivity of stable acetol ions was explained by the introduction of ions **3a** and **5a**. As shown in Table 2.1, which summarizes *ab initio* calculations performed in this work, both ions are stable species, having ΔH_f^o values well below the acetol ion's dissociation limit. Note that the calculated relative

energies agree well with estimates based on the empirical relationship [13] for the stabilization energy of -O•••H•••O- proton-bound dimers. In the absence of further evidence, the experimental results can be rationalized by the sequence **4** → **3a** → **5a** but with either the first or second step taking place at an energy close to the dissociation limit. This mechanism, however, can be tested because it predicts the position of deuterium atoms in the products from labelled precursor molecules, *viz.* :

$CH_3C(=O)CD_2OH^{\bullet+}$ **4**-d_2 → $[CH_3CO\cdots H\cdots O=CD_2]^{\bullet+}$ **3a**-d_2 → $[CH_3C(D)O\cdots H\cdots O=CD]^{\bullet+}$ **5a**-d_2 → CH_3CDOH^+ + $DCO^{\bullet}$

and

$CH_3C(=O)CH_2OD^{\bullet+}$ **4**-d_1 → $[CH_3CO\cdots D\cdots O=CH_2]^{\bullet+}$ **3a**-d_1 → $[CH_3C(H)O\cdots D\cdots O=CH]^{\bullet+}$ **5a**-d_1 → CH_3CHOD^+ + $HCO^{\bullet}$

First , the origins of the H atoms in the product ions need to be established. Figure 2.3 shows the CID mass spectra of $[C_2H_{5-x}D_xO]^+$ (x = 1,2) ions, all generated from *metastable* precursor ions [14], namely acetol and ethanol molecular ions and those of isotopomers, and therefore having comparable internal energies as well as common structures.

Fig. 2.3a shows the CID mass spectrum of metastably generated m/z 45 ions from acetol; it is identical with that of the m/z 45 ions of structure CH_3CHOH^+ [15] generated from metastable ethanol ions. Fig. 2.3b shows the CID mass spectrum of m/z 46 ions from metastable $[CH_3CD_2OH]^{\bullet+}$, which have the structure $[CH_3CDOH]^+$. This CID mass spectrum is indistinguishable from that of the m/z 46 ions produced from metastable $CH_3C(=O)CH_2OD^{\bullet+}$, **4**-$d_1$. Instead of a process involving keto-enol isomerism, the label has become attached to the carbonyl carbon in the rearrangement of the acetol

Table 2.1 Total energies (Hartrees), zero-point vibrational energies (ZPVE) and relative calculated energies (E_{rel}, kcal/mol[a]) for some isomers and components of the (Acetol)$^{\bullet+}$ system.

STRUCTURE		STATE	UHF/4-31G	6-31G*/4-31G	UMP3/6-31G*// 4-31G	ZPVE	E[rel]
$CH_3C{=}O{\cdot\cdot}H{\cdot\cdot}O{=}CH_2$ $^{\bullet+}$	**3 a**	$^2A'$	-266.10292	-266.49315	-267.21675	51.0	-2.1
$CH_3C(=O){\cdot\cdot}H{\cdot\cdot}O{=}CH_2$ $^{\bullet+}$	**3 b**	$^2A'$	-266.09339	-266.48654	-267.19770	50.3	9.2
$CH_3C(=O)CH_2OH$ $^{\bullet+}$	**4**	$^2A'$	-266.10893	-266.49933	-267.21651	52.9	0
$CH_3C(=O)^+{\cdots}O(H)CH_2^{\bullet}$	**4 a**	^2A	-266.09767	-266.48932	-267.21546	50.8	-1.4
	4 b	^2A	-266.09625	-266.48086	-267.21178	51.3	1.7
$CH_3CH{-}O{\cdot\cdot}H{\cdot\cdot}O{=}CH$ $^{\bullet+}$	**5 a**	$^2A'$	-266.10714	-266.50044	-267.22438	50.8	-7.0
$CH_3C(OH){\cdots}H{\cdots}O{=}CH^{\bullet+}$	**5 b**	$^2A'$	-266.09015	-266.48767	-267.21063	50.5	1.3
$CH_2{=}CH{-}O{\cdot\cdot}H{\cdot\cdot}O{=}CH_2$ $^{\bullet+}$	**6**	$^2A''$	-266.12004	-266.50855	-267.23063	51.6	-10.0
$CH_3C^+(OH)CH_2O^{\bullet}$	**7**	^2A	-266.10185	-266.48968	-267.20330	53.7	9.1
	7 a	$^2A'$	-266.11680	-266.50243	-267.21633	52.9	0.5
$CH_3CH(OH)C(H){=}O^{\bullet+}$	**8**	^2A	-266.08602	-266..47858	-267.19666	53.0	12.5
$CH_2{=}C(OH)CH_2OH^{\bullet+}$	**9**	$^2A''$	-266.13215	-266.51786	-267.24622	54.1	-17
TS **4-7**		^2A	-266.07432	-266.46737	-267.19678	50.7	10.2
TS **4a→4b**		^2A	-266.09623	-266.48127	-267.21152	51.1	1.3
TS **4a→3b**		$^2A'$	-266.07050	-266.46776	-267.20331	48.3	3.7
TS **3b→5b**		$^2A'$	-266.07336	-266.46612	-267.19534	47.5	7.9
TS **6-5a**		^2A	-266.03754	-266.43893	-267.18328	48.9	16.8
TS **6-3a**		^2A	-266.01163	-266.40949	-267.13996	48.2	43.3
TS **7-8**		^2A	-266.04875	-266.44946	-267.17204	51.2	26.3

STRUCTURE		STATE	UHF/6-31G**	UMP3/6-31G**//UHF/6-31G**	ZPVE	E[rel]
$CH_3C{=}O{\cdot\cdot}H{\cdot\cdot}O{=}CH_2$ $^{\bullet+}$	**3 a**	$^2A'$	-266.51413	-267.27241	51.5	-2.6
$CH_3C(=O){\cdot\cdot}H{\cdot\cdot}O{=}CH_2$ $^{\bullet+}$	**3 b**	$^2A'$	-266.49990	-267.24714	50.0	11.8
$CH_3C(=O)CH_2OH$ $^{\bullet+}$	**4**	$^2A'$	-266.51727	-267.27055	52.8	0
$CH_3CH{-}O{\cdot\cdot}H{\cdot\cdot}O{=}CH$ $^{\bullet+}$	**5 a**	$^2A'$	-266.52056	-267.27844	50.9	-6.9

STRUCTURE		STATE	UMP2/6-31G*	UMP3/6-31G*//UMP2/6-31G*	ZPVE	E[rel]
$CH_3C{=}O{\cdot\cdot}H{\cdot\cdot}O{=}CH_2$ $^{\bullet+}$	**3 a**	^2A	-267.20105	-267.22100	52.0	3.1
$CH_3C(=O){\cdot\cdot}H{\cdot\cdot}O{=}CH_2$ $^{\bullet+}$	**3 b**	^2A	-267.19411	-267.21151	52.5	9.6
$CH_3C(=O)CH_2OH$ $^{\bullet+}$	**4**	^2A	-267.21226	-267.23024	54.7	0

[a] The relative calculated energies include scaled zero-point vibrational contributions, 0.9 for UHF and 0.96 for UMP2.

molecular ion. This is confirmed by the observations in Fig. 2.3c, which illustrates the CID mass spectrum of the m/z 46 ions from metastable $CH_3C(=O)CD_2OH^{\bullet+}$, **4**-$d_2$. This spectrum is indistinguishable from that of the m/z 46 ions produced from metastable $[CH_3CH_2OD]^{\bullet+}$. Note the enhanced abundance of m/z 20 relative to m/z 19 and the

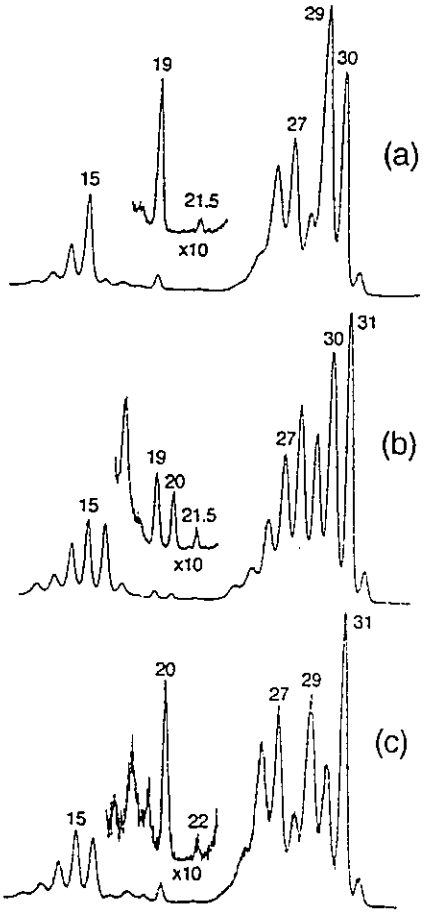

Figure 2.3. Partial CID mass spectra of product ions from dissociation reactions of metastable ions : (a) $C_2H_5O^+$ from $CH_3C(=O)CH_2OH^{\bullet+}$ (**4**) → $C_2H_5O^+ + HCO^{\bullet}$; (b) $C_2H_4DO^+$ from $CH_3CD_2OH^{\bullet+}$ → $CH_3CDOH^+ + D^{\bullet}$ and (c) $C_2H_4DO^+$ from $CH_3C(=O)CD_2OH^{\bullet+}$ (**4**-d_2) → $C_2H_4DO^+ + DCO^{\bullet}$.

doubly charged C_2H_3O ion shifting from m/z 21.5 to m/z 22. Thus the loss of HCO• *cannot* involve the reaction sequence **4→3a→5a**. The experimental observations do not necessarily rule out the generation of O···H···O bridged ions **3a.** However if they are present, they do not, as proposed in the FT-ICR study [7a,b], further isomerize into **5a** prior to the loss of HCO•.

The *ab initio* calculations indicate that it is the isomerization step **4→3a** which is not feasible. At the Hartree-Fock level of theory, all attempts to locate this TS led to the transfer of the hydroxylic H to the carbonyl group (without a concomitant $C(=O)--C(H_2)$ bond cleavage), yielding the stable distonic ion **7** (see also Table 2.1) :

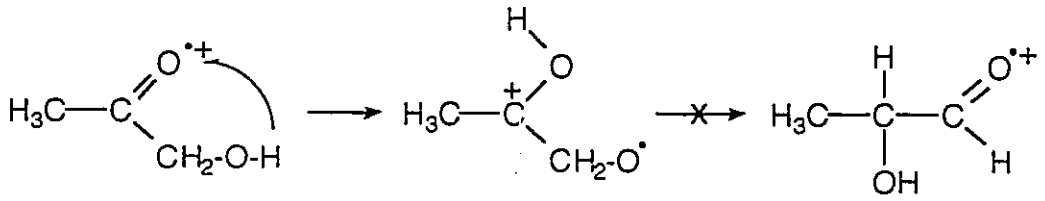

4 **7** **8**

ΔH_f = 138 kcal/mol [9]

Ion **7** has a calculated ΔH_f^0 value some 9 kcal/mol above that of ionized acetol and is separated from it by only a small barrier. Its formation from **4** represents a "cul-de-sac" isomerization [16], since **7** cannot dissociate to products of low combined enthalpy either directly or via further rearrangement, the barrier to ionized lactaldehyde, **8**, being too high. It seems likely that this ion, **7**, or its more stable conformer, **7a** (which, however, cannot be directly generated from **4**), is the species recently shown to react by acetyl replacement in the FT-ICR ion-molecule reaction study of ionized acetol [7a].

While searching for other $[C_3H_6O_2]^{\bullet+}$ ions produced in the fragmentation of larger species, which could possibly shed some more light on the behaviour of ionized

acetol, it was observed that 1-bromo-2,3-dihydroxypropane ($BrCH_2CHOHCH_2OH$, **I**) generated a significant m/z 74 ion in its normal mass spectrum by the loss of HBr (m/z 74, 50 % of base peak, m/z 44 $[C_2H_4O]^{\bullet+}$). The MI mass spectrum of this $C_3H_6O_2^{\bullet+}$ ion contained an intense peak at m/z 45, $[C_2H_5O^+]$ ($T_{0.5}$ = 13 meV), and a weak, narrow m/z 44 peak ($T_{0.5}$ = 1.6 meV). In the corresponding CID mass spectrum, m/z 44 had become the base peak, with little change in the intensity of m/z 45 (now 45%). The CID mass spectrum of the m/z 45 ions generated from the *metastable* m/z 74 species was very closely similar to that for metastably produced $[CH_3CHOH^+]$, whereas that of the (CID generated) m/z 44 ions is compatible with the $C_2H_4O^{\bullet+}$ isomer ionized vinyl alcohol [17], $[CH_2=CHOH]^{\bullet+}$.The NR mass spectrum is shown in Fig 2.2b. It displays only a trace recovery peak at m/z 74 and the spectrum could result largely from collisional ionization of neutral $CH_2=CHOH$ and $CH_2=O$ molecules formed upon dissociative neutralization of the parent ion.

The ion $[BrCH_2CHODCH_2OD]^{\bullet+}$ exclusively lost DBr in its normal mass spectrum, and in the m/z 46 ions derived from metastable $C_3H_5DO_2^{\bullet+}$, the deuterium was exclusively on oxygen, $[CH_3CHOD^+]$. Similarly, m/z 44 $[CH_2=CHOH]^{\bullet+}$ was cleanly displaced to m/z 45. In the NR spectrum, m/z 44 was also cleanly displaced to m/z 45, whereas the other peaks are not shifted.

Clearly this m/z 74 ion is not ionized acetol, nor does it have anything in common with the dissociation of ionized methylacetate. On the basis of the above characteristics, the following structures were considered for the product ions :

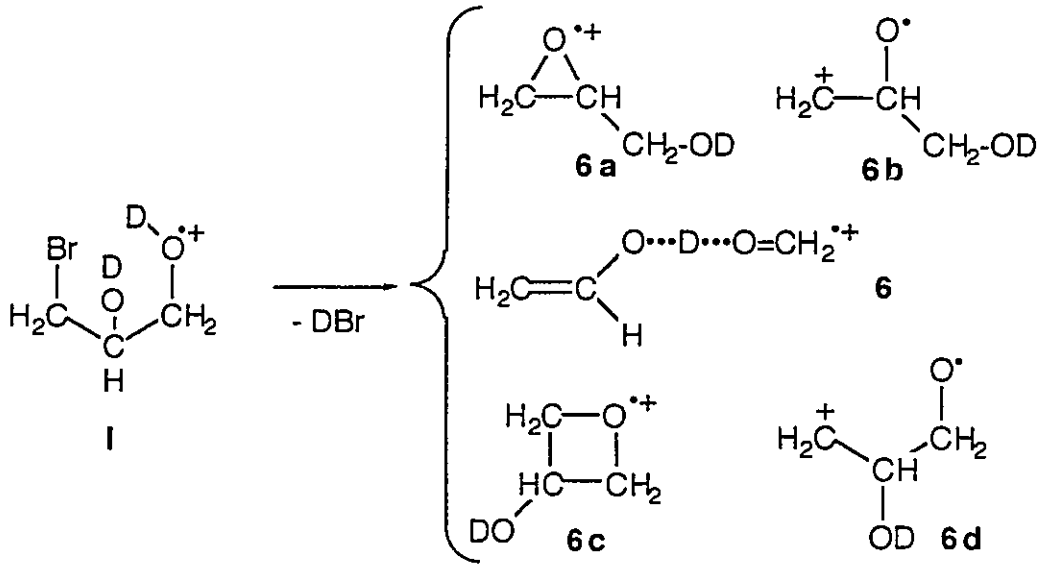

A simple 1,3 elimination from **I** would produce either ionized glycidol **6a** or its C-O ring-opened form **6b**, whereas the 1,4 elimination would yield 2-hydroxyoxetane ions **6c** or ions **6d**. The experimental ΔH^{o}_{f} of the $C_3H_6O_2^{\bullet+}$ product ion from **I** was measured to be ≤ 144 kcal/mol, an upper limiting value [18]. However, the heats of formation of the cyclic product ions **6a** and **6c** are much higher (176 and 164 kcal/mol, respectively [19]), and this precludes their generation from **I**. The same holds for the C-O ring-opened forms **6b** and **6d**, whose ΔH_f values are expected to be even higher than those of their cyclic counterparts [19]. Moreover, metastable glycidol molecular ions, **6a**, show an abundant loss of H_2O in the MI spectrum, a reaction which is absent in the $C_3H_6O_2^{\bullet+}$ ion formed by HBr loss from **I**.

A route for the HBr loss from **I** that may satisfy the product ion enthalpy constraint involves either a 1,3 or a 1,4 elimination with a concomitant C-C cleavage, leading to the -O•••H•••O- hydrogen bridged ion $[CH_2{=}CHO{\cdots}H{\cdots}O{=}CH_2]^{\bullet+}$, **6.** From the calculations (see Table 2.1 and 2.2), ΔH^{o}_{f} (**6**) = 128 kcal/mol was derived which is in excellent agreement with the estimated value. This species, whose optimized geometry (see

Fig. 2.1) is closely similar to that of the extensively studied [8] analogue $[CH_2{=}CHO{\cdots}H{\cdots}OH_2]^{\bullet+}$, may readily yield $CH_2{=}CHOH^{\bullet+}$ following collisional excitation, decompose completely upon neutralization into $CH_2{=}CHOH$ and $CH_2{=}O$, and rearrange to yield the thermochemically less demanding product $[CH_3CHOH^+]$. The calculations further show that this ion, **6** (Table 2.1), has the required properties to satisfy the experimental observations, namely no significant energy barriers to the fragmentation products and a high barrier separating it from ion **3a** $[CH_3C{=}O{\cdots}H{\cdots}O{=}CH_2]^{\bullet+}$, a key player on the methyl acetate ion's hypersurface. The very small kinetic energy release accompanying the production of $[CH_2{=}CHOH]^{\bullet+}$ is also in keeping with it having the characteristics of a (vinyl alcohol) ion / (formaldehyde) molecule complex at the dissociation threshold, analogous to the previously studied vinyl alcohol/ water system [8].

So far several a priori attractive mechanistic possibilities for the loss of $HCO^{\bullet}$ from metastable acetol ions **4** have been able to rule out. It has also become clear that a viable mechanism must satisfy the fate of the D label in the CH_3CHOH^+ product ion. Note that the labelling results also rule out participation of the very stable enol ion $CH_2{=}C(OH)CH_2OH^{\bullet+}$, **9** (see Table 2.2). In addition, the CID mass spectra indicated that the majority of the molecular ions retained an acetyl group, and the insensitivity of m/z 45 to collision gas indicated that the barrier to rearrangement is not far from the dissociation energy to CH_3CO^+.

Next it is considered that $HC{=}O^{\bullet}$ loss from **4** involves the -C···H···O- bridged species $[CH_3C(=O){\cdots}H{\cdots}O{=}CH_2]^{\bullet+}$, **3b**, rather than its -O···H···O- bridged isomer, **3a**. The computations show that **3b** is a minimum on the potential energy surface (PES), lying in a (shallow) well, close to the dissociation limits of **4**. Comparison of the geometries (Fig. 2.1) and energies (Table 2.1) of the two species shows that **3a** differs from **3b** in

that the -C···H···O- bridged ion is less stabilized and that (at the HF level of theory) the bridging hydrogen remains close to the C atom. Thus, whereas **3a** has a strong (and rigid) [8] hydrogen bridge, **3b** is a much more looseiy bound species akin to the ion-dipole complex $CH_3C(H)=O^{\bullet+}/CH_2=O$. Such species are being increasingly considered as intermediates, and *ab initio* calculations indicate that at low internal energies, ionized acetic acid [1b], acetamide [1b], acetone [1b], formic acid [23] and also ethylene glycol [6f] all fragment via such complexes.

A 1,5-H shift in **3b** would produce the -C···H···O- bridged species, **5b**, which by direct bond cleavage will dissociate to the observed products. Such a route accounts for the hydroxyl hydrogen being bound to carbon (not oxygen) in the CH_3CHOH^+ fragment ion :

$CH_3C(=O)CD_2OH^{\bullet+}$ **4**-d_2 → $[CH_3C(=O)\cdots H\cdots O=CD_2]^{\bullet+}$ **3b**-d_2 → $[CH_3C(OD)\cdots H\cdots O=CD]^{\bullet+}$ **5b**-d_2 → CH_3CHOD^+ + $DCO^{\bullet}$

Ion **3b** may not be directly generated from ionized acetol via a 1,3-H shift and a concomitant C-C cleavage: the calculations indicate that the associated four membered ring TS (which has a high $\langle s^2 \rangle$ value) lies well above the dissociation limit for loss of $HCO^{\bullet}$. An energetically feasible route for the formation of ion **3b** involves the participation of ion **4a**, see Figure 2.1. This ion is a strong (acetyl) ion – (CH_2OH) dipole complex [24] formed by stretching the $C(=O)-C(H_2)$ bond in ionized acetol, and rotating the CH_2OH moiety. Elongation of this bond does not immediately lead to dissociation, but it allows the CH_2OH moiety to migrate within the electrostatic field of

Table 2.2 Estimated and Experimental Heats of Formation (kcal/mol) and Relative energies (kcal/mol) for isomers and components of the (acetol) $^{\bullet+}$ system.

STRUCTURE		ΔH_f Experimental	ΔH_f Estimated		E rel(Exp/Est.)	Erel (theory)[a]
$CH_3C(=O)CH_2OH^{\bullet+}$	**4**	138[b]			0	0
$CH_3C=O\cdot\cdot H\cdot\cdot O=CH_2^{\bullet+}$	**3a**	-	138	(c,d)	0	-2
$CH_3CH\text{-}O\cdot\cdot H\cdot\cdot O=CH^{\bullet+}$	**5a**	-	131	(c)	-7	-7
$CH_2=CH\text{-}O\cdot\cdot H\cdot\cdot O=CH_2^{\bullet+}$	**6**	<144	128	(c)	-10	-10
$CH_3CH(OH)C(H)=O^{\bullet+}$	**8**	-	148	(e)	10	12.5
$CH_2=C(OH)CH_2OH^{\bullet+}$	**9**	-	122	(f)	-16	-17
$CH_3CHOH^+ + HCO^{\bullet}$		151[g]			13	10
$CH_3CO^+ + CH_2OH^{\bullet}$		150[g]			12	14
$CH_2=CHOH^{\bullet+} + CH_2=O$		155[g]			17	15

a) see Table 1, the complete set of data for the dissociation products is available upon request; b) this work; c) estimate based on the empirical relationship for -O•H•O- proton bound dimers : SE (kcal/mol) = 30.4 - 0.30 ΔPA (ref. 13) ; SE = stabilization energy relative to the dissociation products of lowest combined enthalpy, PA = proton affinity; appropriate values from ref. 10b; d) from ΔH_f ($CH_3COOCH_3^{\bullet+}$) , **1**, is 139 kcal/mol (10b) and the calculated energy of ion **3a** relative to **1** as reported in ref. 3, one obtains ΔH_f **3a** = 139 kcal/mol ; at the UMP3/6-31G*// UMP2/6-31G* level of theory (Table 2.1) **4** is 3.1 kcal/mol more stable than **3a**. e) ΔH_f of the neutral molecule is -84.7 kcal/mol, by additivity [10a, and using - 7.5 kcal/mol for C-(H)(C)(O)(CO); IE is 0.3-0.4 eV above that of acetol (9.74 eV, this work), cf. IE's of small aldehydes vs analogue ketones in ref. 10b; f) from ΔH_f ($CH_2=C(OH)CH_3^{\bullet+}$)= 158 kcal/mol [10b] and the effect of OH substitution at a non-charge bearing group(ref. 21), - 36 kcal/mol, given by $\Delta(\Delta H_f)$ propane and *n*-propanol (ref. 10b); g) from ref 10b.

the acetyl cation, analogous to loss of OH$^{\bullet}$ from ionized acetic acid [25]. TS **4**→ **4a** has not been defined, but from calculations involving a stepwise elongation of the C(=O)–C(H_2) bond and concomitant rotation, it appears that this process requires very little energy (~1-2 kcal/mol). That the C(=O)–C(H_2) bond in **4** is easily stretched is

further indicated by a geometry optimization at the UMP2/6-31G* level of theory : starting from the optimized 4-31 G geometry of its lowest energy conformer (see Fig. 2.1), it is arrived at a structure in which the bond length has increased from 1.51 to 1.97 Å. The same calculations were performed on the O···H···O bridged ion **3a**, but here the inclusion of electron correlation does not greatly change the geometry.

Since **4a** is an ion-dipole complex, the CH_2OH moiety can rotate with respect to the acetyl cation [21] and donate the hydroxyl hydrogen to the carbonyl C, via TS **4a** → **3b.** Note, see Table 2.1, that when electron correlation and ZPVE corrections are included, TS **4a** → **3b** becomes lower in energy than **3b**. Calculations involving electron correlated geometry optimizations (see above) may solve this problem and provide a more refined description of the proposed isomerization steps. Indeed, although the relative energy has not appreciably changed (see Table 2.1), the MP2 optimized geometry of ion **3b** is more akin to that of TS **4a** → **3b** than the HF optimized structures for **3b** (see Figure 2.1). However, it is not expect that such post-HF computations, which become prohibitively expensive for this system of relatively large ions, will change the overall picture.

Ion **3b** lies close to the thermochemical threshold for formation of CH_3CHOH^+ + H-C=O$^\bullet$ (see Tables 2.1 and 2.2), but well below the dissociation limit for direct bond cleavage into $CH_3C(H)=O^{\bullet+}$ + $CH_2=O$, by 32 kcal/mol [10b]. The ion can be viewed as an (acetaldehyde) ion-(formaldehyde) dipole complex, and rotation of the dipole, the $CH_2=O$ moiety, with respect to the ion, $CH_3C(=O)H^{\bullet+}$, is expected to require little energy [1b]. If the C···H···O bond would remain intact during this rotation, a 1,5-H shift would give ion **5b**, a stable minimum on the PES (see Table 2.1) which may serve as a precursor for direct bond cleavage to CH_3CHOH^+ + HC=O$^\bullet$. However, in the search for the TS describing this transformation, it is located a TS, TS **3b** → **5b**, which indicates

that the CH•••O bond breaks upon rotation and H transfer. TS **3b** → **5b** lies below the dissociation limit, and the coordinate of its imaginary frequency does indeed correspond to H transfer from the CH_2=O group to the carbonyl O atom [26]. Note, see Figure 2.1, that this TS suggests the formation of an O•••H•••C bridged species, $[CH_3C(H)O•••H•••C(H)=O]^{\bullet+}$, **5c**, rather than the O•••H•••O bridged ion, $[CH_3C(H)O•••H•••O=CH]^{\bullet+}$, **5a**. However, ion **5c**, if it exists as a stable minimum at all, does not seem to be accessible from this TS: when the O-H bond is shortened and the H-C bond is simultaneously lengthened along the reaction coordinate, the species appears to oscillate over a flat energy surface close to the dissociation limit until, upon reorientation of the HC=O• dipole, the stable O•••H•••O bridged species **5a** is reached. Note that, analogous to the behavior of ion **3a** in the dissociation chemistry of methyl acetate, the very stable ion **5a** is generated at energies close to the dissociation limit for the loss of HCO•, and thus in the dissociation chemistry of acetol it represents a transient intermediate only.

In summary, the mechanistic picture that emerges from these computations and which satisfies all of the experimental observations involves two consecutive hydrogen transfers in ionized acetol akin to reactions of $CH_2OH^{\bullet}$ with the acetyl ion and of formaldehyde with ionized acetaldehyde (Scheme 2.2).

One final point remains to be addressed : can the recent proposal, based on an FT-ICR study that the -O•••H•••O- bridged isomer **3a** plays a role in the gas-phase ion chemistry of ionized acetol, be excluded? First, MS/MS/MS experiments on the D-labelled acetol isotopomers leave no doubt that metastable ions **4** do *not* dissociate via **3a**. Moreover, the calculations indicate (see above) that transfer of the hydroxylic H atom to the carbonyl group in covalently bound **4** yields the distonic ion

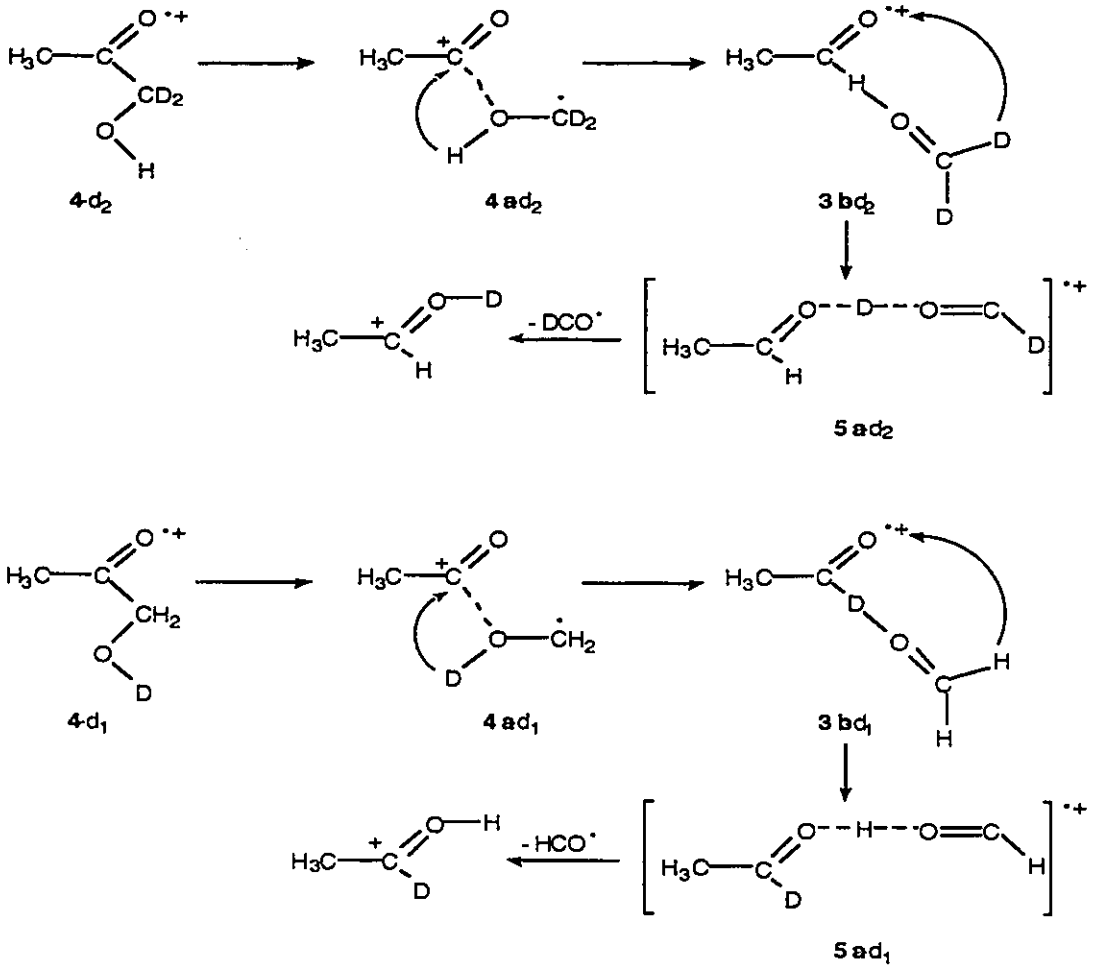

Scheme 2.2

7, not **3a**. On the other hand, the calculations also indicate that **4** can easily adopt the configuration of an ion-dipole complex, **4a**, and it could be argued that this species could serve as the precursor to **3a**. That this is problematic in view of the extensive computational study by Heinrich et al. [3] on the methyl acetate ion PES. In this study, a minimum structure was found akin to the ion **4a**, but with a considerably shorter ion-dipole distance (see structure 7 in Chart I of ref. 3). Such an ion, **4b**, was also found as a minimum in this study : it lies somewhat higher in energy than **4a**, and is connected to it via a low lying TS **4a**→ **4b**, thus indicating that upon ionization, acetol

can access a flat PES characterized by ion-dipole complexes. In the above study the isomerization sequence **4b** → $[CH_3C(OH)OCH_2]^{\bullet+}$, **2**, → **3a** was examined, but the calculated barrier was found to lie far above the experimentally established energy level for dissociation into CH_3-C=O$^+$ + $^\bullet CH_2OH$.

The work of Heinrich et al. [3] also provides a plausible rationalization as to why the acetyl ion and $^\bullet CH_2OH$ dipole components in **4a/b** would not easily interact to form the -O···H···O- bridged isomer **3a**. It was found that a continuous lengthening of the CH_3C=O···$HOCH_2$ bond in **3a** results in a charge distribution which leads to CH_3-C=O$^\bullet$ + $^+CH_2OH$ rather than the more stable products CH_3-C=O$^+$ + $^\bullet CH_2OH$. The dissociation leading to the correct products can occur from the excited state ($^2A''$) of **3a**. This state has the correct charge distribution and it is "symmetry correlated" with the products CH_3-C=O$^+$ / $^\bullet CH_2OH$, but it lies much higher in energy, roughly 20 kcal/mol above the electronic ground state $^2A'$. These findings indicate that the recombination of the CH_3-C=O$^+$ and $^\bullet CH_2OH$ components in **4a** to the -O···H···O- bridged isomer **3a** requires too much energy to compete with rearrangment to the -C···H···O- bridged species **3b** proposed in the mechanism. This intriguing point clearly warrents further investigation using higher levels of theory than those practical at the time of the study by Heinrich et al. It is also noted that in the ion-molecule chemistry of ionized acetol, an acetyl *radical* displacement reaction is proposed [7b] which would be in keeping with the presence of a structure having the charge distribution of ground-state ions **3a**. However, if a facile isomerization **4**→ **3a** does occur, it must be a cul-de-sac with regard to the low-energy dissociation of ionized acetol into CH_3CHOH^+ and $HCO^\bullet$.

References

(1) For selected reviews see : (a) Heinrich, N.; Schwarz, H., Ion and Cluster Ion Spectroscopy and Structure, Maier, J. P., Ed.; Elsevier: Amsterdam, 1989 ; p. 329. (b) Burgers, P.C.; Terlouw, J.K. , Specialist Periodical Reports : Mass Spectrometry; Rose, M.E., Ed.; The Royal Society of Chemistry : London, 1989; Vol. 10, Chapter 2. (c) Radom, L., *Org. Mass Spectrom.* **1991,** *26,* 359. (d) Uggerud, E. *Mass Spectrom. Rev.* **1992**, *11*, 389.

(2) Terlouw, J. K.; Holmes, J. L.; Burgers, P. C. *Int. J. Mass Spectrom. Ion Phys.* **1985,** *66*, 239.

(3) Heinrich, N.; Schmidt, J.; Schwarz, H.; Apeloig, Y.*J. Am. Chem. Soc.*, **1987**, *109*, 1317.

(4) Coitino E.L.; Lledos, A.; Serra R.; Bertran J.; Ventura, O.N. *J. Am. Chem. Soc.*, **1993**, *115*, 9121 and references cited therein.

(5) Arakawa, R. *Bull. Chem. Soc. Jpn.* **1988**, *61*, 3425.

(6) (a) Morton, T.H. *Tetrahedron* **1982**, *38*, 3195. (b) Burgers, P. C.; Holmes, J. L.; Hop, C.E.C.A. ; Postma, R.; Ruttink, P.J.A.; Terlouw, J. K. *J. Am. Chem. Soc.*, **1987**, *109*, 7315. (c) Yates, B.F.; Bouma, W.J.; MacLeod, J.K.; Radom, L. J. Chem. Soc. Chem. Commun. **1987**, 204. (d) Cao, J.R ; George, M.; Holmes, J. L.; Sirois, M ; Terlouw, J. K. ; Burgers, P. C. *J. Am. Chem. Soc.*, **1992**, *114,* 2017. (e) Audier, H.E.; Milliet, A.; Leblanc, D.; Morton, T.H. *J. Am. Chem. Soc.*, **1992**, *114,* 2020. (f) Burgers, P. C.; Ruttink, P.J.A. *Org. Mass Spectrom.* **1993**, *28,* 1087.

(7) (a) Pakarinen, A.; Stirk, K. M.; Vainiotalo, P.; Pakkanen, T. A.; Kenttämaa, H.I.; *Proceedings 41st of the ASMS Conference on Mass Spectrometry and Allied Topics,* San Francisco, **1993**, 1002. (b) For the full paper, which appeared after this work had been submitted, see: Pakarinen, A.; Stirk, K. M.; Vainiotalo, P.; Pakkanen, T. A.; Kenttämaa, H.I., *J. Am. Chem. Soc.*, **1993**, *115*, 12431. (c) Stirk, K.M.; Kiminkinen, L.K.M.; Kenttämaa, H.I. *Chem. Rev.* **1992**, *92*, 1655.

(8) Postma, R.; van Helden, S.P.; van Lenthe, J.H.; Ruttink, P.J.A.; Terlouw, J.K.; Holmes, J.L. *Org. Mass Spectrom.* **1988**, *23*, 503.

(9) The appearance energy (AE) for m/z 43 was measured using energy selected electrons to be 10.35 ± 0.05 eV; the same value within experimental error was obtained for the AE of the weak metastable peak at m/z 43 and that for m/z 45 was measured as 10.30 ± 0.1 eV. These results are in keeping with the fragment ions $[CH_3CO]^+$ and $[CH_3CHOH]^+$ being generated at their thermochemical thresholds (ΔH_f^o $[CH_3COCH_2OH]$ = - 86.5 kcal/mol (by additivity [10a]) ΔH_f^o $[CH_3CO]^+$ = 156 kcal/mol [10b], ΔH_f^o $[CH_3CHOH^+]$ = 139 kcal/mol [10b], ΔH_f^o $[HCO^\bullet]$ = 10.7 kcal/mol [10b] and ΔH_f^o $[CH_2OH^\bullet]$ = - 4.5 kcal/mol [10b]) namely 10.32 eV and 10.25 eV, respectively. The Ionization Energy (IE) of acetol was measured using energy selected electrons, as 9.74 ± 0.05 eV leading to ΔH_f^o $[CH_3COCH_2OH]^{\bullet+}$ = 138 kcal/mol.

(10) (a) Benson,S.W., Thermochemical Kinetics, Wiley-Interscience. New York , 1976. (b) Lias, S.; Bartmess, J. E.; Liebman, J. F.; Holmes, J. L.; Levin , R. D. ; Mallard, W. G. *J. Phys. Chem. Ref. Data*, Vol.17, Suppl. 1, 1988.

(11) The larger part of the m/z 29 peak in this spectrum results from the collision induced dissociative ionization (CIDI) mass spectrum of the neutral species generated from the metastable acetol ions. The CIDI spectrum showed only four significant peaks at m/z 31 (16%), m/z 30 (3%), m/z 29 (100%) and m/z 28 (23%), an observation entirely in keeping with the formation of HCO• and •CH_2OH radicals.

(12) The shape of the latter metastable peak ($T_{0.5}$ = 15 meV) is not Gaussian, having a broader residual collision induced base, beneath a narrow component, also associated with a very small $T_{0.5} \leq 0.5$ meV.

(13) Meot-Ner (Mautner), M. *J. Am. Chem. Soc.*, **1984**, *106*, 1257.

(14) Dissociation in the ion source leads to a mixture of isomeric m/z 45 ions, CH_3CHOH^+ and $CH_2{=}CHOH_2^+$, which obscures the analysis of the position of the label in the product ions generated from the D-labelled isotopomers.

(15) Burgers, P.C.; Terlouw, J.K.; Holmes, J.L. *Org. Mass Spectrom.* **1982**, 17, 369.

(16) Hammerum,S; Vulpius, T.; Audier, H-E. *Org. Mass Spectrom.* **1992**, *27*, 369.

(17) Terlouw, J.K.; Wezenberg, J. ; Burgers, P.C.; Holmes, J.L. *J. Chem. Soc. Chem. Commun.* **1983**, 1121.

(18) From AE (energy selected electrons) = 10.06 eV (this work), ΔH_f ($BrCH_2CHOHCH_2OH$) = -96.5 kcal/mol [10a], and ΔH_f (HBr)= - 9 kcal/mol [10b]. However, considering that in the EI mass spectrum the molecular ion is very weak (≤ 0.1 % of base peak m/z 125) and that the estimated IE ($BrCH_2CHOHCH_2OH$) is approximately equal to the measured AE (m/z 74), the derived ΔH_f (**6**) must be an upper *limiting* value.

(19) The ionization energy (IE) of glycidol , 10.2 eV, combined with its ΔH_f , - 59 kcal/mol (from ref. 20) ,gives ΔH_f(**6a**) = 176 kcal/mol. For ionized 2-hydroxyoxetane (**6c**) ΔH_f ≈ 176 kcal/mol, from ΔH_f $(oxetane)^{\bullet+}$ = 203 kcal/mol (ref. 10b) and the effect of OH substitution at a non-charge bearing site (ref. 21), - 39 kcal/mol, given by $\Delta(\Delta H_f)$ cyclobutanol and cyclobutane (ref. 10b). Ion **6b**, will by analogy with similarly ring opened oxirane (see ref. 22) have a considerably higher ΔH_f than the ring-closed form. Consistent with the oxirane results, the calculations on the distonic ion **6b** showed its derived heat of formation also to be far above that estimated for the ring-closed isomer.

(20) Holmes, J.L.; Terlouw, J.K.; Lossing, F.P . *J. Phys. Chem.* **1976**, *80*, 2860.

(21) Holmes, J.L; Lossing, F.P.; Burgers, P.C. *Int. J. Mass Spectrom. Ion Phys.* **1983**, *47*, 133.

(22) Nobes, R.H.; Bouma, W.; Macleod, J.K.; Radom, L. *Chem. Phys. Lett.* **1987**, *135*, 78.

(23) Ruttink, P.J.A; Burgers, P.C. *Int. J. Mass Spectrom. Ion Processes* **1992**, *113*, 23.

(24) For recent reviews see : (a) Longevialle, P. *Mass Spectrom. Rev.* **1992**, *11*, 157. (b) Morton, T.H. *Org. Mass Spectrom.* **1992**, *27*, 353.

(25) Heinrich, N.; Schwarz, H. *Int. J. Mass Spectrom. Ion Processes* **1987**, *79*, 295.

(26) This TS probably represents the barrier for the transformation **3b** → **5a**, although analysis of the IRC calculation of this TS and the nature of the imaginary frequency provides no direct evidence for rotation of the CH_2=O group concomitant with the H transfer. Note that the energy of this TS is slightly lower than that of ion **3b**.

Addendum to Chapter 2.

Low energy acetol ions $CH_3C(=O)CH_2OH^{\bullet+}$ dissociate to $CH_3C(H)OH^+$ and $HC=O^\bullet$ by a double hydrogen transfer (DHT), a common reaction among oxygen containing radical cations. The work described in Chapter 2 has shown that the isotopologue $CH_3C(=O)$-$CH_2OD^{\bullet+}$ specifically loses $HC=O^\bullet$ to produce $CH_3C(D)OH^+$. This finding refuted an earlier postulated attractive mechanism based on the behaviour of ionized acetol in ion-molecule reactions and led to the proposal formulated in Scheme 2.2 on page 59.

The experimental work described on related compounds in Chapters 3 and 4 of this thesis has prompted Ruttink *et al.* [1] to reexamine the mechanistic proposal described in Chapter 2 using *ab initio* MO calculations at the CEPA//RHF/DZP level of theory complemented with Valence Bond methods. The mechanism [1] indicate that the unimolecular chemistry of ionized acetol can be formulated in terms of two *proton* transfers, taking place in intermediate O•H•O and C•H•O bonded hydrogen bridged radical cations [see Scheme page 65]. The two protons originate from the same moiety and a charge transfer complex is therefore implicated and shown to be involved.

These concepts of proton and charge transfer may well be more generally applicable and they do correctly predict the unimolecular chemistry of ionized acetoin, $CH_3C(=O)CH(CH_3)OH^{\bullet+}$ and related α-ketols described in Chapters 3 and 4.

[1] P.J.A. Ruttink, P.C. Burgers and J.K. Terlouw, *Can. J. Chem.*, (1996) in press.

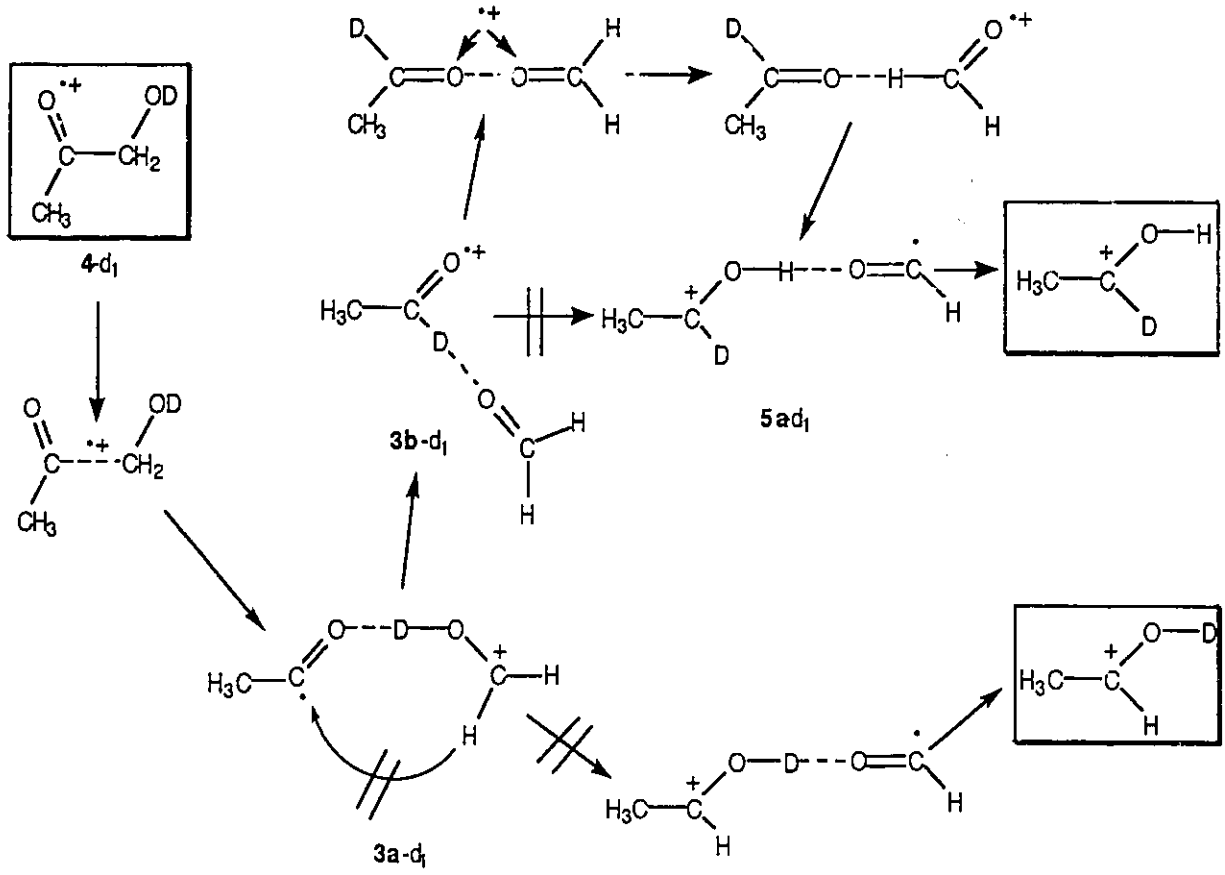
4-d1
3b-d1
5a-d1
3a-d1

CHAPTER 3

C-H···O and O···H···O bonded intermediates in the dissociation of low energy methyl glycolate radical cations

Introduction

Without exaggeration, mass spectrometry, from its inception by Thomson in 1913 [1] and with the advances made by Nier and his contemporaries, has proved to be one of the most powerful and versatile research techniques developed in physical chemistry [2]. Without doubt Professor A.O. Nier has played an inimitable role in the development of modern sector mass spectrometers. For example, in 1940 a milestone was reached when he introduced [3] the sector magnetic analyzer which led to the design of a low resolution instrument [4]. Later, he and his colleagues designed the first double focussing mass spectrometer of high resolution [5], thereby paving the way for the analysis of organic compounds by mass spectrometry.

This work will appear in an article of the same title:

D. Suh, C.A. Kingsmill, P.J.A. Ruttink, P.C. Burgers and J.K. Terlouw, *Int. J. Mass Spectrom. Ion Processes*, in press (1995).

From the early days of organic mass spectrometry, it had been realized that many radical cations formed by electron impact ionization may undergo more or less extensive rearrangement reactions [6]. Indeed, that a rearrangement reaction is involved may already follow from even a cursory examination of the mass spectrum, a simple example being methyl formate whose mass spectrum contains an intense peak at m/z 32 corresponding to the loss of CO [7].

Sometimes, the dissociation behaviour of organic radical cations would appear to border on the bizarre. This is particularly true for the low energy (metastable) ions. Consider for example the behaviour of the $C_3H_6O_2^{\bullet+}$ isomers methyl acetate, $CH_3C(=O)OCH_3^{\bullet+}$ and acetol, $CH_3C(=O)CH_2OH^{\bullet+}$. The former produces $^{\bullet}CH_2OH$ radicals and $CH_3C{\equiv}O^+$ although it does not contain a CH_2OH moiety; by contrast, ionized acetol, which does contain a CH_2OH group, does not produce $^{\bullet}CH_2OH$, but rather $HCO^{\bullet}$ + CH_3CHOH^+ [8].

Hydrogen bonding has been invoked to rationalize the dissociation chemistry of such reactions [9,10,11]. A by now celebrated case is that of ionized methyl acetate whose $^{\bullet}CH_2OH$ loss has been rationalized [12] in terms of O···H···O bonding, (Eq. (1)) :

$$CH_3C(=O)OCH_3^{\bullet+} \rightarrow CH_3C(OH)OCH_2^{\bullet+} \rightarrow [CH_3\text{-}C=O\cdots H\cdots O=CH_2]^{\bullet+},\ \mathbf{a} \rightarrow CH_3CO^+ + {}^{\bullet}CH_2OH \quad (1)$$

More recent work, however, indicates that the C-H···O bonded counterparts of O···H···O bonded ions are perhaps more important intermediates in the decay of oxygen containing radical cations. A case in point is the acetol ion whose remarkable dissociation behaviour has been rationalized in terms of both O···H···O [13] and C-H···O [8] bonded intermediates. Based on characteristic ion/molecule reactions, Pakarinen et al. [13] proposed a mechanism involving O···H···O bonding, (Eq. (2)) :

$CH_3C(=O)CH_2OH^{\bullet+} \rightarrow [CH_3C=O\cdots H\cdots O=CH_2]^{\bullet+}$ **a** $\rightarrow [CH_3C(H)=O\cdots H\cdots O=CH]^{\bullet+} \rightarrow$

$CH_3CHOH^+ + HCO^{\bullet}$ (2)

However, the O···H···O bonded intermediate **a** is the same as that proposed to be generated from metastable ionized methyl acetate, Eq. (1), which yields $CH_3CO^+ + {}^{\bullet}CH_2OH$, but not $CH_3CHOH^+ + HCO^{\bullet}$. indeed, George et al. [8] found Eq. (2) to be incompatible with their D labelling results and they derived a mechanism, supported by ab initio MO calculations, which involves C-H···O bonding, Eq. (3) :

$CH_3C(=O)CH_2OD^{\bullet+} \rightarrow [CH_3C(=O)\cdots O(D)CH_2]^{\bullet+} \rightarrow [CH_3C(=O)\text{-}D\cdots O=CH_2]^{\bullet+} \rightarrow$

$CH_3CDOH^+ + HCO^{\bullet}$ (3)

This mechanism is based, inter alia, on the key observation that the hydroxyl D atom appears in the product ion at the carbenium carbon atom, not at the oxygen atom. This is a remarkable result in so far as C-H···O bonded radical cations are invariably considerably less stable than their O···H···O bridged counterparts [8,9,10]. For example $[CH_3C=O\cdots H\cdots O=CH_2]^{\bullet+}$ is calculated [8] to lie ~ 10 kcal/mol below $[CH_3C(=O)\text{-}H\cdots O=CH_2]^{\bullet+}$ and so loss of $HCO^{\bullet}$ from ionized acetol appears to be kinetically controlled.

Ionized methyl glycolate, $HOCH_2C(=O)OCH_3^{\bullet+}$, **1**, contains both a CH_3O and a CH_2OH group, i.e. it has both the functional groups of methyl acetate and acetol. Thus, a very interesting question was arisen : will **1** dissociate by O···H···O bonding, as in methyl acetate or by C-H···O bonding, as in acetol, or by neither ? It is known that metastable ions **1** predominantly lose $HCO^{\bullet}$ [14] and it will be shown that this reaction proceeds via a mechanism analogous to that of ionized acetol, i.e. via C-H···O bonding ; no evidence was found for a rearrangement analogous to that for ionized methyl acetate.

The methyl glycolate isomer dimethyl carbonate, $CH_3OC(=O)OCH_3$, **2**, was also examined and it is concluded that **1** and **2** rearrange to (a) common intermediate(s) prior to dissociation. Loss of $HCO^{\bullet}$ from **1** requires not more than 10 kcal/mol which further attests to the ease by which C-H···O bonds can be formed in oxygen containing radical cations.

The most important of the other (minor) unimolecular dissociations of **1** (and **2**), *viz.* the formation of CH_2OH^+ which appears to be accompanied by the formation of $CH_3^{\bullet}$ and CO_2 rather than the intact radical $CH_3OC{=}O^{\bullet}$ are also discussed.

Results and Discussion

The Metastable Ion (MI) spectra of **1** and **2** are given in Table 3.1. Both isomers abundantly lose $HCO^{\bullet}$ with minor processes for formation of CH_2OH^+, loss of CO, H_2O and $CH_3^{\bullet}$. Note that these minor processes are more abundant for isomer **2**. The metastable peaks for **1** and **2** were found to be, pairwise, superimposable. Thus, it is very likely that **1** and **2** isomerize to (a) common structure(s) prior to dissociation. First, the major decay, *viz.* the loss of $HCO^{\bullet}$ which was investigated in detail for isomer **1**, is discussed.

Loss of $HCO^{\bullet}$: structure and formation of the $C_2H_5O_2^+$ product ion

Loss of $HCO^{\bullet}$ from both isomers is accompanied by a non-composite Gaussian type metastable peak with a $T_{0.5}$ value of 22 meV (average release : 50 meV). Combined experimental and theoretical studies [16,17] have indicated that at least seven distinct

Table 3.1. Reactions[a] of metastable methyl glycolate and dimethylcarbonate ions.

Precursor molecule		Products formed or neutral lost				
		CH_2OH^+	- HCO$^\bullet$	- CO	- H_2O	- $CH_3^\bullet$
$HOCH_2C(=O)OCH_3$	1	4	100	1	2	2
$CH_3OC(=O)OCH_3$	2[b]	21[56][c]	100[22]	4[230]	3[27]	7[440][d]

[a] Intensities (peak heights) relative to base peak = 100 % ; values in brackets refer to the kinetic energy release, measured at half height ($T_{0.5}$); [b] contains small peaks at m/z 45, $C_2H_5O^+$, and m/z 60 (loss of CH_2O); [c] Assuming co-generation of CH_3O-CO$^\bullet$, see text ; [d] Dished-shaped metastable peak; value from "horns" (T_h).

$C_2H_5O_2^+$ ions exist as stable species in the gas-phase, the best known and most stable of which are the conjugatively stabilized carbenium ions $CH_3C(OH)_2^+$, protonated acetic acid, and H-$C(OH)OCH_3^+$, **3**, protonated methyl formate. Experimentally, the $C_2H_5O_2^+$ isomers can be distinguished by their characteristic collision-induced dissociation (CID) mass spectra [16]; for example, **3** is the only isomer which abundantly undergoes decarbonylation to produce $CH_3OH_2^+$.

The structure of the $C_2H_5O_2^+$ product ion generated from metastable ions **1** and **2** was established through comparative collision experiments as described in the experimental section. The CID mass spectrum of the metastable peak for **1** → $C_2H_5O_2^+$ + HCO$^\bullet$ is shown in Figure 3.1a; this spectrum is virtually identical to that of the $C_2H_5O_2^+$ ion made by the gas-phase protonation of methyl formate, which is known [17] to give **3** and which is distinctly different from those of all other isomers. Hence the following reaction is established :

$$HOCH_2C(=O)OCH_3^{\bullet+}, \mathbf{1}, \rightarrow H\text{-}C(OH)OCH_3^{+} + HCO^{\bullet}$$

Next the origin of the H, C and O atoms lost as $HCO^{\bullet}$ was traced by investigating several specifically labelled molecules and the results are shown in Table 3.2. It is seen that the $HCO^{\bullet}$ radical can originate from both the CH_3O and the CH_2OH groups : the major process involves loss of the CH_2OH oxygen atom, carbon atom and one

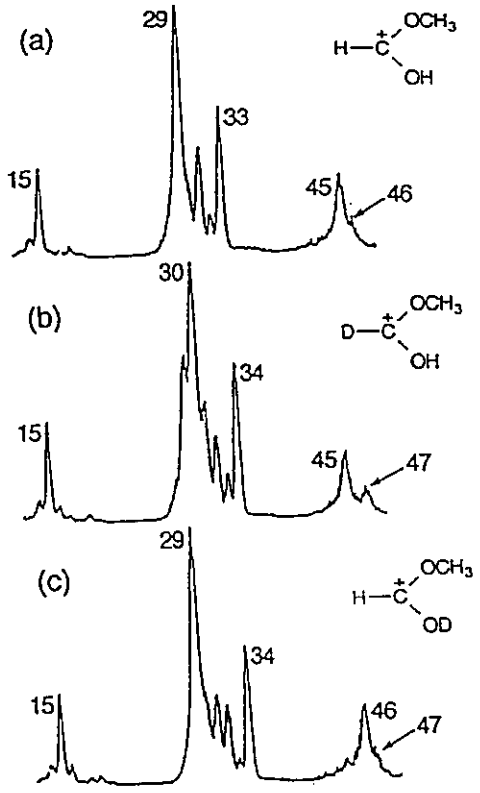

Figure 3.1. Partial CID mass spectra of product ions from dissociation reactions of metastable methyl glycolate ions : (a) $C_2H_5O_2^+$ from $HOCH_2C(=O)OCH_3^{\bullet+}$ (**1**) → $H\text{-}C(OH)OCH_3^+$ (**3**) + $HCO^{\bullet}$; (b) $C_2H_4DO_2^+$ from $DOCH_2C(=O)OCH_3^{\bullet+}$ → $C_2H_4DO_2^+$ + $HCO^{\bullet}$; (c) $C_2H_4DO_2^+$ from $HOCD_2C(=O)OCH_3^{\bullet+}$ → $C_2H_4DO_2^+$ + $DCO^{\bullet}$

Table 3.2. Reactions[a] of metastable methyl glycolate isotopologues[b].

Precursor molecule	Neutral species lost	Calc.[c]
$HOCD_2C(=O)OCH_3$	HCO : DCO = 19 : 81	17 : 83
$HOCH_2C(=O)OCD_3$	HCO : DCO = 88 : 12	87 : 13
$DOCH_2C(=O)OCD_3$	HCO : DCO = 83 : 17	83 : 17
$DOCH_2C(=O)OCH_3$	HCO : DCO = 97 : 3	96 : 4
$HOCH_2C(=^{18}O)OCH_3$	HCO : $HC^{18}O$ = 100 : 0	100 : 0
$HOCH_2C(=O)^{18}OCH_3$	HCO : $HC^{18}O$ = 87 : 13	[d]
$HOCH_2C(=O)O^{13}CH_3$	HCO : $H^{13}CO$ = 87 : 13	[d]
$HOCH_2C(=O)^{18}O^{13}CH_3$	HCO : $H^{13}C^{18}O$ = 87 : 13	[d]

[a] Intensities relative to sum = 100 ; [b] For definition , see ref. 18; [c] Calculated assuming 26% scrambling, see text ; [d] Ratios used to derive degree of scrambling.

methylene H atom, but not the O-H hydrogen atom, while a minor process involves loss of the CH_3O oxygen atom and carbon atom; the keto functionality is not lost as HCO•. The metastable peaks for these two processes in the labelled isotopomers were superimposable and both processes yield the same product ion **3**. Therefore, the minor process may well result from partial isotopic equilibration reactions (scrambling) taking place prior to loss of HCO•, rather than from a distinct mechanism. In fact, if the ratios for the ^{13}C and ^{18}O labelled molecules (see Table 3.2) are taken as showing that 74 % of the HCO• elimination is atom-specific (the major process mentioned above) and that in 26 % of the precursor ions all hydrogen atoms as well as the CH_2OH and CH_3O oxygen and carbon atoms scramble, then the ratios for the D labelled compounds can be accurately reproduced (see Table 3.2).

Hence, the following transformation is established for the major, atom-specific loss :

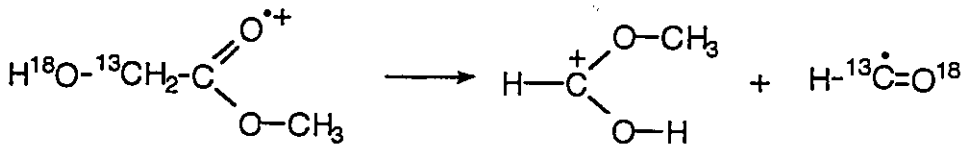

1 3

Based on the above results and by analogy with the two proposals for loss of HCO• from ionized acetol, see above, the following mechanistic possibilities for the atom-specific decay of **1**, which involve O···H···O and C-H···O bonding respectively, see Scheme 3.1, are derived.

As with acetol, a distinction between the two possibilities can be made by determining the fate of the D atom in **1**-Od_1→ (**3**-Od_1 or **3**-Cd_1) through comparative collision experiments. However, because of the partial scrambling process, the product ions, irrespective of the mechanism involved, will not be isotopomerically [18] pure : only 78.3 % will have the connectivity **3**-Od_1 or **3**-Cd_1, while the remainder will have the D at the other positions. Fortunately, this degree of specificity appears more than sufficient to distinguish the two isotopomers of **3**. Reference ions **3**-Od_1 and **3**-Cd_1 were made by the gas-phase deuteronation of methyl formate and by protonation of D-C(=O)OCH_3 respectively. It was observed that the CID mass spectrum (Fig. 3.1b) of the metastable peak for loss of HCO• from **1**-Od_1 was almost identical to that of the **3**-Cd_1 reference ion. Note also that for ion **3**-Cd_1 m/z 45 does not shift to m/z 46, which is entirely compatible with the assigned label position: the most stable $[C,H,O_2]^+$ isomer is HO-C=O^+ [19] formed from **3** via a 1,3-hydrogen shift of the C-H hydrogen to the methyl group. In the complementary experiment, it was observed that

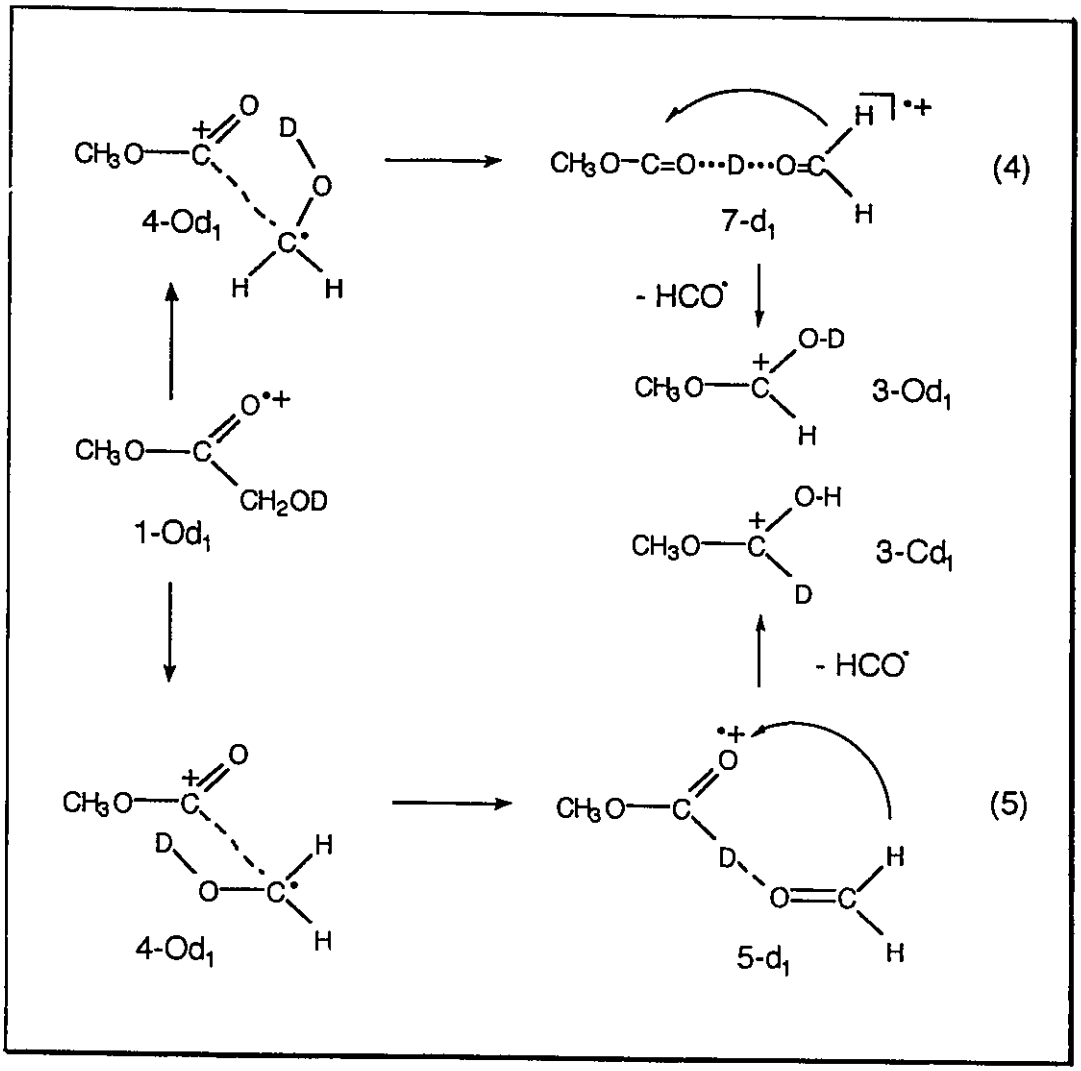

Scheme 3.1

the CID mass spectrum of the metastable peak for loss of DCO· from $HOCD_2C(=O)OCH_3^{\bullet+}$ (Fig 3.1c) was very close to that of the reference ion **3**-Od_1.

Apart from the above comparative experiments, the label position in ion **3**-Cd_1 can also be determined from a detailed albeit qualitative analysis of the CID spectrum of **3**. This can be done by tracing the origins of the connectivity-characteristic base peak at m/z 29 in the CID mass spectrum of **3**. As shown in Figure 3.1a, there are three major peaks in the m/z 29 -33 region. The m/z 29 ion was found to be $HC{\equiv}O^+$ which is

more stable by 33 kcal/mol than its isomer COH^+ [20]; m/z 31 can only be CH_2OH^+, its isomer CH_3O^+ being, on the singlet surface, a transient species only which is dissociative towards $HC{=}O^+ + H_2$ [21] ; m/z 33 can only be $CH_3OH_2^+$.

The $HC{=}O^+$ ion could a priori simply be formed by a 1,3-H shift followed by loss of CH_3OH, i.e. $H\text{-}C(OH)OCH_3^+ \rightarrow H\text{-}C(=O)O(H)CH_3^+ \rightarrow HCO^+$. It is then expected for $D\text{-}C(OH)OCH_3^+$ that this signal cleanly shifts to m/z 30, DCO^+ . However, it follows from Figure 3.1b that this is not the case : an intense signal at m/z 29, HCO^+, remains. Hence, there are at least two different routes to the formylium ion.

To unravel the dissociation reactions of **3**, several isotopologues of **3** were investigated. Fig. 3.2a shows the CID mass spectrum of $HC(OH)^{18}O^{13}CH_3^+$, generated from metastable ions $HOCH_2C(=O)^{18}O^{13}CH_3^{\bullet+}$ (see Table 3.1). There are six intense signals in the m/z 29 - m/z 36 region to wit : m/z 29, HCO^+ ; m/z 30, $H^{13}CO^+$; m/z 31, $HC^{18}O^+$ and/or CH_2OH^+ ; m/z 32, $H^{13}C^{18}O^+$ and/or $^{13}CH_2OH^+$; m/z 34, $^{13}CH_2{}^{18}OH^+$ and/or $^{13}CH_3OH_2^+$ and m/z 36, $^{13}CH_3{}^{18}OH_2^+$.

First, the possible formation of CH_2OH^+, m/z 31, from $HC(OH)^{18}O^{13}CH_3^+$ is considered. This process could simply be formulated as a 1,3-H shift from the CH_3 group to the carbenium center, followed by loss of $^{13}CH_2{}^{18}O$. If this were the case, then the ion $HC(OH)OCD_3^+$ should abundantly form $CHDOH^+$, m/z 32. Figure 3.2c shows the CID mass spectrum of $HC(OH)OCD_3^+$, generated from $HOCH_2C(=O)OCD_3^{\bullet+}$: m/z 32 is virtually absent, whereas the peak at m/z 33 is very intense. Thus $HC(OH)OCD_3^+$ does not produce $CHDOH^+$ via the above process, but rather CD_2OH^+ m/z 33. This ion most likely arises from m/z 36, by consecutive loss of HD i.e. $HC(OH)OCD_3^+ \rightarrow CD_3OH_2^+ (+ CO) \rightarrow CD_2OH^+ + HD$. Thus m/z 31 in the CID mass spectrum of $HC(OH)^{18}O^{13}CH_3^+$, Figure 3.2a, is due **solely** to $HC^{18}O^+$, whereas m/z 29 can only be HCO^+. For $HC(OH)^{18}O^{13}CH_3^+$, the following products are then left: (i) for formylium : HCO^+, $H^{13}CO^+$ and $HC^{18}O^+$; (ii) for

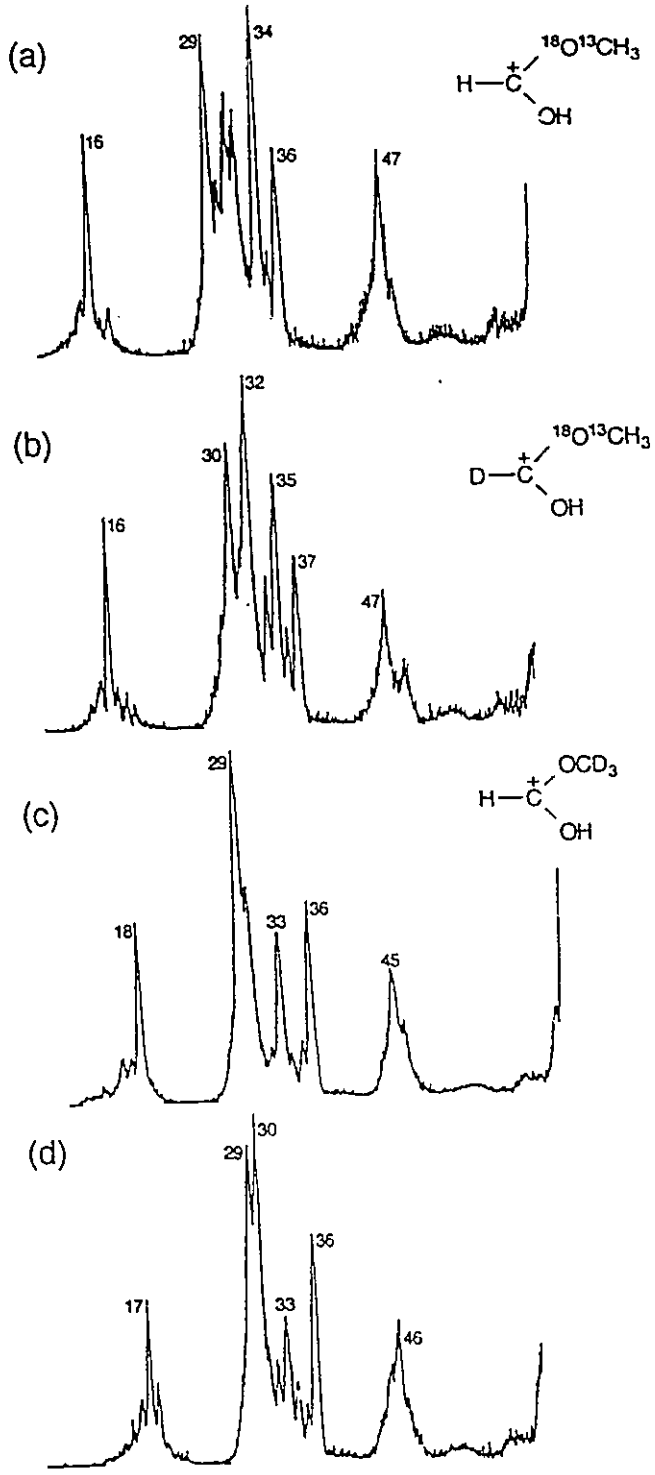

Figure 3.2. Partial CID mass spectra of product ions from dissociation reactions of metastable methyl glycolate ions :

(a)	$HO\text{-}C(H)^{18}O^{13}CH_3^+$	from	$HOCH_2C(=O)^{18}O^{13}CH_3^{\bullet+}$	(- HCO$^\bullet$)
(b)	$HO\text{-}C(D)^{18}O^{13}CH_3^+$	from	$DOCH_2C(=O)^{18}O^{13}CH_3^{\bullet+}$	(- HCO$^\bullet$)
(c)	$HO\text{-}C(H)OCD_3^+$	from	$HOCH_2C(=O)OCD_3^{\bullet+}$	(- HCO$^\bullet$)
(d)	$C_2H_2D_3O_2^+$	from	$CH_3OC(=O)OCD_3^{\bullet+}$	(- HCO$^\bullet$)

hydroxymethylium : $^{13}CH_2OH^+$ and $^{13}CH_2{}^{18}OH^+$; (iii) for protonated methanol, $^{13}CH_3OH_2^+$ and $^{13}CH_3{}^{18}OH_2^+$. Thus, it is as though after activation a mixture of $HC(OH)^{18}O^{13}CH_3^+$ and $HC(^{18}OH)O^{13}CH_3^+$ is formed and these ions dissociate as follows, see Scheme 3.2.

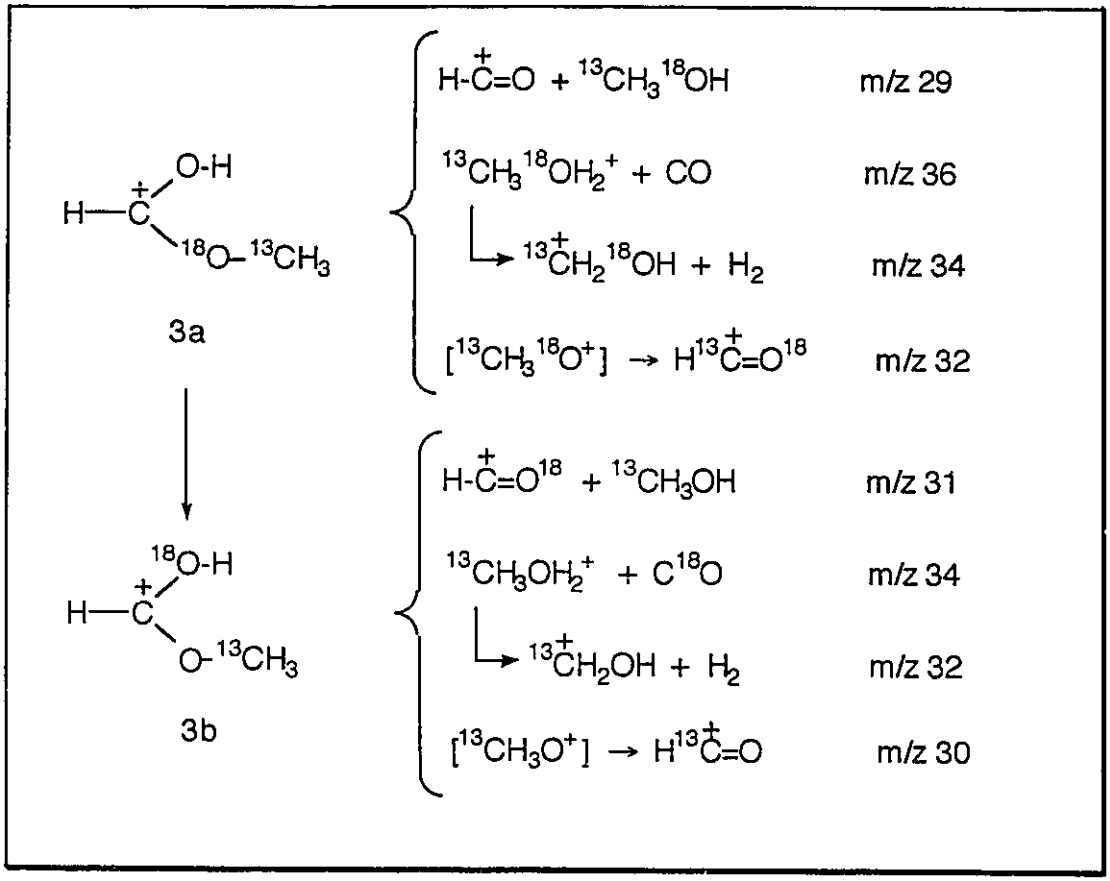

Scheme 3.2

The above transformation **3**a → **3**b most likely proceeds via consecutive 1,3-H and 1,3-CH_3 shifts :

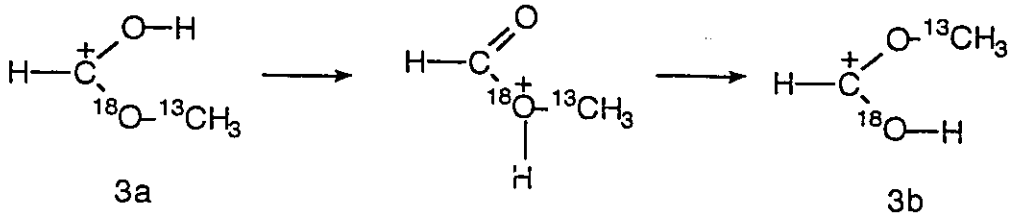

3a 3b

These results are in agreement with those published previously for formation of $CH_3OH_2^+$ [17] , although an alternative interpretation is now offered.

Next, consider Fig. 3.2b which shows the CID mass spectrum of the m/z 65 ions generated from $DOCH_2C(=O)^{18}O^{13}CH_3^{\bullet+}$. When compared with Figure 3.2a, it is seen that m/z 29 is almost cleanly shifted to m/z 30, DCO^+, whereas m/z 31 is cleanly shifted to m/z 32, $DC^{18}O^+$. Considering the above Scheme, this result is only compatible with the structure $DC(OH)^{18}O^{13}CH_3^+$ and *not* with $HC(OD)^{18}O^{13}CH_3^+$. Hence, it is supported not only from comparative experiments but also from the above analysis of the behaviour of labelled ions **3** that the hydroxyl hydrogen of **1** turns up at the carbenium carbon atom of **3** and **not** at the oxygen atom. These results rule out pathway (4) in Scheme 3.1 and it is concluded that the expulsion of $HCO^{\bullet}$ from ionized methyl glycolate may proceed via pathway (5) i.e. **via a C-H···O bonded intermediate.**

Loss of $HCO^{\bullet}$: mechanistic proposals

From the measured Ionization Energy (IE) of methyl glycolate, IE = 10.42 ± 0.05 eV [15], a heat of formation, ΔH_f, of **1** of 106 kcal/mol is obtained (using ΔH_f [ester] = -134 kcal/mol, [20]). Since ΔH_f [**3**] + ΔH_f [$HCO^{\bullet}$] = 92 + 11 = 103 kcal/mol [23], loss of $HCO^{\bullet}$ from **1** is slightly exoergic. The Appearance Energy (AE) for loss of $HCO^{\bullet}$ was also measured , AE = 10.74 ± 0.05 eV [22], and so the dissociation has a forward barrier of ~7 kcal/mol. Thus, for **1** the rearrangements necessary to produce **3** + $HCO^{\bullet}$

must take place within this energy regime. The heat of formation of the dimethyl carbonate ion, **2**, is slightly lower than that of **1** : ΔH_f [**2**] = 103 kcal/mol [23], but within experimental error the TS energies for loss of HCO• from the two isomers are the same (113 kcal/mol for **2**, from AE [m/z 61] = 10.94± 0.05 eV [23] and ΔH_f [ester] = -139 kcal/mol [20]).

The reverse activation energy for **1** is ~ 10 kcal/mol but the average kinetic energy release is only 1 kcal/mol. This indicates that, after passing the highest transition state (corresponding to the AE) the system may enter an attractive surface, such as that for an ion-dipole complex.

Ab initio MO calculations provide an invaluable tool for probing mechanistic proposals. However, even a cursory inspection of the ab initio results given in Table 3.3. (relative energies) and Figure 3.3 (equilibrium geometries) shows that a detailed computational analysis of the unimolecular chemistry of **1** and **2** is impractical. Not only are many stable intermediates energetically accessible (i.e. their relative energies lie below the ~10 kcal/mol limit imposed by experiment), but several of these may have conformers that must be considered as well.

For example, five of the eight possible conformers of **1** are minima which are relatively close in energy (within 4.5 kcal/mol) at the UMP3/6-31G*//6-31G* level of theory : items **1**f, b, c, d and h in Table 3.3 and Fig. 3.3. These five conformers were also studied at the UMP2/6-31G* level of theory and conformer **1**f was found to be the most stable, both with and without inclusion of electron correlation in the geometry optimization. The presence of such a large number of stable intermediates and conformers makes the search for connecting transition states (TS) a formidable task

Table 3.3 Total energies (hartrees), zero-point vibrational energies [ZPVE] and relative calculated E[rel]* energies (kcal/mol) for some isomers of the [methyl glycolate]$^{\bullet+}$ system.

STRUCTURE		STATE	UHF/6-31G**	UMP3/6-31G**// UHF/6-31G**	ZPVE*	E[rel]
$CH_3O(C{=}O)CH_2OH^{\bullet+}$	**1f**	$^2A'$	-341.36295	-342.24505	57.0	0.0
	1b	^2A	-341.35886	-342.24146	57.0	2.2
	1c	$^2A'$	-341.35635	-342.23844	57.1	4.2
	1d	^2A	-341.35880	-342.24128	57.3	2.7
	1h	^2A	-341.35975	-342.24351	57.2	2.6
$CH_3OC(=O)\cdot\cdot H\cdot\cdot O{=}CH_2^{\bullet+}$	**5**	$^2A'$	-341.35087	-342.22672	54.9	9.4
$CH_3OC\text{-}OH\cdots O{=}CH_2^{\bullet+}$	**7**	$^2A'$	-341.35253	-342.24383	54.5	-1.8
$CH_3OC(OH)CH_2O^{\bullet+}$	**8**	$^2A'$	-341.36208	-342.24495	57.9	1.0
$CH_3OC(OH)OCH_2^{\bullet+}$	**9**	^2A	-341.37683	-342.26580	56.9	-13.2
$CH_3O(C{=}O)\cdot\cdot H\cdot\cdot O{=}CH_2^{\bullet+}$	**10**	$^2A'$	-341.32923	-342.22891	53.9	7.0
$CH_3O(H)C(=O)CH_2O^{\bullet+}$	**11**	^2A	-341.34936	-342.23830	56.6	3.8
$CH_3OC(=O)O(H)CH_2^{\bullet+}$	**12**	^2A	-341.34487	-342.23873	56.0	2.9
$CH_2OC(OH)CH_2OH^{\bullet+}$	**13**	^2A	-341.36018	-342.25401	56.4	-6.3
TS **1-8**			-341.34236	-342.23798	55.1	2.6
TS **5-7**			-341.32064	-342.21905	57.7	11.3

*The relative calculated energies include scaled (0.9 for UHF) zero-point vibrational contributions.

and it has therefore been decided to focus on the most important dissociation of **1** *viz.* the loss of HCO$^{\bullet}$. The fact that this loss is largely atom specific greatly reduces the number of mechanistic possibilities, i.e. any mechanism proposed for the major specific loss must be in agreement with all of the labelling results. As argued above, the experiments also indicate that the minor non-specific HCO$^{\bullet}$ loss from **1** is the result of exchange reactions prior to dissociation, most likely with **2** and ions derived therefrom, rather than loss via a different mechanism. Even within these constraints a complete computational picture has not yet been obtained. However, as mentioned

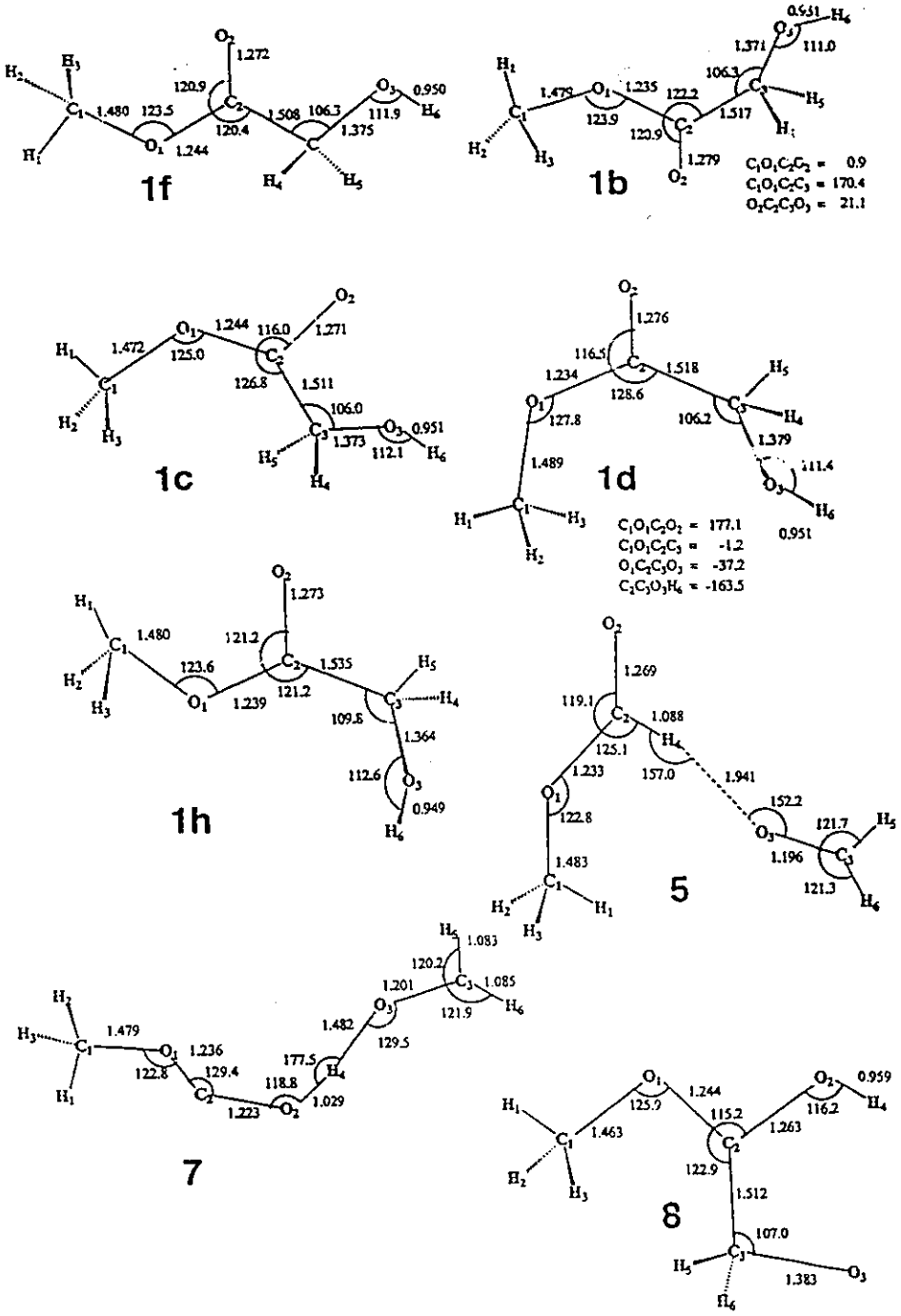

Figure 3.3. Optimized geometries of [methylglycolate]$^{\bullet+}$ isomers and some transition states. Bond lengths in angstroms, bond angles in degrees.

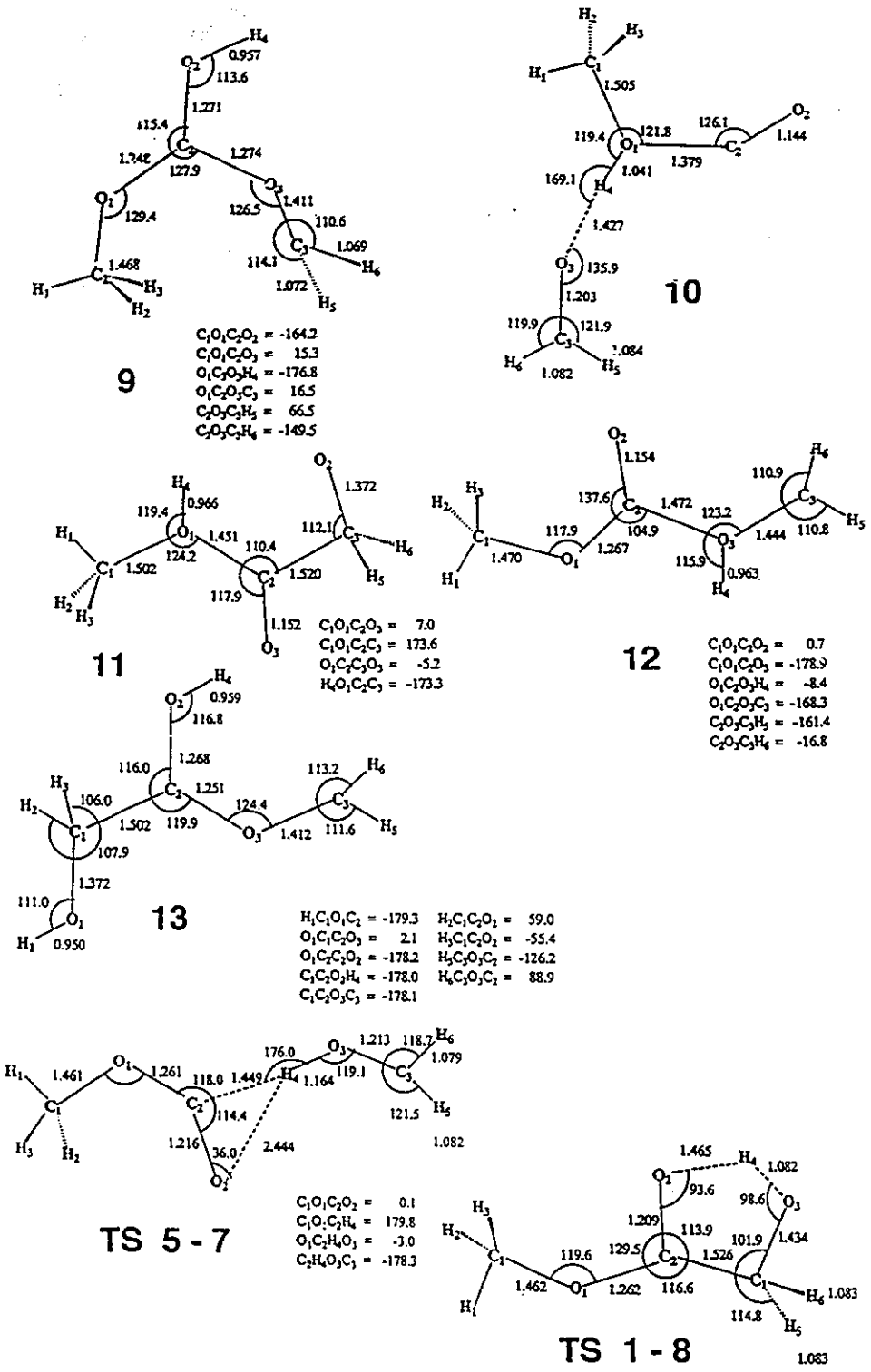

Figure 3.3. Continued.

above, the major specific $HCO^{\bullet}$ loss may well be analogous to that from ionized acetol, $CH_3C(=O)CH_2OH^{\bullet+}$, for which detailed *ab initio* MO calculations [8,24] have been performed; the salient features of these calculations are discussed below and they are extended to include the methyl glycolate ion, see Scheme 3.3.

Elongation of the $C\text{-}C(H_2)$ bond in **1** does not lead to dissociation but to the ion-dipole complex **4**, where the $R\text{-}C{=}O^+$ cation ($R = CH_3$ or CH_3O) interacts with the $^{\bullet}CH_2OH$ dipole. In the case of acetol ($R = CH_3$) ion **4** is clearly a minimum on the PES [8] whereas for the methyl glycolate system, at least at the UHF level of theory, all attempts to determine a structure akin to the ion-dipole complex **4** resulted in the formation of the stable covalently bound ion **12**. However, this is not to say that such an ion-dipole species is energetically inaccessible : considering the experimentally determined ΔH_f values for the $CH_3O\text{-}C{=}O^+$ ion, 120 kcal/mol [23], and the $^{\bullet}CH_2OH$ dipole, - 6 kcal mol, it follows that the cleavage of the $C\text{-}C(H_2)$ bond leading to complete separation of the products is only slightly more energy demanding than the loss of $HCO^{\bullet}$.

Next, the dipole can donate the hydroxyl hydrogen to the $R\text{-}C{=}O^+$ cation to generate **5.** For both acetol [8] and methyl glycolate (Table 3.3) the resulting $C\text{-}H\cdots O$ bridged species **5** has a relatively high energy.

The product ion **3** could be generated therefrom via an H-**atom** shift [8] but, according to our most recent calculations on acetol [24], this step may be too energy demanding. Rather, since **5** is an ion-dipole complex, the formaldehyde dipole can migrate within the electrostatic field of the $R\text{-}C(H){=}O^{\bullet+}$ ion. In this step the relative orientation of the $R\text{-}C(H){=}O$ and $CH_2{=}O$ units is changed such that a charge transfer may

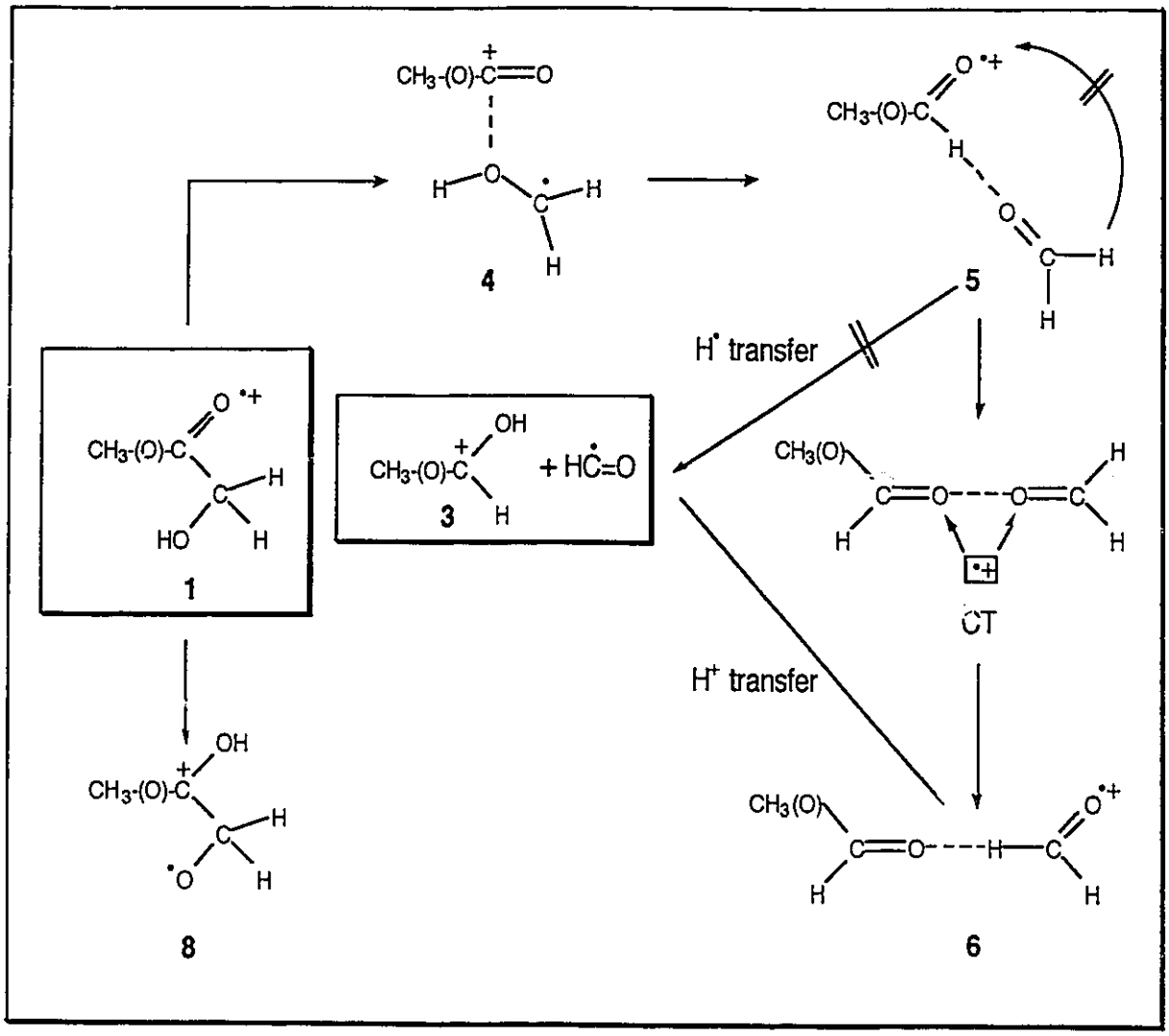

Scheme 3.3

take place without affecting the total energy [25]. For methyl glycolate the ionization energies of $CH_3OC(H)=O$ and $CH_2=O$ are almost the same (10.82 and 10.87 eV respectively [20]), whereas both molecules have substantial dipole moments, 1.77 and 2.33 D [26] respectively; thus the charge localization in the charge transfer complex CT will be determined by the relative orientation of the two units, i.e. **5** or **6**, see Scheme 3.3.

The measured AE for **1** (R = CH_3O) corresponds to a TS energy of 113 kcal/mol, see above. The respective components' energies of the proposed CT complex are very similar, viz. 138 and 140 kcal/mol for $CH_3OC(H)=O^{\bullet+}/O=CH_2$ and $CH_3OC(H)=O/O=CH_2^{\bullet+}$ respectively. Hence for CT to be accessible, a stabilization energy of 27 kcal/mol is needed which, considering the significant dipole moments of the components, is a very reasonable value [11]. The hydrogen bridge in structures **5** and **6** may provide additional stabilization with respect to CT. Ion **6** can smoothly donate a **proton** to $CH_3OC(H)=O$, leading to **3** + $HCO^{\bullet}$; further details will be discussed in our forthcoming computational study of the acetol system [24]. Note that the mechanistic proposal of Scheme 3.3 also adequately explains the remarkable behaviour of acetoin, $CH_3C(=O)CH(CH_3)OH^{\bullet+}$, whose $^{18}O/D$ labelled isotopomer $CH_3C(=^{18}O)CH(CH_3)OD^{\bullet+}$ loses $CH_3CO^{\bullet}$ and $CH_3C^{18}O^{\bullet}$, to cleanly produce the product ions $CH_3C(D)^{18}OH^{+}$ and $CH_3C(H)OD^{+}$ respectively [27].

Both for acetol and methyl glycolate, the O···H···O bridged ion **7** is considerably more stable than its C-H···O bridged counterpart **5** (see Table 3.3), but nevertheless loss of $HCO^{\bullet}$ proceeds via the less stable species. According to the calculations on acetol [8,24] and methyl glycolate (this work), **7** cannot be generated directly from **1** : migration of the hydroxyl hydrogen to the keto oxygen is not acccompanied by C-C(H_2) cleavage but rather leads to the distonic ion **8**, which for both systems represents a cul-de-sac isomerization [28]. In the methyl glycolate system, ion **8** might further communicate with the distonic ion **13**, via a 1,5-H shift, but this stable ion cannot account for the atom specific $HCO^{\bullet}$ loss. Note too, that for the methyl glycolate system another O···H···O bridged ion can be envisaged, viz. ion **10**. This species has been invoked in an earlier work on the loss of CO [15] but, see below, it probably too may not be generated directly from **1**.

As far as the charge distribution in the O···H···O bridged ion **7** is concerned there is an interesting difference between the two systems, in that for the acetol system the Mulliken analysis and the geometry indicate that **7** is best described as having the charge on the CH_2O moiety : $CH_3C^{\bullet}=O\cdots H\text{-}O\text{-}CH_2^{+}$. The methyl glycolate derived ion, however, is better represented as depicted in Scheme 3.4. This difference may be related to the fact that ionized dioxycarbenes are much better stabilized than alkyl(hydr)oxy carbenes (compare : $\Sigma\Delta H_f\ CH_3OCOH^{\bullet+} + CH_2O$ and $\Sigma\Delta H_f\ CH_3OCO^{\bullet} + CH_2OH^{+}$, 132 vs 128 kcal/mol, with $\Sigma\Delta H_f\ CH_3COH^{\bullet+} + CH_2O$ and $\Sigma\Delta H_f\ CH_3CO^{\bullet} + CH_2OH^{+}$, 180 vs 162 kcal/mol [20,29]).

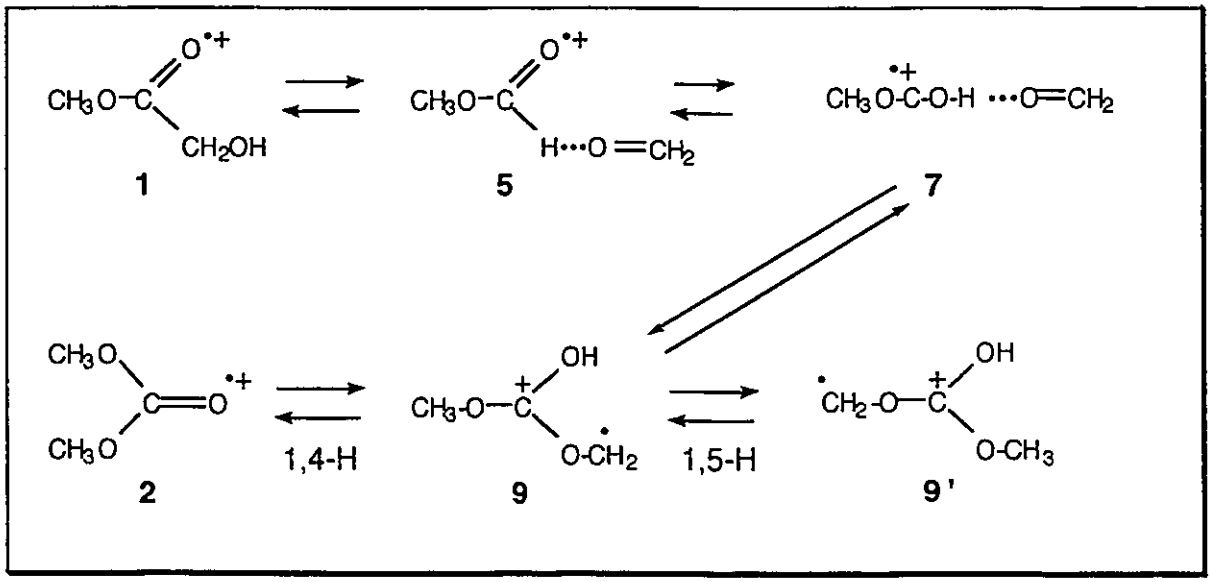

Scheme 3.4

The calculations on methyl glycolate do indicate that, albeit only at energies close to the measured threshold, the O···H···O bonded isomer **7** may be accessible, from ion **5** via TS **5-7** (see Table 3.3). This transformation, see Scheme 3.4, can be viewed as

the 1,2-H shift $CH_3O\text{-}C(H)O^{\bullet+} \rightarrow CH_3O\text{-}C\text{-}OH^{\bullet+}$ catalyzed by formaldehyde [24] ; the formaldehyde dipole in **5** attacks the C(=O)-H proton and then donates it to the keto atom of the $CH_3O\text{-}C{=}O$ moiety. Note that solitary $CH_3O\text{-}C\text{-}OH^{\bullet+}$ is c. 7 kcal/mol more stable than ionized methyl formate, compare 11.2 kcal/mol for the corresponding ions complexed with formaldehyde, i.e. ions **5** and **7.**

What is the fate of **7**? The calculations on acetol [24] indicate that the formaldehyde molecule in **7** cannot donate an H atom to the ionized carbene moiety. Instead, it is proposed that the formaldehyde dipole migrates within the electrostatic field of the $CH_3O\text{-}C\text{-}OH^{\bullet+}$ ion to yield the very stable distonic ion **9**, see Scheme 3.4. Such a dipole migration has also been found to be the key step in the dissociation of ionized methyl acetate [12] i.e. $CH_3C(OH)OCH_2^{\bullet+} \rightarrow CH_3C{=}O\cdots H\cdots O{=}CH_2^{\bullet+}$. Ion **9** may undergo a degenerate 1,5-H shift, **9 - 9'**, and communicate via a 1,4-H shift with the dimethyl carbonate ion **2.**

It is tentatively proposed that this sequence of events, as depicted in Scheme 3.4, provides a rationale for the closely similar MI characteristics and energetics of **1** and **2.** It may also account for the partial scrambling reactions observed for **1**, which may largely find their origin in its communication with **2.**

That extensive scrambling occurs in the loss of HCO$^{\bullet}$ from ions **2** follows from the following observations. In $CH_3OC(=O)OCD_3^{\bullet+}$, an isotopomer of **2**, H/D exchange reactions of all H and D atoms occur to the statistical limit. The ratio for HCO$^{\bullet}$: DCO$^{\bullet}$ loss from $CH_3OC(=O)OCD_3^{\bullet+}$ was found to be 1:1, although this does not necessarily reflect complete H/D randomization; this ratio could equally well be due to specific losses.

However, analysis of the isotopomer $CH_3OC(=O)O^{13}CD_3^{\bullet+}$ clearly shows that the latter is not the case. Moreover, the CID spectra of the metastable peaks for loss of HCO$^{\bullet}$ and DCO$^{\bullet}$ from $CH_3OC(=O)OCD_3^{\bullet+}$ demonstrate that extensive H/D exchange reactions have taken place. Consider the CID mass spectrum of the metastable peak

for loss of HCO$^{\bullet}$ from $CH_3OC(=O)OCD_3^{\bullet+}$ shown in Figure 3.2d. It is seen, especially from the m/z 17 : m/z 18 ratio, that $CH_3OC(=O)OCD_3^{\bullet+}$ has undergone significantly more H/D exchange reactions than $HOCH_2C(=O)OCD_3^{\bullet+}$, see Figure 3.2c. Note that a relatively high energy barrier must separate **1** and **2** (as was found in this study, see TS **5-7**) to allow for the atom specific loss of HCO$^{\bullet}$ from **1.**

Upon collisional activation of **1** and **2**, an additional abundant signal is produced, m/z 45, which labelling experiments show is $COOH^+$. The O···H···O bonded intermediate **7** is a prime candidate for $COOH^+$; **7** can lose upon activation both $CH_3^{\bullet}$ and CH_2=O. Note, in agreement with the above, that for $DOCH_2C(=O)OCH_3^{\bullet+}$ this signal cleanly shifts to m/z 46, $COOD^+$.

Finally, the methyl lactate radical cation, $HOCH(CH_3)C(=O)OCH_3^{\bullet+}$, a higher homologue of **1**, shows a unimolecular behaviour which resembles that of **1**. Like **1**, it displays an MI spectrum dominated by **3**, resulting from the loss of $CH_3C{=}O^{\bullet}$; also present is a sizeable peak at m/z 45, CH_3CHOH^+, along with minor losses of $CH_3^{\bullet}$ and CO, which are both characterized by a large kinetic energy release [31].

The position of the label in the m/z 62 ions **3** generated by the (specific) loss of $CH_3C{=}O^{\bullet}$ from the metastable ions $DOCH(CH_3)C(=O)OCH_3^{\bullet+}$ and $HOCD(CH_3)C(=O)OCH_3^{\bullet+}$ has been examined. These isotopomers appear to produce ions **3**-CD_1 and **3**-OD_1 respectively (spectra not shown), which leads to proposal that the loss of $CH_3C{=}O^{\bullet}$ occurs analogously to that for HC=O$^{\bullet}$ from **1.**

*Formation of CH_2OH^+ from **1** : a direct bond cleavage reaction ?*

As shown in Table 3.1, metastable ions **1** and **2** show four more minor processes of which the generation of CH_2OH^+ is the most prominent. The losses of $CH_3^{\bullet}$ and CO have been discussed in detail before [15] : both losses were proposed to occur (by

direct bond cleavage) from the O···H···O bridged isomer **10**, $CH_3O(C=O)\cdots H\cdots O=CH_2^{\bullet+}$ to yield the product ions $O=C=O\cdots H\cdots O=CH_2^+$ and $CH_3O\cdots H\cdots O=CH_2^{\bullet+}$ respectively. In the earlier study it was proposed that **10** (see Figure 3.3) is directly generated from **1** but now an alternative mechanism is provided. It had already been proposed, see Scheme 3.4, that ion **5** can rearrange to **7** via a formaldehyde catalyzed 1,2-H shift.

Similarly, ion **5** can also isomerize to **10** again via a formaldehyde catalyzed 1,2-H shift followed by loss of CO, i.e. :

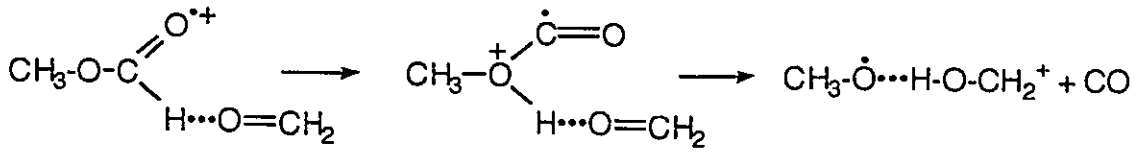

5 **10**

The formation of CH_2OH^+ from **1** could simply be formulated as a simple bond cleavage reaction, i.e., **1**→ $CH_2OH^+ + CH_3O\text{-}C=O^{\bullet}$. Isomer **2** could then form CH_2OH^+ after isomerization into **1**, according to Scheme 3.4. However, the labelling results (see below) do not support this proposal and there is a convincing energetic argument against it as well. The AE's for CH_2OH^+ generated from **1** and **2** were measured as 10.82 ± 0.05 and 10.96 ± 0.05 eV respectively [22] and these values lead to a common TS energy of 114 kcal/mol ($\Delta H_f[CH_3OC(=O)OCH_3]$ = -139 kcal/mol [23]). This TS energy is very close to that for loss of $HCO^{\bullet}$ (113 kcal/mol for both **1** and **2**), as expected for competing reactions. However, the calculated thermochemical threshold for $CH_2OH^+ + CH_3O\text{-}C=O^{\bullet}$ is 128 kcal/mol [20,29], far above the measured value ! Now, it is known that the radical $CH_3O\text{-}C=O^{\bullet}$ is thermodynamically less stable, by 19 kcal/mol [29], than the products $CH_3^{\bullet} + CO_2$; in fact the thermochemical threshold for

formation of $CH_2OH^+ + CO_2 + CH_3^\bullet$ is 109 kcal/mol which is slightly below the measured value. Hence, it is concluded that generation of CH_2OH^+ involves the (concerted?) formation of $CH_3^\bullet$ and CO_2.

Further evidence for this proposal comes from collisionally induced dissociative ionization (CIDI) experiments [30]. The CIDI mass spectrum of **1** and also that of **2**, see Figure 3.4a, is dominated by m/z 29 which results from ionization of $HCO^\bullet$, the dominant neutral lost in the MI spectrum. However, there is clearly no signal present at m/z 59, reionized $CH_3O\text{-}C{=}O^\bullet$, the ostensible neutral product formed together with CH_2OH^+. Note that this is not because $CH_3O\text{-}C{=}O^\bullet$ radicals are intrinsically unstable : they are clearly generated (along with CO) in the dissociation of dimethyl oxalate metastable ions, $CH_3OC(=O)C(=O)OCH_3^{\bullet+} \rightarrow CH_3O\text{-}C{=}O^+ + CH_3O\text{-}C{=}O^\bullet$, as witnessed by the m/z 59 signal in the CIDI spectrum, Fig. 3.4b. Thus the CIDI spectrum confirms the proposal that CH_2OH^+ is not generated by a simple bond cleavage in **1**. Rather, the ion may originate from the consecutive reactions **1**$\rightarrow [\mathbf{1}\text{-}CH_3]^+ \rightarrow CH_2OH^+ + CO_2$ or **1**$\rightarrow [\mathbf{1}\text{-}CO_2]^{\bullet+} \rightarrow CH_2OH^+ + CH_3^\bullet$ or from a synchronous formation of the neutrals.

Returning to the CIDI spectra of **1** and **2**, it is noted that a telltale peak is present at m/z 44, $CO_2^{\bullet+}$, which arises from reionized CO_2. Loss of CO_2 could not be detected in the MI spectrum of **1** and this suggests that the m/z 44 peak in Fig. 4a arises from **1**$\rightarrow [\mathbf{1}\text{-}CH_3]^+ \rightarrow CH_2OH^+ + CO_2$ or the "three particle" formation **1** $\rightarrow CH_2OH^+ + CO_2 + CH_3^\bullet$.

However, there is another possibility which should be considered : the MI spectrum of **2**, which shows a more intense CH_2OH^+ ion than **1**, also contains a signal at m/z 46, albeit of very low intensity (0.3 % of base peak at m/z 61). The source generated m/z 46 ions clearly have the structure $CH_3O(H)CH_2^{\bullet+}$, the only $C_2H_6O^{\bullet+}$ isomer which abundantly loses $CH_3^\bullet$ in its MI and CID spectrum, with a small energy release [32].

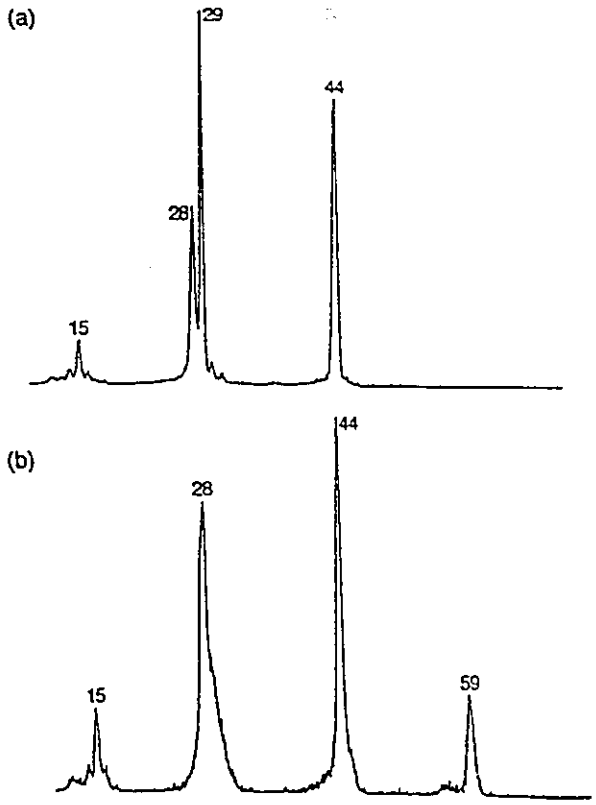

Figure 3.4. Collision-Induced Dissociative Ionization (CIDI) mass spectrum of : (a) ionized dimethylcarbonate, **2** and (b) ionized dimethyl oxalate. The CIDI spectrum of ionized methyl glycolate, **1**, is similar to that of **2** but with a more prominent m/z 29 signal.

Assuming that the metastably generated ions from **2** have this structure too, one could argue that the CH_2OH^+ ions in the MI spectra of **1** and **2** originate from the consecutive reaction **1** → **2**→ [**2**- CO_2]$^{\bullet+}$ → $CH_2OH^+ + CH_3^{\bullet}$. Formation of CH_2OH^+ from **1** would then involve communication with the PES of **2** and this, as shown by the following labelling results, is indeed likely.

Noting that all metastable losses from **2** show a very extensive degree of scrambling, the reactions of labelled ions **1** for the CH_2OH^+ formation are summarized in Table 3.4. The keto functionality does not appear in the CH_2OH^+ ion but the oxygen

and carbon atoms of the $HOCH_2$ and OCH_3 moieties have become indistinguishable. Note that one step, namely a degenerate 1,5-hydrogen shift in **9**, see Scheme 3.4, is sufficient to account for this result. The results for the D-labelled compounds indicate that significant H/D randomizations take effect of all hydrogen and deuterium atoms, but not to the statistical limit. For example, the statistical limit for $HOCH_2C(=O)OCD_3$ is m/z (31:32:33:34) = I (5:45:45:5) and so there is a measured surplus for m/z 31, CH_2OH^+. By trial and error the intensity distributions were found to be compatible with the following : 10 % of the formation of hydroxy methylium is atom-specific and involves the generation of the intact CH_2OH moiety, whereas 90 % of the ions undergo scrambling of the methylene and methyl hydrogen atoms via reversible 1,5-H shifts, i.e. **9** → **9'**; of these 90 % about half also undergo scrambling of all hydrogen atoms via reversible 1,4-H shifts, i.e. **9** → **2**, see Scheme 3.4. That ions **9** prefer 1,5-H shifts rather than 1,4-H shifts is not surprising since 1,5-H shifts invariably have lower activation energies than 1,4-H shifts.

When comparing the results for $HCO^\bullet$ loss and formation of CH_2OH^+ from **1**, it is seen that the less intense metastable peak (CH_2OH^+, see Table 3.1) is associated with more extensive H/D equilibrations (90 % vs. 26 %). This is precisely what is expected as the more intense metastable peak (loss of $HCO^\bullet$) may well have a slightly lower activation energy, so that a smaller fraction of these ions communicates with the PES of **2** where extensive scrambling takes place.

Thus the formation of CH_2OH^+ from **1** does not involve loss of $CH_3O\text{-}C{=}O^\bullet$ as an intact radical, neither does it involve the consecutive or concerted loss of $CH_3^\bullet$ and CO_2 prior to extensive communication with the PES of **2.** In fact, the reaction may well proceed

Table 3.4. Formation of $^{+}CH_2OH$ [a] from metastable methyl glycolate isotopologues[b].

Precursor molecule	m/z of daughter ion			
	31	32	33	34
$HOCD_2C(=O)OCH_3$	23	52	25	
$HOCH_2C(=O)OCD_3$	12	52	35	2
$DOCH_2C(=O)OCD_3$		21	57	22
$DOCH_2C(=O)OCH_3$	19	81		
$HOCH_2C(=^{18}O)OCH_3$	100			
$HOCH_2C(=O)^{18}OCH_3$	48		52	
$HOCH_2C(=O)O^{13}CH_3$	51	49		
$HOCH_2C(=O)^{18}O^{13}CH_3$	46			54

[a] Intensities relative to sum = 100 ; [b] For definition , see ref. 18.

from **2** or intermediates accessible to **2** via a low barrier. In the above section, the possibility of the sequence **1** → **2** → $[\mathbf{2}\text{-}CO_2]^{\bullet+}$ → $CH_2OH^+ + CH_3^{\bullet}$ is considered. However, there is an overriding energetic argument against this : as shown in ref. 32, the process $CH_3O(H)CH_2^{\bullet+} \rightarrow CH_2OH^+ + CH_3^{\bullet}$ has an energy barrier of c. 1.4 eV and therefore this consecutive reaction cannot explain the threshold generation of CH_2OH^+ from **1** / **2**. Therefore, the process may actually involve the sequence **1** → **2** → $[\mathbf{2}\text{-}CH_3^{\bullet}]^+ \rightarrow CH_2OH^+ + CO_2$ [33] or a concerted loss, perhaps from the O···H···O bridged ion **7**. Unfortunately, the extensive atom scrambling observed for this process prevents analysis of the product ion connectivities which would greatly facilitate a computational approach to elucidate the mechanism of this seemingly simple reaction.

Conclusions

There are now four experimentally well documented cases of radical cations of the type $HOCH(R_1)C(=O)R_2^{\bullet+}$ which may dissociate via intramolecular C-H···O bonding, *viz.* acetol, $R_1 = H$, $R_2 = CH_3$ [8], acetoin, $R_1 = R_2 = CH_3$ [27], methyl glycolate, $R_1 = H$, $R_2 = OCH_3$ and methyl lactate, $R_1 = CH_3$, $R_2 = OCH_3$ [this work]. These species all dissociate by loss of $R_1CO^{\bullet}$ by double hydrogen transfer. Because the molecular and product ions undergo little or no isotopic scrambling, the associated mechanism may be traced using specifically labelled compounds. The results lead to the conclusion that the above losses proceed via the C-H···O bonded intermediate $R_1C(H)=O\cdots H\text{-}C(=O)R_2^{\bullet+}$,**5**. It is further proposed, from *ab initio* calculations, that **5** do not lose $R_1CO^{\bullet}$ via a hydrogen atom shift from neutral $R_1C(H)=O$ to ionized $H\text{-}C(=O)R_2^{\bullet+}$. Rather, charge transfer takes place in **5** from $H\text{-}C(=O)R_2^{\bullet+}$ to the aldehyde which thus becomes charged. Because it is now charged, the aldehyde can rotate and donate a **proton** to $H\text{-}C(=O)R_2$ after which dissociation follows. The methyl glycolate system is complicated by the possibility of isomerization to the symmetrical species $CH_3OC(=O)OCH_3$, **2**, leading to loss of positional identity of labels; for loss of $HCO^{\bullet}$ this rearrangement plays a minor role and the mechanism is not compromised by it. However, for the minor processes, including formation of CH_2OH^+, this isomerization is almost complete and this seriously hampers the elucidation of the associated mechanisms. What is clear, however, is that formation of CH_2OH^+ is accompanied by the appearance of $CH_3^{\bullet}$ and CO_2 rather than the intact radical $CH_3OC{=}O^{\bullet}$, which is an unusual type of metastable dissociation.

References

1 J.J. Thomson : Rays of Positive Electricity and Their Application to Chemical Analysis, Longmans, Green & Co., Ltd., London (1913).

2 W.A. Bryce, in C.A. McDowell (Ed.), Mass Spectrometry, McGraw-Hill, New York, Chapter 3 (1963).

3 A.O. Nier, *Phys. Rev.*, **50**, 212 (1940).

4 H.A. Straus, *Phys. Rev.*, **59**, 430 (1941).

5 (a) A.O. Nier, T.R. Roberts and E.G. Franklin, *Phys. Rev.*, **75**, 346 (1949); (b) A.O. Nier and T.R. Roberts, *Phys. Tev.*, **81**, 507 (1951); (c) T.L. Collins, A.O. Nier and W.H. Johnson, *Phys. Rev.*, **84**, 717 (1951).

6 See for example : (a) J.L. Holmes, *Org. Mass Spectrom.*, **28**, 1388 (1993); (b) S. Meyerson, *Anal. Chem.*, **66**, 960 (1994).

7 N. Heinrich, T. Drewello, P.C. Burgers, J.C. Morrow, J. Schmidt, W. Kulik, J.K. Terlouw and H. Schwarz, *J. Am. Chem. Soc.*, **114**, 3776 (1992).

8 M. George, C.A. Kingsmill, D. Suh, J.K. Terlouw and J.L. Holmes, *J. Am. Chem. Soc.*, **116**, 7807 (1994).

9 N. Heinrich and H. Schwarz, in J.P. Maier (Ed.), Ion and Cluster Ion Spectroscopy and Structure, Elsevier, Amsterdam, p. 329 (1989).

10 P.C.Burgers and J.K.Terlouw, in M. E. Rose (Ed.), Specialist Periodical Reports : Mass Spectrometry, The Royal Society of Chemistry , London, Vol. 10, Ch. 2 (1989).

11 R.D. Bowen, *Org. Mass Spectrometry*, **28**, 1577 (1993).

12 N. Heinrich, J. Schmidt, H. Schwarz and Y. Apeloig, *J. Am. Chem. Soc.*, **109**, 1317 (1987).

13 J.M.H. Pakarinen, P. Vainiotalo, T.A. Pakkanen and H.I. Kenttämaa, J. *Am. Chem. Soc.*, **115**, 12431 (1993).

14 J.D.S. Golden and D.J. Manning, *Org. Mass Spectrom.*, **3**, 1467 (1970).

15 P.C. Burgers, J.L. Holmes, C.E.C.A. Hop, R. Postma, P.J.A. Ruttink and J.K. Terlouw, *J. Am. Chem. Soc.*, **109**, 7315 (1987).

16 H. Halim, Ph.D thesis, Technische Universität Berlin (1986).

17 B.L.M. van Baar, H. Halim, J.K. Terlouw and H. Schwarz, *J. Chem. Soc. Chem. Commun.*, 728 (1986).

18 J.I. Seeman, H.V. Secor, R. Disselkamp and F.R. Bernstein, *J. Chem. Soc. Chem. Commun.*, 713 (1992).

19 See for example : P.C. Burgers, A.A. Mommers and J.L. Holmes, *J. Am. Chem. Soc.*, **105**, 5976 (1983) .

20 (a) S.W. Benson, Thermochemical Kinetics, 2nd ed. Wiley-Interscience, New York (1976); (b) S.G. Lias, J.E. Bartmess, J.F. Liebman, J.L. Holmes, R.D. Levin and W.G. Mallard, *J.Phys. Chem. Ref. Data*, **17** (suppl. 1) (1988).

21 (a) W.J. Bouma, R.H. Nobes and L. Radom, *Org. Mass Spectrom.*, **17**, 315 (1982); (b) P.C. Burgers and J.L. Holmes, *Org. Mass Spectrom.*, **19**, 452 (1984); (c) E.E. Ferguson, J. Roncin and L. Bonazolla, *Int. J. Mass Spectrom. Ion Processes*, **79**, 215 (1987).

22 F.P. Lossing, unpublished results

23 M.C. Blanchette, J.L. Holmes, C.E.C.A. Hop, F.P. Lossing, R. Postma, P.J.A. Ruttink and J.K. Terlouw, *J. Am. Chem. Soc.*, **108**, 7859 (1986).

24 P.J.A. Ruttink, P.C. Burgers and J.K. Terlouw,*Can. J. Chem.* (1995) submitted.

25 P.J.A. Ruttink and P.C. Burgers, *Org. Mass Spectrom.* **28**, 1087 (1993).

26 D.R. Lide (Ed.), Handbook of Chemistry and Physics, 73rd edn, CRC Press, Baca Raton, Fl (1992).

27 D. Suh, P.C. Burgers and J.K. Terlouw, *Int. J. Mass Spectrom. Ion Processes*, **144**, L1 (1995).

28 S. Hammerum, T. Vulpius and H.-E. Audier, *Org. Mass Spectrom.*, **27**, 369 (1992).

29 J.L. Holmes, F.P. Lossing and P.M. Mayer, *J. Am. Chem. Soc.*, **113**, 9723 (1991).

30 S. Tajima, Y. Nagai, O. Sekiguchi, M. Fujishige and N. Uchida, *J. Am. Soc. Mass Spectrom.*, **6**, 202 (1995).

31 See for example : J.K. Terlouw and H. Schwarz, *Angew. Chem. Int. Ed. Engl.*, **26**, 805 (1987).

32 (a) P.C. Burgers, J.L. Holmes, J.K. Terlouw and B. van Baar, *Org. Mass Spectrom.*, **20**, 202 (1985); (b) R. Postma, P.J.A. Ruttink, B. van Baar, J.K. Terlouw, J.L. Holmes and P.C. Burgers, *Chem. Phys. Letters*, **123**, 409 (1986).

33 Note that loss of $CH_3^{\bullet}$ is associated with a large kinetic energy release (KER) (see Table 1) whereas CH_2OH^+ is produced with little extra translational energy. This is not to say that CH_2OH^+ cannot be generated via $[M\text{-}CH_3^{\bullet}]^+$: it is usually only the lower end of the first KER that is effective inconsecutive reactions and thus the overall value for the KER will be smaller than that for loss of $CH_3^{\bullet}$: see C.J. Proctor, B. Kralj, A.G. Brenton and J.H. Beynon, *Org. Mass Spectrom.*, **15**, 619 (1980).

CHAPTER 4

Low energy acetoin ions $CH_3C(=O)C(H)(OH)CH_3^{\bullet+}$ decompose to $CH_3CO^{\bullet}$ and CH_3CHOH^+ via a remarkable "hidden rearrangement"

C-H···O bonded ions are being increasingly postulated as intermediates to rationalize the dissociation chemistry of oxygen containing radical cations [1]. However, at first sight their O···H···O bonded isomeric forms are more attractive intermediates because of their higher thermodynamic stability [1a,b]. A case in point is ionized acetol, $CH_3C(=O)CH_2OH^{\bullet+}$ whose remarkable dissociation behaviour has very recently been rationalized in terms of O···H···O [2] and C-H···O [3] bonded intermediates. The metastable molecular ions decay in the μs time-frame, by double hydrogen transfer, to $CH_3CHOH^+ + HCO^{\bullet}$. Based on characteristic ion/molecule reactions, Pakarinen et al. [2] proposed a mechanism involving the O···H···O bonded key intermediate **a,** (Eq. (1)) :

$$CH_3C(=O)CH_2OH^{\bullet+} \rightarrow [CH_3C=O\cdots H\cdots O=CH_2]^{\bullet+},\ \mathbf{a} \rightarrow [CH_3C(H)=O\cdots H\cdots O=CH]^{\bullet+} \rightarrow CH_3CHOH^+ + HCO^{\bullet} \qquad (1)$$

The work described here was published under the above title:

D. Suh, P.C. Burgers and J.K. Terlouw, *Int. J. Mass Spectrom. Ion Processes*, **144**, L1 (1995).

George et al. [3] found this pathway to be incompatible with their D labelling experiments and they derived a mechanism supported by *ab initio* MO calculations involving the C-D···O bonded ion **b**, (Eq. (2)) :

$$CH_3C(=O)CH_2OD^{\bullet+} \rightarrow CH_3C^+(=O)\cdots O(D)CH_2^{\bullet} \rightarrow [CH_3C(=O)\text{-}D\cdots O{=}CH_2]^{\bullet+}\ \mathbf{b} \rightarrow CH_3CDOH^+ + HCO^{\bullet} \qquad (2)$$

The latter mechanism is based, inter alia, on the key observation that the hydroxyl D atom , as shown above, turns up in the product ion at the carbenium carbon atom, *not* at the oxygen atom. It also provides an attractive rationale for the loss of $RCO^{\bullet}$ from ionized methyl glycolate, $HOCH(R)C(=O)OCH_3^{\bullet+}$ (R = H) and methyl lactate (R = CH_3) [4].

Ionized acetol's higher homologue ionized acetoin, $CH_3C(=O)C(H)(OH)CH_3^{\bullet+}$, **1**, undergoes one abundant dissociation in the μs timeframe, viz. **1** → $CH_3CO^{\bullet}$ + CH_3CHOH^+, **4**, prima facie a simple bond cleavage reaction. The structure of the $C_2H_5O^+$ product ion **4**, generated from *metastable* ions **1**, was established through comparative collision experiments using a BE_1E_2 mass spectrometer (B = magnet, E = electric sector) as described in ref. 3. The structure of the $C_2H_3O^{\bullet}$ radical, $CH_3C{=}O^{\bullet}$, was determined by collision-induced dissociative ionization (CIDI) mass spectrometry [5].

From energetic measurements, it follows that the reaction produces the CH_3CHOH^+ product ion **4** close to the thermochemical threshold : the critical energy is only 8 ± 1 kcal/mol #1,but nevertheless the reaction produces a very intense metastable peak, ~ 3 % of the unperturbed ion beam. Very intense [9] and exceedingly narrow [10] metastable peaks – the associated kinetic energy release measured at half height

#1 Appearance energy $C_2H_5O^+$ = 10.02 ± 0.05 eV [6]. This value leads, using ΔH_f [acetoin] = -94.6 kcal/mol (by additivity [7], and using -5 kcal/mol for the term C(H)(CO)(C)(O) [6]) and ΔH_f [$CH_3C{=}O^{\bullet}$] is -6 kcal/mol [8], to a measured ΔH_f $CH_3C(H)OH^+$ of 142 ± 1 kcal/mol, close to the known value of 139±1 kcal/mol [8]. The ionization energy of acetoin is 9.68 ± 0.05 eV [6].

($T_{0.5}$) is only 0.07 kcal/mol – have been linked to dissociation of intermediate ion-dipole complexes and so it is surmised that the above ostensible simple bond cleavage might in actuality be ion-dipole mediated. In fact, as an alternative to simple bond cleavage, loss of $CH_3C{=}O^{\bullet}$ from **1** could proceed analogous to loss of $HC{=}O^{\bullet}$ from ionized acetol i.e. (Eq. (3)) :

$$CH_3C(=O)CH(OD)CH_3^{\bullet+}, \textbf{1}\text{-OD} \rightarrow CH_3C^{+}(=O)\cdots O(D)CHCH_3^{\bullet}, \textbf{2} \rightarrow$$
$$[CH_3C(=O)\text{-}D\cdots O{=}C(H)CH_3]^{\bullet+}, \textbf{3} \rightarrow CH_3CDOH^{+}, \textbf{4}\text{-CD} + CH_3CO^{\bullet} \qquad (3)$$

Note that complex **2** could also dissociate directly to CH_3CHOD^{+}, **4**-OD. If these processes , i.e. Eq. (3) and direct dissociations, are in competition then for **1**-OD a mixture of $CH_3C(D)OH^{+}$, **4**-CD, and $CH_3C(H)OD^{+}$, **4**-OD, should be formed. As shown in ref. [3], the position of the label in ions **4** can be determined by comparative MS/MS/MS experiments and indeed the CID mass spectrum of the ions generated by loss of $CH_3C{=}O^{\bullet}$ from metastable **1**-OD (not shown) was clearly compatible with a mixture of **4**-OD and **4**-CD. Next, the isotopomer $CH_3C(=^{18}O)C(H)(OH)CH_3^{\bullet+}$, **1**-CO* (obtained by exchange of acetoin with $H_2{}^{18}O$ in acid medium) was examined. Metastable ions **1**-CO* form not only $CH_3C(H)OH^{+}$, **4**, but also $CH_3C(H)^{18}OH^{+}$, **4**-*OH, in a 1 : 1 ratio, again compatible with competition of direct bond cleavage and rearrangement , see Eq (3). The CID mass spectrum of metastably generated **4**-*OH from **1**-CO* is shown in Fig. 4.1A. Further, the doubly labelled metastable ion $CH_3C(=^{18}O)CH(OD)(CH_3)^{\bullet+}$, **1**-ODCO*, forms m/z 46 and m/z 48 ions. Their CID mass spectra are shown in Fig. 4.1B and C respectively : the m/z 46 spectrum (Fig. 4.1B) was superimposable upon that of metastably generated reference ions $CH_3C(H)OD^{+}$ (produced by loss of $DCO^{\bullet}$ from $CH_3C(=O)CD_2OH^{\bullet+}$ or loss of $H^{\bullet}$ from $CH_3CH_2OD^{\bullet+}$ [3]). The m/z 48 ion could be $CH_3C(D)^{18}OH^{+}$, **4**-CD*OH, and/or $CH_3C(H)^{18}OD^{+}$, **4**-*OD. Figure 4.1D shows the CID mass

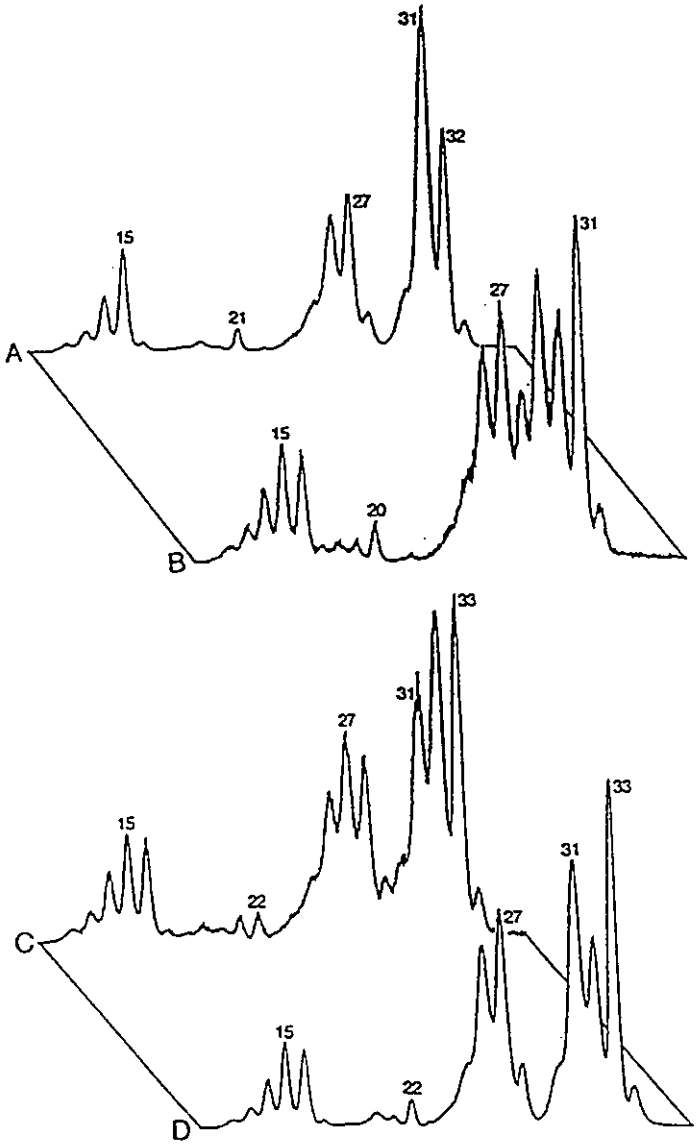

Figure 4.1. Partial CID mass spectra of product ions from dissociation reactions of metastable acetoin and ethanol ions:

(A) $CH_3CH^{18}OH^+$ from $CH_3C(=^{18}O)C(H)(OH)CH_3^{\bullet+} \rightarrow C_2H_5{}^{18}O^+ + CH_3CO^{\bullet}$;

(B) CH_3CHOD^+ from $CH_3C(=^{18}O)C(H)(OD)CH_3^{\bullet+} \rightarrow C_2H_4DO^+ + CH_3C^{18}O^{\bullet}$;

(C) $CH_3CD^{18}OH^+$ from $CH_3C(=^{18}O)C(H)(OD)CH_3^{\bullet+} \rightarrow C_2H_4D^{18}O^+ + CH_3CO^{\bullet}$;

(D) $CH_3CH^{18}OD^+$ from $CH_3CH_2{}^{18}OD^{\bullet+} \rightarrow C_2H_4D^{18}O^+ + H^{\bullet}$.

spectrum of pure reference ions **4**-*OD (from the metastable loss of H$^{\bullet}$ from $CH_3CH_2{}^{18}OD^{\bullet+}$). Comparison of Fig. 4.1C and D leaves little doubt that the m/z 48 ions generated from **1**-ODCO* have the connectivity of the isotopomer $CH_3C(D){}^{18}OH^+$, **4**-CD*OH.

The above observations can be rationalized on the basis of competition between simple bond cleavage and a rearrangement as depicted in Eq. (3). They rule out a mechanism involving O···H···O bonding like the one proposed by Pakarinen et al. [2] for acetol ions.

The product ion ratio for simple bond cleavage and rearrangement of **1**-CO* is exactly 1:1. The ratio for **1**-ODCO* is 1.6 : 1 and this results, see below, from a ZPVE (zero-point vibrational energy) isotope effect. The 1:1 ratio could be a coincidence but the current *ab initio* calculations for acetol [11], when applied to acetoin, point to a mechanism which would nicely account for the observed degeneracy. For acetol, a transition state with structure $[CH_3C(H)=O\cdots H\cdots C(H)=O]^{\bullet+}$ (TS **3b-5a** in ref. 3) was located for the transformation $[CH_3C(=O)\text{-}H\cdots O=CH_2]^{\bullet+}$ **b** → $CH_3C(H)OH^+$ + HCO$^{\bullet}$; this reaction would require rotation of the $O=CH_2$ unit, but the calculations did not provide evidence for such a rotation [3]. It has now been found [11] that this TS actually connects the products, not with **b** but rather with the H-bridged complex $CH_3C(H)=O\cdots H\text{-}C(H)=O^{\bullet+}$, **c**, where the charge is on the formaldehyde moiety, and which can produce the products by *proton* transfer. By contrast, in ion **b** the charge is on the acetaldehyde unit and to generate $CH_3C(H)OH^+$ therefrom requires an H-*atom* shift, which, according to the calculations requires too much energy. Instead, these ion **b** can transform to **c** via the charge-transfer complex $[CH_3C(H)=O\cdots O=CH_2]^{\bullet+}$ [11]. Preliminary calculations indicate that a similar sequence can also occur in **1** and by analogy to acetol ions the sequence of events depicted in Scheme 4.1 is derived.

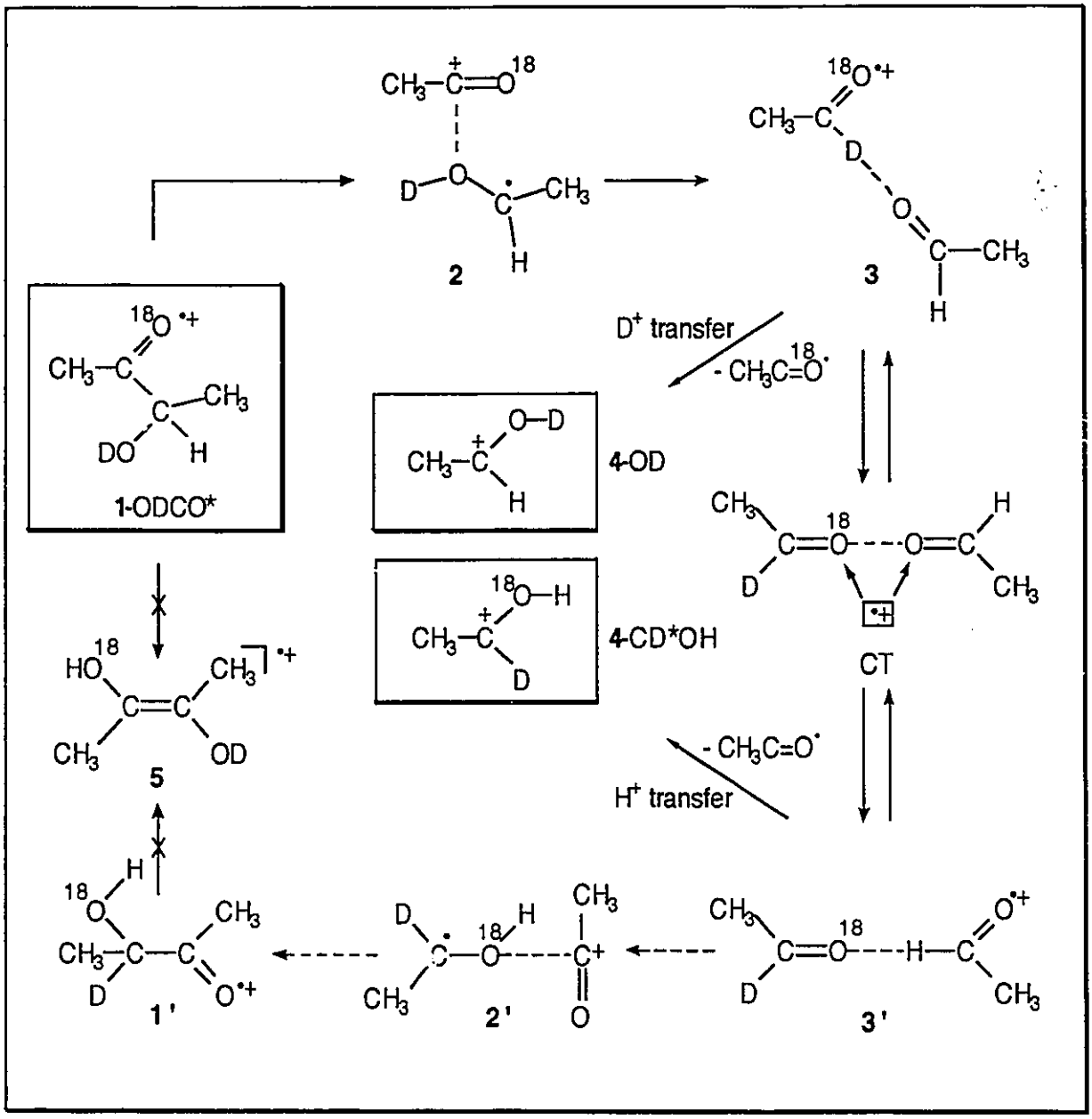

Scheme 4.1

Elongation of the central C-C bond in **1** does not immediately lead to dissociation, but rather to the ion-dipole complex **2**, where the CH_3CO^+ cation interacts with the $CH_3C(H)OH^•$ dipole. Next, the $CH_3C(H)OH^•$ moiety can donate the hydroxyl hydrogen to

the acetyl cation [12] to generate **3**. In this species the charge is on the $CH_3C(D)=^{18}O^{\bullet+}$ unit and to generate $CH_3C(D)^{18}OH^+$ from **3** requires an H-atom shift, which, see above, would be too energy demanding to occur within the narrow energy constraint (8 kcal/mol) imposed by experiment. Ions **3**, it is proposed, have two other options : (i) they can donate a *deuteron* (D^+) to the neutral $CH_3C(H)=O$ unit to produce $CH_3C(H)OD^+$ + $CH_3C^{18}O^{\bullet}$; (ii) since **3** is an ion-dipole complex, the neutral $CH_3C(H)=O$ can migrate within the electrostatic field of the $CH_3C(D)=^{18}O^{\bullet+}$ion. In this step, **3**→CT→**3'**, the relative orientation of the two acetaldehyde units is changed such that the dipole moments of the two moieties are oriented towards each other and charge transfer (CT) may take place easily. Such a charge transfer complex was also proposed as the key step in the unimolecular chemistry of ionized ethylene glycol [13]. The equilibria in Scheme 4.1 would account for the observed 1:1 product ion ratio. Considering that the product ion ratio **4** : **4**-*OH from **1**-CO* remained 1:1 upon collisional activation #2 and that only 8 kcal/mol is available to **1**, the interconversions depicted in Scheme 4.1 are very facile processes indeed.

#2 The CID mass spectrum of **1** remains dominated by the m/z 45 $CH_3C(H)OH^+$ ion but two more prominent peaks appear, viz. m/z 43 (CH_3CO^+, 20 %) and m/z 44 (17 %). The m/z 44 ions clearly are $CH_2=C(H)OH^{\bullet+}$ and not $CH_3C(H)=O^{\bullet+}$: the $T_{0.5}$ value for the 3ffr metastable loss of $H^{\bullet}$ from the 2ffr collisionally formed ions was large, 430 meV [14]. Formation of $CH_2=C(H)OH^{\bullet+}$ requires 8 kcal/mol more than formation of $CH_3C(H)OH^+$ [8] and is therefore absent in the MI spectrum. Most simply, these ions are formed from **2** (and **2'**) via donation of the $HOC(H)CH_3$ methyl hydrogens to the acetylium ion. For **1**-CO*, m/z 44 is split into m/z 44 and m/z 46 in a ratio of 1:1, whereas for **1**-d m/z 44 shifts to m/z 45, as expected from Scheme 4.1.

Neutralization-Reionization (NR) experiments [15] further support the intermediacy of ion-dipole complexes in the dissociation of **1** : one-electron reduction of **1** with cyclopropane followed by reionization with O_2 does not yield a detectable recovery signal in the NR spectrum but to signals due to decomposition of neutralized **1** into $CH_3CO^{\bullet}$, $CH_3C(H)=O$ and/or $CH_2=C(H)OH$, and $CH_3C(H)OH^{\bullet}$. These findings strongly point to collapse of **1** (whose neutral counterpart is stable) to species which have no neutral counterpart, such as **2** and **3**, and which after reduction disintegrate to $CH_3CO^{\bullet}$, $CH_3C(H)=O$ and $CH_3C(H)OH^{\bullet}$.

The preferred formation of $CH_3C(H)OD^+$ over $CH_3C(D)^{18}OH^+$ from **1**-ODCO* vis `a vis the equal product ratios for **1**-CO*, can be rationalized in terms of isotopic fractionation resulting from differences in the ZPVE's of the products, analogously to the behaviour of the N-acetyliminium ion [16]. Calculations using the DZP (double zeta + polarization) [17] basis set yield 4021 cm^{-1} for the O-H bond stretch frequency in $CH_3C(H)OH^+$, whereas that for the C-H bond is much smaller, 3362 cm^{-1}. The ZPVE difference (using a scaling factor of 0.9 [18]) between $CH_3C(H)OD^+$, **4**-OD and $CH_3C(D)^{18}OH^+$, **4**-CD*OH, is then calculated to be 0.24 kcal/mol in favour of **4**-OD. Although small, this difference is larger than the average kinetic energy release (0.14 kcal/mol) and thus **4**-OD is, at threshold, formed at a faster rate than **4**-CD*OH, i.e. the deuterium atom prefers the stronger bond of the product ion.

Finally, a simple but incorrect alternative explanation for the 1:1 product ratio observed for **1**-ODCO* might be proposed. Ions **1**-ODCO* and **1'**, see Scheme 4.1, are formally related by 1,3-hydrogen shifts via the (very stable) ionized enediol $CH_3(DO)C=C(^{18}OH)CH_3^{\bullet+}$, **5**, and a facile interconversion **1**-ODCO* → **5** → **1'** would account for the observed 1:1 ratio. However, such 1,3-hydrogen shifts are known to have much larger activation energies than the energy (8 kcal/mol) available to **1**, e.g.

for acetol ions the barrier for the analogous 1,3-H shift was calculated to be 28.4 kcal/mol [19]. To remove all ambiguity, the unlabelled isotopomer of **5** (from ionized $CH_3C(=O)C(OH)(CH_3)CH_2OH$ [20], by loss of CH_2O) has independently been generated and, not unexpectedly for an ionized enediol, an intense recovery signal was observed in its characteristic NR spectrum. As mentioned above, no such signal could be detected in the NR spectrum of **1**.#3

Summarizing, it is concluded that the $CH_3CO^{\bullet}$ loss from low energy acetoin ions is a truly hidden rearrangement reaction [23] and is proposed that the sequence sketched in Scheme 4.1 provides a rationale for this remarkable dissociation behaviour. Further work is in progress and will be published in due course. Finally it is noted that the results and the proposed mechanism indicate that *ionized* secondary α-ketols may well dissociate via double hydrogen transfer [24] in addition to or to the exclusion of decay via thermally induced processes of the neutral molecules [25], but that *ionized* tertiary α-ketols cannot undergo such fragmentations [25].

#3 The above type of rearrangement through an enediol is known to occur in neutral systems , for example in the interaction of reducing sugars with aqueous alkali, the Lobry de Bruyn and Alberda van Ekenstein rearrangement [21] or the acid-catalyzed acyloin transformation of α-ketols [22] and so it is conceivable that the rearrangement **1** → **1'** takes place in *molecules* thermally energized in the inlet system of the mass spectrometer. However, from the intensity ratio of m/z 45 : m/z 47 in the normal mass spectrum (4 : 1, corrected for unlabelled material) it follows that thermal rearrangement occurs, if at all, to no more than 20 %. In fact, it can reasonably be argued that the above m/z 47 is the result of rearrangement of the ions (Scheme 4.1) and that high energy molecular ions prefer (80 %) direct cleavage to m/z 45.

References

1 For selected references see : (a) N. Heinrich and H. Schwarz, in J.P. Maier (Ed.), Ion and Cluster Ion Spectroscopy and Structure, Elsevier, Amsterdam, p. 329 (1989); (b) P.C.Burgers and J.K.Terlouw, in M. E. Rose (Ed.), Specialist Periodical Reports : Mass Spectrometry, The Royal Society of Chemistry , London, Vol. 10, Ch. 2 (1989); (c) R.D. Bowen, *Org. Mass Spectrometry*, **28**, 1577 (1993).

2 J.M.H. Pakarinen, P. Vainiotalo, T.A. Pakkanen and H.I. Kenttämaa, *J. Am. Chem. Soc.*, **115**, 12431 (1993).

3 M. George, C.A. Kingsmill, D. Suh, J.K. Terlouw and J.L. Holmes, *J. Am. Chem. Soc.*, **116**,7807 (1994).

4 D. Suh, C.A. Kingsmill, P.J.A. Ruttink, P.C. Burgers and J.K. Terlouw, *Int. J. Mass Spectrom. Ion Processes*, **146/147**, 305 (1995).

5 P.C. Burgers, J.L. Holmes, A.A. Mommers, J.E. Szulejko and J.K. Terlouw, *Org. Mass Spectrom.*, **19**, 442 (1984).

6 F.P. Lossing and J.L. Holmes, private communication 1994.

7 S.W. Benson, Thermochemical Kinetics, 2nd ed. Wiley-Interscience,New York (1976).

8 S.G. Lias, J.E. Bartmess, J.F. Liebman, J.L. Holmes, R.D. Levin and W.G. Mallard, *J.Phys. Chem. Ref. Data*, **17** (suppl. 1) (1988).

9 J-D Shao, T. Baer, J.C. Morrow and M.L. Fraser-Monteiro, *J. Chem. Phys.*, **87**, 5242 (1987).

10 For selected references see : (a) S. Hammerum, *Mass Spectrom. Rev.* **7**, 123 (1988); (b) P.J.A. Ruttink, *J. Phys. Chem.*, **91**, 703 (1987).

11 P.J.A. Ruttink, P.C. Burgers and J.K. Terlouw, *Can. J. Chem.* (1995) submitted.

12 N. Heinrich and H. Schwarz, *Int. J. Mass Spectrom. Ion Processes*, **79**, 293 (1987).

13 P.J.A. Ruttink and P.C. Burgers, *Org. Mass Spectrom.*, **28**, 1087 (1993).

14 J.L. Holmes and J.K. Terlouw, *Can. J. Chem.*, **53**, 2076 (1975).

15 For a recent review see : N. Goldberg and H. Schwarz, *Acc. Chem. Res.*, **27**, 347 (1994).

16 P.C. Burgers, C.A. Kingsmill, G.A. McGibbon and J.K. Terlouw, *Org. Mass Spectrom.*, **27**, 398 (1992).

17 T.H. Dunning, Jr, *J. Chem. Phys.* , **53**, 2823 (1970).

18 J.A. Pople, H.B. Schlegel, R. Krishan, D.J. de Frees, J.S. Binkley, M.J. Frisch, R.A. Whiteside, R.F. Hout, Jr and W.J. Hehre, *Int. J. Quantum. Chem.*, **15**, 269 (1981).

19 C.A. Kingsmill and J.K. Terlouw, unpublished UMP3/6-31G*//4-31G + ZPVE result.

20 J. Cologne and Y. Vaginay, *Bull. Soc. Chim. France*, 3140 (1965).

21 J.C. Sowden and R. Schaffer, *J. Am. Chem. Soc.*, **74**, 505 (1952).

22 A.E. Favorskii, *Bull. Soc. Chim. France*, **39**, 216 (1926).

23 H. Schwarz, *Top. Curr. Chem.*, **97**, 1 (1981).

24 M.J. Frearson and D.J. Brown, *J. Chem. Soc. (C)*, 2909 (1968).

25 (a) R.T. Aplin and M.J. Frearson, *Chem. and Ind.*, 1663 (1969); (b) C.A. Brown and C. Djerassi, *J. Chem. Soc. (C)*, 2550 (1969).

CHAPTER 5

The Unimolecular Chemistry of the Enol of Ionized Methyl Glycolate : Formation of the Hydrogen-Bridged Radical Cation $[CH_3\text{-}O(H)\cdots H\cdots O{=}CH]^{\bullet +}$

In solution the keto-enol tautomeric equilibrium generally favours the keto structure [1]. This is because in general neutral ketones are less acidic (i.e. have lower heats of formation, ΔH_f), than their enol counterparts. It is now well known that one-electron oxidation of organic molecules often leads to a reversal of thermodynamic stability; for example, enol radical cations are invariably more stable than their ketone tautomers [2].

Nevertheless, large barriers for keto-enol transformations may prevent enolization of solitary ketone radical cations. Thus, prior to dissociation ionized acetone does not rearrange to the more stable enol form, because the barrier for the 1,3-hydrogen shift is prohibitively high, 51 kcal/mol [3]. By contrast, in ionized methyl acetate, the almost complete loss of positional identity of the hydrogen atoms observed to take place prior to dissociation has been interpreted in terms of fast keto-enol tautomerizations. In this

The work presented here has been appeared in an article having the same title:

D. Suh, P.C. Burgers and J.K. Terlouw, *Rapid Commun. Mass Spectrom.*, **9**, 862 (1995).

case the tautomerization takes place via a more circuitous route through a distonic ion, eq (1) (R = H), which can be formed from the keto (and the enol ion) via a facile 1,4-hydrogen shift, requiring only 11 kcal/mol [4] ; thus the distonic ion greatly accelerates tautomerization.

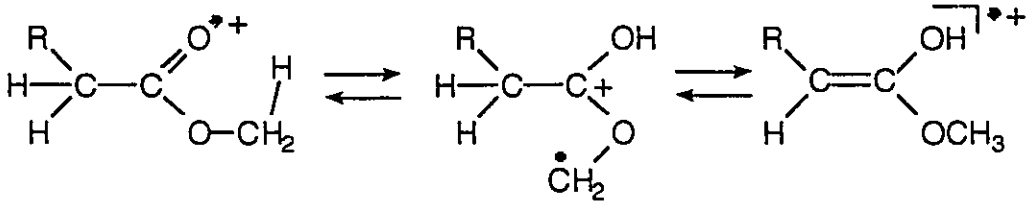

1[keto]$^{\bullet+}$ **3**[distonic]$^{\bullet+}$ **2**[enol]$^{\bullet+}$ (1)

Recently, the unimolecular chemistry of ionized methyl glycolate, $HOCH_2C(=O)OCH_3^{\bullet+}$,**1** (R=OH) [5a] was studied in detail. Metastable ions **1** undergo one major dissociation, *viz.* loss of HCO$^{\bullet}$ to produce H-C(OH)OCH_3^+ with a surprisingly small activation energy (0.3 eV) and with surprisingly limited (~24%) hydrogen randomization reactions. It was proposed that the hydrogen atoms became indistinguishable by isomerization of **1** into ionized dimethyl carbonate, CH_3O-C(=O)-$OCH_3^{\bullet+}$. Although no evidence was found for the intermediacy of the enol ions $HOCH=C(OH)OCH_3^{\bullet+}$, **2**, five of the six hydrogen atoms in **1** could lose their positional identity by a facile keto-enol tautomerization via the distonic ion $HOCH_2C(OH)OCH_2^{\bullet+}$,**3**, eq.(1), R = OH. To investigate this possibility ion **2** (see eq. (2)) has been generated via two independent pathways, *viz.* by the McLafferty rearrangement of ionized methyl 2-hydroxy-isovalerate, **M1**, and dimethyl tartrate, **M2**, and its, as will become evident, intriguing unimolecular chemistry has been investigated.

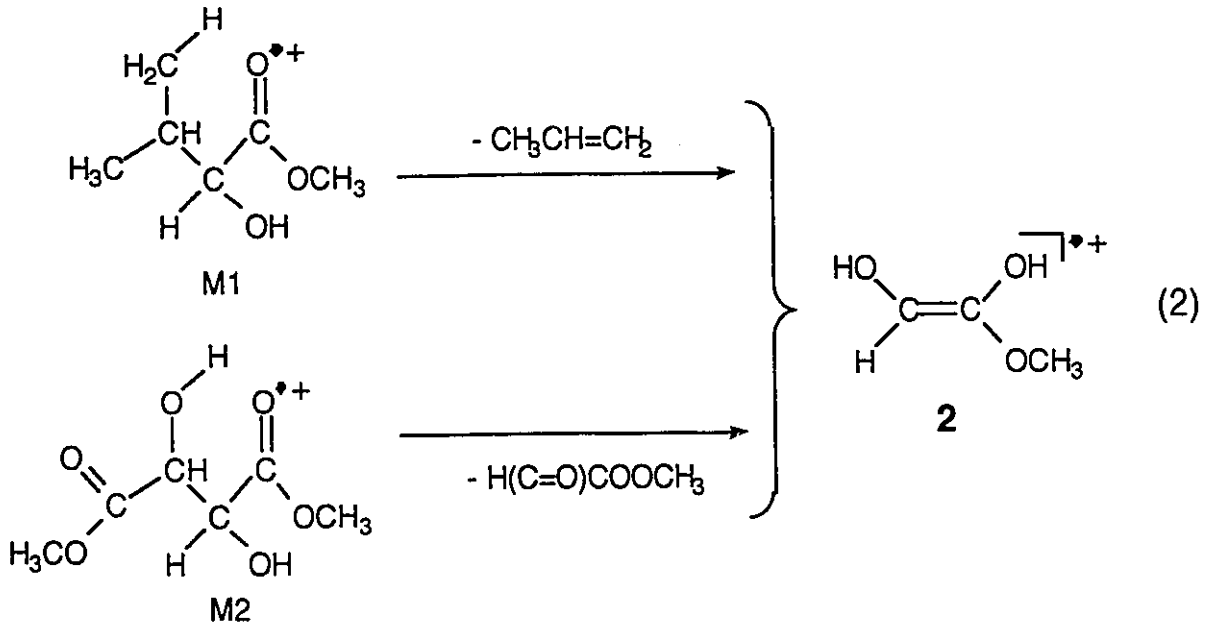

Results and discussion

The metastable ion (MI) spectra of **2** and its keto form **1** [5a] are given in Table 5.1. It is seen that these spectra are totally different : thus, while metastable ions **1** decay almost completely via loss of HCO•, ions **2** do not undergo this reaction at all. Rather, they dissociate by four competing channels, namely to CH_3•, CO and to the conjugate pair CH_3OH and $CH_3OH_2^+$. Note that for the reactions of the same stoichiometry (losses of CH_3• and CO) different amounts of kinetic energy are released ($T_{0.5}$ values in Table 1). These results indicate that **1** and **2** do not interconvert prior to dissociation. Assuming that such a tautomerization would most easily proceed via **3**, the above results show that either **1** $\rightleftarrows$ **3** and/or **2** $\rightleftarrows$ **3** does not occur.

Table 5.1 Reactions of the metastable methyl glycolate ion (1) and its enol (2).

	Daughter ion formed and/or neutral lost[a]					
Precursor ion	CH_2OH^+	$CH_3OH_2^+$	CH_3OH	$HCO^\bullet$	CO	$CH_3^\bullet$
$HOCH_2C(=O)OCH_3^{\bullet+}$, **1**	4 [56]	-	-	100 [22]	1 [230]	2 [570]
$HOCH=C(OH)OCH_3^{\bullet+}$, **2**	-	35 [50]	75 [38]	-	50 [330]	100 [68]
$DOCH=C(OD)OCH_3^{\bullet+}$, **2**-$(Od)_2$	-	15[b]	20[c]	-	15	100

[a] MI spectra obtained in the second field-free region (8 keV ions) using precursor ion M2. The intensities (± 5 %) are relative to base peak equal to 100 % ; the values in parentheses refer to kinetic energy release (meV), measured from the peak width at half height ($T_{0.5}$). [b] Connectivity is $CH_3OD_2^+$ determined by comparative MS/MS/MS experiments. [c] Connectivity is CH_3OD determined by comparative MS/MS/MS experiments.

Reactions of metastable ions ***2***

Since it is concerned with competing, slow dissociations, all four dissociations probably have similar energy requirements, although for the loss of CO ($T_{0.5}$ = 330 meV, see Table 5.1) a large reverse term may be involved. An estimation of the critical energy for these dissociations comes from the following. From Table 5.1 it is seen that loss of CH_3OH has the smallest T value, $T_{0.5}$ = 38 meV, and so it may be reasonably assumed that this reaction has the smallest reverse term. The collision-induced dissociation (CID) mass spectrum of the $[M\text{-}CH_3OH]^{\bullet+}$ product ions generated from metastable ions of **2** is shown in Fig. 5.1A. It contains intense peaks at m/z 30, which tandem (MS/MS/MS) experiments show is $HOCH^{\bullet+}$ [6], m/z 29, $HC{=}O^+$, and m/z 41, loss

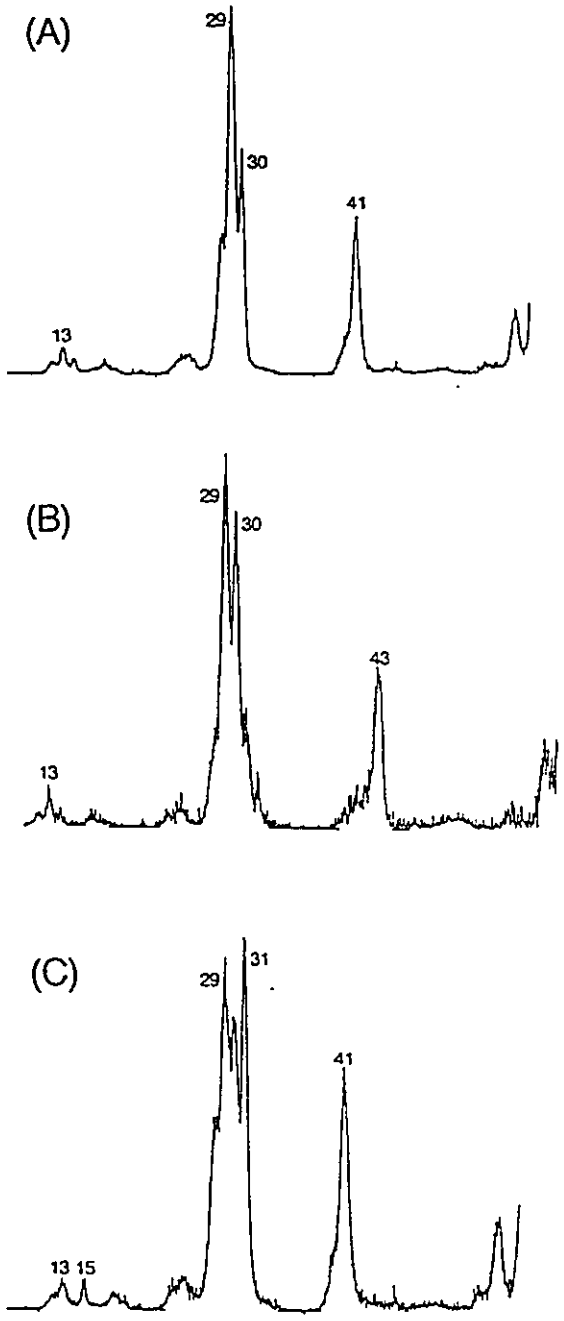

Figure 5.1. The collision-induced mass spectra of product ions from dissociation reactions of metastable enol ions of methyl glycolate, **2**:

(a) $HO(H)C{=}C{=}O^{\bullet+}$ from $HO\text{-}CH{=}C(OH)(OCH_3)^{\bullet+}$ (**2**) (- CH_3OH);

(b) $HO(H)C{=}C{=}{}^{18}O^{\bullet+}$ from $HO\text{-}CH{=}C({}^{18}OH)(OCH_3)^{\bullet+}$ (**2**-^{18}O) (- CH_3OH);

(c) $DO(H)C{=}C{=}O^{\bullet+}$ from $DO\text{-}CH{=}C(OD)(OCH_3)^{\bullet+}$ (**2**-$(Od)_2$) (- CH_3OD).

of OH•, indicative of the structure HO(H)C=C=O•+, **8**. ΔH_f [**8**] has not been measured , but it can be estimated from the computed ΔH_f of HO(H)C=C=CH_2•+, 216 kcal/mol [7], assuming that the effect of OH substitution on the ΔH_f's of ionized ketene and allene are the same. From ΔH_f[ketene]•+ - ΔH_f[allene]•+ = -59 kcal/mol [8], ΔH_f [**8**] = 157 kcal/mol is obtained. This yields a threshold energy for loss of CH_3OH (ΔH_f = -48 kcal/mol [8]) of 109 kcal/mol. Adding this to the average T value (2 kcal/mol) an upper limit for the threshold energy of ~ 111 kcal/mol is obtained and it is proposed that this value represents the transition state energy for all metastable dissociations.

According to the *ab initio* calculations executed at the UMP3/6-31G•//6-31G• level of theory [5b], ions **2** (Z-isomer) are 33 kcal/mol more stable than **1**, in agreement with the general finding that ionized enols are more stable, thermodynamically, than their keto forms [2]. Since ΔH_f [**1**] = 106 kcal/mol [5a], ΔH_f [**2**] = 73 kcal/mol so the critical energy for the dissociations of ions **2** is 38 kcal/mol.

The reactions of various metastable isotopologues are summarized in Table 5.2 and that all dissociations, except loss of methanol from **2**-Od_1, show atom specific behaviour.

Table 5.2 Reactions of metastable labelled methyl glycolate enol ions .

Precursor ion	Daughter ion formed and/or neutral lost[a]				[M-CO]•+ loses[a]
DOCH=C(OH)OCH_3•+, **2**-Od_1	CH_3•	CO	CH_3OH (1.1)[b] CH_3OD (1.0)	CH_3OHD^+	HCO•
HOCH=C(OH)OCD_3•+, **2**-Cd_3	CD_3•	CO	CD_3OH	$CD_3OH_2^+$	HCO•
DOCH=C(OD)OCH_3•+, **2**-$(Od)_2$	CH_3•	CO	CH_3OD and DO(H)C=C=O•+	$CH_3OD_2^+$	HCO•
HOCH=C(^{18}OH)OCH_3•+,**2**-^{18}O	CH_3•	C^{18}O	CH_3OH and HO(H)C=C=^{18}O•+	$CH_3OH_2^+$	HCO• (c)

[a] From MI spectra obtained in the second field-free region, 8 keV ions. The connectivities were determined by comparative MS/MS/MS experiments, see text. [b] Intensity ratio. [c] From [M-C^{18}O]•+.

Loss of $CH_3^\bullet$

The CID mass spectrum of the metastably generated $[M\text{-}CH_3]^+$ product ions generated from metastable ions of **2** (Fig. 5.2A) is entirely different from that of the $[M\text{-}CH_3]^+$ ions from **1** [5a] (Fig. 5.2B). Loss of $CH_3^\bullet$ from **1** has been proposed to yield the proton bound dimer $[CH_2{=}O\cdots H\cdots O{=}C{=}O]^+$ [5a] and an attractive structure for the ions derived from the enol **2** is the "capto-dative" [9] carbenium ion $HC(=O)C(OH)_2^+$, **9a**. The direct bond cleavage of lowest energy requirement in this ion involves the formation of m/z 29, $HC{=}O^+$, which is the base peak in the CID mass spectrum ($\Sigma\Delta H_f$ $[HC{=}O^+ + :C(OH)_2]$ = 148 kcal/mol whereas $\Sigma\Delta H_f$ $[C(OH)_2^{\bullet+} + HC{=}O^\bullet]$ = 186 kcal/mol [8,10]).

ΔH_f **[9a]** is estimated to be 70 kcal/mol [11], yielding a calculated threshold energy for the loss of $CH_3^\bullet$ of 105 kcal/mol (ΔH_f $[CH_3^\bullet]$ = 35 kcal/mol [8]). This value lies below the limiting value for the loss of methanol, consistent with the larger $T_{0.5}$ value for methyl loss, see Table 5.1. A possible mechanism for loss of $CH_3^\bullet$ is presented in Scheme 5.1.

In principle, loss of $CH_3^\bullet$ could be a simple bond cleavage in **2b** to produce the ion $HO(H)CCOOH^+$, **9b**. Such a process was proposed to occur in the related enol of ionized glycine methyl ester, $H_2NCH{=}C(OH)OCH_3^{\bullet+}$ [13].

Ion **9b** is undoubtedly less stable than its isomer **9a** because, in contrast to **9a**, it has only one electron donating group attached to the carbenium ion centre [14]. ΔH_f **[9b]** can be estimated from the following isodesmic reactions, using known ΔH_f's from ref. 8 and using a carbenium ion stabilization energy (SE) of zero for the COOH functionality [15], i.e. $SE_1 = SE_2$:

$CH_3^+ + CH_3OH \rightarrow CH_4 + CH_2OH^+$ $\quad SE_1$ = 63 kcal/mol

$CH_3^+ + HOCH_2COOH \rightarrow CH_4 + HOCHCOOH^+$ $\quad SE_2$ = 63 kcal/mol

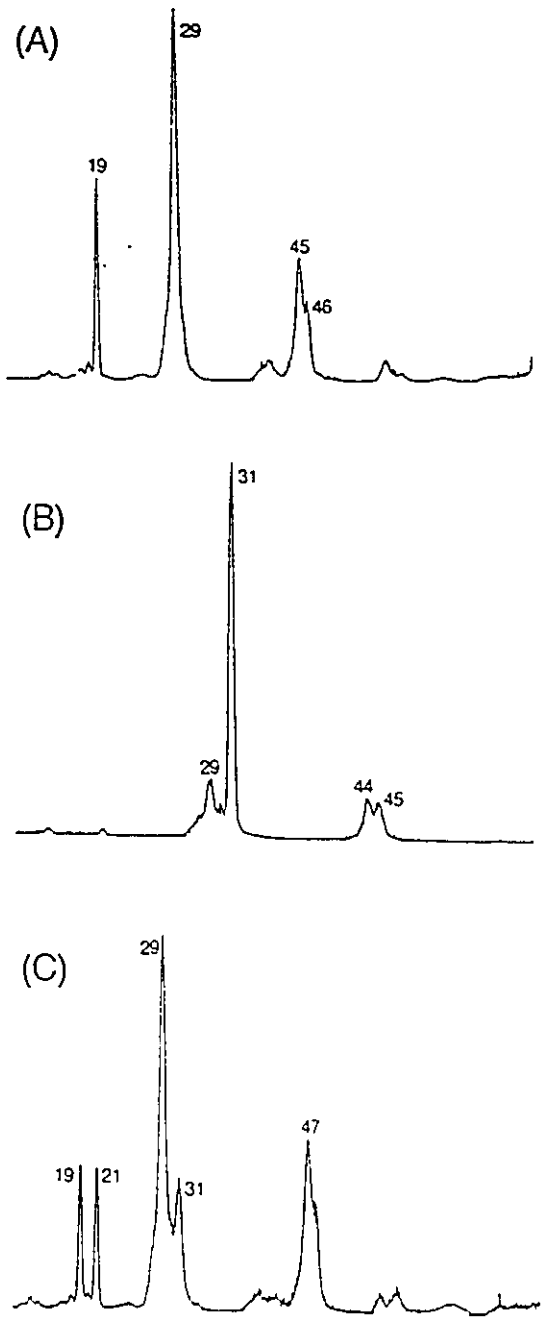

Figure 5.2. The collision-induced mass spectra of product ions from dissociation reactions of metastable enol ions of methyl glycolate, **2**:

(a) $HC(=O)C(OH)_2^+$ from $HO\text{-}CH{=}C(OH)(OCH_3)^{\bullet+}$ (**2**) ($-CH_3^{\bullet}$);

(b) $[CH_2{=}O\cdots H\cdots O{=}C{=}O]^+$ from $HO\text{-}CH_2C(=O)OCH_3^{\bullet+}$ (**1**) ($-CH_3^{\bullet}$);

(c) $HC(=O)C(OH)(^{18}OH)^+$ from $HO\text{-}CH{=}C(^{18}OH)(OCH_3)^{\bullet+}$ (**2**-^{18}O) ($-CH_3^{\bullet}$).

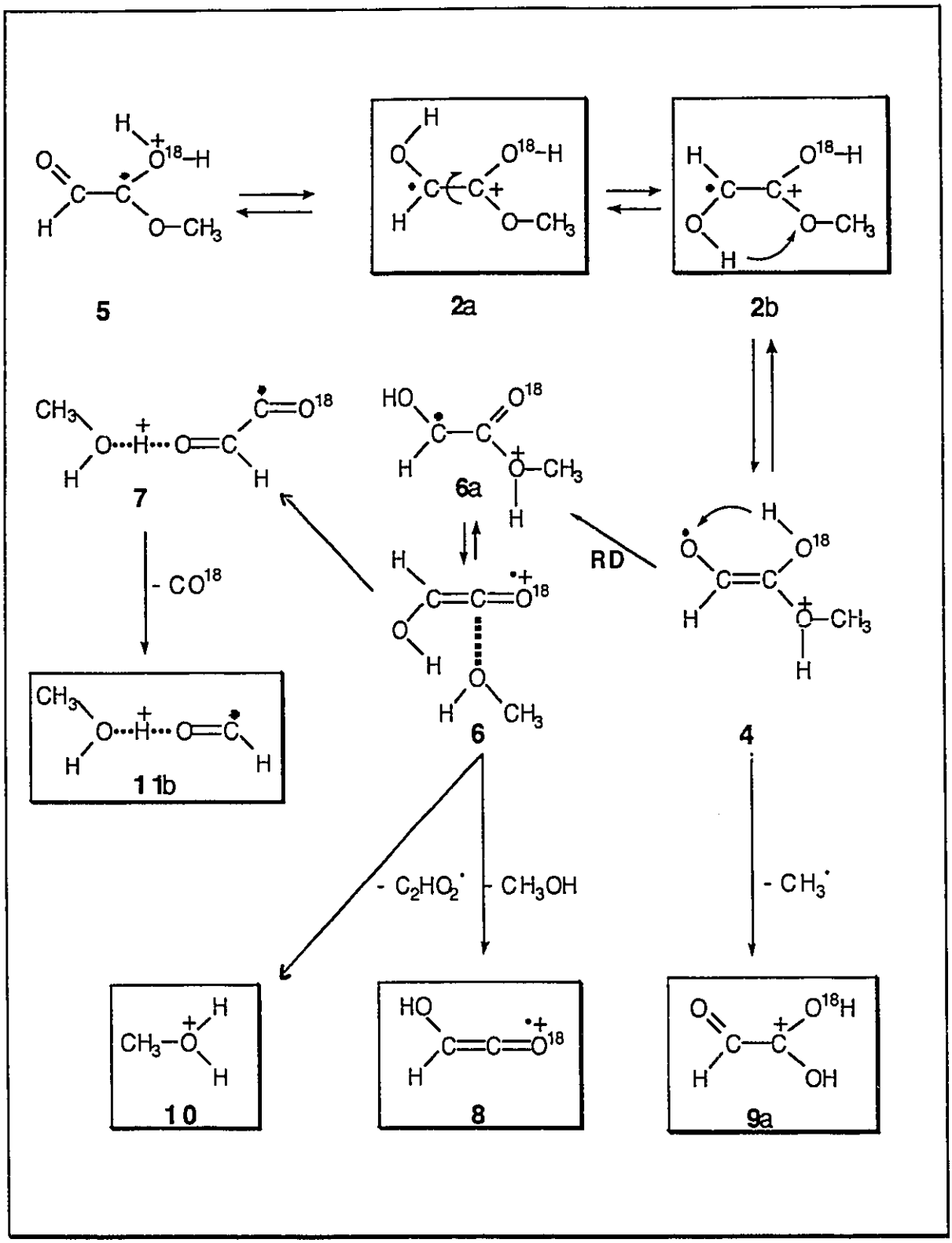

Scheme 5.1

ΔH_f [$HOCH_2COOH$] is estimated to be -139 kcal/mol [16]. One then obtains ΔH_f [**9b**] = 77 kcal/mol, leading to a calculated threshold of 112 kcal/mol and this would make ion ΔH_f **9b** just accessible. However, in view of the significant kinetic energy release, see Table 5.1, the more stable ion **9a** is the more likely candidate. Indeed, note that the $C(OH)_2^{\bullet+}$ ions, generated after collisional activation of **9a**, may decompose further by loss of $OH^{\bullet}$, to produce COH^+ [17]. According to Scheme 5.1, **2**-^{18}O should produce $HC(=O)C(OH)(^{18}OH)^+$; this ion, upon CID , should produce $HC{\equiv}O^+$, m/z 29 and $HO\text{-}C^{18}OH^{\bullet+}$, which decays further to COH^+, m/z 29 and $C^{18}OH^+$, m/z 31; this is precisely what is observed, the m/z 29 : m/z 31 ratio in the CID mass spectrum of $HC(=O)C(OH)(^{18}OH)^+$ being 3 : 1, see Fig. 5.2C. With respect to the non-occurence of the tautomerization **1** → **2** it can now be concluded that since **2**-Cd_3 does not eliminate $CD_2H^{\bullet}$, see Table 5.2, the interconversion **2** → **3** does not take place, i.e. **2** $\overset{?}{\rightleftharpoons}$ **3**.

Loss of CH_3OH and formation of $CH_3OH_2^+$

From Table 5.2, it can be seen that the original methoxy group is lost as CH_3OH. Furthermore, the hydroxyl hydrogens are lost to approximately the same extent pointing to hydrogen exchange between the two OH groups prior to loss of CH_3OH, most likely via the interconversion **2a** → **5**, see Scheme 5.1 (the *ab initio* calculations [5b] show that ions **2a** and **2b** have virtually the same heats of formation). A similar exchange was observed between the NH_2 and OH groups in $H_2NCH{=}C(OH)OCH_3^{\bullet+}$, the enol of ionized glycine methyl ester [13].

Highly structure characteristic peaks in the CID mass spectrum of the product ion $HO(H)C{=}C{=}O^{\bullet+}$, **8** are m/z 30, $HOCH^{\bullet+}$, and m/z 41, loss of $OH^{\bullet}$; using these fragmentations it could be established from MS/MS/MS experiments that **2**-^{18}O produces $HO(H)C{=}C{=}^{18}O^{\bullet+}$ and that **2**-$(Od)_2$ generates $DO(H)C{=}C{=}O^{\bullet+}$, see Fig. 5.1B and

C and Table 5.2. A plausible mechanism for loss of CH_3OH, see Scheme 5.1, involves a 1,4-hydrogen shift in ion **4** to produce the distonic ion **6a**. Alternatively, **6a** could be formed directly from **2b** via a 1,3-hydrogen shift, as proposed for $H_2NCH=C(OH)OCH_3^{\bullet+}$, [13].

Considering the *ab initio* calculations on the related ketene/water system [18] it seems likely, see Scheme 5.1, that ion **6a** freely interconverts with the (hydroxyketene) ion - (methanol) dipole complex **6** which then loses CH_3OH. Note, however, that the $T_{0.5}$ value for loss of CH_3OH is not typical of a dissociating ion-dipole complex, i.e. it is not exceedingly small; for example the $T_{0.5}$ value for loss of H_2O from $CH_2=C=O^{\bullet+}/H_2O$ is only 0.2 meV. Indeed, using an ion-dipole stabilization energy of ~20 kcal/mol [19], ΔH_f [**6**] of ~ 90 kcal/mol is derived, and so loss of CH_3OH may well take place above the threshold (see next section).

Metastable ions **2** (see Table 5.1) also produce $CH_3OH_2^+$, **10** ; the structure of the neutrals co-generated most likely are intact $O=CH-C=O^{\bullet}$ and/or $HO-C=C=O^{\bullet}$ radicals rather than $HC=O^{\bullet}$ + CO because the calculated threshold energy for formation of **10** + $HC=O^{\bullet}$ + CO is 120 kcal/mol [8], significantly above the limiting value of 111 kcal/mol. Furthermore, the neutralization-reionization (NR) mass spectrum of **2** (Fig. 5.4D) contains a telltale peak at m/z 56 which most likely originates from reionized $O=CH-C=O^{\bullet}$ and/or $HO-C=C=O^{\bullet}$ which dissociates further by $H^{\bullet}$ loss.

The ion-dipole complex **6** is also a prime candidate for formation of $CH_3OH_2^+$: because **6** can dissociate directly to ionized hydroxyketene (see above), the charge in **6** will reside on that moiety which can thus donate a **proton** [20] , as opposed to a hydrogen atom, to the CH_3OH molecule. Note (see Table 5.2) that since the **2**-$(Od)_2$-labelled compound specifically forms m/z 35, $CH_3OD_2^+$ from MS/MS/MS experiments, to the exclusion of m/z 34 (i.e the $DO(H)C=C=O^{\bullet+}$ ion in the ion-dipole complex

specifically transfers a D^+ to the methanol molecule), the neutral generated is O=CH-C=O•. Unfortunately ΔH_f[O=CH-C=O•] is not known. Also, MS/MS/MS experiments show that **2**-Cd_3 specifically forms $CD_3OH_2^+$. The proposed mechanism for formation of $CH_3OH_2^+$ is shown in Scheme 5.1.

Decarbonylation .

Prima facie, loss of CO could occur from ion **6a** via the least motion extrusion [21] to generate the ylid ion **11a** , eq. (3) :

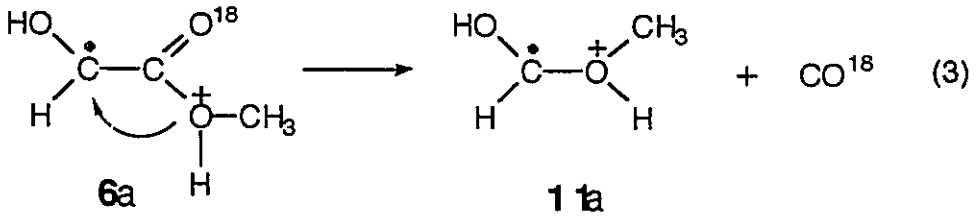

ΔH_f [**11a**] can be estimated from the effect of OH substitution (-36 kcal/mol [22]) on the non-charge bearing site of the ylid ion CH_2-O(H)-$CH_3^{\bullet+}$ (ΔH_f = 176 kcal/mol [23]) leading to ΔH_f [**11a**] = 140 kcal/mol and a threshold energy for **11a** + CO of 114 kcal/mol., slightly above the limiting value of 111 kcal/mol. Since, from the large $T_{0.5}$ value (330 meV, see Table 5.1), a large reverse term must be involved, ion **11a** can be discarded on energetic grounds. It was observed that the [M-CO]$^{\bullet+}$ daughter ion undergoes one CID unimolecular dissociation, *viz.* loss of HCO• to produce $CH_3OH_2^+$ ($\Sigma\Delta H_f$ = 147 kcal/mol [8]) This observation also eliminates ion **11a** as possible candidate, as this ion is expected (barring reverse terms) to lose CH_3• by a simple bond cleavage to produce the stable ion $HC(OH)_2^+$ ($\Sigma\Delta H_f$ = 131 kcal/mol [8]).

In a recent computational study [20] on the unimolecular isomerization and dissociation reactions of $HOCH_2CH_2OH^{\bullet+}$, it was found that the most stable $C_2H_6O_2^{\bullet+}$

isomer is the hydrogen-bridged ion-dipole complex $[CH_3\text{-}O(H)\cdots H\cdots O{=}C\text{-}H]^{\bullet+}$, **11b**, in the dissociative configuration for loss of HCO$^{\bullet}$. Its ΔH_f was computed at 130 kcal/mol and so **11b** is energetically accessible from **2**, ΔH_f [**11b**] + ΔH_f [CO] = 104 kcal/mol; the reverse term would then be ~7 kcal/mol, and this could account for the large $T_{0.5}$ value observed (Table 5.1). The related species $[CH_3\text{-}O\cdots H\cdots O{=}CH_2]^{\bullet+}$ [24] which is also predicted to lose HCO$^{\bullet}$ has a computed energy of 145 kcal/mol [20] and thus is not accessible from **2**.

It was observed from MS/MS/MS/MS experiments that the m/z 36 $[CH_2D_3O]^+$ ions, formed from collisionally activated $[M\text{-}CO]^{\bullet+}$ ions generated from metastable **2**-Cd_3 precursor ions, upon CID specifically form CD_3^+ and so m/z 36 has the connectivity $CD_3OH_2^+$ (see Fig. 5.3). An important clue as to the identity of the $[M\text{-}CO]^{\bullet+}$ daughter ion

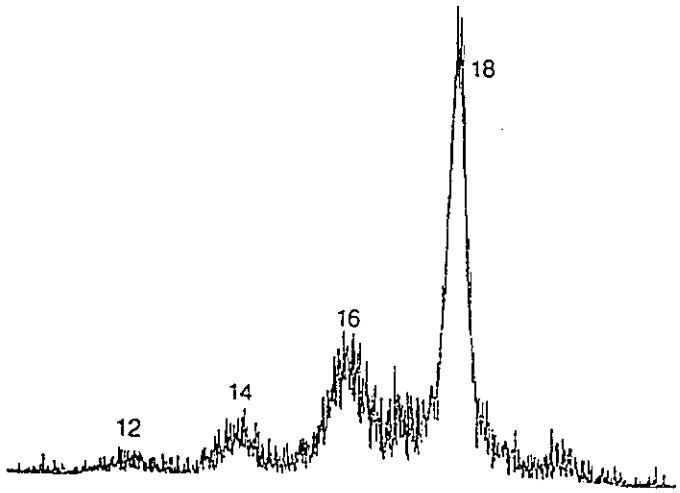

Figure 5.3. MS/MS/MS/MS experiment on HO-CH=C(OH)$(OCH_3)^{\bullet+}$ → [M - CO]$^{\bullet+}$ → [M - CO]$^{\bullet+}$ - HCO$^{\bullet}$ → CD_3^+ (see text for discussion).

follows from the behaviour of the various $[M\text{-}CO]^{\bullet+}$ isotopologues, see Table 5.2. It is seen that the decarbonylated product ions specifically lose the vinylic H-C-O group. Hence, the following sequence is established , eq. (4) :

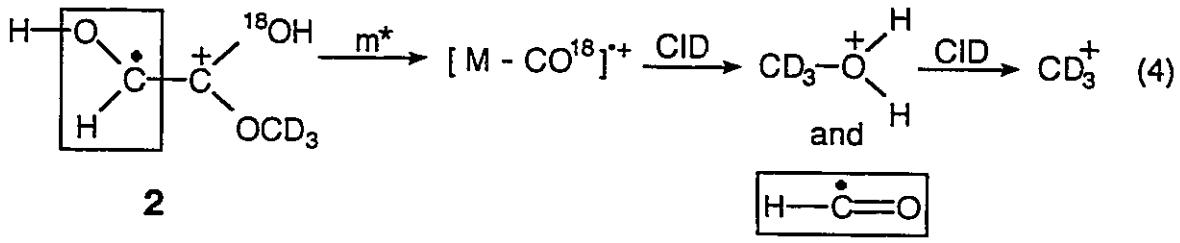

2 (4)

A product ion which rationalizes the above is indeed ion **11b** and a mechanism for its formation is presented in Scheme 5.1 : the ion-dipole complex **6** undergoes reorientation to the hydrogen-bridged species **7** which then undergoes decarbonylation.

It appears that decarbonylation of **2** is an extremely slow process. This becomes evident from a comparison of the CID mass spectra of ions **2** generated in the ion source (Fig. 5.4B) and of the ions **2** generated from metastable M2 molecular ions (m* 132→90) (Fig. 5.4C).

The spectrum of Fig. 5.4B reflects both low energy, metastable and high energy, CID processes, whereas Fig. 5.4C can only obtain peaks due to high energy, fast CID reactions. It can be seen that [M-CO]$^{\bullet+}$ is virtually absent in Fig. 5.4C (but that it is a sizeable signal in Fig. 5.4B) and this indicates that decarbonylation does not compete at high internal energies. This is also borne out by the near absence of [M-CO]$^{\bullet+}$ in the NR spectrum of **2** (Fig. 5.4D). NR processes are known to sample target ions of low internal energies, followed by fast , high energy dissciation of the reionized molecular ions [25]. Indeed, if a delayed analysis is performed, i.e. if the "survivor" ions (S) are allowed to live for *ca.* 10^{-5} s and an MI spectrum is then obtained, [M-CO]$^{\bullet+}$ becomes an important peak (see Fig. 5.4E). In fact, it can be seen that the spectrum in Fig. 5.4E is closely similar to the normal MI spectrum (Fig. 5.4A). (These results also show that

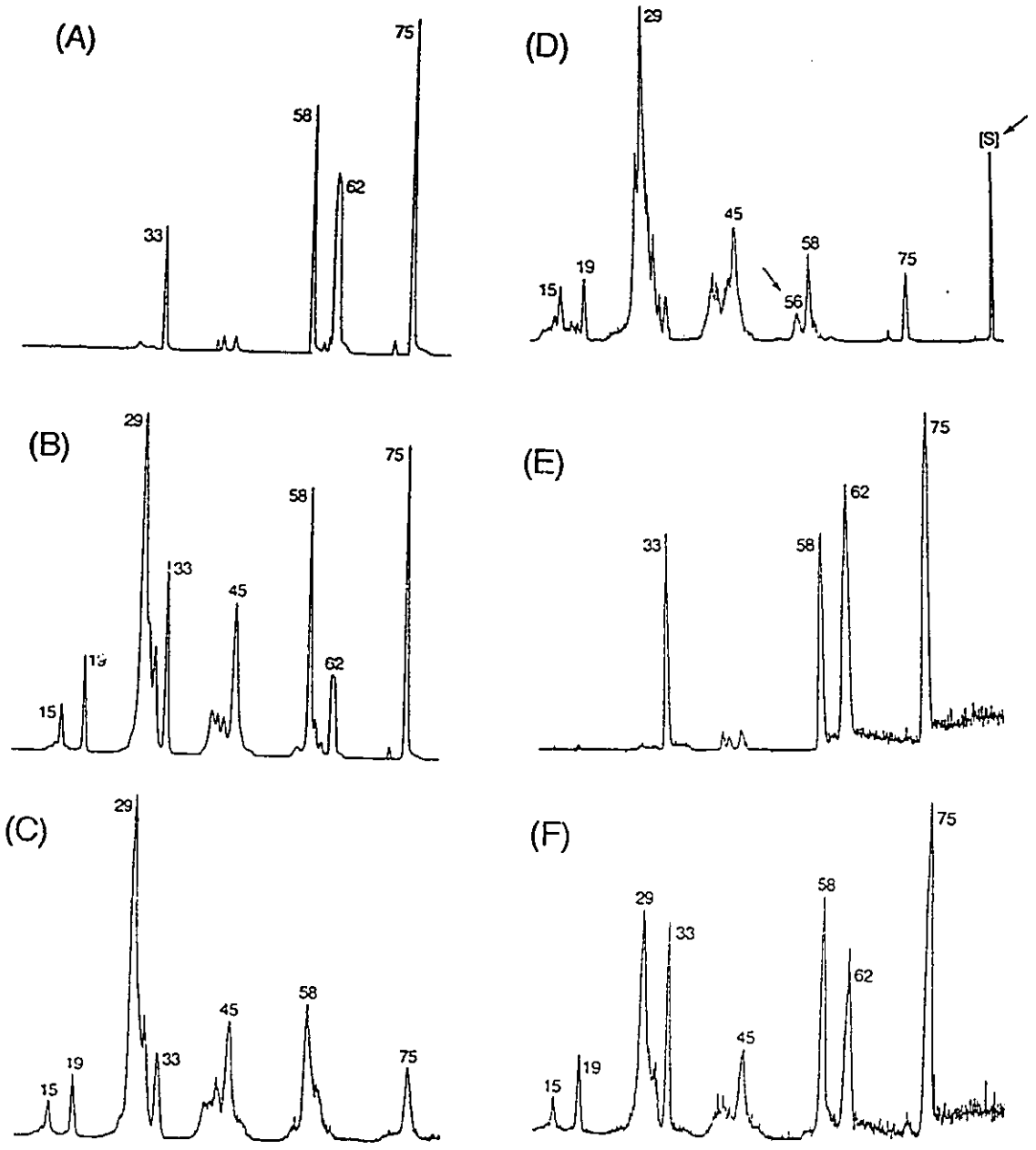

Figure 5.4. Mass spectra of ionized enol of methyl glycolate, **2**: (a) metastable ion mass spectrum; (b) collision-induced dissociation mass spectrum of ions generated in the ion source; (c) as (b), but of ion generated from metastable ion, see text; (d) neutralization-reionization mass spectrum; (e) metastable ion mass spectrum of the survivor ion [S] in (d); (f) collision-induced dissociation mass spectrum of the survivor ion [S] in (d).

the neutral enol of **2** is a stable species which does not rearrange to methyl glycolate, compare spectra Fig. 5.4B and F). It is therefore proposed that ion **7** is formed very slowly from **6** and moreover, that it only leads to CO loss. Alternatively, it is ion **7** itself which dissociates slowly.

From Table 5.1 it can be seen that for **2**-$(Od)_2$ a large isotope effect (~3) operates against the losses of CO, CH_3OH and O=C(H)-C=O$^{\bullet}$. This is interpreted in terms of **4** → **6** (or **2b** → **6**) being rate determining (i.e. unidirectional) in agreement with the large $T_{0.5}$ value for the loss of CH_3OH from the ion-dipole complex **6** mentioned in the preceding section. Upon CID of **2**, two other major processes occur, *viz.* formation of $HC{=}O^+$ and HO-C=O$^+$ (see Fig. 5.4B). Ion **4** may account for $HC{=}O^+$, whereas **2** may produce HO-C=O$^+$ (+ $CH_3^{\bullet}$ + HCOH) indicating that **2** → **4** is not rate-determining; all labelling experiments (not shown) are in agreement with this proposal.

It is clear from the above that **1** and **2** do not interconvert prior to dissociation. For methyl acetate the keto-enol isomerization (eq. (1), R = H) requires 11 kcal/mol and a similar value may pertain to ions **1**. However, it has been established [5] that the $HOCH_2$ functionality of ions **1** triggers an even more facile rearrangement which eventually leads to loss of HCO$^{\bullet}$ and this reaction requires only 7 kcal/mol, corresponding to a transition state energy of 113 kcal/mol. A similar situation pertains for the enol ions **2**. Here, isomerization into **3** via a 1,4-hydrogen shift cannot compete with the formation of **6** (and with loss of $CH_3^{\bullet}$ from **4**). Note also that the isomerization **2** → **6** takes place at virtually the same energy (111 kcal/mol) as does loss of HCO$^{\bullet}$ from **1**. Hence **1** and **2** do not tautomerize simply because their dissociation processes require less energy. This behaviour nicely parallels that of the ionized methyl ester of glycine and its enol, which, too, do not interconvert prior to dissociation and exhibit their own unimolecular chemistry [13].

References

1 F.A. Carey and R.J. Sundberg, Advanced Organic Chemistry, Part A : Structure and Mechanisms, Plenum Press, New York (1984).

2 (a) J.L. Holmes and F.P. Lossing, *J. Am. Chem. Soc.* **102**, 1591 (1980); (b) F. Turecek, in Z. Rappoport (Ed.), The Chemistry of Enols, Wiley, Chichester, 1990, pp. 95-146; (c) G. Bouchoux, *Mass Spec. Rev.* **7**, 1 (1988); ibid. **7**, 203 (1988).

3 N. Heinrich, F. Louage, C. Lifshitz and H. Schwarz, *J. Am. Chem. Soc.* **110**, 8183 (1988).

4 N. Heinrich, J. Schmidt, H. Schwarz and Y. Apeloig, *J. Am. Chem. Soc.* **109**, 1317 (1987).

5 (a) D. Suh, C.A. Kingsmill, P.J.A. Ruttink, P.C. Burgers and J.K. Terlouw, *Int. J. Mass Spectrom. Ion Processes* (in press); (b) C.A. Kingsmill, J.T. Francis and J.K. Terlouw, in preparation.

6 (a) P.C. Burgers, A.A. Mommers and J.L. Holmes, *J. Am. Chem. Soc.* **105**, 5976 (1983) ; (b) R. Feng, C. Wesdemiotis and F.W. McLafferty, *J. Am. Chem. Soc.* **109**, 6521 (1987).

7 M.L. McKee and L. Radom, *Org. Mass Spectrom.* **28**, 1238 (1993).

8 S.G. Lias, J.E. Bartmess, J.F. Liebman, J.L. Holmes, R.D. Levin and W.G. Mallard, *J.Phys. Chem. Ref. Data* **17** (suppl. 1) (1988).

9 P.C. Burgers, K.J. van den Berg, H. Visser and J.K. Terlouw, *Int. J. Mass Spectrom. Ion Processes* **101**, 83 (1990).

10 J.S. Francisco, *J. Chem. Phys.* **96**, 1167 (1992).

11 J.L. Holmes, personal communication, 1995. Estimate based on the effect of OH substitution on $H(C=O)CHOH^+$ (ΔH_f = 132 kcal/mol [12]), using the enthalpy difference between CH_2=CH-$CHOH^+$ and CH_2=CH-$C(OH)_2^+$, 62 kcal/mol.

12 M.C. Blanchette, J.L. Holmes, C.E.C.A. Hop, F.P. Lossing, R. Postma, P.J.A. Ruttink and J.K. Terlouw, *J. Am. Chem. Soc.* **108**,7859 (1986).

13 G. Depke, N. Heinrich and H. Schwarz, *Int. J. Mass Spectrom. Ion Processes* **62**, 119 (1984).

14 Ring closure to HO-CH-C(OH)-O^+ would generate a carbenium centre attached to two stabilizing electronegative atoms, but at the expense of ring strain, see ref. 16.

15 D. Suh, C.A. Kingsmill, P.J.A. Ruttink, J.K. Terlouw and P.C. Burgers, *Org. Mass Spectrom.* **28**, 1270 (1993).

16 From ΔH_f [CH_3COOH] [8] and using the enthalpy difference between $CH_3C(=O)OCH_3$ [8] and $HOCH_2C(=O)OCH_3$ [5a].

17 P.C. Burgers, G.A. McGibbon and J.K. Terlouw, *Chem. Phys. Lett.* **224**, 539 (1994).

18 R. Postma, P.J.A. Ruttink, J.K. Terlouw and J.L. Holmes, *J. Chem. Soc., Chem. Commun.* (1986) 683.

19 A stabilization energy of 20 kcal/mol has been obtained for the complex CH_2=CHOH$^{\bullet+}$/CH_3OH, see : R. Postma, P.J.A. Ruttink, F.B. van Duijneveldt, J.K. Terlouw and J.L. Holmes, *Can. J. Chem.*, **63**, 2798 (1985).

20 P.J.A. Ruttink and P.C. Burgers, *Org. Mass Spectrom.* **28**, 1087 (1993).

21 T. Drewello, N. Heinrich, W.P.M. Mass, N.M.M. Nibbering, T. Weiske and H. Schwarz, *J. Am. Chem. Soc.* **109**,4810 (1987).

22 J.L. Holmes, F.P. Lossing and P.C. Burgers, *Int. J. Mass Spectrom. Ion Phys.* **47**, 133 (1983).

23 J.L. Holmes, F.P. Lossing , J.K. Terlouw and P.C. Burgers, *J. Am. Chem. Soc.* **104**,2931 (1982).

24 P.C. Burgers, J.L. Holmes, C.E.C.A. Hop, R. Postma, P.J.A. Ruttink and J.K. Terlouw, *J. Am. Chem. Soc.* **109**,7315 (1987).

25 (a) D.E. Drinkwater and F.W. McLafferty, *Org. Mass Spectrom.* **28**, 378 (1993 ?) ; (b) G.A. McGibbon, P.C. Burgers and J.K. Terlouw, *Eur. Mass Spectrom.* submitted.

CHAPTER 6

The Chemistry of Ionized Ethyl Glycolate, $HOCH_2CO_2C_2H_5^{\bullet+}$, and Its Enol Isomer, $HOCH{=}C(OH)OC_2H_5^{\bullet+}$. Formation of Ionized and Neutral Trihydroxyethylene

Introduction

Keto-enol tautomerism is one of the most fundamental rearrangements in organic chemistry [1]. This process occurs in condensed phases, often assisted by facile acid or base catalyzed intermolecular hydrogen transfers, and in the dilute gas-phase, where only intramolecular hydrogen transfers are feasible. Whereas neutral species containing the carbonyl group are normally much more stable than their enol isomers (especially when simple ketones are considered), the ionized enols are generally lower in energy than their keto tautomers [2]. Many reactions of isolated organic ions involve keto-enol tautomerism, which frequently proceeds in two (or more) steps via intermediate distonic ions as indicated in eq. (1) for simple methyl esters.

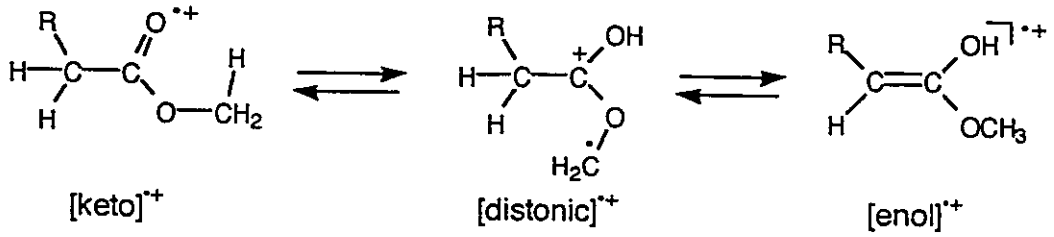

(1)

Thus, in these systems, keto-enol tautomerization does not take place directly via an energetically demanding (~50 kcal/mol [3] for R=H) and consequently slow 1,3-hydrogen shift : [keto]•+→ [enol]•+. Instead, two less energy demanding (~12 kcal/mol [4] for R=H) and therefore more rapid 1,4-hydrogen shifts lead to interconversion of ionized keto and enol forms via a distonic ion: [keto]•+→ [distonic]•+→ [enol]•+. An important consequence of the above is that both keto and enol ions invariably show the same dissociation behaviour [2c].

The unimolecular chemistry of ionized methyl glycolate [5], and its enol, (eq.1: R=OH) [6] was recently reported and it was discoverd that, in contrast to the expectations from the above precedent, these species do not tautomerize at all, as they decay via completely different channels. It appeared that for each tautomer the CHOH functionality opens up facile rearrangement/dissociation pathways, whose energy requirements lie below the tautomerization barrier. In particular, for this ionized methyl ester, the CHOH group triggers a type of reaction which other α-ketols also undergo, namely a facile double hydrogen [7] transfer as indicated in eq. (2).

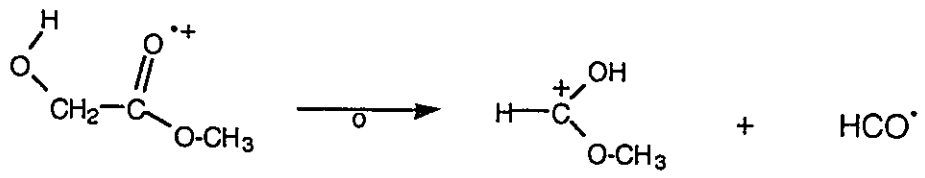

(2)

For the proto-type ionized α-ketol, acetol, this reaction has been studied in

detail by state-of-the-art *ab initio* molecular orbital (MO) calculations and the derived mechanism is given elsewhere [7].

It has been established that for ionized methyl glycolate $HCO^{\bullet}$ loss requires only 8 kcal/mol [5] and so tautomerization cannot compete. Since 1,5-H shifts may be expected to require even less energy than 1,4-H shifts (i.e. < 12 kcal/mol) it was intrigued by the possibility that the higher homologue ethyl glycolate, **1**, might well undergo tautomerization via consecutive 1,5-H shifts prior to dissociation, see eq. (3).

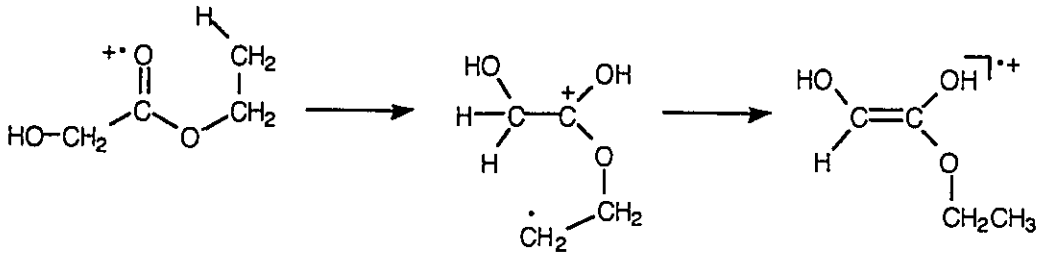

1 **3** **2** (3)

It is found that this indeed to be the case, but the tautomerization appears to be unidirectional, i.e. **1**→ (**3** →) **2**, but **2**↮ (**3** →) **1**. Surprisingly, however, it is observed that the ethyl group opens up at the other end of the ion an even more facile reaction than the expected $HCO^{\bullet}$ loss, namely elimination of C_2H_4 to produce the remarkably stable proto-type unsaturated ionized triol, trihydroxyethylene, $HO\text{-}C(H)=C(OH)_2^{\bullet+}$, **4**, via a reaction which is very similar to ethylene loss from the well studied ionized phenyl ethyl ether [8] and related systems [9] and ethyl onium ions [10].

Results and Discussion

Overview and comparison with $HOCH_2CO_2CH_3^{\bullet+}$ and $HOCH{=}C(OH)OCH_3^{\bullet+}$

Ionized ethyl glycolate, $HOCH_2CO_2C_2H_5^{\bullet+}$, **1**, may be generated directly from the neutral precursor. The only technical problem with this method is the ease of self-protonation, which gives rise to an abundant $(M+H)^+$ ion at m/z 105, which complicates the appearance of the spectrum. The isomeric ionized enol, $HOCH{=}C(OH)OC_2H_5^{\bullet+}$, **2**, may be generated indirectly by dissociative ionization of diethyl tartrate (eq. 4) or by propene loss via the McLafferty rearrangement of ionized ethyl 2-hydroxyisovalerate (eq. 5).

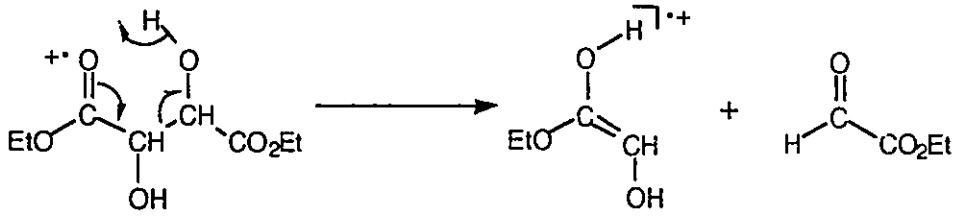

(4)

2

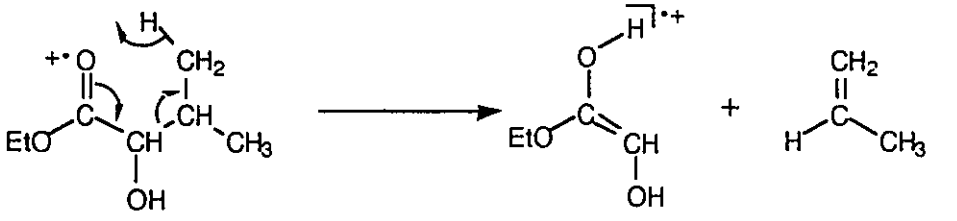

(5)

2

The metastable ion (MI) spectra of **1** and **2** are given in Table 6.1. It can be seen that both tautomers abundantly expel C_2H_4 with closely similar kinetic energy releases ($T_{0.5}$). However, **1** also undergoes three minor competing reactions, loss of H_2O, $HCO^{\bullet}$

and formation of m/z 59; therefore, **1** is able to reach transition states and intermediates which are inaccessible to **2**.

Table 6.1. Reactions of metastable **1** and **2**.

Precursor	Ion Structure	Neutral Lost	RA[a]	$T_{1/2}$[b]
$HOCH_2CO_2Et$	$HOCH_2CO_2C_2H_5^{\bullet+}$	H_2O	5	
		C_2H_4	83	24
		$HCO^{\bullet}$	4	
		$HOCO^{\bullet}$	8	
$(CH_3)_2CHCH(OH)CO_2Et$	$HOCH{=}C(OH)OC_2H_5^{\bullet+}$	C_2H_4	>99	25

[a] RA = Relative abundance, measured by peak heights and normalized to a total of 100 units for dissociation of metastable ions; [b] $T_{0.5}$ = Kinetic energy (in meV) estimated from the width at half-height of the appropriate metastable peak.

Moreover, MS/MS/MS experiments, see below, reveal that the fragment ion produced by C_2H_4 loss from both **1** and **2** is ionized trihydroxyethylene, $HO\text{-}C(H){=}C(OH)_2^{\bullet+}$ and this suggests that prior to dissociation **1** tautomerizes into **2** which in turn can directly form **4** via a hydrogen shift. However, **2** does not tautomerize (back) to **1**, because the side reactions characteristic of **1** are not observed for **2**. This conclusion also follows from labelling data as discussed below.

A clear contrast exists between the related chemistries of **1** and **2**, in which unidirectional tautomerism is important, and the behaviour of the lower homologues, $HOCH_2CO_2CH_3^{\bullet+}$ and $HOCH{=}C(OH)OCH_3^{\bullet+}$, in which tautomerism is insignificant [5,6]. This contrast reflects the influence of the larger O-ethyl group in **1** and **2**, which faciliates

the hydrogen transfers necessary for tautomerism. Thus, enolization of $HOCH_2CO_2CH_3^{\bullet+}$ would require two 1,4-H shifts (eq. 1), but the corresponding process in **1** involves 1,5-H shifts (eq. 3), which are known to be more facile.

Reactions of $HOCH{=}C(OH)OC_2H_5^{\bullet+}$

It is logical to present a detailed discussion of the chemistry of **2** first because it is simpler than that of **1**. As can be seen from Table 6.2, loss of C_2H_4 occurs from the O-ethyl group with highly selective β-hydrogen transfer. Thus, $HOCH{=}C(OH)OCH_2CD_3^{\bullet+}$ and $HOCH{=}C(OH)OCD_2CH_3^{\bullet+}$ expel $C_2H_2D_2$ with only very minor contributions from other labelled ethylenes (3 % C_2HD_3 and 6 % C_2H_3D, respectively), but $DOCH{=}C(OH)O\text{-}CH_2CH_3^{\bullet+}$ loses only C_2H_4 (Table 6.2). The preponderance of $C_2H_2D_2$ loss also excludes the possibility of CO loss from **2**; this deduction is consistent with the absence of $C^{18}O$ loss from $HOCH{=}C(OH)^{18}OCH_2CH_3^{\bullet+}$.

Table 6.2. Reactions of metastable isotopologues of **2**.

Ion Structure	Neutral Lost[a]
$DOCH{=}C(OH)OC_2H_5^{\bullet+}$	C_2H_4
$HOCH{=}C(OH)OCD_2CH_3^{\bullet+}$	$C_2H_2D_2$
$HOCH{=}C(OH)CH_2CD_3^{\bullet+}$	$C_2H_2D_2$

[a] Specificity at least 95 %.

This pronounced site-selectivity in ethylene loss from labelled analogues of **2** is closely similar to that found in ethylene elimination from ionized phenyl ethyl ether [8]

and onium ions of general structure $R^1R^2C{=}Z^+CH_2CH_3$ (Z = O, S, NH, NCH_3) [10]. All these reactions may be explained in terms of mechanisms involving ion-radical or ion-neutral complexes, in which proton transfer occurs in a complex comprising a bridged non-classical ethyl cation coordinated to a neutral component. Transfer of the bridging proton, which originates from the terminal methyl group, to an atom of the neutral component then explains the observed site-selectivity. In the case of **2**, the neutral species is the radical derived by hydrogen abstraction from one of the geminal hydroxy groups in trihydroxyethylene (Scheme 6.1). It is not possible from the current data to determine whether **6** is a true ion-radical complex, in which at least one of the components is able to rotate freely with respect to the other, or a transition state. Neither is it possible to delineate the geometry of **6**, which may be better described as a transient proton-bridged complex, in which the proton is being irreversibly transferred from carbon to oxygen. Nevertheless, the generic features of this fragmentation (highly selective β-proton transfer and the moderate $T_{0.5}$ value of ~ 25 meV) are typically of those found in ion-neutral- mediated fragmentations.

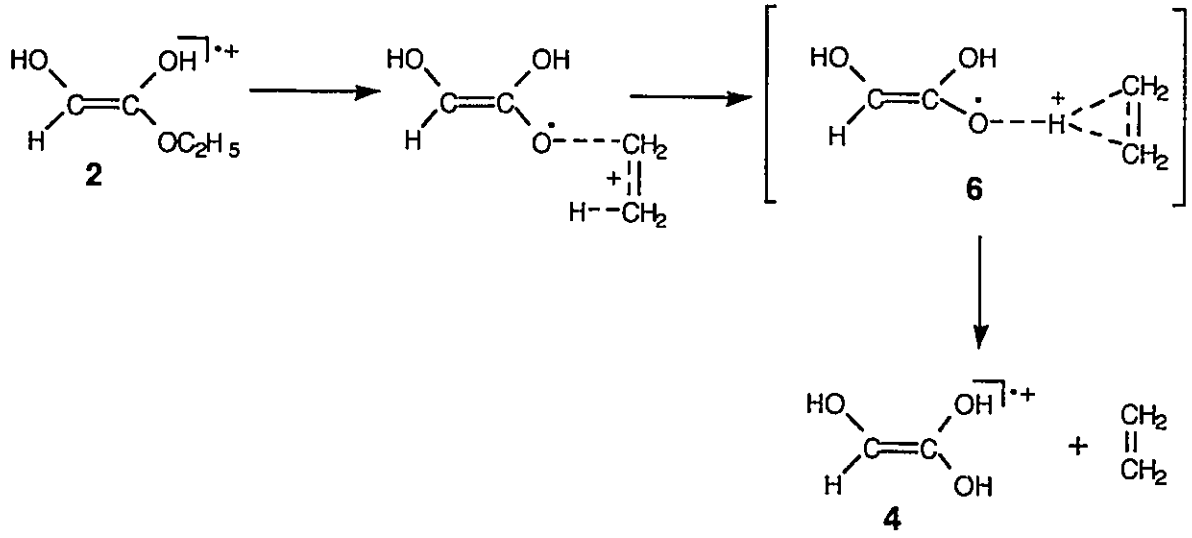

Scheme 6.1

The labelling results are thus perfectly compatible with the formation of ionized trihydroxyethylene, which is the enol of glycolic acid, $HOCH_2C(=O)OH^{\bullet+}$, **5**. The collision-induced dissociation (CID) mass spectrum of **5** has been reported [11] and is dominated by loss of CO_2 which produces the proto-type ylid ion $^{\bullet}CH_2OH_2^+$ at m/z 32, see Fig. 6.1a. The spectrum of the fragment ions generated by loss of C_2H_4 from metastable ions **2** is shown in Fig. 6.1b and it can be seen that this spectrum is totally different from that for **5**; note that m/z 32 is absent. In fact, the spectrum in Fig. 6.1b can be rationalized in terms of structure **4** as follows. Upon activation, cleavage of the C-C bond leads to the ionized carbenes $HCOH^{\bullet+}$, m/z 30 [12] and $HOCOH^{\bullet+}$, m/z 46 [12a,13]. The former is known subsequently to lose $H^{\bullet}$ to form preferentially HCO^+ [14] (m/z 29 base peak), while $HOCOH^{\bullet+}$ may lose $H^{\bullet}$ [12a,13c] to produce $HOCO^+$, m/z 45.

In addition, ions **4** lose H_2O to generate m/z 58 and by comparison of reference spectra this fragmentation leads to $HO\text{-}CH{=}C{=}O^{\bullet+}$ [6], which may further decompose to $HCOH^{\bullet+}$, m/z 30, which represents an alternative route to m/z 30 and m/z 29. From this analysis, the fate of the label in various labelled precursors can be traced. Thus, $HO\text{-}CH{=}C(OH)OCH_2CD_3^{\bullet+}$ forms only $HOCH{=}C(OH)(OD)^{\bullet+}$, whereas $HO\text{-}CH{=}C(OH)^{18}O\text{-}CH_2CH_3^{\bullet+}$ clearly generates $HOCH{=}C(OH)(^{18}OH)^{\bullet+}$. Thus, loss of C_2H_4 from **2** appears to be well characterized in that it can be formulated as a simple hydrogen shift as depicted in Scheme 6.1.

Reactions of $HOCH_2CO_2C_2H_5^{\bullet+}$

As mentioned above the major fragmentation route of **1** is loss of C_2H_4. It was observed that the CID mass spectrum of the *metastably* generated fragment ions was superimposable on Fig. 6.1b and so it is concluded that loss of C_2H_4 from **1**, too, leads to $HOCH{=}C(OH)_2^{\bullet+}$ to the exclusion of $HOCH_2C(=O)OH^{\bullet+}$.

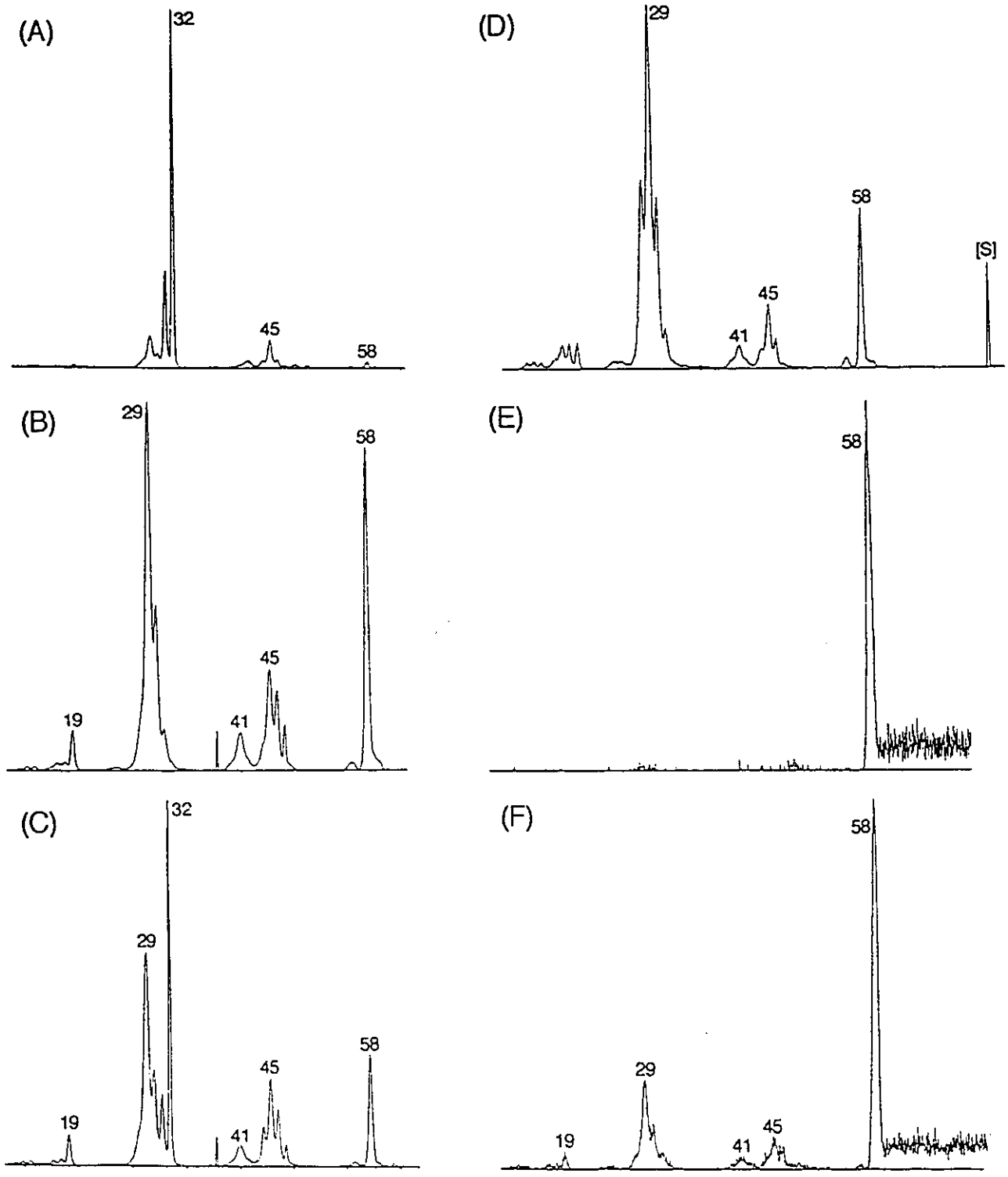

Figure 6.1. Collision-induced dissociation (CID) mass spectra of (a) $HOCH_2CO_2H^{\bullet+}$, **5**; (b) $HOCH{=}C(OH)_2^{\bullet+}$, **4**; (c) $C_2H_4O_3^{\bullet+}$ ions generated from **1** in the ion source; and (d) neutralization-reionization (NR) mass spectrum of **4**; (e) metastable ion (MI) and (f) CID mass spectra of the survivor ions [S] from NR of **4**.

However, in contrast to the corresponding fragmentation of **2**, C_2H_4 elimination from **1** does not involve β-proton transfer with high selectivity. Thus, both $HOCH_2CO_2CD_2CH_3^{\bullet+}$ and $HOCH_2CO_2CH_2CD_3^{\bullet+}$ expel $C_2H_2D_2$ and C_2H_3D in the ratio 73 : 27 ; moreover, $HOCD_2CO_2CH_2CH_3^{\bullet+}$ loses C_2H_3D and C_2H_4 in the ratio 75 : 25, when only the latter would be expected on the basis of hydrogen transfer exclusively from the O-ethyl group.

The preferential participation of one hydrogen atom from the methylene group of the hydroxymethyl substituent which results in C_2H_3D loss from $HOCD_2CO_2CH_2CH_3^{\bullet+}$ is strong evidence for enolization of **1** to **2** prior to the bulk of ethylene elimination. Thus, a 1,5-H shift in $HOCD_2CO_2CH_2CH_3^{\bullet+}$ leads to the distonic ion $HOCD_2C^+(OH)CH_2CH_2^{\bullet}$, which undergoes a specific 1,5-D shift to give $HOCD{=}C(OH)CH_2CH_2D^{\bullet+}$ (Scheme 6.2). The deuterium atom that is transferred to the ethyl group by this relay of hydrogen transfers is now ideally situated to participate in ethylene loss. Moreover, this tautomerism is unidirectional, as there is no significant contribution from $C_2H_2D_2$ elimination from $HOCD_2CO_2CH_2CH_3^{\bullet+}$, which would be expected if a route existed for transfer of both deuterium atoms to the O-ethyl substituent via reversible tautomerism of labelled analogues of **1** and **2**.

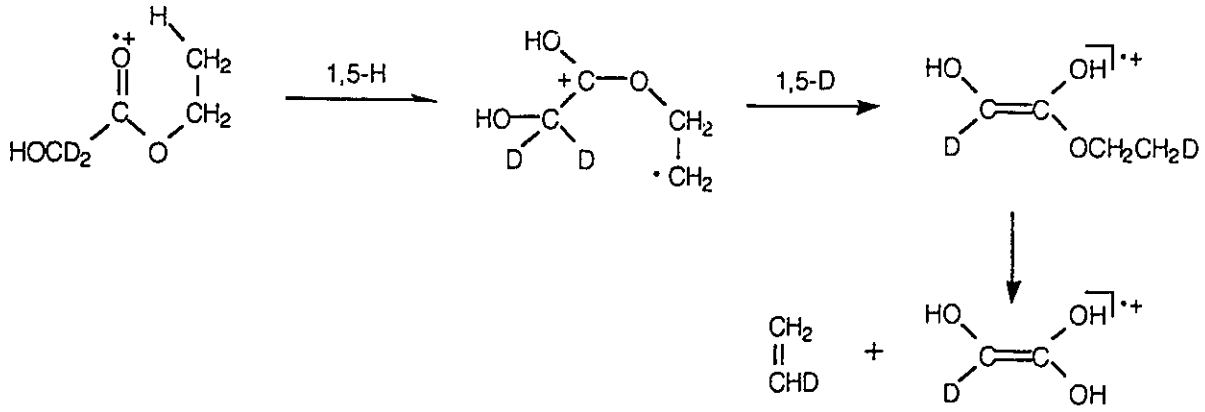

Scheme 6.2

However, this mechanism does not account for the contribution from apparent α-hydrogen transfer from the O-ethyl group in ethylene loss. It seems unlikely that the site-selectivity of the final step, ejection of ethylene from labelled analogues of **2**, should vary so strongly depending on whether the radical cation is formed directly or by tautomerism of **1**. The occurrence of β-hydrogen transfer in ethylene loss from the analogous ionized phenyl ethyl ethers [8] and related onium ions [10] over a wide range of energies also militates against such an explanation of the contrasting site-selectivities in ethylene elimination from **1** and **2**.

A possible explanation is that **3** may undergo a degenerate 1,2-shift, which alters the connectivity of the heavy atom skeleton and renders the two methylene groups derived from the O-ethyl group equivalent, Scheme 6.3. Analogous 1,2-shifts occur with great facility in other β-distonic ions [15,16]. For example, *ab initio* calculations indicate that the 1,2-OH_2 shift in the β-distonic ion CH_2-CH_2-$OH_2^{\bullet+}$ has a low barrier [16]. Indeed, at an internal energy of 12 kcal/mol (i.e. 7 kcal/mol below the threshold for dissociation to $C_2H_4^{\bullet+}$ + H_2O) this species may be more accurately described as an ethylene radical cation to which a water molecule is attached, with freedom to move along and around the positively charged ethylene rod, rather than a β-distonic ion with a localized C-O σ-bond [16]. It will be shown in the following section that a similar situation may apply in the case of the distonic ion **3**. The dissociation limit of *ionized* $C_2H_4^{\bullet+}$ and *neutral* $HOCH_2COOH$ lies only a few kcal/mol above the energy requirement for the dissociation to **4** + C_2H_4. Consequently, by analogy with the $C_2H_4^{\bullet+}/H_2O$ system, the degenerate rearrangement converting **3** into **3'** could be described in terms of a species in which a neutral glycolic acid molecule is able to move along and around the charged ethylene rod.

Provided that this skeletal rearrangement does occur, it is possible to interpret the labelling data in some detail. Table 6.3 gives the experimental ratios for loss of $C_2H_{4-n}D_n$ from labelled analogues of **1** and those calculated (second column) on the basis of the sequence **1** → **3** (⇄ **3'**) → **2** → **4**, as sketched in Scheme 6.3.

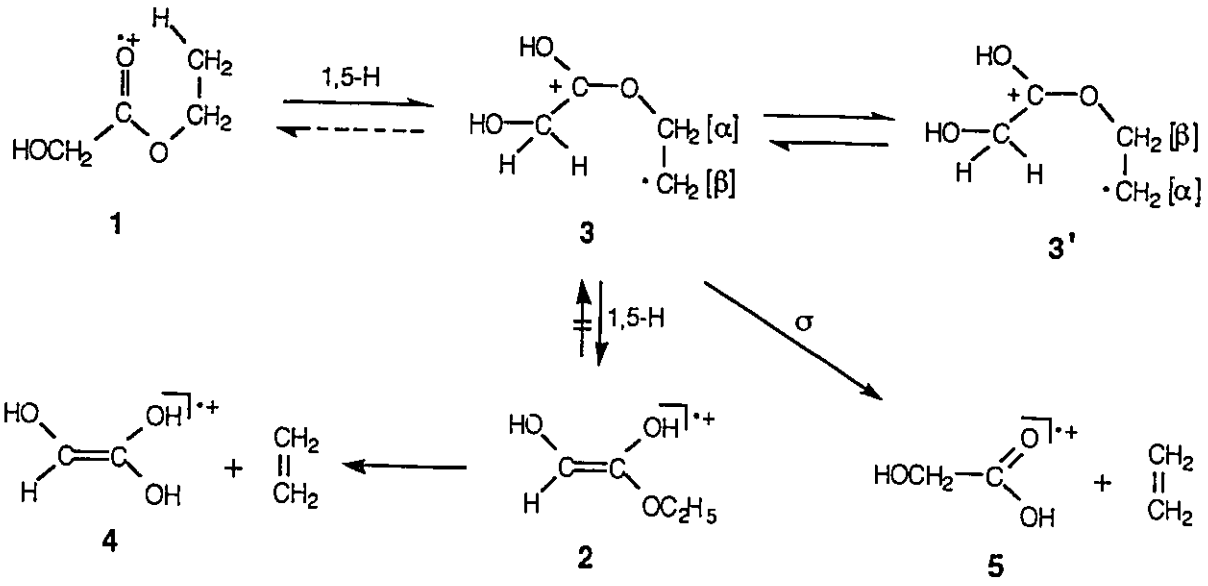

Scheme 6.3

Table 6.3. Observed and calculated ratios of $C_2H_{4-n}D_n$ loss from isotopologues of **1**.

Ion Structure	Neutral Lost	RA[a] Exp.[b]	Calc.[c]	Calc.[d]
$HOCD_2CO_2C_2H_5^{\bullet+}$	C_2H_4	25	33	26
	C_2H_3D	75	67	74
$HOCH_2CO_2CD_2CH_3^{\bullet+}$	C_2H_3D	27	33	26
$HOCH_2CO_2CH_2CD_3^{\bullet+}$	$C_2H_2D_2$	73	67	74

[a] See footnotes to Table 6.1; [b] Experimental; [c] Calculated, isotope effect $k_H/k_D = 1.0$, see text; [d] As in (c) but $k_H/k_D = 1.40$.

The agreement between these predicted ratios and those found experimentally is only reasonably good. However, it becomes excellent if an isotope effect of 1.4:1 favouring H^+ over D^+ transfer on the final step (**2**→**4**) is postulated (see third column of Table 6.3). The occurrence of a moderate isotope effect of this magnitude is not uncommon. Thus, all experiments are in agreement with enolization of **1** prior to

dissociation, provided that the methylene hydrogens in **3** become identical, pairwise, via the sequence **3** → **3'**, and that this reaction does not occur when starting from **2**, see Scheme 6.3. This is in good agreement with our conclusion, see above, that the tautomerization is unidirectional, i.e. **2** does not rearrange to **3**. Note that ion **3** could directly lose C_2H_4 to produce the keto product **5**, but because **5** lies much higher in energy than **4** (see below) this reaction cannot compete with formation of **4** from metastable ions **1** and **2**.

Alternatively, **2** may be formed from **1** via two consecutive 1,4-H shifts involving the distonic ion $HOCH_2C(OH)OCHCH_3^{\bullet+}$, **8**, rather than via **3**. Indeed, recent MO calculations [17a] indicate that a 1,5-H shift resulting in the formation of a primary radical centre (e.g., **1** →**3**) requires about the same energy as a 1,4-H shift leading to the production of a secondary radical centre (e.g., **1**→ **8**). Therefore, the route involving two successive 1,4-H shifts (**1**→ **8** → **2**) could conceivably compete with that involving two consecutive 1,5-H shifts (**1**→**3**(⇄**3'**)→**2**). However, the observation that $HOCH_2CO_2CD_2CH_3^{\bullet+}$ and $HOCH_2CO_2CH_2CD_3^{\bullet+}$ expel C_2H_3D and $C_2H_2D_2$ in the same ratio (see Table 3) militates against this possibility because the sequence **1**→ **8**→**2** erodes the positional integrity of the methylene group in the O-ethyl substituent. In contrast, this observation is naturally explained by the sequence **1** → **3**(⇄**3'**)→**2** shown in Scheme 6.3, as discussed previously. It is noted that generalizations concerning the relative ease of hydrogen transfers through cyclic transition states of different sizes cannot always be reliably extrapolated to a particular case. Thus, detailed studies of the reactions of ionized di-butyl ether and related species reveal that a 1,4-H shift from carbon to oxygen resulting in the production of a secondary radical is preferred over the alternative 1,5-H shift in which a primary radical centre is formed [17b]. However, in the case of **1**, the labelling results are equally clear in establishing a preference for the opposite site-selectivity : the 1,5-H shift is preferred to the alternative 1,4-shift.

The CID mass spectrum of $C_2H_4O_3^{\bullet+}$ ions generated from **1** in the *ion source* is shown in Fig. 6.1c. It can be seen, from the appearance of m/z 32 [11] (compare Figs. 6.1a and 6.1b) that ions **4** are clearly generated in admixture with **5**. This is precisely what is expected as ions generated in the *ion source* have larger internal energies than those formed from metastable ions. This further attests to the intermediacy of the distonic ion **3**.

Thermochemistry of C_2H_4 loss: appearance energy measurements and ab initio calculations.

To obtain a more accurate description of the potential energy surface associated with the loss of C_2H_4 from **1** and **2**, several appearance energy (AE) measurements were performed. The AE for loss of C_3H_6 (ΔH_f = 4.8 kcal/mol [18]) from ethyl 2-hydroxyisovalerate (ΔH_f = -164.6 kcal/mol [19]) (eq. 5) was measured, using energy selected electrons [20], AE = 10.19 ± 0.05 eV, leading to ΔH_f (**2**) = 66 kcal/mol. The AE for formation of m/z 76 (consecutive losses of C_3H_6 and C_2H_4), again using energy selected electrons, was 12.03 ± 0.05 eV. However, this value could equally well relate to the consecutive losses of C_2H_4 and C_3H_6, rather than vice versa and may thus have no bearing on the loss of C_2H_4 from **2**. Therefore, the AE of the metastable peak m/z 104 → m/z 76 was measured by a comparative method [21] ; in this way the process studied is unequivocal, namely loss of C_2H_4 from **2** to generate **4**. The AE thus obtained, 12.2 = 0.1 eV, is close to that obtained above (12.03 eV), so the more accurate and precise value obtained by energy selected electrons will be used. This value leads to an apparent ΔH_f (**4**) = 95 kcal/mol. The keto form, **5**, is estimated to have a ΔH_f of 105 kcal/mol [22] and this would indicate a marginal keto-enol stabilization energy (compare a stabilization energy of 23 kcal/mol for the ionized

acetic acid keto/enol system [18]). However, it is entirely possible that the above AE measurements actually reflect the barrier for the hydrogen transfer reaction **2** → **4**.

To test this possibility, the Gaussian 2 (G2) *ab initio* method [23] is employed - utilizing the MP2 approximation, known as G2(MP2) theory - which has been shown to yield results within 'chemical' accuracy (2-3 kcal / mol). The methodology, optimized structures and energetic information derived from the calculations are outlined in the theoretical methods section, Figure 6.2 and Table 6.4, respectively. Preceding the G2(MP2) calculation, the most stable ionic and neutral conformers of **4** had to be found. Four ionic and four corresponding neutral conformers, illustrated in Figure 6.2 as structures **4a** - **4h**, were investigated at the MP3/6-31G**//HF/6-31G* level of theory. From the relative energies in Table 6.4, ion structure **4d** and its corresponding neutral structure **4h** were found to be the most stable conformers and thus candidates for subsequent G2(MP2) calculations. Via the G2(MP2) method, we obtain $\Delta H_f^{298} = -107.4$ kcal / mol for the neutral, **4h** (MP2(FULL)/6-31G* geometry; see Figure 6.2). Addition of the ionization energy obtained by taking the difference in the G2(MP2) energies (see Table 6.4) between **4d** and **4h** yields a ΔH_f^{298} of 71.6 kcal / mol for ion **4d.** This leads to a reasonable keto/enol stabilization energy of 33 kcal/mol. Thus, by combination of experiment and theory we derive for the enol ion **2** the energy diagram shown in the right part of Fig. 6.3. It can be seen that the activation energy for loss of C_2H_4 from **2** is 42 kcal/mol with a reverse term of 24 kcal/mol. These values are very reminiscent of C_2H_4 loss from ionized phenyl ethyl ether [8a] (48 and 28 kcal/mol, respectively), again indicating that similar mechanisms may be involved. Moreover, the kinetic energy releases are very similar (25 meV for **2** and 30 meV for ionized phenyl ethyl ether [8a]) and small compared to the reverse terms. This indicates that ions **2** also most probably dissociate via an ethyl ion-radical complex, as shown in Scheme 6.1, where free energy flow between the moieties is minimal [9] and where

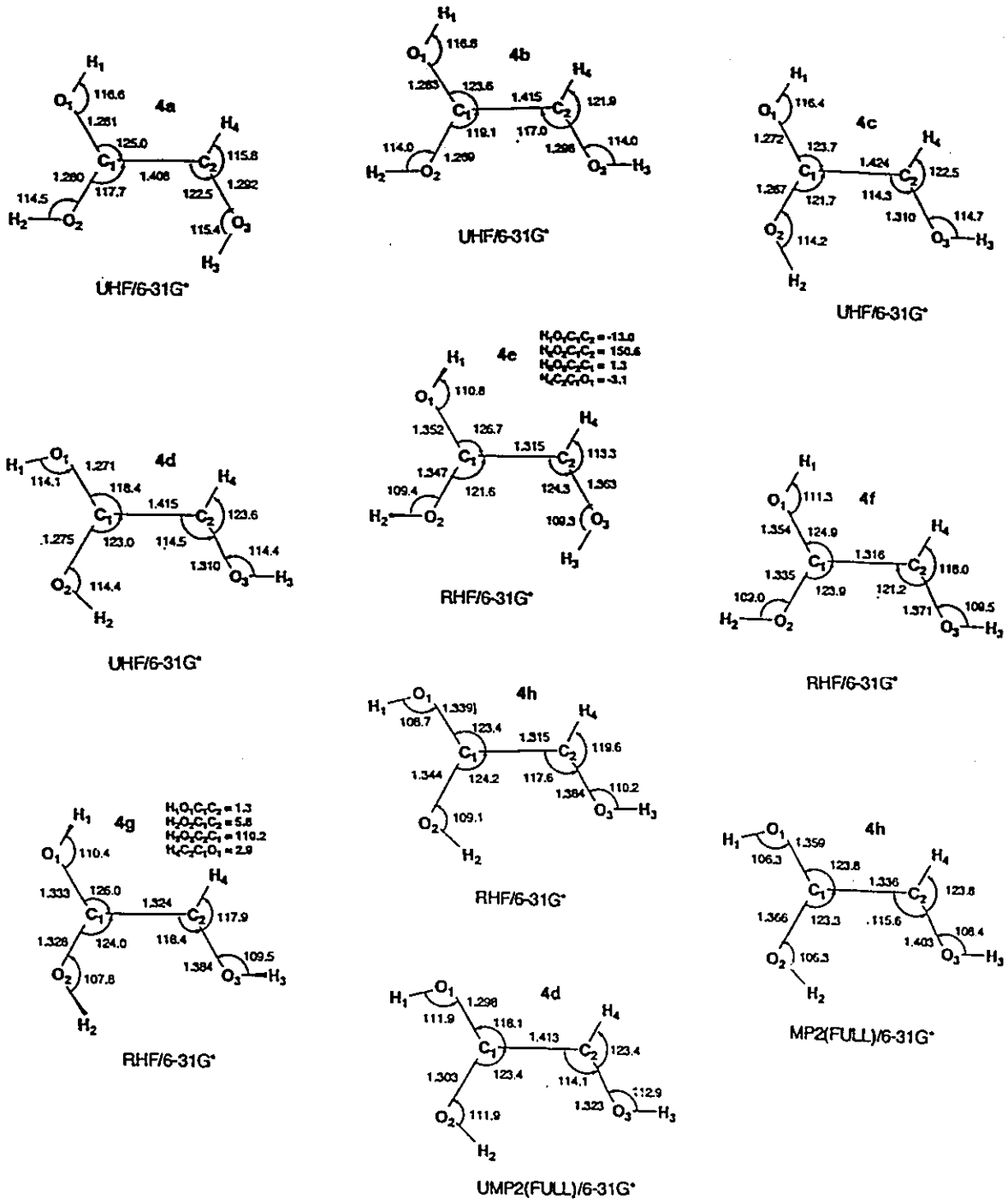

Figure 6.2. HF/6-31G* and MP2(FULL)/6-31G* optimized geometries for ionic and neutral conformers of trihydroxyethylene.

Table 6.4. Total Energies (Hartrees), Zero Point Vibrational Energies (ZPVE, kcal/mol) Relative Energies (E_{rel}, kcal/mol), G2(MP2) Energies (Hartrees) and ΔH_f values (kcal/mol) for Ionic (**4a-d**) and Neutral (**4e-h**) Isomers of Trihydroxyethylene.

Structure	E(HF/6-31G*)	E(MP3/6-31G**//HF/6-31G*)	ZPVE	State	E_{rel}[a]
4a	-302.359301	-303.170878	45.6	$^2A''$	4.3
4b	-302.360018	-303.170727	45.4	$^2A''$	4.6
4c	-302.359063	-303.168986	45.3	$^2A''$	5.6
4d	-302.368870	-303.178012	45.4	$^2A''$	0.0
4e	-302.595090	-303.437145	44.7	^1A	-163.2
4f	-302.587895	-303.429551	43.9	$^1A'$	-159.2
4g	-302.597608	-303.438715	45.3	^1A	-163.7
4h	-302.596896	-303.438371	44.7	$^1A'$	-164.0

Structure	E (MP2 (FULL) /6-31G*)	E (MP3 /6-31G**// MP2 (FULL) /6-31G*)	State	E_{rel}[b]
4h	-303.399448	-303.439770	$^1A'$	-164.2
4d	-303.142850	-303.179060	$^2A''$	0.0

Structure	G2 (MP2) (0 K)	G2 (MP2) (298 K)	ΔH_f^0	ΔH_f^{298}
4h	-303.833306	-303.828414	-105.3	-107.4
4d	-303.548500	-303.543172	73.4	71.6

a) E(MP3 /6-31G**//6-31G*) + 0.8929 x ZPVE ; b) E(MP3/6-31G**//MP2 (FULL) /6-31G*) + 0.8929 x ZPVE; E_{rel} is with respect to ion **4d** .

the reverse term is only weakly coupled to the translational separation of the products [24] leading to a relatively small $T_{0.5}$ value. The similarity between the dissociation of **2** and phenyl ethyl ether is also manifest from the magnitude of the isotope effect associated with the H^+/D^+ transfer. Above an isotope effect of 1.40 ± 0.07 for the H^+/D^+

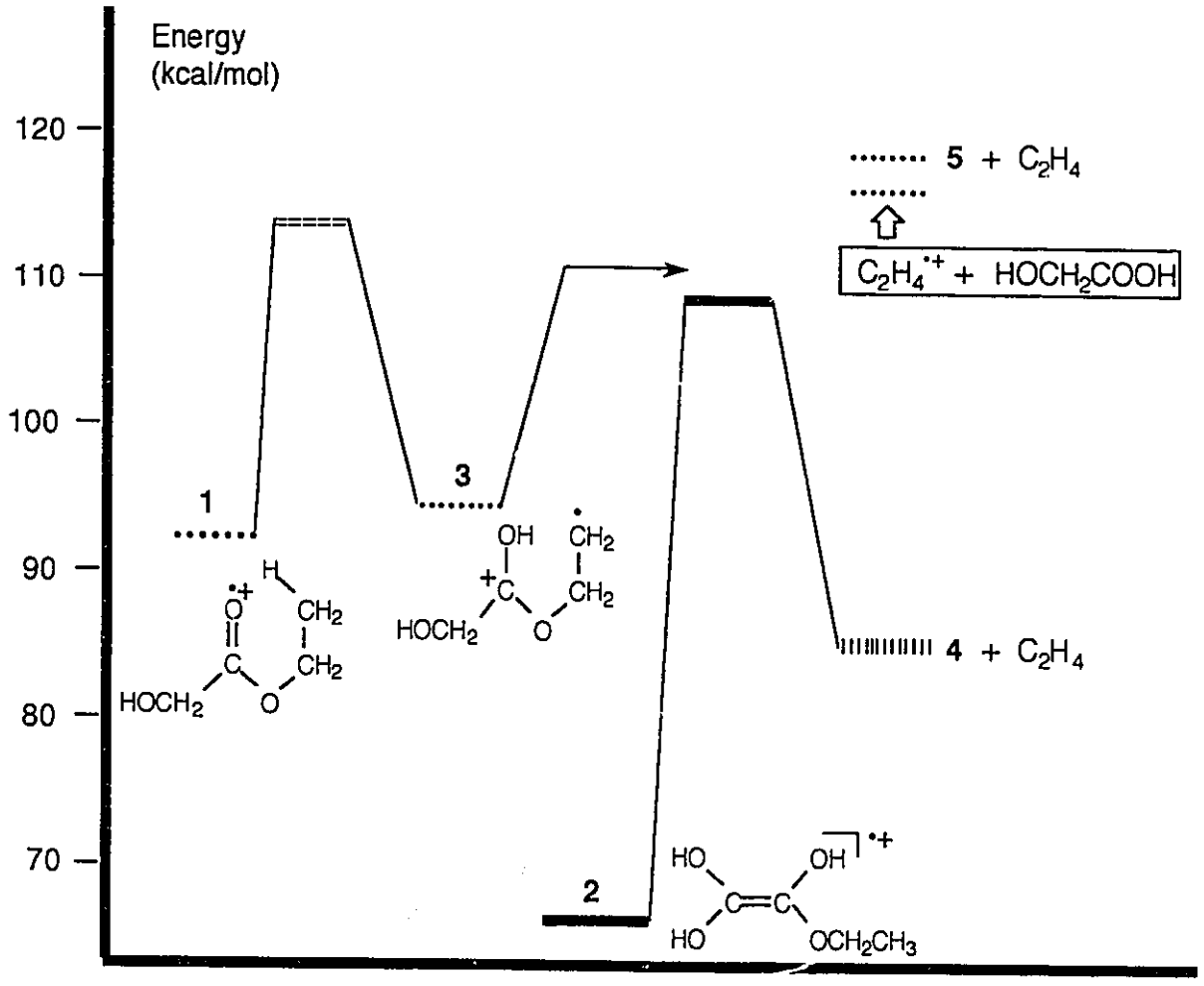

Figure 6.3 Potential energy diagram for the (unidirectional)isomerization and dissociation of ionized ethyl glycolate, **1** and its ionized enol, **2**.

transfer **2** → **4** was postulated; for the H^+/D^+ transfer in ionized phenyl ethyl ether, an isotope effect of 1.5:1 has been deduced [8b]. Similar isotope effects have been

observed for other ionized alkyl phenyl ethers for which there is evidence that they too fragment via exothermic proton transfers in alkyl ion-phenoxy complexes [9]. A detailed picture of the potential surface in the region of the transition state is not available. However, a simple model whereby the relative rates of reaction of an exothermic H^+ versus D^+ transfer through the transition state is related to the velocity of H^+ and D^+ through the transition state would predict an isotope effect of $\sqrt{2}$. It is surmised that an isotope effect of this magnitude may well be indicative of an exothermic proton transfer in an (alkyl)ion-radical complex.

The heat of formation of ion **1** has not been measured, but can be reliably estimated from the difference (14 kcal/mol) in the heats of formation of ionized ethyl acetate and ionized methyl acetate [18] and by subtracting this difference from the known heat of formation of ionized methyl glycolate [15]; this procedure gives ΔH_f = 92 kcal/mol as indicated in Fig.6.3.

ΔH_f of the distonic ion **3** can be estimated from the following thermodynamic cycle. Starting from ethyl propionate, $CH_3CH_2C(=O)OCH_2CH_3$, ΔH_f = -111 kcal/mol [18] and by using a C-H bond dissociation energy of 100 kcal/mol [19], it is estimated for the radical $CH_3CH_2C(=O)OCH_2CH_2^{\bullet}$: ΔH_f = - 41 kcal/mol (ΔH_f [H$^{\bullet}$] = 52 kcal/mol) [18]. Next, using a proton affinity of 200 kcal/mol typical for aliphatic esters [18] it is estimated for the distonic ion $CH_3CH_2C^+(OH)OCH_2CH_2^{\bullet}$: ΔH_f = 125 kcal/mol. Finally, using an OH substitution increment on a non-charge bearing site of ~31 kcal/mol (for example the difference in ΔH_f of neutral propane and ethanol [18]), it is obtaind for the distonic ion $HOCH_2C^+(OH)OCH_2CH_2^{\bullet}$: ΔH_f = 94 kcal/mol, about the same as for the keto ion, see Fig. 6.3.

The calculated threshold for formation of *ionized* $C_2H_4^{\bullet+}$ and *neutral* glycolic acid ($\Delta H_f[C_2H_4^{\bullet+}]$ = 254 kcal/mol and ΔH_f[glycolic acid] = -139.5 kcal/mol [22]) is also shown in Fig. 6.3. It is evident that this dissociation limit lies only a few kcal/mol above the

energy required to promote loss of C_2H_4 from **1**; indeed, it actually lies slightly below the dissociation limit for production of **5** and C_2H_4.

As discussed previously, MO calculations [16] indicate that the distonic ion CH_2-CH_2-$OH_2^{\bullet+}$ may assume a structure in which the water molecule may move freely from one carbon atom of the ionized ethylene to the other at an internal energy 7 kcal/mol below the treshold for formation of $C_2H_4^{\bullet+}$ and H_2O . By analogy with this system, the neutral glycolic acid molecule in the distonic ion **3** may also acquire such freedom to migrate from one carbon atom of the ionized ethylene to the other at an internal energy a few kcal/mol below that needed to form $C_2H_4^{\bullet+}$ + $HOCH_2COOH$. This possibility, **3** $\rightleftarrows$ $HOCH_2C(=O)OH\cdots CH_2=CH_2^{\bullet+}$ $\rightleftarrows$ **3'** , allows the labelling results to be understood.

It had been concluded above that ions **1** give rise to minor high energy side reactions, notably the degenerate isomerization observed for the distonic ion, **3** → **3'**, see Scheme 6.3, which are not observed when starting from ion **2**. This indicates, see Fig. 6.3, that the transformation **1** → **3** produces the distonic ion at elevated internal energies, which allow the occurence of such energy demanding processes. At the same time, it had been shown from labelling data that the isomerization **3** → **2** is unidirectional, i.e. that **2** → **3** does not in fact occur. Thus the dissociation **2** → **4** itself occurs at a faster rate than the isomerization **2** → **3**. Barring differences in frequency factors, this indicates that the transition state for the isomerization **2** → **3** lies above the threshold for C_2H_4 loss from **2**, as indicated in Fig. 6.3. Thus when ions **3** are formed from **1** they have sufficient internal energy to undergo the degenerate isomerization and other side reactions, whereas ions **3** cannot be formed from **2** at all. From the above it follows that starting from **1**, the first step, i.e. **1** → **3** is rate-determining. However, the labelling data were more consistent with the operation of an isotope effect in the final step. These observations are not in conflict : since the first step involves migration of one of the methyl hydrogen atoms of the OCH_2CH_3 group

of **1**, any isotope effect in this step would not be apparent from the labelled ions studied, the OCH_2CD_3 and OCD_2CH_3 esters. It has been indicated that at least one of the side reactions observed for **1**, i.e. formation of m/z 59, procedes from the distonic ion **3**.

Formation of m/z 59 could in principle be formulated as a simple cleavage process to produce $HOCH_2CO^+ + CH_3CH_2O^\bullet$. The calculated threshold energy for this reaction is 119 kcal/mol, from ΔH_f [$HOCH_2CO^+$] = 125 kcal/mol [25] and ΔH_f [$CH_3CH_2O^\bullet$] = - 6 kcal/mol [19]. However, the fact that ionized glycolic acid is not produced in the loss of C_2H_4, see above, but that it nevertheless requires less energy than formation of $HOCH_2CO^+$, see Fig. 6.3, led it to be believed that m/z 59 might not be the result of the above simple bond breaking process. Indeed, the CID mass spectrum of the metastably generated m/z 59 ions, shown in Fig. 6.4, is not compatible with any known $C_2H_3O_2^+$ structure [25]; rather it is indicative of $C_3H_7O^+$ ions [26] and so formation of m/z 59 involves the loss of $HOCO^\bullet$. As is shown in Scheme 6.4, the distonic ion **3** is a prime candidate to rationalize the loss of $HOCO^\bullet$: attack of the undoubtedly reactive radical site on the OH group followed by O-C cleavage leads to the reactive configuration **3a**.

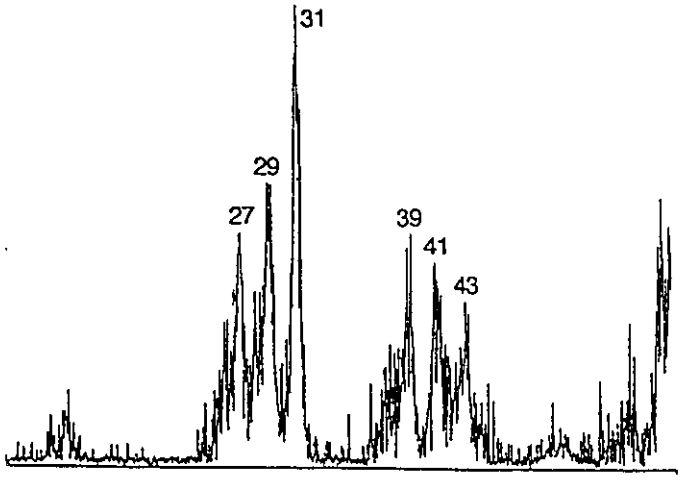

Figure 6.4. Collision-induced dissociation (CID) mass spectrum of m/z 59 ions generated from metastable $HOCH_2CO_2CH_2CH_3^{\bullet+}$, **1**, ions.

Note that the combined enthalpies of the proposed product ion, protonated oxetane, and HOCO• is 103 kcal/mol [18] and so these products are energetically accessible. In addition, the interconversion **3a** → **3b**, see Scheme 6.4, via 1,4-H shifts explains an otherwise puzzling observation : $HOCH_2C(=O)OCD_2CH_3^{\bullet+}$ shows specific loss of HOCO• but on the other hand it loses both C_2H_3D and $C_2H_2D_2$, see Table 6.3, whereas $HOCH_2C(=O)OCH_2CD_3^{\bullet+}$ shows losses of both HOCO• and DOCO• in a ratio of *ca.* 1. Inspection of Schemes 6.3 and 6.4 reveals that this is precisely what is expected.

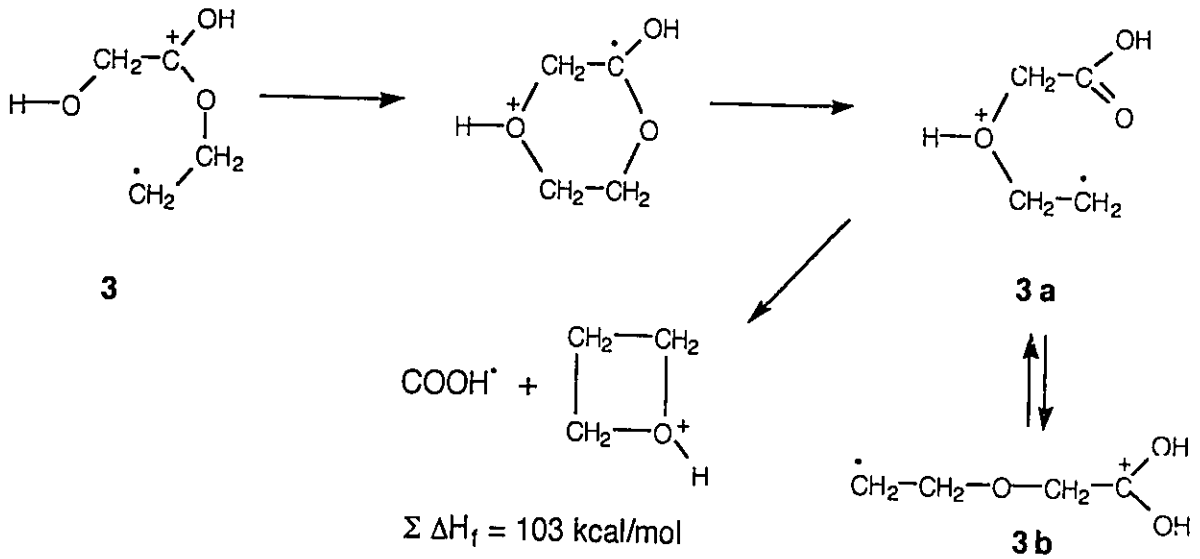

Scheme 6.4

Another minor process observed for **1**, but not for **2**, is loss of HCO•. Upon collisional activation, loss of C_2H_4 remains the dominant process for both **1** and **2**, see Figs. 6.5a and b. Other peaks that are present are at m/z 29, 45 and 58. However, it can clearly be seen that **1**, compared to **2**, contains a considerably more intense signal at m/z 75, arising from the expected loss of HCO• by double proton transfer which occurs so dominantly in ionized methyl glycolate and where there is no competition from ethylene loss. It is proposed that the same mechanism applies to ethyl glycolate.

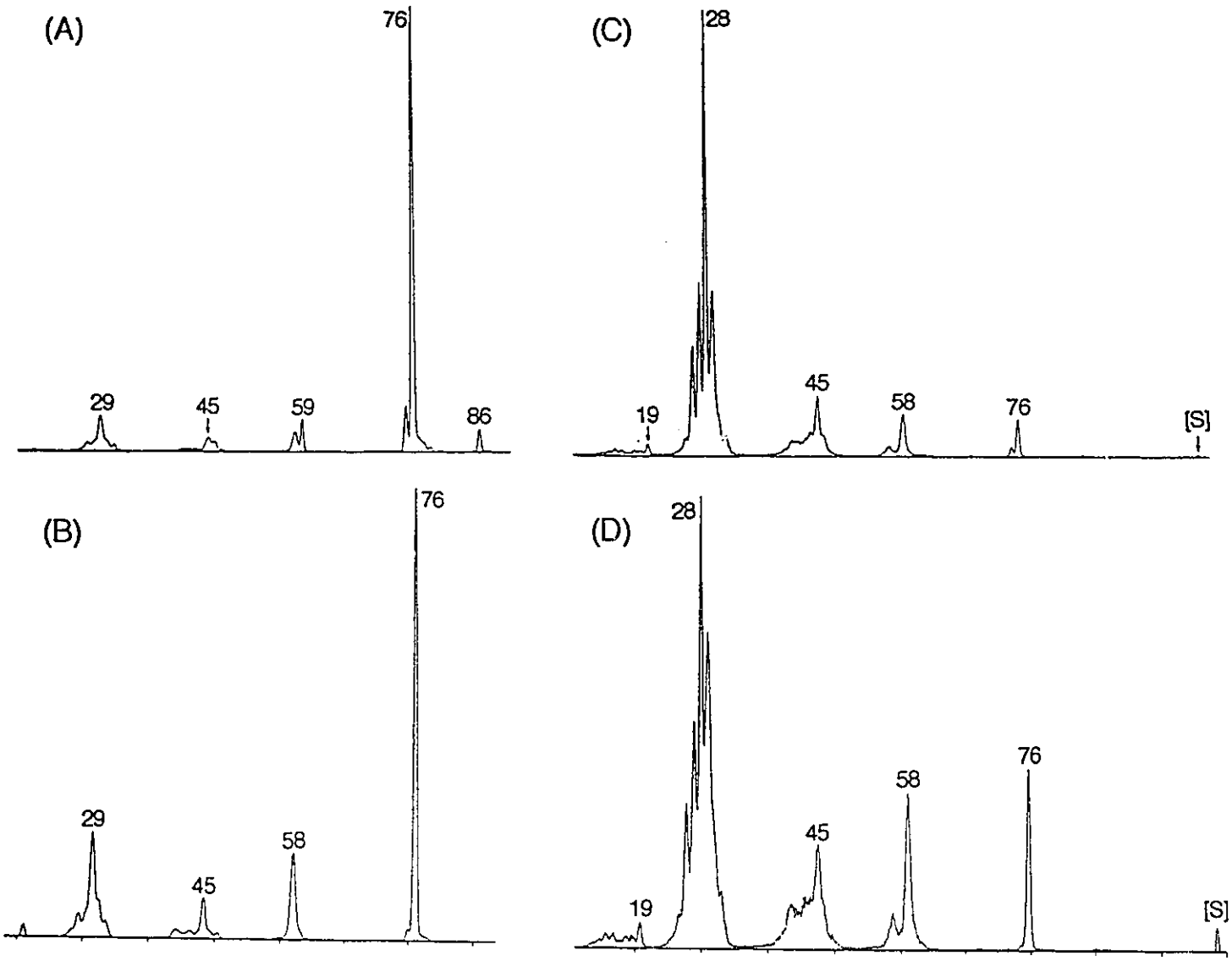

Figure 6.5. Collision-induced dissociation (CID) mass spectra of (a) $HOCH_2CO_2CH_2CH_3^{\bullet+}$, **1**; (b) $HOCH{=}C(OH)OCH_2CH_3^{\bullet+}$, **2**; and neutralization-reionization (NR) mass spectra of (c) $HOCH_2CO_2CH_2CH_3^{\bullet+}$, **1**and (d) $HOCH{=}C(OH)OCH_2CH_3^{\bullet+}$, **2**.

The neutralization-reionization (NR) mass spectra of **1** and **2** are also given in Figs. 6.5c and d. These spectra are dominated by ionized ethylene and its fragments at m/z 28, 27 and 26. According to the energy diagram it is possible that the metastably generated ethylene is generated in an excited state [27] and this may lead to an enhanced ionization cross section. Furthermore, the observation that a sizable survivor ion signal is present in the NR spectrum of **2**, whereas m/z 59, 75 and 86 (signals characteristic for the keto structure **1**) are absent, is good evidence that the neutral enol of ethyl glycolate, 1,2-dihydroxy-1-ethoxy ethylene is a stable species in the gas phase.

Finally it is noted that the rearrangement products m/z 59 and m/z 86 appear with significant abundances in the CID spectrum of **1** , see Fig. 3a, but that they are absent from the corresponding NR spectrum, Fig. 3c. This parallels observations from previous studies [27] that NR leads to reduced isomerization reactions (for example to reduced scrambling reactions in labelled ions [27a,b]) compared to CID.

Ionized and neutral trihydroxyethylene, $HOCH{=}C(OH)_2$

The specific production of ionized trihydroxyethylene, **4**, the enol isomer of ionized glycolic acid, **5**, by ethylene loss from **2** allows its chemistry to be studied. Its CID mass spectrum has already been discussed in some detail for structure assignment purposes.

Metastable ions **4** fragment solely by loss of water and as revealed by MS/MS/MS data this fragmentation yields ionized hydroxyketene [6]. The ion $HOCH{=}C(OH)^{18}OH^{\bullet+}$, generated by loss of C_2H_4 from $HOCH{=}C(OH)^{18}OC_2H_5^{\bullet+}$, loses H_2O and $H_2{}^{18}O$ in a ratio of *ca.* 1:1, whereas $HOCH{=}C(OH)(OD)^{\bullet+}$ loses HDO and H_2O in a ratio of 1.4 : 1.The mechanism outlined in Scheme 6.5 may explain these observations; note that this

mechanism is the same as that derived for the loss of methanol from the enol of ionized methyl glycolate [6]. This mechanism predicts a ratio for HDO and H_2O loss of 1:1, but note that reversibility of the first step leads to an increase in HDO loss, as observed. (Fast interconversion of **4**, **4a** and **4b** prior to water elimination would lead to an expected ratio of 2:1). The activation energy is estimated to be 27 kcal/mol (from ΔH_f [HOCH=C=O$^{\bullet+}$] = 157 kcal/mol [6], ΔH_f [**4**] = 72 kcal/mol [this work] and ΔH_f [H_2O] = -58 kcal/mol [18]); this value is very similar to that (36 kcal/mol) calculated for loss of methanol from the ionized enol of methyl glycolate [6].

The NR mass spectrum of **4** is shown in Fig. 6.1d. The structure characteristic fragments at m/z 29, 30 and 58, together with the presence of an intense survivor signal, are good indications that neutral trihydroxyethylene is a stable species which does not isomerize to glycolic acid. Definitive evidence for the existence of neutral **4**

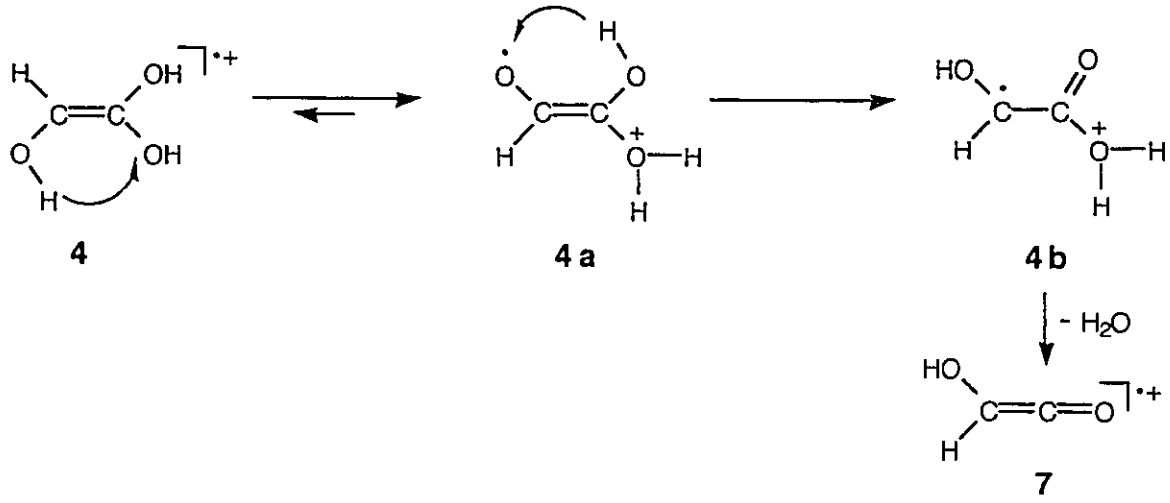

Scheme 6.5

comes from a delayed analysis of the survivor ions. In this experiment the survivor ions are selectively transmitted through the second sector of our triple sector machine and these selected ions are then allowed to dissociate spontaneously leading to the MI spectrum of the neutralized-reionized species (NR/MI, see Fig. 6.1e) or induced to

dissociate by CID, leading to the NR/CID spectrum, Fig. 6.1f. It can clearly be seen from Figs. 6.1e and f, in particular from the presence of an intense signal at m/z 58 and the absence of any detectable signal at m/z 32, that the enol neutrals have completely retained their structure and that they do not at all rearrange to their tautomeric glycolic acid counterparts, $HOCH_2COOH$.

Conclusions

The chemistry of ionized ethyl glycolate and its enol isomers is rich and interesting. Although the behaviour of the lower homologues, ionized methyl glycolate and its enol isomer do not undergo tautomerism, unidirectional enolization via two 1,5-H shifts dominates the reactions of ionized ethyl glycolate, which expels ethylene by two distinct routes, to give a mixture of ionized glycolic acid and its enol isomer. In contrast, the ionized enol isomer loses ethylene via a single channel to form only the ionized enol of glycolic acid with a strong preference for β-hydrogen transfer, which is not found for the keto isomer. The distonic ion $HOCH_2C^+(OH)OCH_2CH_2^{\bullet}$, which appears to undergo a facile degenerate rearrangement, plays a crucial role in the chemistry of ionized ethyl glycolate; however, it does not participate in the fragmentation of the ionized enol of ethyl glycolate. The ionized enol isomer of glycolic acid, which is stable in the gas phase and survives neutralization-reionization, also has interesting chemistry, dominated by water loss after 1,4-hydrogen transfers to give ionized hydroxyketene.

References

1. F.A. Corey and R.J. Sundberg, Advanced Organic Chemistry, Part A: Structure and Mechanism, Plenum Press, New York (1984).
2. (a) J.L. Holmes and F.P. Lossing, *J. Am. Chem. Soc.*, **102**, 1591 (1980); (b) F. Turecek, in Z. Rappoport (Ed.), The Chemistry of Enols, John Wiley, Chichester, pp. 95-146 (1990); (c) G. Bouchoux, *Mass Spectrom. Rev.*, **7**, 1 (1988); ibid., **7**, 203 (1988).
3. N. Heinrich, F. Lenage, C. Lifshitz and H. Schwarz, *J. Am. Chem. Soc.*, **110**, 8183 (1987).

4. N. Heinrich, J. Schmidt, H. Schwarz and Y. Apeloig, *J. Am. Chem. Soc.*, **109**, 1317 (1987).
5. D. Suh, C.A. Kingsmill, P.J.A. Ruttink, P.C. Burgers and J.K. Terlouw, *Int. J. Mass Spectrom. Ion Processes*, **146/147**, 305 (1995).
6. D. Suh, P.C. Burgers and J.K. Terlouw, *Rapid Commun. Mass Spectrom.*, **9**, 862 (1995).
7. P.J.A. Ruttink, P.C. Burgers and J.K. Terlouw, *Can. J. Chem.*, (1995) submitted.
8. (a) M.C. Blanchette, J.L. Holmes and F.P. Lossing, *Org. Mass Spectrom.*, **24**, 673 (1989); (b) D. Harnish and J.L. Holmes, *J. Am. Chem. Soc.*, **113**, 9729 (1991).
9. See for example, E.L. Chronister and T.H. Morton, *J. Am. Chem. Soc.*, **112**, 133 (1990) and references cited therein.
10. See for example, R.D. Bowen, *Org. Mass Spectrom.*, **28**, 1577 (1993) and references cited therein.
11. J.L. Holmes, F.P. Lossing, J.K. Terlouw and P.C. Burgers, *J. Am. Chem. Soc.*, **104**, 2931 (1982).
12. (a) P.C. Burgers, A.A. Mommers and J.L. Holmes, *J. Am. Chem. Soc.*, **105**, 5976 (1983); (b) R. Feng, C. Wesdemiotis and F.W. McLafferty, *J. Am. Chem. Soc.*, **109**, 6521 (1987).
13. (a) E. Uggerud, W. Koch and H. Schwarz, *Int. J. Mass Spectrom. Ion Processes*, **73**, 187 (1986); (b) W.J. Bouma, J.K. McLeod and L. Radom, *Int. J. Mass Spectrom. Ion Processes*, **33**, 87 (1980); (c) P.C. Burgers, J.L. Holmes and J.K. Terlouw, *J. Chem. Soc. Chem. Commun.*, 642 (1984).
14. P.C. Burgers, J.L. Holmes, W.J. Bouma and L. Radom, *J. Am. Chem. Soc.*, **108**, 1767 (1986).
15. For reviews see: (a) S. Hammerum, *Mass Spectrom. Rev.*, **7**, 123 (1988); (b) P.C. Burgers and J.K. Terlouw, in M.E. Rose (Ed.) Specialist Periodical Report: Mass Spectrometry, The Royal Society of Chemistry, London, Vol. 10, Chapter 2 (1989).
16 R. Postma, P.J.A. Ruttink, B.L.M. van Baar, J.K. Terlouw, J.L. Holmes and P.C. Burgers, *Chem. Phys. Lett.*, **123**, 409 (1986).
17 (a) V. Brenner, A. Milliet, P. Mourgues, G. Ohanessian and H.-E. Audier, *J. Chem. Phys.*, **99**, 10837 (1995); (b) R.D. Bowen, D. Suh and J.K. Terlouw, *Org. Mass Spectrom.*, **29**, 791 (1994).
18. S.G. Lias, J.E. Bartmess, J.F. Liebman, J.L. Holmes, R.D. Levine and W.G. Mallard, *J. Phys. Chem. Ref. Data 17* (Suppl. 1) (1988).
19. S.W. Benson, Thermochemical Kinetics, 2nd ed., Wiley-Interscience, New York (1976).
20. F.P. Lossing and J.C. Traeger, *Int. J. Mass Spectrom. Ion Phys.*, **19**, 9 (1976).
21. P.C. Burgers and J.L. Holmes, *Org. Mass Spectrom.*, **17**, 123 (1982).
22. J.L. Holmes, personal communication 1995.
23. (a) L.A. Curtiss, K. Raghavachari, G.W. Trucks and J.A. Pople, *J. Chem. Phys.*, **94**, 7221 (1991); (b) L.A. Curtiss, K. Raghavachari and J.A. Pople, *J. Chem. Phys.*, **98**, 1293 (1993).
24. D. Harnish and J.L. Holmes, *Org. Mass Spectrom.*, **29**, 213 (1994).
25. M.C. Blanchette, J.L. Holmes, C.E.C.A. Hop, F.P. Lossing, R. Postma, P.J.A. Ruttink and J.K. Terlouw, *J. Am. Chem. Soc.*, **108**, 7859 (1986).
26. S.J.A. Curtis and A.G. Harrison, *J. Am. Chem. Soc.*, **1**, 301 (1990).
27. (a) D.E. Drinkwater and F.W. McLaffferty, *Org. Mass Spectrom.*, **28**, 378 (1993); (b) P.C. Burgers, G.A. McGibbon and J.K. Terlouw, *Eur. Mass Spectrom.*, **1**, 261 (1995); (c) S. Beranova and C. Wesdemiotis, *J. Am. Soc. Mass Spectrom.*, **5**, 1093 (1994).

CHAPTER 7

Reactions of Ionized Dibutyl Ether

Introduction

The reactions of ionized ethers contain many interesting features At high internal energies (e.g. fragmentations occuring rapidly in the ion source), α-cleavages producing oxonium ions tend to dominate, especially at 70 eV ionizing electron energy [1]. However, at lower internal energies, a variety of interesting rearrangements often compete strongly with these α-cleavages. Thus, intense peaks arising by expulsion from the molecular ion of an alkenyl radical, $C_nH_{2n-1}^{\bullet}$, are found when the mass spectra of unbranched dialkyl ethers, $(C_nH_{2n+1})_2O^{\bullet+}$, are recorded at low ionizing electron energies [2]. Similar double hydrogen transfer (DHT) processes have been reported in the fragmentation of smaller alcohols and ethers, as is exemplified by the presence of significant $[M-C_3H_5]^+$ signals in the 70 and 12 eV spectra of $(CH_3)_2CHCH_2OH^{\bullet+}$ [3,4]. These unusual fragmentations have been interpreted by

The work presented here was based on an article under the above title:

R.D. Bowen, D. Suh and J.K. Terlouw, *Org. Mass Spectrom.*, **29**, 791 (1994).

means of mechanisms in which distonic ions (DIs) [5,6] and ion-neutral complexes (INCs) [7-13] play crucial roles in the hydrogen transfer and skeletal isomerization steps. The loss of an alkane, C_nH_{2n+2}, derived from an α-alkyl group and a β-hydrogen atom from a neighbouring α-substituent is also common [13,17], as is illustrated by the expulsion of C_3H_8 from metastable $C_3H_7(CH_3)CHOCH_3^{\bullet+}$ species. INC-mediated mechanisms have also been applied to explain this class of reactions. A third common fragmentation is elimination of $C_2H_5^{\bullet}$ from ionized ethers derived from primary butyl and larger homologous alcohols [13-16,18,19]. This process entails rearrangement of the 'heavy atom' skeleton, which can be envisaged to take place by a direct 1,3-ROH shift which converts the appropriate DI into an isomer in which the oxygen atom is now attached to the original γ-carbon atom. Alternatively, it may be visualized in two stages involving ring closure of the hydrocarbon chain containing the radical site to give an INC comprising an ionized alkylcyclopropane and ROH, followed by ring opening in a different sense to form the rearranged DI. A second 1,4-H shift then returns the hydrogen atom from oxygen to the radical centre, yielding an ionized ether derived from a secondary alcohol [20]. Expulsion of $C_2H_5^{\bullet}$ then occurs by α-cleavage (Scheme 7.1).

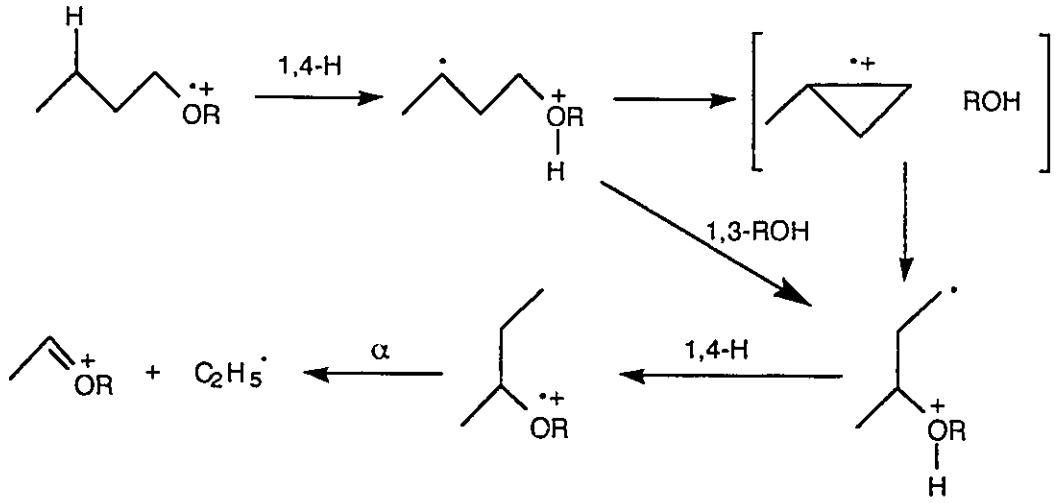

Scheme 7.1

In the course of research on the chemistry of oxonium ions [21], several isomers of $C_4H_9OC_4H_7D_2$ and $C_4H_7D_2OC_4H_7D_2$ were prepared in order to generate and investigate the reactions of labelled analogues of $CH_3CH_2CH_2CH_2{}^+O{=}CHCH_3$. The mass spectra of these labelled dibutyl ethers revealed that the initial 1,4-H/D shift was apparently influenced by a sizeable isotope effect. Consequently, a more extensive range of labelled dibutyl ethers was synthesized in order to permit a detailed scrutiny of the reactions of $(C_4H_9)_2O^{\bullet+}$ species.

Results and Discussion

The reactions of metastable $C_8H_{18}O^{\bullet+}$ radical-cations generated by ionization of di-*n*-butyl ether (**1**), *n*-butyl *sec*-butyl ether (**2**) and di-*sec*-butyl ethers (**3**) are repo:ted in Table 7.1. Collisional activation (CA) [22-24] spectra and neutralization-reionization mass spectra (NRMS) [25-28] of isomeric species formed as $\mathbf{1}^{\bullet+}$, $\mathbf{2}^{\bullet+}$ and $\mathbf{3}^{\bullet+}$ are

Table 7.1. Reactions of metastable ionized dibutyl ethers

	Neutral species lost													
	$CH_3^{\bullet}$		$C_2H_5^{\bullet}$		C_2H_6		$C_4H_7^{\bullet}$		$C_4H_9^{\bullet}$		C_4H_{10}		$C_4H_{10}O$	
Precursor structure	RA[a]	T[b]	RA	T	RA	T	RA	T	RA	T	RA	T	RA	T
$CH_3CH_2CH_2CH_2OCH_2CH_2CH_2CH_3$	2	1.6	87	1.9			5	1.7	3	1.7	2	1.9	2	1.8
$CH_3CH_2CH_2CH_2OCH(CH_3)CH_2CH_3$	36	0.9	20	1.6	39	1.4	1	[c]	3	[c]	1	[c]	1	[c]
$CH_3CH_2(CH_3)CHOCH(CH_3)CH_2CH_3$	41	0.8	4	1.5	55	1.1								

[a] RA = relative abundance (%), measured by metastable peaks areas and normalized to a total of 100 units for ions dissociating in the second field-free region; [b] T = kinetic energy release (kJ/mol) as estimated from the width at half-height of the corresponding metastable peak; all the metastable peaks had a Gaussian or approximately Gaussian profile; [c] Peak too weak to permit accurate measurement.

given in Tables 7.2 and 7.3, respectively. New data on the dissociation of metastable $C_6H_{13}O^{\bullet+}$ product ions formed by $C_2H_5^{\bullet}$ elimination from **1**$^{\bullet+}$, **2**$^{\bullet+}$ and **3**$^{\bullet+}$ are compared with older results in Table 7.4; the CA spectra of these oxonium ions are summarized in Table 7.5.

Comparison of the chemistry of 1$^{\bullet+}$, 2$^{\bullet+}$ and 3$^{\bullet+}$

Overview of the reactions of metastable 1$^{\bullet+}$, 2$^{\bullet+}$ and 3$^{\bullet+}$

The reactions of metastable **1**$^{\bullet+}$ differ markedly from those of **2**$^{\bullet+}$ and **3**$^{\bullet+}$. Ions formed from **1** expel predominantly $C_2H_5^{\bullet}$, with much smaller contributions for loss of $CH_3^{\bullet}$, $C_4H_7^{\bullet}$, $C_4H_9^{\bullet}$ and $C_4H_{10}O$. The relative abundance (RA, expressed as a percentage of the total metastable ion current for dissociation of **1**$^{\bullet+}$) for $C_2H_5^{\bullet}$ elimination exceeds 85%; of the other reactions, only $C_4H_7^{\bullet}$ loss has an RA greater than 3%. These data are in good agreement with those reported previously [14]. All the fragmentations give rise to approximately Gaussian metastable peaks, corresponding to moderate kinetic energy releases (KER, in each case, $T_{1/2}$, the KE release estimated from the width at half-height of the appropriate metastable peak, lies in the range 1.6-1.9 kJ/mol). In contrast, **2**$^{\bullet+}$ and particularly **3**$^{\bullet+}$ lose much less $C_2H_5^{\bullet}$ (RA=20 and 4%, respectively), but expulsion of $CH_3^{\bullet}$ and C_2H_6, which are of minor and negligible importance starting from **1**$^{\bullet+}$, become dominant (RA=35-40 and 40-55%, respectively). This contrasting reactivity of radical-cations generated from ethers containing isomeric butyl groups appears to be typical. Parallel effects have been found for lower homologues (e.g. the corresponding ionized butyl ethyl ethers) [14,16]. Alkane (in this system, C_2H_6) loss is much more abundant in the fragmentation of ionized secondary ethers because it yields thermodynamically more

favourable products and has a lower critical [29] energy than alkyl radical (in this case, $C_2H_5^{\bullet}$) elimination by α-cleavage. However, starting from the primary ionized ether, the unidirectional rearrangement illustrated in Scheme 7.1 produces a significantly more energized population of radical-cations with the ionized secondary ether structure, which show an enhanced preference for direct dissociation via α-cleavage and a reduced tendency to undergo the additional hydrogen transfer that must precede alkane loss. The observation that the $T_{1/2}$ value for $C_2H_5^{\bullet}$ loss from $\mathbf{1}^{\bullet+}$ (1.9 kJ/mol) exceeds that starting from $\mathbf{2}^{\bullet+}$ (1.6 kJ/mol) supports this view. The higher energy ions formed by rearrangement of $\mathbf{1}^{\bullet+}$ fragment at an increased rate [30] and with a greater average KE release [31]. Moreover, it is known that the ratio of $C_2H_5^{\bullet}$ to C_2H_6 losses from radical-cations generated from ethers often shows a very pronounced dependence on the average internal energy of the dissociating ions [32]. Consequently, the divergent behaviour of $\mathbf{1}^{\bullet+}$, $\mathbf{2}^{\bullet+}$ and $\mathbf{3}^{\bullet+}$ is intelligible. In particular, the chemistry of $\mathbf{1}^{\bullet+}$ and $\mathbf{2}^{\bullet+}$ may be interpreted by means of Scheme 7.1 ($R=CH_3CH_2CH_2CH_2$).

A proportion of metastable radical-cations formed as $\mathbf{2}^{\bullet+}$ may undergo a similar isomerization of the *n*-butyl group to give $\mathbf{3}^{\bullet+}$ prior to $C_2H_5^{\bullet}$ elimination. This interpretation is in line with the slightly greater $T_{1/2}$ value for $C_2H_5^{\bullet}$ loss from $\mathbf{2}^{\bullet+}$ compared with that for fragmentation of $\mathbf{3}^{\bullet+}$ (1.5 kJ/mol). Parallel trends are found in the $T_{1/2}$ values for other common fragmentations ($CH_3^{\bullet}$ and C_2H_6 expulsion) of $\mathbf{2}^{\bullet+}$ and $\mathbf{3}^{\bullet+}$. However, despite the trends in the $T_{1/2}$ values it is unlikely that when $\mathbf{2}^{\bullet+}$ is formed by isomerization of $\mathbf{1}^{\bullet+}$ further rearrangement to $\mathbf{3}^{\bullet+}$ takes place. Such rearrangements of the *n*-butyl to *sec*-butyl substituents are slow and rate limiting; consequently, a second isomerization of the previously unrearranged butyl group of $\mathbf{2}^{\bullet+}$ formed from $\mathbf{1}^{\bullet+}$ would be pre-empted by faster alternative precesses, particularly $C_2H_5^{\bullet}$ elimination.

*Structure of the $C_8H_{18}O^{\bullet+}$ radical-cations formed as **1**$^{\bullet+}$, **2**$^{\bullet+}$ and **3**$^{\bullet+}$*

Further valuable insight is provided by the CA and NRMS of the parent $C_8H_{18}O^{\bullet+}$ species. The distinctive CA spectra reveal that ions formed as **1**$^{\bullet+}$, **2**$^{\bullet+}$ and **3**$^{\bullet+}$ have each a retained a discrete identity after a period of several microseconds. All the spectra contain prominent $(M-C_2H_5)^+$ peaks at m/z 101; however, these signals contain contributions from the dissociation of ions that have not been energized by collision. Apart from these peaks, the spectra of **1**$^{\bullet+}$ and **2**$^{\bullet+}$ are dominated by the product ion at m/z 56 $[(M-C_4H_{10}O)^{\bullet+}]$; in contrast, the ion at m/z 57 $[(M-C_4H_9O)^+]$ is more abundant than that at m/z 56 in the spectrum of **3**$^{\bullet+}$. However, the spectra of **1**$^{\bullet+}$ and **2**$^{\bullet+}$ are not identical. These data suggest that some (but not all) non-decomposing ions formed as **1**$^{\bullet+}$ isomerize to **2**$^{\bullet+}$.

None of the CA spectra contains even moderately intense $(M-C_3H_7)^+$ signals at m/z 87. In the case of **3**$^{\bullet+}$, this is hardly surprising: no intact propyl group is present in the initial structure. Similarly, although **2**$^{\bullet+}$ does contain a $CH_3CH_2CH_2CH_2O$ substituent, which might be expected to undergo $C_3H_7^{\bullet}$ loss by α-cleavage, it is plausible to suppose that this process would be swamped by the energetically more favourable α-cleavages of the $CH_3CH_2(CH_3)CH$ group. However, the very low intensity of the $(M-C_3H_7)^+$ peak in the CA spectra of **1**$^{\bullet+}$ may be more significant. It is possible, but unlikely, that the energy deposited in non-decomposing ions is rarely sufficient to permit $C_3H_7^{\bullet}$ loss by α-cleavage to compete effectively. A more probable alternative explanation is that only a comparatively small proportion of these species remain as **1**$^{\bullet+}$ because most have rearranged to other more stable structures. Likely contenders for such structures include the DIs and the INC involved in isomerization of **1**$^{\bullet+}$ to **2**$^{\bullet+}$ (Scheme 7.1, R=C_4H_9). All these species might be expected to fragment readily on collisional activation via loss of $C_4H_{10}O$ to give m/z 56, because each contains an *n*-butanol molecule as an intact entity.

Tables 7.2/3. Collisional activation and neutralization-reionization mass spectra of $C_4H_9OC_4H_9^{\bullet+}$ radical-cations.

m/z	*n*-C_4H_9O-*sec*-C_4H_9		(n-C_4H_9)$_2O$		(*sec*-C_4H_9)$_2O$	
	CA[a]	NR[a]	CA	NR	CA	NR
115	(85)	<1	3		(184)	3
101	(390)	8	(160)		(805)	40
100	(64)		1		(168)	
87	3	1	4	1		
85	5	1	1		8	6
83	3			13		
75	(10)		(12)			
74	10		1			
73	18	3	11	3	11	13
59	5	8		1	13	21
57	59	49	29	30	100	100
56	100	50	100	50	42	38
55	18	24	9	41	13	19
45	18	25	3	7	58	45
43	8	18	3	38	11	20
42		23		17		
41	21	48	10	46	26	45
39	10	39	4	39	11	38
31	3	11	2	48	3	4
29	15	100	5	100	24	65
28	6	46	2	43	8	28
27	8	51	3	58	11	32
15		3		2		3

[a] RI = relative intensity, measured by peak height and normalized to a value of 100 units for the most intense signal containing no significant contribution (greater than 2% of the total ion current for fragmentation of metastable $C_4H_9OC_4H_9^{\bullet+}$, see Table 7.1) from the dissociation of ions that were not energized by collision. Values in parentheses (corresponding to loss of $CH_3^{\bullet}$, $C_2H_5^{\bullet}$, C_2H_6 and $C_4H_7^{\bullet}$) contain significant contributions from the dissociation of ions that were not energized by collision.

Parallel conclusions may be drawn from the NR spectra: **1**$^{\bullet+}$, **2**$^{\bullet+}$ and **3**$^{\bullet+}$ exhibit distinctive spectra, but the spectrum of **1**$^{\bullet+}$ has many features in common with that of **2**$^{\bullet+}$ and both bear almost no resemblance to that of **3**$^{\bullet+}$. Thus, **1**$^{\bullet+}$ and **2**$^{\bullet+}$ show enhanced propensities for producing m/z 29 [although this signal arises mainly from collision-induced ionization of $C_2H_5^{\bullet}$ neutral species produced by the unimolecular dissociation of $(C_4H_9)_2O^{\bullet+}$], whereas **3**$^{\bullet+}$ exhibits a preference for forming the same product (m/z 57) as is favoured in its CA spectrum.

The NR spectra do not contain appreciable peaks corresponding to $C_8H_{18}O^{\bullet+}$ species that have survived neutralization and reionization without fragmenting. The absence of such 'survivor' signals suggests strongly that most or all of the radical-cations generated as **1**$^{\bullet+}$, **2**$^{\bullet+}$ and **3**$^{\bullet+}$ have rearranged after a few microseconds to isomers which do not have stable neutral counterparts. Consequently, neutralization produces neutral species that dissociate before being reionized. This conclusion is perhaps somewhat tentative in the case of **3**$^{\bullet+}$ because this species is much more vulnerable to fragmentation than **1**$^{\bullet+}$ and **2**$^{\bullet+}$. Therefore, it is conceivable that some ions formed as **3**$^{\bullet+}$ do retain their initial structure, but that after neutralization to **3**, reionization produces a population of **3**$^{\bullet+}$ species that are energized sufficiently highly to cause almost all of them to fragment. A comparable situation is unlikely to apply for **1**$^{\bullet+}$ and **2**$^{\bullet+}$ because these radical-cations, particularly **1**$^{\bullet+}$, are much less susceptible to extensive fragmentation than **3**$^{\bullet+}$. Moreover, the spectra of **1**$^{\bullet+}$ and **2**$^{\bullet+}$ show very few signals above m/z 57, but strong peaks at m/z 87, $[M\text{-}C_3H_7]^+$, and m/z 101, $[M\text{-}C_2H_5]^+$, respectively, arising by α-cleavage would be expected if **1**$^{\bullet+}$ and **2**$^{\bullet+}$ retained their original structure until neutralization and reionization.

An especially interesting feature of the NR spectrum of **1**$^{\bullet+}$ is the presence of an intense signal at m/z 31. This ion must be $CH_2{=}OH^+$ and it almost certainly arises by

ionization and fragmentation of *n*-butanol formed by neutralization of species generated as $\mathbf{1}^{\bullet+}$. This finding is explicable if a significant proportion of the ions generated as $\mathbf{1}^{\bullet+}$ have attained structures containing an intact *n*-butanol entity when they are neutralized. It is noteworthy in this connection that *n*-butanol displays a negligible molecular ion signal in its conventional electron impact (EI) mass spectrum, which is dominated by the base peak at m/z 31, corresponding to $CH_2{=}OH^+$; similar behaviour is expected following collisional ionization. The corresponding peaks at m/z 31 in the spectra of $\mathbf{2}^{\bullet+}$ and $\mathbf{3}^{\bullet+}$ are much weaker, as would be expected if only $\mathbf{1}^{\bullet+}$ rearranges freely to structures containing a complete *n*-butanol molecule.

Structure of the $C_6H_{13}O^+$ ions formed from $\mathbf{1}^{\bullet+}$, $\mathbf{2}^{\bullet+}$ and $\mathbf{3}^{\bullet+}$

The reactions of metastable $[M\text{-}C_2H_5]^+$ ions formed by ionization and fragmentation of **1** and **2** are similar, whereas those of ions generated from **3** are noticeably different, especially in the distinctive ratios (1.5+0.2 and 11+1, respectively) for $H_2O{:}C_4H_8$ loss (see Table 7.4). These data suggest that $C_2H_5^{\bullet}$

Table 7.4 Reactions of metastable $C_6H_{13}O^+$ ions[a,b]

Precursor structure	Probable ion structure	Neutral species lost							
		H_2O		C_3H_6		$CH_3CH{=}O$		C_4H_8	
		RA	T	RA	T	RA	T	RA	T
$CH_3CH_2CH_2CH_2OCH_2CH_2CH_2CH_3$	$CH_3CH{=}O^+CH_2CH_2CH_2CH_3$	43	2.4	6	~3[c]	18	2.0	32	2.0
$CH_3CH_2CH_2CH_2OCH(CH_3)CH_2CH_3$	$CH_3CH{=}O^+CH_2CH_2CH_2CH_3$	52	2.1	7	~4[c]	10	1.9	31	1.8
$CH_3CH_2(CH_3)CHOCH(CH_3)CH_2CH_3$	$CH_3CH{=}O^+CH(CH_3)CH_2CH_3$	78	2.1	6	~6[c]	8	1.6	7	1.6

[a] See footnote to Table 7.1; RAs were normalized to a total of 100 units for dissociation of $C_6H_{13}O^+$ ions in the second field-free region; [b] See footnote to Table 7.1; all the metastable peaks were Gaussian or near Gaussian profile except for those arising from C_3H_6 loss, which were composite; [c] Composite peak.

expulsion from both **1**$^{\bullet+}$ and **2**$^{\bullet+}$ affords a common structure (presumably $CH_3CH_2CH_2CH_2^+O{=}CHCH_3$, **4**) but the corresponding fragmentation of **3**$^{\bullet+}$ leads to an isomeric species (probably $CH_3CH_2(CH_3)CH^+O{=}CHCH_3$, **5**). Although the behaviour of metastable ions can be strongly influenced by energy effects [33], which means that the ratios of competing reactions cannot always be regarded as a reliable criterion for structure elucidation, these results do seem clear. Moreover, the agreement of the current data with those reported previously [34] in a study of the chemistry of the four isomeric $C_4H_9^+O{=}CHCH_3$ ions is very good.

There are minor discrepancies in the ratios of the competing reactions of the metastable $[M\text{-}C_2H_5]^+$ ions formed from **1**$^{\bullet+}$ and **2**$^{\bullet+}$. Ions generated from **2**$^{\bullet+}$ show an enhanced tendency to lose H_2O and a diminished propensity for C_4H_8 elimination relative to the values found for ions formed from **1**$^{\bullet+}$. This deviation slightly skews the ratios towards those found for ions generated from **3**$^{\bullet+}$. These minor differencies may merely reflect internal energy effects. Alternatively, it is possible that when $C_6H_{13}O^+$ oxonium ions are formed from **2**$^{\bullet+}$ at longer lifetimes and lower average internal energies, some isomerization to **3**$^{\bullet+}$ may precede $C_2H_5^{\bullet}$ elimination. As a result, the reactions of ions generated in this way may contain a minor contribution from the dissociation of rearranged ions that are actually **5**. However, any such effect is small; there is no doubt that the reactions of ions generated from **1**$^{\bullet+}$ and **2**$^{\bullet+}$ are closely similar, but those formed from **3**$^{\bullet+}$ are distinctly different.

Collisional activation mass spectra provide a more reliable means of distinguishing between isomeric structures that exist in potential energy wells. The CA spectra of the ions produced by $C_2H_5^{\bullet}$ loss from **1**$^{\bullet+}$ and **2**$^{\bullet+}$ are very similar and diagnostically different from the spectrum of ions formed from **3**$^{\bullet+}$ (see Table 7.5). Thus, the signals at m/z 26-29, 41 and especially 58 and 85 are much more intense in the spectra of $C_6H_{13}O^+$ ions formed from fragmentation of **1**$^{\bullet+}$ and **2**$^{\bullet+}$ than those in the spectrum of

Table 7.5. Collisional activation spectra of $C_6H_{13}O^+$ radical-cation.

m/z	Precursor: *n*-C_4H_9O-*sec*-C_4H_9 RI[a]	Precursor: (*n*-C_4H_9)$_2$O RI[a]	Precursor: (*sec*-C_4H_9)$_2$O RI[a]
85	42	42	14
83	(212)	(39)	(335)
73	4	3	
72	6	6	8
71	8	8	5
59	(25)	(6)	(32)
58	63	69	14
57	(454)	(400)	(311)
56	83	94	100
55	25	25	22
54	8	8	5
53	8	8	8
45	(638)	(422)	(411)
44	25	25	35
43	75	72	68
42	25	28	22
41	100	100	70
39	46	44	32
31	6	6	3
29	79	83	49
28	38	39	19
27	54	53	35
15	4	3	3

[a] RI = relative intensity, measured by peak height and normalized to a value of 100 units for the most intense signal containing no contribution from the dissociation of ions that were not energized by collision. Values in parentheses (corresponding to loss of H_2O, C_3H_6, $CH_3CH{=}O$ and C_4H_8) contain contributions from the dissociation of ions that were not energized by collision.

the corresponding ions generated from **3**$^{\bullet+}$. The ratios of the intensities of the peaks at m/z 85 and 44 are 1.68, 1.68 and 0.40, in the CA spectra of ions formed from **1**$^{\bullet+}$, **2**$^{\bullet+}$ and **3**$^{\bullet+}$, respectively. Consequently, $C_2H_5^{\bullet}$ loss from **3**$^{\bullet+}$ yields a different structure (**5**) to that (**4**) formed from **1**$^{\bullet+}$ and **2**$^{\bullet+}$.

This proposal is supported by the relative abundances of doubly charged product ions formed from the $[M\text{-}C_2H_5]^+$ species after collision. Reasonably intense signals at m/z 49 and 50 are found in the charge stripping (CS) spectra of $C_6H_{13}O^+$ ions generated from **1** and **2**. In contrast, the corresponding peaks formed from ions generated from **3** have less than one tenth the intensity of those produced from **1**. Further, the ratios of the intensities of the doubly charged peaks at m/z 49 and 50 are 1.5:1, 1.4:1 and 0.6:1 for $[M\text{-}C_2H_5]^+$ ions formed from **1**, **2** and **3**, respectively. These results are consistent with the proposal that $C_2H_5^{\bullet}$ elimination from **1**$^{\bullet+}$ and **2**$^{\bullet+}$ gives **4**, whereas the same fragmentation of **3**$^{\bullet+}$ yields **5**.

All these results support the generalized mechanism of Scheme 7.1: **1**$^{\bullet+}$ and **2**$^{\bullet+}$ have a related chemistry, in which **1**$^{\bullet+}$ isomerizes unidirectionally to **2**$^{\bullet+}$. The reactions of **3**$^{\bullet+}$ are related to those of **1**$^{\bullet+}$ and **2**$^{\bullet+}$ in that some ions generated as **2**$^{\bullet+}$ may rearrange to **3**$^{\bullet+}$, but few ions (if any) that rearrange from **1**$^{\bullet+}$ to **2**$^{\bullet+}$ undergo a second isomerization to **3**$^{\bullet+}$.

Reactions of **1**$^{\bullet+}$

Elimination of $C_2H_5^{\bullet}$

As noted previously, $C_2H_5^{\bullet}$ loss dominates the chemistry of metastable $C_8H_{18}O^{\bullet+}$ species formed from **1**. Considerable information on this fragmentation can be gained by examining the behaviour of ionized ethers in which either or both butyl substituents

contains a CD_2 residue. Tables 7.6 and 7.7 give the reactions of metastable analogues of $\mathbf{1}^{\bullet+}$ generated from $C_4H_7D_2OC_4H_9$ and $C_4H_7D_2OC_4H_7D_2$ ethers,

Table 7.6 Reactions of metastable $C_4H_7D_2OCH_2CH_2CH_2CH_3^{\bullet+}$ radical-cations

	Precursor structure					
	1-1,1-d_2		1-2,2-d_2		1-3,3-d_2	
Neutral specis	$CH_3CH_2CH_2CD_2OC_4H_9$		$CH_3CH_2CD_2CH_2OC_4H_9$		$CH_3CD_2CH_2CH_2OC_4H_9$	
lost(or mass[c])	RA[a]	T[b]	RA	T	RA	T
$CH_3^{\bullet}$	1.9	1.6	1.7	1.6	1.3	1.5
$C_2H_5^{\bullet}$	48.1	1.8	49.3	1.8	68.4	1.9
$C_2H_4D^{\bullet}$					12.8	1.9
$C_2H_3D_2^{\bullet}$	38.7	1.7	39.3	1.7		
$C_4H_7^{\bullet}$ (55)	2.5	1.7	2.6	1.7	2.3	1.8
(56)	1.0	1.5	0.7	1.7	4.1	2.0
(57)	2.5	1.7	2.0	1.8	2.6	1.8
(58)	0.3	1.3	0.2	1.5	2.7	2.1
(59)	2.0	2.0	1.7	2.1	2.9	2.1
$C_4H_8D_2$ (60)	0.8	2.3	0.8	2.1	0.3	~2
$C_4H_{10}O$	0.6	2.1	0.4	2.0	1.0	1.6
C_4H_9DO	0.3	1.6	0.2	1.4	0.7	1.6
$C_4H_8D_2O$	1.2	2.0	1.0	1.9	1.0	1.8

[a,b] See footnotes to Table 7.1; [c] Values quoted in atomic mass units (u); the isotopic constitution of the neutral species having masses of 56, 57, 58 and 59 u cannot be elucidated with confidence from these data.

respectively. It is immediately evident that the reactions of metastable analogues of $\mathbf{1}^{\bullet+}$ formed from ethers with either an α- or β-CD_2 group in the same butyl substituent

are strikingly similar, particularly with regard to $C_2H_{5-n}D_n^{\bullet}$ expulsion. Moreover, the common behaviour of these species differs conspicuously from that of the corresponding isomer containing a γ-CD_2 group.

Table 7.7. Reactions of metastable $C_4H_7D_2OC_4H_7D_2^{\bullet+}$ radical-cations

	Precursor Structure					
	1-1,1,1',1'-d_4		1-2,2,2',2'-d_4		1-3,3,3',3'-d_4	
Neutral specis	$(CH_3CH_2CH_2CD_2)_2O$		$(CH_3CH_2CD_2CH)_2O$		$(CH_3CD_2CH_2CH_2)_2O$	
lost(or mass[c])	RA[a]	T[b]	RA	T	RA	T
$CH_3^{\bullet}$	2.0	1.5	2.0	1.6	0.9	1.6
$C_2H_5^{\bullet}$					7.7	1.8
$C_2H_4D^{\bullet}$					48.7	1.7
$C_2H_3D_2^{\bullet}$	87.7	1.8	90.5	1.8	0.6	1.5
56	2.0	1.9	1.0	1.5	5.7	2.0
57	2.7	1.9	1.1	2.0	8.7	1.7
58	0.3	1.3	0.3	1.7	7.8	1.6
59	2.0	1.8	1.8	2.0	6.8	1.9
60	<0.2	-[d]	<0.2	-[d]	3.0	1.7
61	0.4	2.1	1.5	2.1	1.5	1.7
C_4H_9DO	<0.3	-[d]			1.1	1.7
$C_4H_8D_2O$	2.0	2.5	1.1	2.1	4.8	1.6
$C_4H_7D_3O$	0.3	1.8	<0.3	1.6	2.7	1.8

[a,b] See footnotes to Table 7.1; [c] Values quoted in atomic mass units (u); the isotopic constitution of the neutral species having masses of 56, 57, 58, 59, 60 and 61 u cannot be elucidated with confidence from these data; [d] Peak too weak to permit meaningful estimate of T.

Table 7.7 Continued

Neutral specis lost(or mass[c])	Precursor Structure: 1-1,1,3',3'-d_4 $CH_3CH_2CH_2CD_2OCH_2CH_2CD_2CH_3$ RA[a]	T[b]	1-2,2,3',3'-d_4 $CH_3CH_2CD_2CH_2OCH_2CH_2CD_2CH_3$ RA	T
$CH_3^{\bullet}$	1.4	1.8	1.6	1.7
$C_2H_5^{\bullet}$	4.8	2.0	4.6	1.9
$C_2H_4D^{\bullet}$	16.7	2.0	16.7	1.9
$C_2H_3D_2^{\bullet}$	58.3	1.7	58.0	1.8
56	2.3	1.9	2.8	2.4
57	5.1	1.9	3.8	2.3
58	1.6	1.4	1.9	2.1
59	2.2	1.7	2.5	2.3
60	2.8	1.9	3.7	2.9
61	0.8	1.9	0.5	~2
C_4H_9DO	<0.2	-[d]	<0.2	-[d]
$C_4H_8D_2O$	2.4	1.9	2.5	2.2
$C_4H_7D_3O$	1.2	1.9	1.2	2.0

[a,b] See footnotes to Table 7. Values quoted in atomic mass units (u); the isotopic constitution of the neutral species having masses of 56, 57, 58, 59, 60 and 61 u cannot be elucidated with confidence from these data; [d] Peak too weak to permit meaningful estimate of T.

Thus, both $CH_3CH_2CH_2CD_2OCH_2CH_2CH_2CH_3^{\bullet+}$ (**1**-1,1-$d_2^{\bullet+}$) and $CH_3CH_2CD_2CH_2O$-$CH_2CH_2CH_2CH_3^{\bullet+}$ (**1**-2,2-$d_2^{\bullet+}$) expel $C_2H_5^{\bullet}$ (from the unlabelled butyl substituent) and $C_2H_3D_2^{\bullet}$ (from the dideuteriated butyl group) in comparable amounts, but essentially no $C_2H_4D^{\bullet}$. Furthermore, the RAs and $T_{1/2}$ values for the fragmentations of these $C_4H_7D_2OC_4H_9^{\bullet+}$ species are the same within experimental error. In contrast, $CH_3CD_2CH_2CH_2OCH_2CH_2CH_2CH_3^{\bullet+}$ (1-3,3-$d_2^{\bullet+}$) eliminates mainly (~68% of the total

metastable ion current or ~85% of that for ethyl radical loss) $C_2H_5^{\bullet}$, a little (~13% of ethyl radical loss) $C_2H_4D^{\bullet}$ (from the dideuteriated butyl group) but essentially no $C_2H_3D_2^{\bullet}$. These data may be understood in terms of Scheme 7.2.

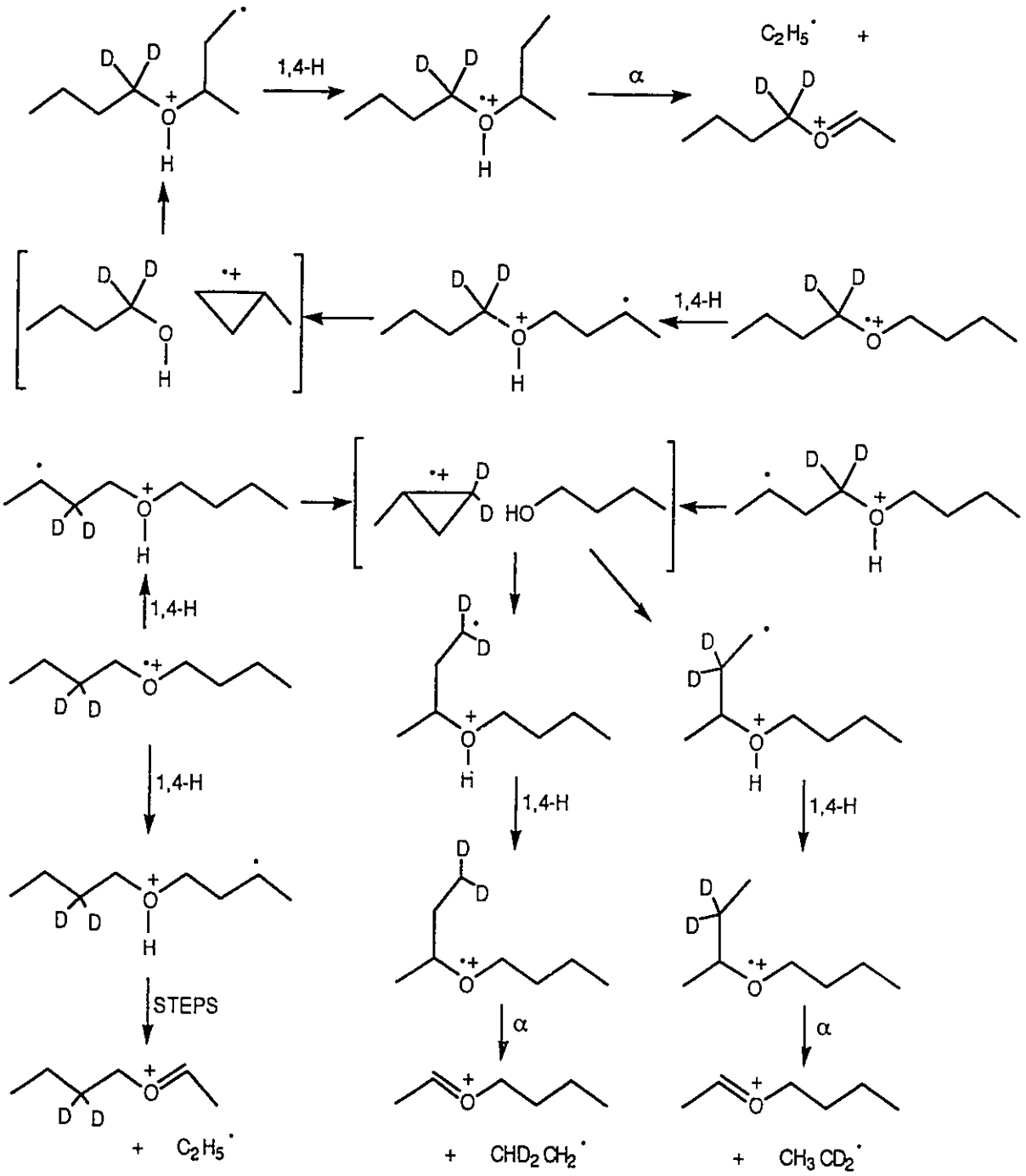

Scheme 7.2

Ethyl radical loss from both **1**-1,1-$d_2^{\bullet+}$ and **1**-2,2-$d_2^{\bullet+}$ begins with a 1,4-H shift to oxygen, followed by a skeletal isomerization that may be visualized as occurring via the INC [$CH_3CH_2CH_2CH_2OH$ $\overline{CH_2CD_2CHCH_3}^{\bullet+}$] in which the original α- and β-CD_2 groups have been rendered equivalent. After recombination of the components to give a labelled DI containing a rearranged skeleton, a second 1,4-H shift returns the protium atom from oxygen to carbon to give an ionized dideuteriated *sec*-butyl *n*-butyl ether, which then expels $C_2H_3D_2^{\bullet}$ by α-cleavage. A parallel mechanism involving isomerization of the unlabelled butyl groups accounts for $C_2H_5^{\bullet}$ loss. The rate of $C_2H_5^{\bullet}$ elimination from the C_4H_9 substituent is slightly greater than that of $C_2H_3D_2^{\bullet}$ loss from the $C_4H_7D_2$ group because the 1,4-H shift from the labelled substituent is influenced by a small secondary isotope effect. The fact that almost identical isotope effects (1.25 and 1.24 overall, or 1.12 and 1.11 (i.e. $\sqrt{1.25}$ and $\sqrt{1.24}$), respectively, per deuterium atom) discriminate against the 1,4-H shift which initiates ethyl expulsion from the labelled butyl group of **1**-1,1-$d_2^{\bullet+}$ and **1**-2,2-$d_2^{\bullet+}$ is interesting. The magnitude of these secondary isotope effects would normally vary with the distance separating the origin of the migrating hydrogen atom from the site of deuteriation [35]. The invariance of the isotope effects may indicate that the transition state has a geometry in which α- and β-CD_2 groups occupy a similar location with respect to the γ-CH_2 residue which is being disrupted by the 1,4-H shift. If this explanation is correct, it would be evidence that the skeletal rearrangement involves rate-limiting formation of an INC comprising an ionized methylcyclopropane. In any event, it seems clear that the 1,4-H shift is the slow step in ethyl loss from **1**$^{\bullet+}$ and its labelled analogues.

In contrast to **1**-1,1-$d_2^{\bullet+}$ and **1**-2,2-$d_2^{\bullet+}$, elimination of an ethyl radical from the partially deuteriated butyl substituent of **1**-3,3-$d_2^{\bullet+}$ entails a 1,4-D shift to oxygen and the subsequent skeletal rearrangement involves [$CH_3CH_2CH_2CH_2OD$ $\overline{CH_2CH_2CDCH_3}^{\bullet+}$].

When the deuterium atom is transferred back to carbon, $CH_3CH_2CH_2CH_2O$-$CD(CH_3)CH_2CH_2D^{\bullet+}$ is formed; consequently, $C_2H_4D^{\bullet}$ is lost (Scheme 7.3). Loss of $C_2H_5^{\bullet}$ occurs from the unlabelled butyl group by a competing route beginning with a 1,4-H shift to oxygen. A substantial primary isotope effect (~5.4:1, overall) favours the 1,4-H shift over the 1,4-D shift, as would be expected if this step is rate limiting.

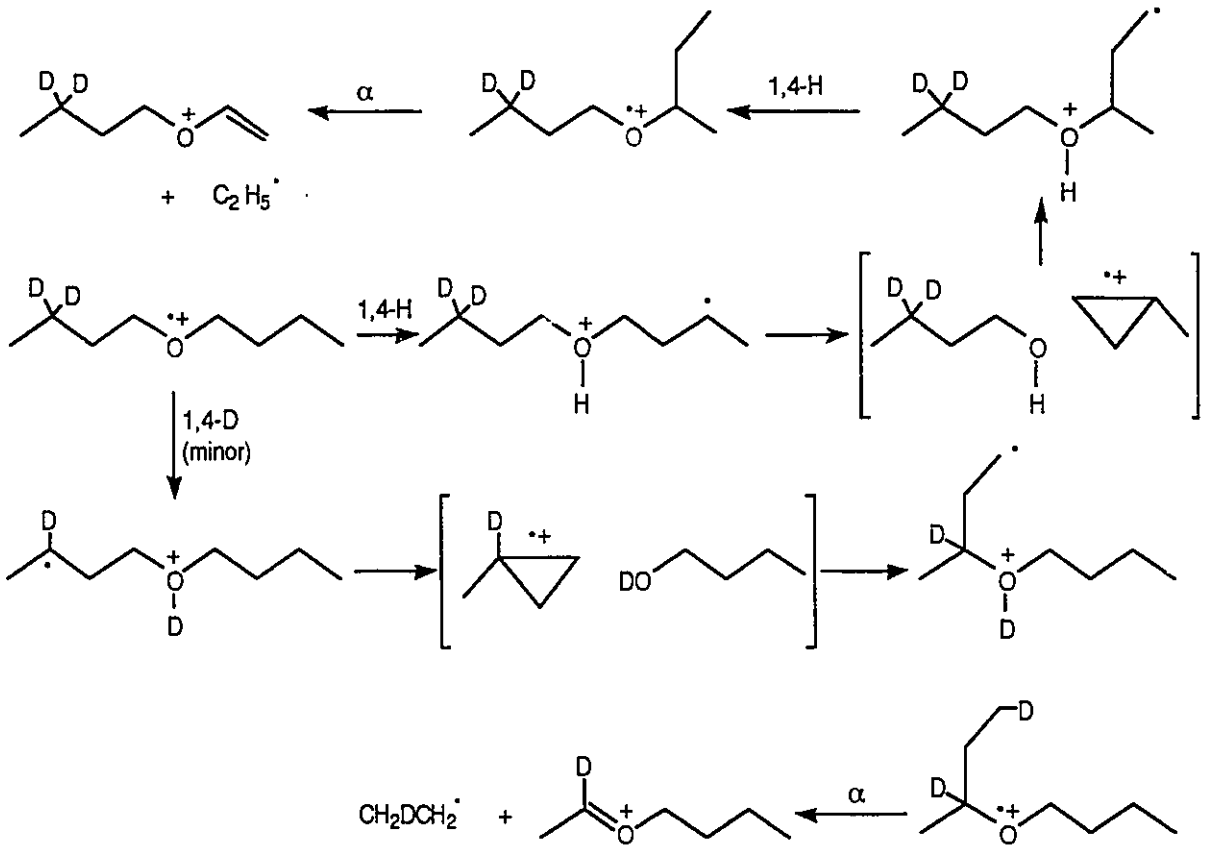

Scheme 7.3

Parallel trends are seen in $C_2H_{5-n}D_n^{\bullet}$ elimination from corresponding pairs of $C_4H_7D_2OC_4H_7D_2^{\bullet+}$ species. Thus, $CH_3CH_2CH_2CD_2OCD_2CH_2CH_2CH_3^{\bullet+}$ (**1**-1,1,1',1'-$d_4^{\bullet+}$) and $CH_3CH_2CD_2CH_2OCH_2CD_2CH_2CH_3^{\bullet+}$ (**1**-2,2,2',2'-$d_4^{\bullet+}$) both expel exclusively $C_2H_3D_2$ (from one of the dideuteriated butyl groups) in ethyl radical elimination. These fragmentations occur after rearrangement of one of the $C_4H_7D_2$ substituents

initiated by a 1,4-H shift (Scheme 7.4). The isomeric pair of radical-cations generated

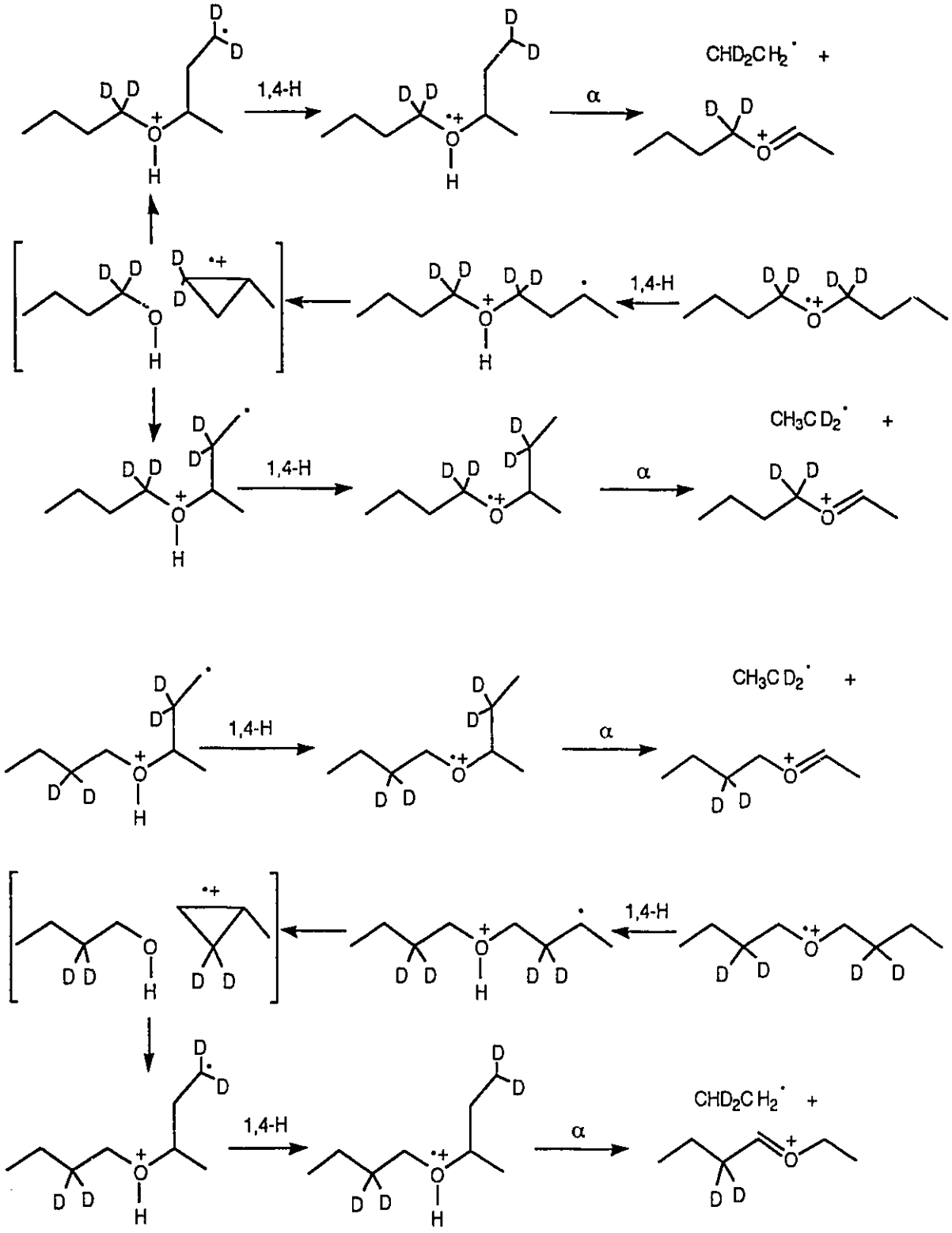

Scheme 7.4

as $CH_3CH_2CH_2CD_2OCH_2CH_2CD_2CH_3^{\bullet+}$ (**1**-1,1,3',3'-$d_4^{\bullet+}$) and $CH_3CH_2CD_2CH_2OCH_2CH_2$-$CD_2CH_3^{\bullet+}$ (**1**-2,2,3',3'-$d_4^{\bullet+}$) display a common reactivity that differs from that of **1**-1,1,1',1'-$d_4^{\bullet+}$ and **1**-2,2,2',2'-$d_4^{\bullet+}$. The main dissociation channel is still $C_2H_3D_2^{\bullet}$ expulsion (~73% of ethyl radical loss), but there is a sizable contribution from $C_2H_4D^{\bullet}$ elimination (~21%). These processes take place after rearrangements initiated by a 1,4-H shift in the 1,1-d_2- or 2,2-d_2-butyl substituent or a 1,4-D shift in the 3,3-d_2-butyl group, respectively (Scheme 7.5). A moderately large overall isotope effect (~3.5:1) favours the 1,4-H over the 1,4-D shift, thus confirming that this step is rate-limiting in $C_2H_{5-n}D_n^{\bullet}$ loss. The fifth isomer, **1**-3,3,3',3'-$d_4^{\bullet+}$, has a unique reactivity, differing from those of **1**-1,1,1',1'-$d_4^{\bullet+}$ and **1**-2,2,2',2'-$d_4^{\bullet+}$ or **1**-1,1,3',3'-$d_4^{\bullet+}$ and **1**-2,2,3',3'-$d_4^{\bullet+}$. Elimination of $C_2H_4D^{\bullet}$ (~85%) becomes the dominant fragmentation; it entails a 1,4-D shift in the one of the 3,3-d_2-butyl substituents, leading eventually to rearrangement to $CH_3CD_2CH_2CH_2OCD(CH_3)CH_2CH_2D^{\bullet+}$ (Scheme 7.6).

There are minor signals for loss of $C_2H_5^{\bullet}$ (~6% from both **1**-1,1,3',3'-$d_4^{\bullet+}$ and 1-2,2,3',3'-$d_4^{\bullet+}$; ~14% from **1**-3,3,3',3'-$d_4^{\bullet+}$) which cannot be explained simply in terms of Schemes 7.5 and 7.6. These fragmentations may occur after additional hydrogen transfers have taken place, either within or between the individual butyl substituents. One possibility involves limited isomerization of the appropriate INC, $[C_4H_{9-n}D_nOD\ \overline{CH_2CH_2CDCH_3}^{\bullet+}]$, to a DI having the same heavy atom skeleton as ionized *n*-butyl isobutyl ether and this route eventually leads to formation of a $C_4H_{9-n}D_nOCD(CH_2D)CH_2CH_3^{\bullet+}$ species, which then loses $C_2H_5^{\bullet}$ by α-cleavage. Thus, 1-3,3,3',3'-$d_4^{\bullet+}$ isomerizes to $CH_3CD_2CH_2CH_2OCD(CH_2D)CH_2CH_3^{\bullet+}$ via $[CH_3CD_2CH_2CH_2OD\ \overline{CH_2CH_2CDCH_3}^{\bullet+}]$, $CH_3CD_2CH_2CH_2O^+DCH_2CD(CH_2^{\bullet})CH_3$ and $[CH_3CD_2CH_2CH_2OH\ \overline{CH_2CH_2CDCH_2D}^{\bullet+}]$ (Scheme 7.7). This interpretation is plausible given the known

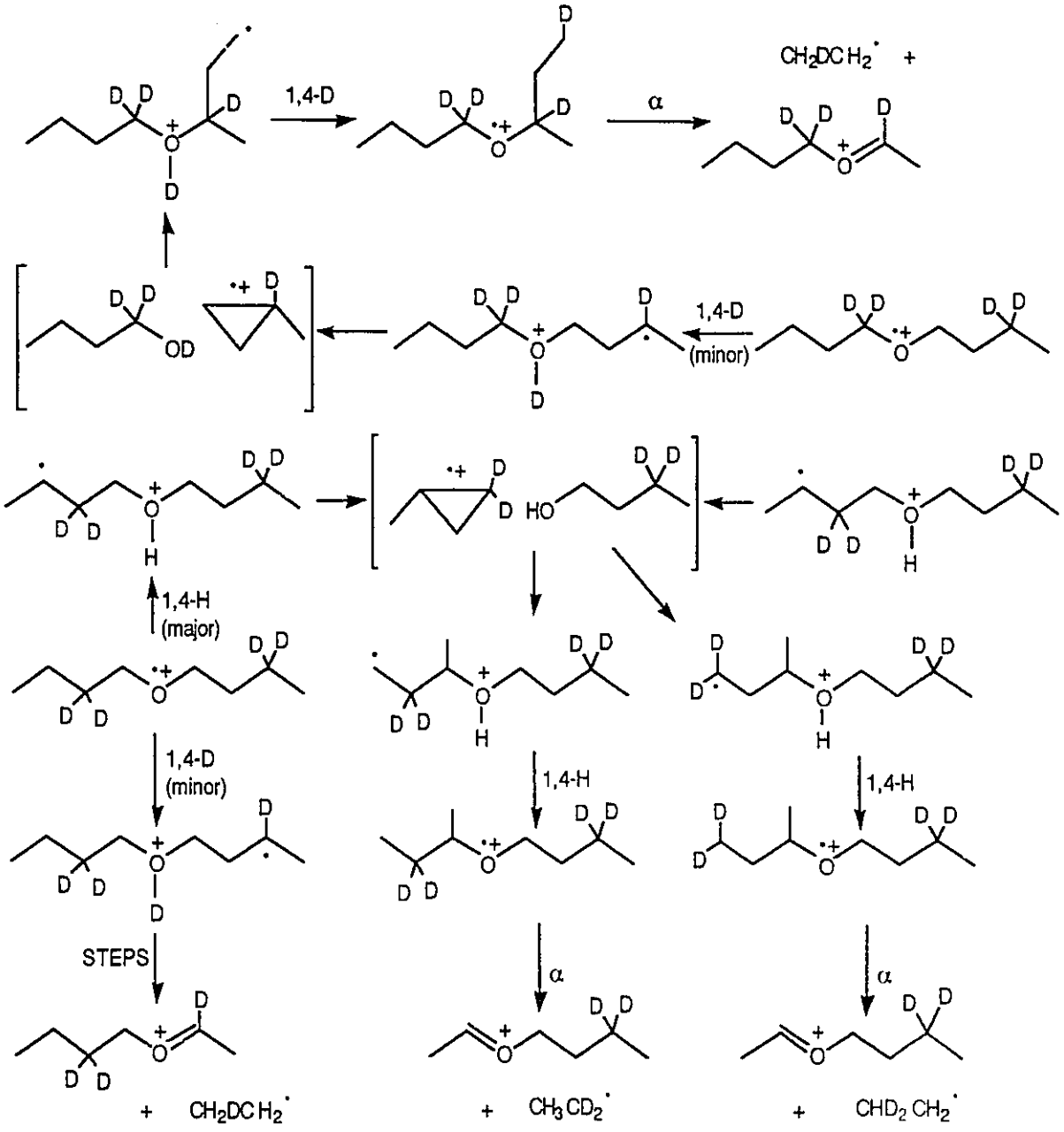
1,4-D
α
CH2DCH2· +
1,4-D
(minor)
1,4-H
(major)
1,4-D
(minor)
1,4-H
1,4-H
STEPS
α
α
+ CH2DCH2·
+ CH3CD2·
+ CHD2CH2·

Scheme 7.5

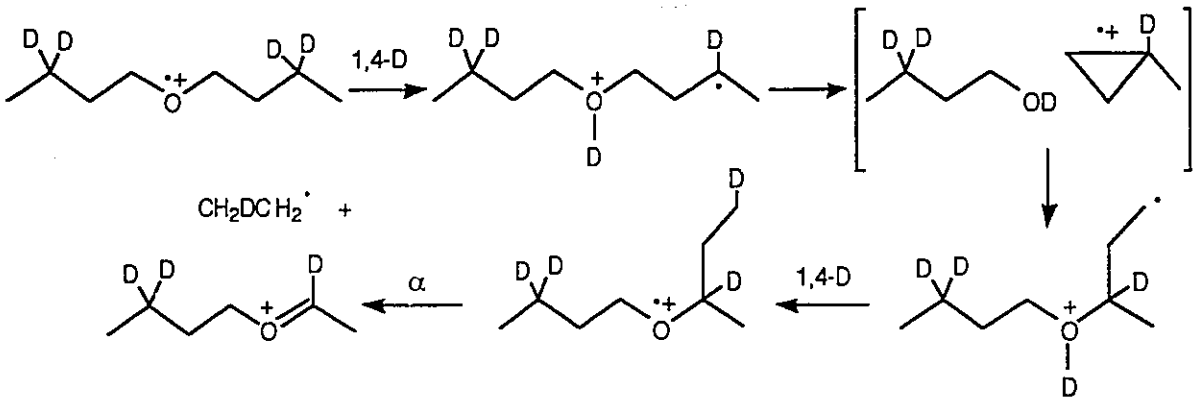

Scheme 7.6

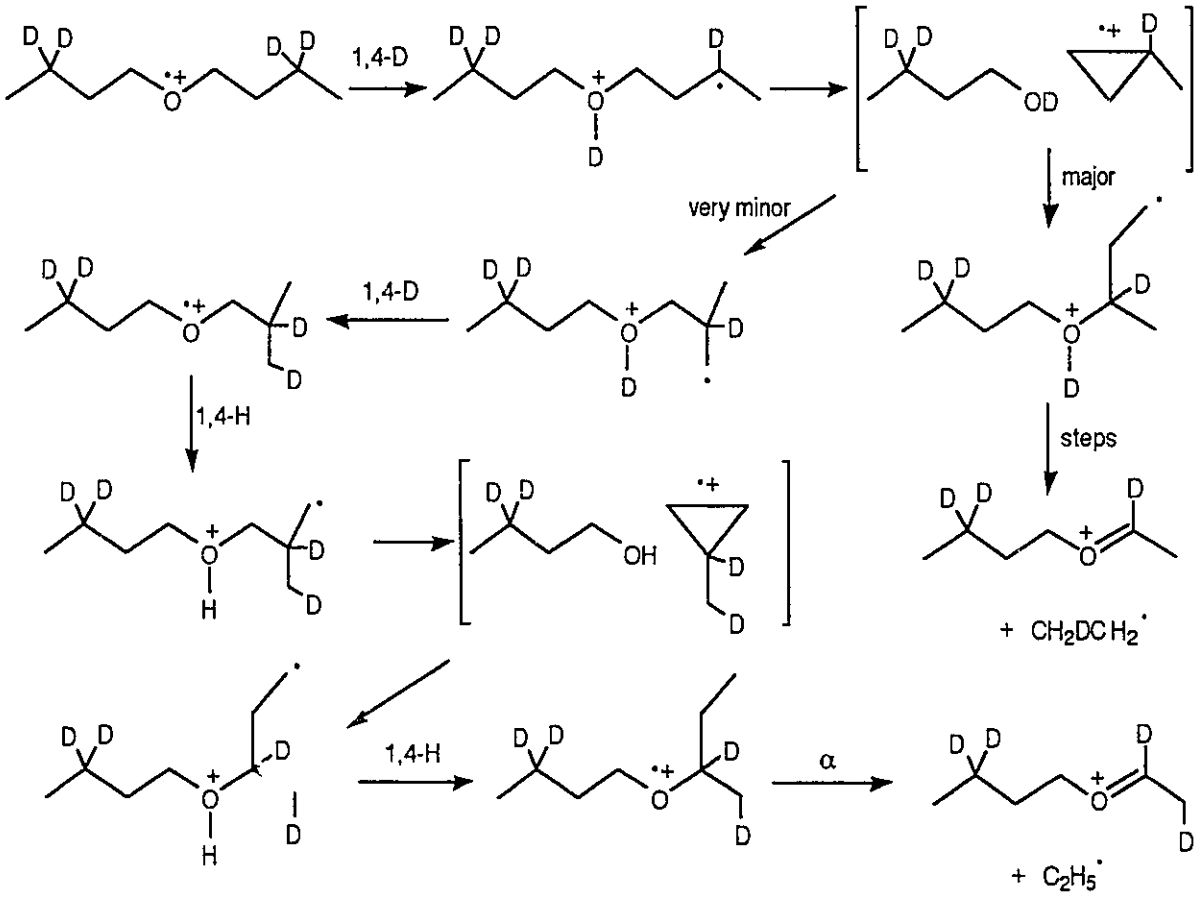

Scheme 7.7

similarity between the reactions of isomeric ionized *n*- and isobutyl alkyl ethers, which points to rearrangement of both to a common intermediate (e.g. the INC [ROH $\overline{CH_2CH_2CHCH_3}^{\bullet+}$]). However, the labelling data show that interconversion of *n*- and isobutyl skeletons via this route cannot be rapid and reversible: only a minor percentage of the INCs [$C_4H_{9-n}D_nOD$ $\overline{CH_2CH_2CDCH_3}^{\bullet+}$] rearrange to DIs containing an isobutyl skeleton (e.g. $C_4H_{9-n}D_nO^+DCH_2CD(CH_2^{\bullet})CH_3$); most isomerize instead to isomeric DIs with a *sec*-butyl connectivity (e.g. $C_4H_{9-n}D_nO^+DCD\ (CH_3)CH_2CH_2^{\bullet}$). The preference shown by [$C_4H_{9-n}D_nOD$ $\overline{CH_2CH_2CDCH_3}^{\bullet+}$] for isomerizing to the DI in the *sec*-butyl series is understandable because the ionized methylcyclopropane should exhibit some of the characteristics expected from its open chain distonic form, $^{\bullet}CH_2CH_2CD^+CH_3$, which would be attacked more readily by nucleophiles at the more heavily substituted carbon atom.

Relative rates of elimination of $C_2H_5^{\bullet}$ and competing fragmentations

The isotope effects on the initial 1,4-hydrogen shift are most clearly seen by comparing the rates of ethyl radical loss from an unlabelled and partially deuteriated butyl group in the same ionized ether. However, isotope effects are also evident on the relative rates of ethyl radical elimination and the minor competing processes. The total amount of ethyl radical loss ($\Sigma RA(C_2H_{5-n}D_n^{\bullet})$) is barely affected by deuteriation on either or both α- or β-carbon atoms ($\Sigma RA(C_2H_{5-n}D_n^{\bullet})$=87-90%). In contrast, deuteration on only one of the γ-carbon atoms appreciably reduces the total amount of ethyl radical elimination ($\Sigma RA(C_2H_{5-n}D_n^{\bullet})$=79-81%); moreover, deuteration of both γ-carbon atoms strongly suppresses this fragmentation ($\Sigma RA(C_2H_{5-n}D_n^{\bullet})$=57%). These trends confirm that the 1,4-hydrogen shift is rate limiting in ethyl radical expulsion. They also serve to emphasize how strongly the competition amongst the various fragmentations

of ionized ethers depends on the internal energy of the decomposing ions. The transition state energies for the 1,4-D shifts initiating rearrangement of a $CH_2CH_2CD_2CH_3$ group are slightly higher than those of the 1,4-H shifts which begin the corresponding isomerization of a $CH_2CH_2CH_2CH_3$ substituent. Therefore, the average internal energy of the dissociating ions that have isomerized via the 1,4-D shifts is marginally higher than that of ions which have rearranged via the 1,4-H shifts. The higher energy ions will show an increased tendency for fragmenting via processes which involve the minimum further rearrangement, especially if these additional steps entail reorganization of the heavy atom skeleton [30,31]. Several of the alternative dissociations (loss of labelled butenyl or butyl radicals or butanols) require only relatively facile hydrogen transfers but little or no further skeletal rearrangement after formation of the relavant INC $[C_4H_{9-n}D_nOD\ \overline{CH_2CH_2CDCH_3}^{\bullet+}]$. Consequently, these processes compete more effectively with $C_2H_{5-n}D_n^{\bullet}$ expulsion starting from analogues of $\mathbf{1}^{\bullet+}$ which are deuterated in the γ-position; this effect is especially noticeable in the reactions of **1**-3,3,3',3'-$d_4^{\bullet+}$, in which there are two γ-CD_2 groups and all the dissociating ions that eliminate $C_2H_{5-n}D_n^{\bullet}$ have an elevated average internal energy because they have undergone a 1,4-D shift. Outline mechanisms for elimination of $C_4H_7^{\bullet}$, $C_4H_9^{\bullet}$, C_4H_{10} and $C_4H_{10}O$ from $\mathbf{1}^{\bullet+}$ are shown in Scheme 7.8. Unfortunately, the labelling data shed little light on how these minor processes take place because the signals for the various fragmentations are weak and frequently overlap with one another.

Structure of the radical-cations generated from $C_4H_7D_2OC_4H_9$ and $C_4H_7D_2OC_4H_7D_2$

The reactions of the members of the three related pairs of metastable $C_4H_7D_2OC_4H_9^{\bullet+}$ and $C_4H_7D_2OC_4H_7D_2^{\bullet+}$ species in which the butyl substituents have

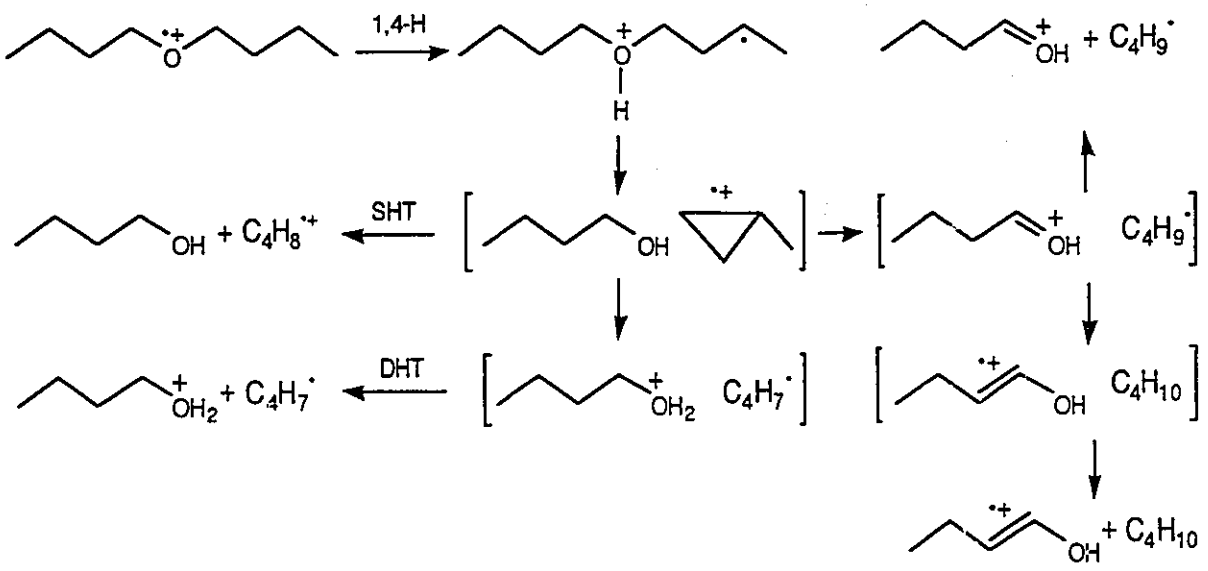

Scheme 7.8

CD_2 residues in the α- or β-position (**1**-1,1-$d_2$$^{\bullet+}$/**1**-2,2-$d_2$$^{\bullet+}$, **1**-1,1,1',1'-$d_4$$^{\bullet+}$/-**1**-2,2,2',2'-$d_4$$^{\bullet+}$ and **1**-1,1,3',3'-$d_4$$^{\bullet+}$/**1**-2,2,3',3'-$d_4$$^{\bullet+}$) are almost identical. However, the CA and NR spectra of the members of each of these pairs show significant differences (Tables 7.8 and 7.9, respectively).

There are two reasons why differences are apparent in the CA and NR spectra, but not in the corresponding metastable ion spectra. First, only one of the two *n*-butyl groups in the $C_4H_7D_2OC_4H_9$$^{\bullet+}$ and $C_4H_7D_2OC_4H_7D_2$$^{\bullet+}$ radical-cations needs to be isomerized before $C_2H_{5-n}D_n$$^{\bullet}$ loss becomes possible. Second, most (or possibly all) of the dissociations that are evident in the metastable ion spectra arise by fragmentation of the isomerized butyl substituent. In particular, the dominant reaction, loss of $C_2H_{5-n}D_n$$^{\bullet}$ occurs specifically from whichever butyl group has been rearranged. When the butyl substituent which is not involved in the isomerization is the same for both members of a related pair of ions, the rearrangment converts the other group into a

sec-butyl structure from which a common $C_2H_{5-n}D_n^{\bullet}$ species is expelled. Thus, isomerization of the labelled butyl substituent in **1**-1,1-$d_2^{\bullet+}$ and **1**-2,2-$d_2^{\bullet+}$ forms the same mixture of $CH_3CH_2CH_2CH_2OCH(CH_3)CD_2CH_3^{\bullet+}$ and $CH_3CH_2CH_2CH_2OCH(CH_3)$-$CH_2CHD_2^{\bullet+}$; both these species may eliminate $C_2H_3D_2^{\bullet}$ by α-cleavage (Scheme 7.2). The parts of the CA and NR spectra which originate from the fraction of ions generated as **1**-1,1-$d_2^{\bullet+}$ and **1**-2,2-$d_2^{\bullet+}$ which undergo rearrangement of the labelled butyl group are likely to be very similar. All fragmentations involving dissociation of the unlabelled *n*-butyl group should be identical; of those arising by disruption of the labelled *sec*-butyl substituent, $C_2H_3D_2^{\bullet}$ loss by α-cleavage will be much the most important, thus disguising the different distribution of deuterium atoms within the $C_4H_7D_2$ entity. However, isomerization of the unlabelled butyl substituent of **1**-1,1-$d_2^{\bullet+}$ and **1**-2,2-$d_2^{\bullet+}$ affords $CH_3CH_2(CH_3)CHOCD_2CH_2CH_2CH_3^{\bullet+}$ and $CH_3CH_2(CH_3)CHOCH_2CD_2$-$CH_2CH_3^{\bullet+}$, respectively. The unlabelled *sec*-butyl groups in these species should dissociate in a virtually identical fashion, but the different labelled *n*-butyl substituents should show distinct fragmentations. Parallel arguments apply for the other pair of $C_4H_7D_2OC_4H_9^{\bullet+}$ and $C_4H_7D_2OC_4H_7D_2^{\bullet+}$ radical-cations which show almost identical metastable ion spectra but appreciably different CA and NR spectra.

Nevertheless, the distinctive CA and NR spectra of isomeric species containing α-CD_2 and β-CD_2 residues bear a closer resemblance to each other than to the spectra of the corresponding radical-cation with a γ-CD_2 group. Thus, the relative intensities of the group of important peaks at m/z 56-58 in the CA spectra of **1**-1,1-$d_2^{\bullet+}$ and **1**-2,2-$d_2^{\bullet+}$ are the same within experimental error. In contrast, in the spectrum of **1**-3,3-$d_2^{\bullet+}$ the signals at m/z 57 and 58 are approximately doubled and reduced by four fifth, respectively, in relative intensity. These signals appear to arise predominantly by elimination of a molecule of butanol from $C_4H_7D_2OC_4H_9^{\bullet+}$, presumably by collision-induced fragmentation of the appropriate DI or by separation

Table 7.8. Collisional activation and neutralization-reionization mass spectra of $C_4H_7D_2OCH_2CH_2CH_2CH_3^{\bullet+}$ radical-cations.

	Precursor structure					
	1-1,1-d_2		1-2,2-d_2		1-3,3-d_2	
m/z	CA[a]	NR[b]	CA	NR	CA	NR
103	(204)		(204)		(227)	
102					(42)	
101	(160)		(161)			
77	12		12		11	
73	13		13		11	
59	25	15	24	15	23	12
58	93	45	95	38	20	36
57	32	34	32	35	65	39
56	100	42	100	37	100	42
55	9	29	8	27	8	28
54	3	10	2	8	3	11
44	4	14	4	21	2	19
43	8	47	7	31	5	37
42	8	35	7	32	6	30
41	13	12	10	23	8	21
39	5	41	5	35	4	34
33	1	29		7		
32						21
31	4	95	4	100	3	47
30	4	34	4	32	3	33
29	8	100	8	93	6	100
28	5	53	5	48	5	53
27	6	62	5	62	5	56

[a] See footnote to Table 7.4; RI values are normalized to a value of 100 units for the most intense peak excluding those (shown in parentheses) arising by loss of an ethyl radical which are prominent in the fragmentation of the corresponding radical-cations that were not energized by collision; [b] See footnote a to Table 7.3.

Table 7.9. Collisional activation and neutralization-reionization mass spectra of $C_4H_7D_2OC_4H_7D_2^{\bullet+}$ radical-cations.

	Precursor structure					
	1-1,1,1',1'-d_4		1-2,2,2',2'-d_4		1-3,3,3',3'-d_4	
m/z	CA[a]	NR[b]	CA	NR	CA	NR
105	(191)		(187)		(16)	
104			(93)		(93)	
77	4		4		15	
76	1		2		18	
75	6		9		13	
59	23	22	23	18	28	39
58	100	73	100	44	32	100
57	11	32	12	24	28	71
56	3	23	3	10	7	41
55	9	22	5	18	28	21
46	1	5	1	4	18	39
45	3	16	4	24	2	51
44	2	19	3	18	3	34
43	5	50	5	26	5	64
42	6	42	6	22	6	55
41	3	41	4	18	4	41
40	3	28	2	19	3	52
39	2	34	2	15	2	41
33	1	55		3		<8
32		16		4	2	76
31	3	100	4	100	3	54
30	4	53	4	35	4	88
29	3	73	4	36	3	79
28	3	45	3	31	3	54
27	2	49	2	24	2	56

[a,b] See footnote to Tables 7.3 and 7.8.

Table 7.9. Continued.

m/z	Precursor structure: 1-1,1,3',3'-d_4 CA[a]	1-1,1,3',3'-d_4 NR[b]	1-2,2,3',3'-d_4 CA	1-2,2,3',3'-d_4 NR
105	(11)		(13)	
104	(39)		(47)	
103	(153)		(167)	
77	13		11	
76	5		7	
75	11		12	
59	33	30	33	25
58	100	66	100	56
57	33	43	33	36
56	5	26	5	19
55	33	11	33	7
45	3	30	4	31
44	3	23	3	20
43	6	44	7	36
42	8	39	8	31
41	4	30	4	21
40	3	33	4	19
39	2	30	3	19
34		17		5
33	<0.5	11	<0.5	6
32	1	14	1	19
31	4	100	4	100
30	5	56	6	49
29	4	52	4	48
28	3	48	4	41
27	3	41	3	31

[a,b] See footnote to Tables 7.3 and 7.8.

of the components of the corresponding INC. Both **1**-1,1-$d_2^{\bullet+}$ and **1**-2,2-$d_2^{\bullet+}$ will rearrange to a DI or INC containing either unlabelled butanol (via a 1,4-H shift to oxygen from the $CD_2CH_2CH_2CH_3$ or $CH_2CD_2CH_2CH_3$ group) or a dideuterated butanol ($CH_3CH_2CH_2CD_2OH$ or $CH_3CH_2CD_2CH_2OH$ via a 1,4-H shift from the $CH_2CH_2CH_2CH_3$ group). Moreover, the rates of these two 1,4-H shifts should be almost the same, with only a marginal preference for abstracting the hydrogen atom from the unlabelled substituent. Therefore, this region of the CA spectra of **1**-1,1-$d_2^{\bullet+}$ and **1**-2,2-$d_2^{\bullet+}$ is dominated by $[M\text{-}C_4H_7D_2OH]^{\bullet+}$ and slightly smaller $[M\text{-}C_4H_9OH]^{\bullet+}$ peaks at m/z 56 and 58, respectively. In contrast, the analogous processes in **1**-3,3-$d_2^{\bullet+}$ involve a 1,4-H shift from the $CH_2CH_2CH_2CH_3$ group (to form $CH_3CD_2CH_2CH_2OH$) or a 1,4-D shift from the $CH_3CD_2CH_2CH_2$ group (to form $CH_3CH_2CH_2CH_2OD$); the former should occur more rapidly than the latter. Further, there is now no facile route for formation of $CH_3CH_2CH_2CH_2OH$. Consequently, the CA spectrum of **1**-3,3-$d_2^{\bullet+}$ shows a strong $[M\text{-}C_4H_7D_2OH]^{\bullet+}$ signal, an appreciably less intense $[M\text{-}C_4H_9OD]^{\bullet+}$ peak and a much weaker $[M\text{-}C_4H_9OH]^{\bullet+}$ signal.

Another interesting point to emerge from the CA spectra concerns the $[M\text{-}C_3H_{7\text{-}n}D_n]^+$ peaks. These signals are very faint (typically having a relative intensity of 3-8% of the $[M\text{-}C_2H_{5\text{-}n}D_n]^+$ peaks). However, they are significant because they appear to arise mainly by α-cleavage of an unrearranged *n*-butyl substituent. Thus, **1**-1,1-$d_2^{\bullet+}$ shows a moderate $[M\text{-}C_3H_7]^+$ peak (8%) at m/z 89, but negligible $[M\text{-}C_3H_6D]^+$ and $[M\text{-}C_3H_5D_2]^+$ peaks ($\leqslant$1%) at m/z 88 and 87, respectively, because the α-CD_2 residue is always retained in the oxonium ion produced by α-cleavage. In contrast, $[M\text{-}C_3H_7]^+$ and $[M\text{-}C_3H_5D_2]^+$ signals of approximately equal intensity (~5%) are found in the CA spectra of **1**-2,2-$d_2^{\bullet+}$ and **1**-3,3-$d_2^{\bullet+}$ because there is a roughly equal probability of expelling an unlabelled propyl radical or one containing the intact β-CD_2 or γ-CD_2 residue. Similar trends are found in the $[M\text{-}C_3H_7]^+$, $[M\text{-}C_3H_6D]^+$ and $[M\text{-}C_3H_5D_2]^+$ peaks at m/z 91, 90 and 89 in the spectra of the $C_4H_7D_2OC_4H_7D_2^{\bullet+}$ radical-cations.

The weakness of these $[M\text{-}C_3H_{7-n}D_n]^+$ peaks suggests that relatively few of even the lowest species generated as labelled analogues of **1**$^{\bullet+}$ retain their original skeletal structure; most have isomerized to a DI or INC or the appropriate variant(s) of **2**$^{\bullet+}$. Indeed, it is possible (but unlikely) that all the species formed as **1**$^{\bullet+}$ have rearranged to **2**$^{\bullet+}$ (the weak $[M\text{-}C_3H_{7-n}D_n]^+$ signals would then be ascribed to α-cleavage of the unisomerized *n*-butyl substituent of **2**$^{\bullet+}$). The selectivity of $C_2H_{5-n}D_n^{\bullet}$ elimination indicates that those analogues that do remain as ionized di-*n*-butyl ether tend not to undergo any isomerizations which might erode the positional integrity of the α-, β- and γ-methylene groups.

Only one additional deduction can be made with confidence from the NR spectra. This concerns the signals at m/z 31-34 corresponding to $CH_2{=}OH^+$ and its labelled analogues. These peaks may be attributed, at last in part, to α-cleavage of $C_4H_{10-n}D_nO^{\bullet+}$ radical-cations which arise by ionization of butanol molecules that were formed after neutralization of the parent $C_4H_7D_2OC_4H_9^{\bullet+}$ or $C_4H_7D_2OC_4H_7D_2^{\bullet+}$ species. Neutralization of either an INC or DI containing $C_4H_{10-n}D_nO$ as an intact entity would yield an unstable $C_8H_{18-m}D_mO$ neutral which should separate spontaneously to give $C_4H_{10-n}D_nO$ and $C_4H_{8+n-m}D_{m-n}$ components. Reionization then affords the corresponding $C_4H_{10-n}D_nO^{\bullet+}$ and $C_4H_{8+n-m}D_{m-n}^{\bullet+}$ radical-cations. An appreciable signal at m/z 33 (29%) corresponding to $CD_2{=}OH^+$ is present in the spectrum of **1**-1,1-$d_2^{\bullet+}$; this reflects the possibility of forming $CH_3CH_2CH_2CD_2OH$ via a 1,4-H shift to oxygen from the unlabelled butyl substituent. Much weaker peaks (7 and ~1%, respectively) at m/z 33 are found in the spectra of **1**-2,2-$d_2^{\bullet+}$ and **1**-3,3-$d_2^{\bullet+}$, as would be anticipated since the formation of $CD_2{=}OH^+$ (or $CHD{=}OD^+$) is difficult when there is no α-CD_2 group. However, a significant signal at m/z 32 (21%) appears in the spectrum of **1**-3,3-$d_2^{\bullet+}$; this reflects the possibility of a 1,4-D shift with eventual formation of

$CH_3CH_2CH_2CH_2OD$, which yields $CH_2{=}OD^+$ after ionization and α-cleavage. Similarly, **1**-1,1,3',3'-$d_4$$^{\bullet+}$ displays an appreciable peak (17%) at m/z 34, corresponding to $CD_2{=}OD^+$, arising by ionization and dissociation of $CH_3CH_2CH_2CD_2OD$. All these findings lend support to the general mechanism proposed for isomerization and dissociation of **1**$^{\bullet+}$ and its labelled analogues.

Conclusion

The reactions of ionized di-*n*-butyl ether are logically interpreted in terms of unidirectional skeletal isomerization to ionized *n*-butyl *sec*-butyl ether via a mechanism involving distonic ions and an ion-neutral complex comprising *n*-butanol and ionized methylcyclopropane. The rate-limiting step in this rearrangement is the initial 1,4-hydrogen shift. This step is subject to a sizeable isotope effect of ~5:1 favouring a 1,4-H over a 1,4-D shift. The main fragmentation, ethyl radical elimination, occurs by α-cleavage of the *sec*-butyl group in the isomerized ionized ether. A relatively small proportion of the low-energy, undissociated radical cations generated as ionized di-*n*-butyl ether still retain this structure after a period of ~10 μs.

References

1. F.W. McLafferty, *Anal. Chem.*, **29**, 1782 (1957).
2. M. Spiteller-Friedmann and G. Spiteller, *Chem. Ber.*, **100**, 79 (1967).
3. S. Tajima, J. van der Greef and N.M.M. Nibbering. *Org. Mass Spectrom.*, **3**, 551 (1978).
4. R.D. Bowen and D.H. Williams, *J. Chem. Soc. Chem. Commun.*, 836 (1981).
5. B.F. Yates, W.J. Bouma and L. Radom, *J. Am. Chem. Soc.*, **106**, 5805 (1984).

6. S. Hammerum, *Mass Spectrom. Rev.*, **7**, 123 (1988).
7. T.H. Morton, *Tetrahedron*, **38**, 3195 (1982).
8. D.J. McAdoo, *Mass Spectrom. Rev.*, **7**, 363 (1988).
9. B.L.M. van Baar, J.K. Terlouw, S. Akkok, W. Zummack and H. Schwarz, *Int. J. Mass Spectrom. Ion Processes*, **81**, 217 (1987); N. Heinrich and H. Schwarz in Ion and Cluster Ion Spectroscopy, Ed., J.P. Maier, p. 329, Elsevier, Amsterdam (1988).
10. D.J. McAdoo, *Mass Spectrom. Rev.*, **7**, 363 (1988).
11. S. Hammerum, Fundamentals of Gas-Phase Ion Chemistry, Ed., K.R. Jennings, p. 379, Kluwer, Dordrecht (1990); R.D. Bowen, *Acc. Chem. Res.*, **24**, 364 (1991).
12. P. Longevialle, *Mass Spectrom. Rev.*, **11**, 157 (1992).
13. D.J. McAdoo and T.H. Morton, *Acc. Chem. Res.*, **26**, 295 (1993).
14. C.E. Hudson and D.J. McAdoo, *Org. Mass Spectrom.*, **14**, 109 (1979).
15. C.E. Hudson, R.D. Lemer, R. Aleman and D.J. McAdoo, *J. Phys. Chem.*, **84**, 551 (1980).
16. H.E. Audier, G. Bouchoux, Y. Hoppilliard and A. Milliet, *Org. Mass Spectrom.*, **17**, 382 (1982).
17. S. Hammerum, *J. Chem. Soc. Chem. Commun.*, 858 (1988); S. Hammerum and H.E. Audier, *J. Chem. Soc. Chem. Commun.*, 860 (1988).
18. S. Bernasek and R.G. Cooks, *Org. Mass Spectrom.*, **3**, 127 (1970).
19. R.D. Bowen and A. Maccoll, *J. Chem. Soc., Perkin Trans. 2*, 1101 (1985); 2363 (1990).
20. For a recent review of this and other reactions of ionized ethers, see F. Turecek, Supplement E: The Chemistry of Hydroxyl, Ether and Peroxide Groups, Ed., S. Patai, Vol. 2, p. 373, Wiley, Chichester (1993).
21. R.D. Bowen, A.W. Colburn and P.J. Derrick, *J. Chem. Soc. Chem. Commun.*, 1274 (1989); R.D. Bowen and P.J. Derrick, *Org. Mass Spectrom.*, **26**, 1197 (1993).
22. K. Levsen and H. Schwarz, *Angew. Chem. Int. Ed. Engl.*, **15**, 503 (1976); K. Levsen and H. Schwarz, *Mass Spectrom. Rev.*, **2**, 77 (1983).
23. R.G. Cooks (Ed.), Collision Spectroscopy, Plenum Press, New York (1978).
24. J. Bordas-Nagy and K.R. Jennings, *Int. J. Mass Spectrom. Ion Processes*, **100**, 217 (1990).
25. J. K. Terlouw and H. Schwarz, *Angew. Chem. Int. Ed. Engl.*, **26**, 805 (1987).
26. C. Wesdemiotis and F.W. McLafferty, *Chem. Rev.*, **87**, 465 (1985).
27. J.L. Holmes, *Mass Spectrom. Rev.*, **8**, 513 (1989).
28. H. Schwarz, *Pure Appl. Chem.*, **61**, 53 (1989).
29. The expression 'critical energy' corresponds conceptually to the term 'activation energy'. A. Maccoll, *Org. Mass Spectrom.*, **15**, 225 (1980).
30. G. Hvistendahl and D.H. Williams, *J. Am. Chem. Soc.*, **97**, 3097 (1975).

31. R.G. Cooks, J.H. Beynon, R.M. Caprioli and G.R. Lester, Metastable Ions, Elsevier, Amsterdam (1973).

32. J.C. Traeger, C.E. Hudson and D.J. McAdoo, *J. Phys. Chem.*, **94**, 5714 (1990).

33. A.N.H. Yeo and D.H. Williams, *J. Am. Chem. Soc.*, **93**, 395 (1971).

34. R.D. Bowen and D.H. Williams, *J. Chem. Soc., Perkin Trans. 2*, 1411 (1980).

35. S. Ingemann, S. Hammerum and P.J. Derrick, *J. Am. Chem. Soc.*, **110**, 3869 (1988), and references cited therein.

CHAPTER 8

Mechanism of Propene and Water Elimination from the Oxonium Ion $CH_3CH{=}O^+CH_2CH_2CH_3$

Introduction

The task of understanding the reactions of isolated ions continues to be a challenging theme in organic mass spectrometry. Much progress has been made during the past 20 years or so in providing mechanistically satisfying explanations for many isomerization and fragmentation processes. In particular, it has been demonstrated that great insight can be gained by examining the reactions of metastable ions. Metastable ions have relatively low internal energies and they eventually dissociate with excess energies in the transition states that are small and comparable to those found in solution chemistry [1]. Moreover, the lifetimes (typically *ca.* 10 μs) of metastable ions are generally too long to permit interference from isolated

This chapter is based on a paper under the above title:

R.D. Bowen, D. Suh and J.K. Terlouw, *J. Chem. Soc. Perkin Trans. 2*, 119 (1995).

electronic states. As a result, it is often possible to describe the chemistry of metastable ions by means of a potential energy profile (PEP) model [2], in which it is assumed that all possible rearrangements and dissociation steps occur from the gound state, with the relative rates of these competing processes being crucially dependent on the associated critical energies [3].

Sometimes, the chemistry of metastable ions can be adequately explained by means of mechanisms involving only conventional ion structures (*i.e.* ones in which the atoms are connected by ordinary covalent links and the usual rules of valency hold good) and steps that are familiar in classical solution reactions. However, certain processes cannot be interpreted in this manner. In such systems, mechanisms in whcih ion-neutral complexes (INCs) [4-14] play important roles in permitting cation rearrangements, hydrogen transfers and skeletal rearrangements often offer a means of understanding previously inexplicable phenomena.

INC-mediated mechanisms have been of particular value in describing the chemistry of onium ions $R_1R_2C{=}Z^+R_3$ (Z=O,S,NR_4; R_1,R_2,R_3,R_4=H,C_nH_{2n+1}) and related species [15]. Recent work on propene elimination from a propyl group attached to nitrogen in immonium ions $R_1R_2C{=}N(R_4)^+C_3H_7$ (R_4=CH_3,C_2H_4,C_3H_7) [16,17] and protonated propylamines [18] has provided strong evidence that these processes proceed via INCs. An important point is that the site-selectivity in the hydrogen transfer step in propene elimination from these ions is inconsistent with the mechanism that has traditionally been offered to rationalise this ubiquitous process, [reaction (1)], in which a β-hydrogen migrates to nitrogen in a four-membered ring

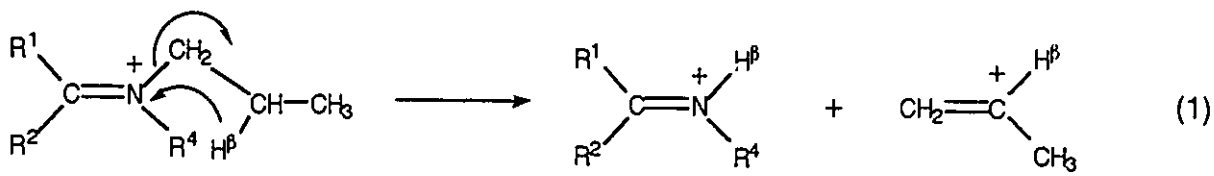

(1)

transition state [19]. This traditional explanation requires that specific β-hydrogen transfer must accompany alkene expulsion, whereas the experimental data show a distinct preference for α- and γ-hydrogen transfer. However, the observed site-selectivity is accommodated by an INC-mediated mechanism because unidirectional rearrangement of the incipient propyl cation to the more stable isopropyl isomer converts the α-methylene group and one of the β-hydrogen atoms into a second methyl group. Abstraction of a proton from either of the two methyl groups of the resultant isopropyl cation then occurs, so that α-, β- and γ-hydrogen transfer from the original propyl group to nitrogen is found in the ratio 2:1:3, to a first approximation [16,17].

A slightly earlier study [20] of the analogous metastable oxonium ions $CH_2{=}O^+CH_2CH_2CH_3$ and $CH_2{=}O^+CH(CH_3)_2$ led to subtly different conclusions. These ions expel water and formaldehyde in closely similar ratios [21], suggesting that they interconvert with one another and/or a common structure before dissociating. Furthermore, labelling experiments reveal that the hydrogen atoms of the eliminated molecule of water originate almost at random from the seven of the initial propyl substituent [20]. These findings were also interpreted in terms of an INC-mediated mechanism; however, unlike their analogues in the immonium ion and protonated propylamine systems, the cation rearrangement step was considered to be reversible. The interconversion of the isomeric propyl and isopropyl cations allows the seven hydrogen atoms within the propyl group to undergo extensive site-exchange before the hydrogen transfers to oxygen take place.

The divergent behaviour of the oxonium ions and the immonium ions or protonated propylamines suggests that the site-selectivity in the hydrogen transfer steps depends on the nature of the cation rearrangement. The distinctive selectivity found in the

chemistry of the immonium ions and protonated propylamines appears to reflect a unidirectional isomerization of the incipient cation. If this hypothesis is correct, a similar selectivity should be observed in propene loss from oxonium ions in which the rearrangement is not reversible. Another explanation is that a different site-selectivity occurs when there is a more basic nitrogenous component in the INCs, because the proton transfer step is more exothermic and less likely to be reversible. If this view is correct, the site-selectivities in propene and water loss from oxonium ions may always differ from those found for the corresponding reactions of their immonium ion analogues. The second interpretation is less attractive than the first because it interprets the differences in the site-selectivities solely in terms of the presence or absence of a particular element, rather than the influence of energetic and kinetic factors on the mechanism of fragmentation. The two alternative explanations can be distinguished by examining the behaviour of $CH_3CH{=}O^+CH_2CH_2CH_3$ [22], which is known [23] to rearrange unidirectionally to $CH_3CH{=}O^+CH(CH_3)_2$ before dissociating.

Results and discussion

The reactions of metastable oxonium ions generated as $CH_3CH{=}O^+CH_2CH_2CH_3$, **1**, and six of its specifically labelled analogues are reported in Table 8.1. These data give the relative abundance (RA, as measured from the area of the corresponding metastable peak and quoted as a percentage of the total) and kinetic energy (KE) release ($T_{0.5}$, as estimated from the width at half-height of the appropriate metastable peak) for each dissociation of the $C_5H_{11-n}D_nO^+$ ions.

The new data confirm and refine the earlier exploratory work [21-23] on **1**. Elimination of water and propene from metastable **1** occurs in approximately equal

Table 8.1. Reactions of metastable $C_5H_{11-n}D_nO^+$ ions

	Neutral species lost[ab]															
	H_2O		HOD		D_2O		C_3H_6		$C_3H_5D^\bullet$		$C_3H_4D_2$		$C_3H_3D_3$		$C_3H_2D_4$	
Ion structure	RA[a]	T[b]	RA	T	RA	T	RA	T	RA	T	RA	T	RA	T	RA	T
$CH_3CH{=}O^+CH_2CH_2CH_3$	45.0	1.6					55.0	1.3								
$CH_3CH{=}O^+CHDCH_2CH_3$	32.1	1.5	9.4	1.6			15.2	1.2	43.2	1.2						
$CH_3CH{=}O^+CD_2CH_2CH_3$	21.6	1.6	18.6	1.4	~0		3.3	~1	21.5	1.3	35.1	1.3				
$CH_3CH{=}O^+CH_2CD_2CH_3$	22.1	1.6	6.5	1.5	~0		3.9	~1	17.1	1.3	50.4	1.4				
$CH_3CH{=}O^+CH_2CH_2CD_3$	8.7	1.5	28.2	1.4	<0.1		2.9	~1	<0.5		31.1	1.4	29.1	1.4		
$CH_3CD{=}O^+CH_2CH_2CH_3$	38.9	1.5	<0.2		~0		54.5	1.3	6.6	1.0						
$CD_3CD{=}O^+CH_2CH_2CH_3$	31.2	1.6	8.9	1.6	~0		52.4	1.3	0.7	~1.2	0.5	~1	3.6	~1	2.8	~0.9

[a] RA = relative abundance, measured by metastable peak areas arising from dissociation of ions in the second field-free region of the VG Analytical ZAB-R mass spectrometer and normalized to a total of 100 units. Values are quoted to the first decimal place solely in order to avoid introducing rounding errors. [b] T = Kinetic energy release (in kJ/mol) estimated from the width at half-height of the associated metastable peak.

quantities. The hydrogen atoms of the expelled neutral species mainly originate from the propyl group. However, some minor discrepancies are found in the behaviour of labelled analogues of **1**. The older work [22] found that $CD_3CD{=}O^+CH_2CH_2CH_3$ lost specifically C_3H_6 and H_2O, thus leading to the conclusion that only the hydrogen (in this case protium) atoms from the propyl group of **1** are always selected in the neutral product. The new (and more extensive) labelling data reported in this work show that this conclusion is a slight oversimplification: the atoms of the eliminated water and propene molecules are indeed usually chosen from those of the propyl group, but the atoms of the two-carbon chain (particularly those of the methyl group) also participate to an appreciable extent.

Both water and propene elimination produce Gaussian metastable peaks. Neither the shape of the metastable peaks nor the associated KE releases ($T_{0.5}$=1.5±0.1 kJ/mol) for water loss are significantly affected by deuteriation. Similarly, the KE releases for elimination of propene from the initial propyl group lie in the range 1.2-1.4 kJ/mol. However, for the minor signals for loss of propene molecules that are not derived simply by hydrogen abstraction from the intact propyl substituent, the $T_{0.5}$ values (1.0±0.2 kJ/mol) appear to be slightly smaller. This trend is probably significant and it is discussed later. The invariance of the $T_{0.5}$ values associated with expulsion of water and most propene molecules is consistent with fragmentation *via* INC-mediated routes in which no bond to hydrogen is broken in the final dissociation step. Furthermore, the KE releases are typical of the small to moderate values that have been reported in analogous systems in which the chemistry has been interpreted in terms of INCs.

Even a cursory inspection of the new labelling data reveals that the site-selectivity in water loss from **1** is very different from that (almost random probability of transferring any two of the seven protium or deuterium atoms of the original propyl group) found for labelled analogues of $CH_2{=}O^+CH_2CH_2CH_3$. Similarly, the site-selectivity in propene loss is nowhere near that which would be anticipated on the basis of reaction (1); moreover, the observed site-selectivity differs significantly from that predicted by assuming that any one of the seven hydrogen atoms of the initial propyl group is transferred to oxygen during the reaction. However, propene loss from labelled analogues of **1** does show a clear resemblance to the corresponding reaction of the analogous immonium ions. Consequently, it appears that the chemistry of **1** involves a unidirectional rearrangement of the incipient propyl cation to its isopropyl isomer, followed by proton abstraction from either of the methyl groups. Detailed mechanisms for propene and water loss from **1** are best considered separately.

Elimination of Propene

Earlier work interpreted propene loss from **1** in terms of an INC-mediated mechanism which resulted in production of the most stable isomer of $C_2H_5O^+$, $CH_3CH{=}OH^+$, as the fragment ion [4,22]. The four isomeric $C_2H_5O^+$ ions, $CH_3CH{=}OH^+$, $CH_2{=}O^+CH_3$, $CH_2{=}CHOH_2^+$ and $\overline{CH_2CH_2OH}^+$ can be differentiated on the basis of their collisional activation (CA) spectra [24-26]. Fig. 8.1 shows the CA spectrum of the $C_2H_5O^+$ product ions fromed by fragmentation of metastable $C_5H_{11}O^+$ ions generated

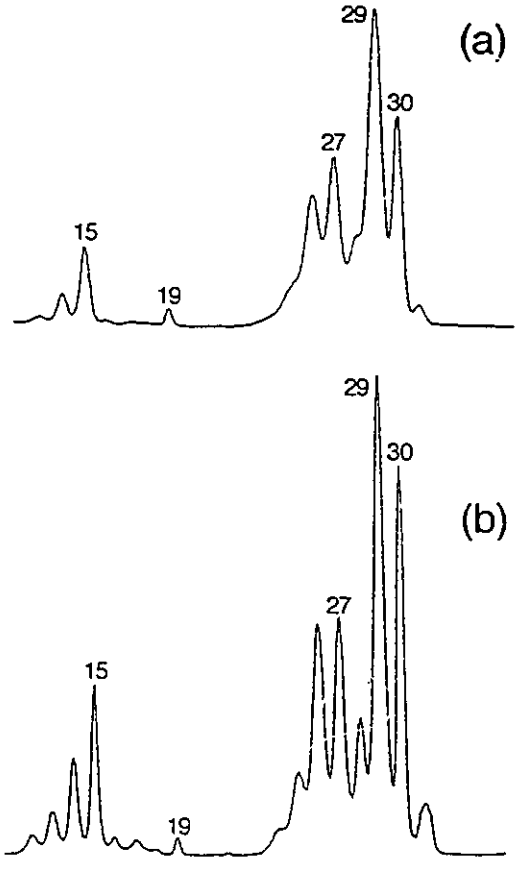

Figure 8.1 Partial collisional activation mass spectra of $C_2H_5O^+$ ions derived (*a*) by loss of C_3H_6 from metastable $CH_3CH{=}O^+CH_2CH_2CH_3$ ions and (*b*) by loss of $H^\bullet$ from metastable $CH_3CH_2OH^{\bullet+}$ radical cations.

as **1**. This spectrum is indistinguishable from that of $CH_3CH{=}OH^+$ reference ions produced from metastable $CH_3CH_2OH^{\bullet+}$ (by loss of $H^\bullet$), thus confirming the earlier mechanistic deduction.

Table 8.2 gives the ratios of partially labelled propenes that are lost from labelled analogues of **1**, together with those expected on the basis of five models.

Model A assumes that specific β-hydrogen transfer occurs via reaction (1). This model is grossly in error: there is actually a strong discrimination against β-hydrogen transfer, as is shown most clearly by the loss of predominantly $C_3H_4D_2$ (71%) from $CH_3CH{=}O^+CH_2CD_2CH_3$, which is predicted by model A to lose only C_3H_5D. The inadequacy of reaction (1), whcih has been known for almost 30 years [27], was recently underlined in definitive studies of propene loss from labelled analogues of $R_1R_2C{=}N(R_4)^+CH_2CH_2CH_3$ and $CH_2CH_2CH_2NH_3^+$ [16-18]. However, despite this clear demonstration of its inaccuracy, reaction (1) is still widely held to be an adequate general explanation of this ubiquitous class of alkene elimination.

Model B corresponds to random transfer of any one of the seven protium or deuterium atoms from the original propyl group to oxygen in propene loss from labelled analogues of **1**. This model reproduces the experimental data far more accurately than model A does, but it cannot explain the appreciably different behaviour of $CH_3CH{=}O^+CD_2CH_2CH_3$ and $CH_3CH{=}O^+CH_2CD_2CH_3$. It underestimates the probability of α- and γ-hydrogen transfer while overestimating the likelihood of β-hydrogen transfer.

The ratios quoted for model C are derived from the mechanistic description of Scheme 8.1. After the requisite C-O bond in **1** has been sufficiently strectched, a 1,2-H shift occurs unidirectionally in the developing propyl cation in **1a**. Proton abstraction

Table 8.2. Observed and calculated ratios of $C_3H_{6-n}D_n$ lost from labelled analogues of 1

Ion structure	Neutral species lost	Obs.	Expected from Model[a,b] A	B	C	D	E
$CH_3CH{=}O^+CHDCH_2CH_3$	C_3H_6	26	0	14	17	20	24-28 (26)
	C_3H_5D	74	100	86	83	80	72-76 (74)
$CH_3CH{=}O^+CD_2CH_2CH_3$	C_3H_6	5	0	0	0	0	4-8 (6)
	C_3H_5D	36	0	29	33	42	38-44 (40)
	$C_3H_4D_2$	59	100	71	67	58	52-54 (54)
$CH_3CH{=}O^+CH_2CD_2CH_3$	C_3H_6	5	0	0	0	0	0-6 (5)
	C_3H_5D	24	100	29	17	20	22-28 (22)
	$C_3H_4D_2$	71	0	71	83	80	72-74 (73)
$CH_3CH{=}O^+CH_2CH_2CD_3$	C_3H_6	5	0	0	0	0	0-6 (5)
	C_3H_5D	<1	0	0	0	0	0-5 (1)
	$C_3H_4D_2$	49	0	43	50	50	45-50 (49)
	$C_3H_3D_3$	46	100	57	50	50	45 (45)
$CH_3CD{=}O^+CH_2CH_2CH_3$	C_3H_6	89	100	100	100	100	90-100 (92)
	C_3H_5D	11	0	0	0	0	5-10 (8)
$CD_3CD{=}O^+CH_2CH_2CH_3$	C_3H_6	87	100	100	100	100	90
	C_3H_5D	1	0	0	0	0	0
	$C_3H_4D_2$	<1	0	0	0	0	0
	$C_3H_3D_3$	6	0	0	0	0	0-10 (5)
	$C_3H_2D_4$	5	0	0	0	0	0-10 (5)

[a] Values normalized to a total of 100 units for propene loss. [b] See text for details of models.

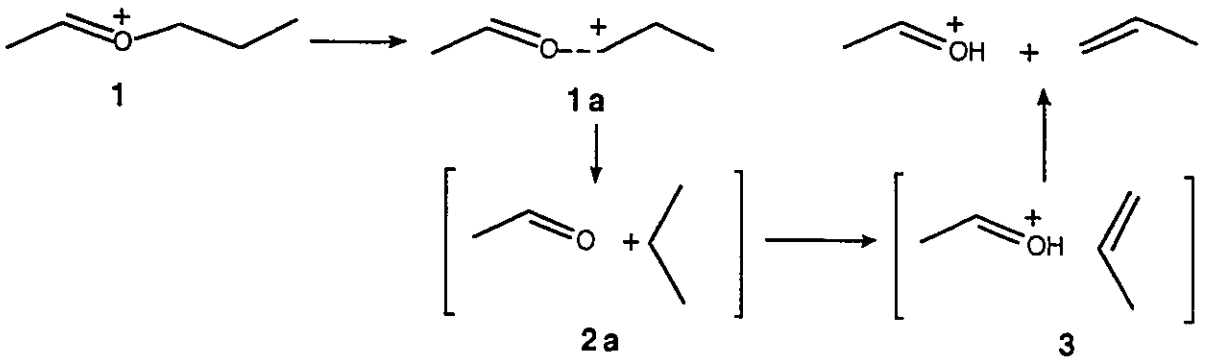

Scheme 8.1

from either of the two methyl groups in the incipient isopropyl cation in the INC, **2a**, with equal probability and without interference from any isotope effects, then gives the second INC **3**, comprising $CH_3CH{=}OH^+$ and $CH_2CH{=}CH_3$. Separation of **3** into its components results in propene elimination. This model gives a good first approximation to the experimental data. In particular, it accounts for the discrimination against β-hydrogen transfer because only one of the two hydrogen atoms in the initial β-methylene group is moved by the 1,2-shift into a position (a new methyl group derived from the α-methylene residue and the migrating hydrogen atom) from which it can be transferred to oxygen. Thus, $CH_3CH{=}O^+CHDCH_2CH_3$ and $CH_3CH{=}O^+CH_2CD_2CH_3$ undergo eventual H-transfer (resulting in C_3H_5D and $C_3H_4D_2$ loss, respectively) and D-transfer (resulting in C_3H_6 and C_3H_5D expulsion, respectively) in quite similar ratios because the isopropyl cation, from which proton or deuteron abstraction occurs, contains one CH_3 and one CH_2D group ($CH_3CH^+CH_2D$ and $CH_3CD^+CH_2D$, respectively).

Although model C provides a reasonable first approximation to the observed ratios for $C_3H_{6-n}D_n$ loss from labelled analogues of **1**, it slightly underestimates the contribution from α- and β-hydrogen transfer. A refinement in the form of a preference factor, *p*, favouring hydrogen abstraction from the methyl group derived from the original α-methylene residue compensates for this deficiency. This preference factor

arises because the components of the INC **3** do not enjoy complete rotational freedom; instead, there is a slightly increased probability of abstracting a proton from the methyl group derived from the α-methylene residue because the oxygen atom initially is located nearer to this methyl group than to the more distant γ-methyl group of the original propyl substituent. Similarly, the influence of a small inverse secondary isotope effect (k_H per deuterium atom) must be considered on the hydrogen transfer step. This isotope effect discriminates against transfer of a protium atom from a methyl group that does not contain any deuterium atoms. The origin of this unusual inverse isotope effect also lies in rotational effects. The rate of H-transfer from the CH_3 group in a $CH_3CH^+CHD_2$ cation will be reduced compared with that of H-transfer (or D-transfer) from the CHD_2 group because the centre of mass of the cation is shifted slightly away from the CH_3 group towards the CHD_2 group. Consequently, the atoms of the CH_3 group are marginally less likely to spend time in the near vicinity of the oxygen atom than are those of the CHD_2 group.

Model D corresponds to a system in which p=1.4 and k_H=0.9. Similar values for p and k_H have been found in propene loss from immonium ions containing propyl groups [16]. In some cases (e.g. $CH_3CH{=}O^+CD_2CH_2CH_3$), the effects induced by p and k_H reinforce each other (both favour hydrogen transfer from the methyl group derived from the α-methylene residue); in others (e.g. $CH_3CH{=}O^+CH_2CH_2CD_3$), they oppose one another (p favours transfer from the substituent formed from the α-methylene residue, whereas k_H acts to the advantage of transfer from the original γ-methyl group). Model D reproduces the observed site-selectivity in the hydrogen transfer step from the original propyl substituent quite accurately.

In order to account for the minor (but significant) contribution for hydrogen transfer from the isolated two-carbon unit of **1**, it is necessary to allow for the possibility of a skeletal rearrangement whcih destroys the positional integrity of the $CH_3CH{=}O$ entity.

Such a skeletal isomerization could arise by recombination of the components of **3** to give the open-chain cation, $CH_3CHOHCH_2CH^+CH_3$, **4**, which then rearranges to $CH_3CH^+CH_2CHOHCH_3$, **4'**, before expelling propene, Scheme 8.2. Independent studies

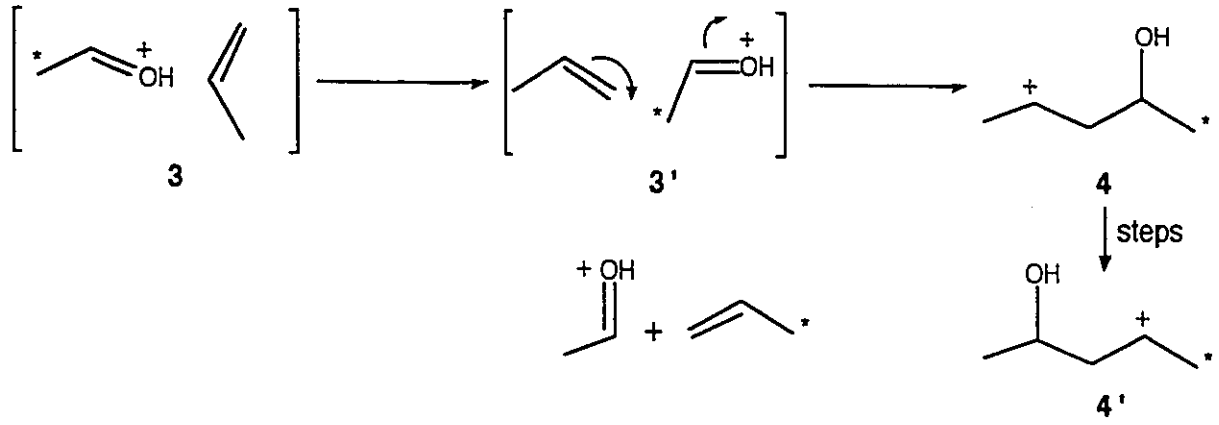

Scheme 8.2

of the chemistry of the related oxonium ion, $CH_3CH_2CH_2C(CH_3)=OH^+$, **5**, have shown that this isomer of **1** expels H_2O and C_3H_6 in slow dissociations [28-30]. Furthermore, although propene loss from labelled analogues of **5** proceeds with predominant retention of the γ-methyl group in the neutral fragment, there is a minor contribution (*ca.* 20%) from another route in whcih this substituent remains in the ionic fragment. This minor component can be explained by several mechanisms. Thus, open-chain cations such as $CH_3CHOHCH^+CH_2CH_3$, **6**, and **4**, are accessible to **5** *via* 1,2-H shifts; these species can then undergo ring-closure and ring-opening *via* either protonated oxiranes [28] or oxetanes [29], thus allowing the hydroxy group to migrate from C(2) to C(4) of the five-carbon chain.

Alternatively, a series of 1,2-H and 1,2-alkyl shifts permits **5** to rearrange to **5'** *via* a sequence of steps that does not require rupture of the initial C-O bond (Scheme 8.3) [29-30]. Attempts to distinguish between these mechanisms by examining the

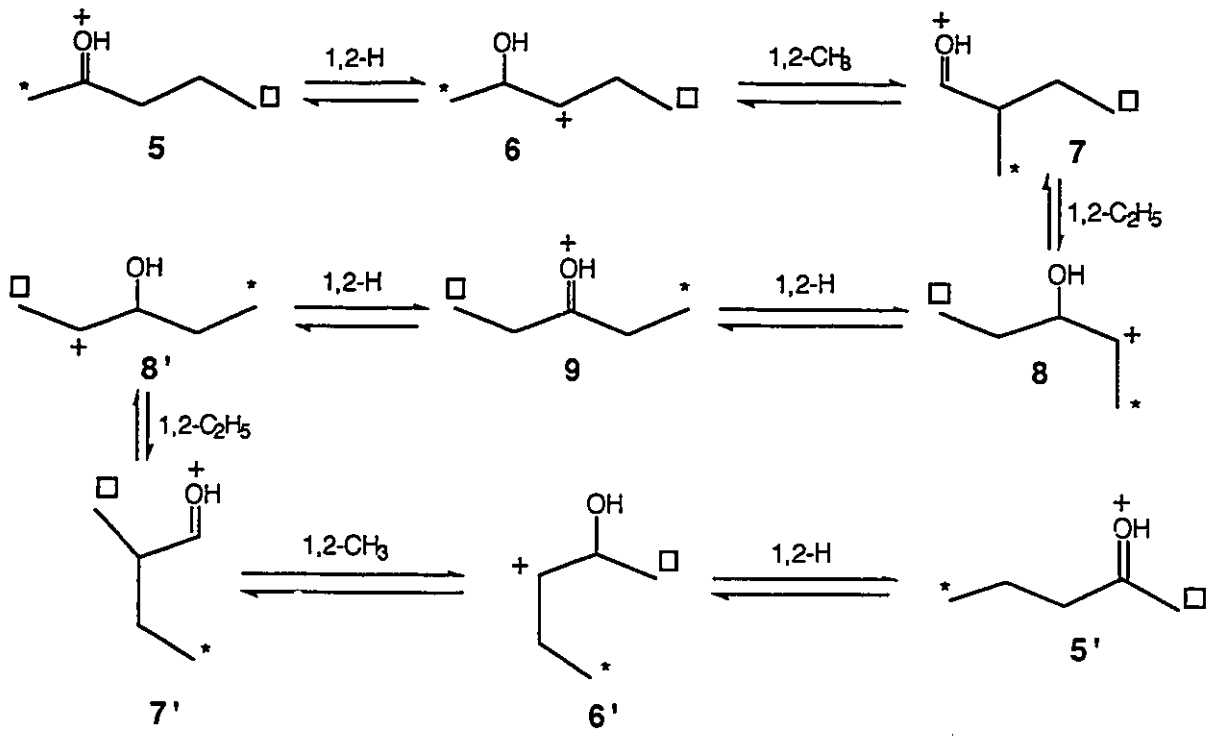

Scheme 8.3

behaviour of ^{13}C-labelled variants of **5** [e.g. $CH_3CH_2CH_2{}^{13}C(CH_3)=OH^+$] have not yet given conclusive results [30]: the carbon atom initially attached to oxygen is predominantly retained in the fragment ion (as would be expected from Scheme 8.3), but there appears to be a small contribution (*ca.* 10-20%) from a route in whcih the C-O bond is broken (as would be anticipated on the basis of the alternative routes involving protonated cyclic ethers). In the case of the lower homologue, $CH_3CH_2CH=OH^+$, the analogous reaction (ethene elimination) definitely proceeds without dislocation of the C-O bond, as is shown by the loss of C_2H_4 with high specificity from $CH_3CH_2{}^{13}CH=OH^+$ [31,32].

Fortunately, the residual doubt concerning the nature of the skeletal isomerization(s) which convert **5** into **5'** (or **4** into **4'**) creates only a minor uncertainty in estimating the ratios of $C_3H_{6-n}D_n$ that should be lost from labelled analogues of **1**.

Model E corresponds to a situation in which the bulk (90%) of ions dissociate according to model D, but 10% of the INCs comprising protonated acetaldehyde and propene recombine to give **4** (or a labelled analogue) which undergoes further isomerization to **4'** before finally losing propene. The quoted range of values spans the maximum uncertainty in the ratios; the value in parentheses is the ratio considered to be most likely.

Model E clearly offers an excellent approximation to the experimental data: it accomodates the ratios of labelled propenes derived from the initial propyl substituent of **1** and also allows for the minor contribution for inclusion in the eliminated propene of some of the atoms of the two carbon entity. The behaviour of $CD_3CD{=}O^+CH_2CH_2CH_3$ is especially interesting. The CD_3 group tends to be incorporated intact when partially deuteriated propene is expelled: both $C_3H_2D_4$ and $C_3H_3D_3$ are lost in moderate abundance (RA=6), but C_3H_5D and $C_3H_4D_2$ are very rarely eliminated. The negligibly small quantity of $C_3H_4D_2$ loss reflects the difficulty in eroding the positional integrity of the methyl groups of **4**, which evidently migrate intact in the steps which result in isomerization to **4'**. A similar deduction can be made from the observation that $CH_3CH{=}O^+CH_2CH_2CD_3$ expels almost no C_3H_5D.

The proposal that a small percentage of propene loss from **1** involves the recombination of the components of the INC **3** may seem rather contrived, particularly since the binding energy of this complex may be relatively low. However, alternative mechanisms [e.g. reaction (2)] for isomerization of the skeleton of **1** are at least equally speculative.

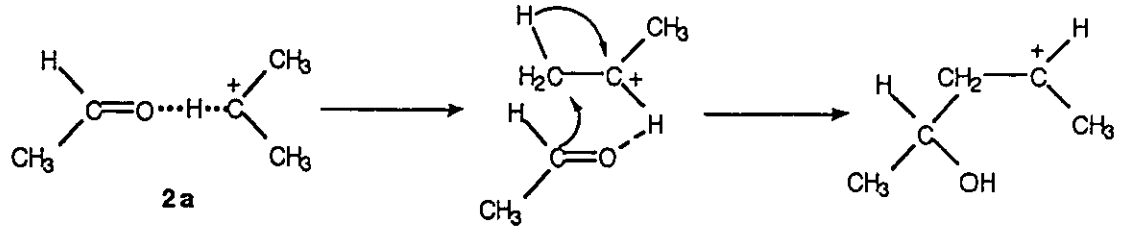

(2)

Some circumstantial evidence supporting the mechanism of Scheme 8.3 is found in the appreciably smaller KE releases accompanying propene losses which are considered to involve the recombination of the components of **3**. This trend appears to be significant and would be intelligible provided that the tendency of the dissociating ions to react in this manner increased as their average internal energy decreases. When these ions with a reduced average internal energy eventually expel propene, a smaller KE release should be observed. In contrast, the higher energy ions are more likely to fragment by eliminating propene directly, without undergoing the additional rearrangement entailed in recombination of **3** to **4**. Consequently, a somewhat greater excess energy is present in the transition state, thus slightly increasing the KE release.

In conclusion, propene elimination from **1** may be understood in some detail by means of an INC-mediated mechanism in which unidirectional rearrangement of a developing propyl cation to its more stable isopropyl isomer precedes hydrogen transfer from either of the methyl groups of the isomerized cation. This mechanism correctly accounts for the site-selectivity of hydrogen transfer from the propyl group to oxygen. Propene loss from **1** resembles the corresponding fragmentation of the analogous immonium ions [16,17] and protonated alkylamines [18] containing a propyl substituent. This finding indicates that the observed site-selectivity reflects the occurrence of a unidirectional rearrangement of the incipient cation from the unstable propyl structure to the stable isopropyl isomer, rather than the presence of nitrogen in the initial ion. A particularly interesting finding is the influence of an unusual inverse isotope effect on the rates of hydrogen transfer from the methyl groups of the isopropyl cation formed by this isomerization. An isotope effect of this kind was first documented in propene expulsion from the analogous immonium ions [16]; it appears that such isotope effects may be typical in these INC-mediated processes.

Elimination of Water

Loss of H_2O from oxonium ions such as **1** in which the oxygen atom is flanked on both sides by carbons must involve extensive rearrangement. This process cannot be explained solely in terms of conventional intermediates. However, INC-mediated mechanisms have been applied successfully to give a detailed interpretation of water loss from $CH_2{=}O^+CH_2CH_2CH_3$, $CH_2{=}O^+CH(CH_3)_2$ and their labelled analogues [20,23].

Table 8.3 gives the ratios of H_2O, HOD and D_2O that are lost from labelled analogues of **1**, together with the ratios expected on the basis of four models.

Model F corresponds to random selection of any two of the 11 protium or deuterium atoms from the $C_5H_{11-n}D_nO^+$ ion in the expelled molecule of water. Model G restricts the statistical selection to the seven protium or deuterium atoms in the initial propyl substituent. Neither of these models accounts for the experimental facts to even a first approximation. Both seriously overestimate the abundance of D_2O loss [as is particularly clear in the case of $CD_3CD{=}O^+CH_2CH_2CH_3$ (model F) and $CH_3CH{=}O^+CH_2CH_2CD_3$ (model G)]. Similarly, neither of these models can explain the different ratios of H_2O, HOD and D_2O which are eliminated from $CH_3CH{=}O^+CD_2CH_2CH_3$ and $CH_3CH{=}O^+CH_2CD_2CH_3$. The probabilities of incorporating the hydrogen atoms on the five distinct sites of **1** in the eliminated water are obviously not identical: those on the α- and γ-carbons of the propyl group are more readily transferred to oxygen than those on the β-carbon; moreover, the likelihood of transferring a hydrogen atom that was originally part of the isolated two-carbon entity of **1** to oxygen is smaller still. In addition, there is a strong discrimination against selecting two hydrogen atoms from the same carbon atom. Thus, $CH_3CH{=}O^+CH_2CH_2CD_3$, which would be expected to expel 5-14% of D_2O in water elimination, actually undergoes this reaction to a negligible extent (<1%).

Table 8.3. Observed and calculated ratios of $H_{2-n}D_nO$ lost from labelled analogues of 1

Ion structure	Neutral species lost	Obs.	Expected from Model[a,b] F	G	H	I
$CH_3CH{=}O^+CHDCH_2CH_3$	H_2O	77	82	71	67	70
	HOD	23	18	29	33	30
$CH_3CH{=}O^+CD_2CH_2CH_3$	H_2O	54	65	48	33	40
	HOD	46	32	48	67	60
	D_2O	0	2	4	0	0
$CH_3CH{=}O^+CH_2CD_2CH_3$	H_2O	77	65	48	67	70
	HOD	23	32	48	33	30
	D_2O	0	2	4	0	0
$CH_3CH{=}O^+CH_2CH_2CD_3$	H_2O	24	51	29	0	13
	HOD	76	44	57	100	87
	D_2O	<1	5	14	0	0
$CH_3CD{=}O^+CH_2CH_2CH_3$	H_2O	>99	82	100	100	100
	HOD	<1	18	0	0	0
$CD_3CD{=}O^+CH_2CH_2CH_3$	H_2O	78	38	100	100	75
	HOD	22	51	0	0	25
	D_2O	0	10	0	0	0

[a] Values normalized to a total of 100 units for water loss. [b] See text for details of models.

Model H attempts to allow for these trends by assuming that the transfer of the first hydrogen atom to oxygen is delayed until isomerization of the developing propyl cation has occurred. These steps correspond to those required in propene loss (Scheme 8.1). Once the first hydrogen transfer has taken place, recombination of the components of **3** gives **4**, which then undergoes a second hydrogen transfer from the more distant methyl group, *via* a favourable six-membered ring transition state, to yield the protonated homoallyl alcohol, **10**. Cleavage of the C-O bond (probably with

rearrangement of the developing $C_5H_9^+$ cation) then results in expulsion of H_2O (Scheme 8.4). This mechanism explains why the two hydrogen atoms of the eliminated water are very rarely selected from the same carbon atom of the propyl group: the first hydrogen atom is abstracted from one of the methyl groups of the isopropyl cation in **3**; the other methyl group then becomes the more distant methyl substituent in **4**, from which the second hydrogen is abstracted in the rearrangement leading to **10**. Scheme 8.4 also accommodates the discrimination against selecting a hydrogen atom from the β-methylene residue in the eliminated water because only one of these two hydrogen atoms is moved to a site from which it may be subsequently transferred to oxygen in either of the appropriate steps (**2a** → **3** or **4** → **10**). Model H

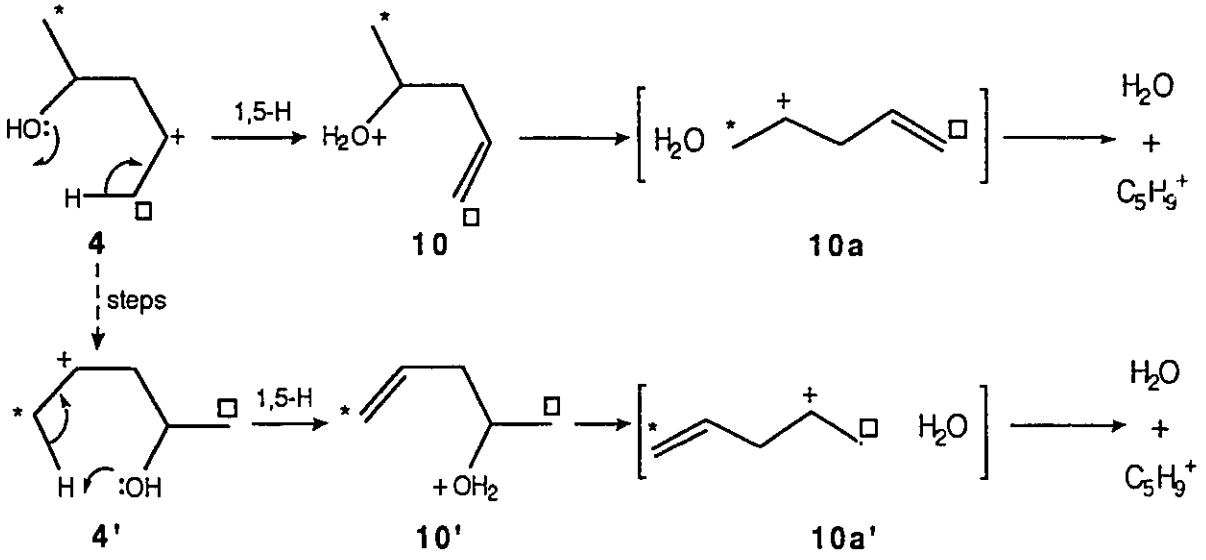

Scheme 8.4

successfully accounts for the trends in the ratios of H_2O, HOD and D_2O which are lost from labelled analogues of **1**. In particular, it explains the divergent behaviour of $CH_3CH{=}O^+CD_2CH_2CH_3$ and $CH_3CH{=}O^+CH_2CD_2CH_3$ (the former expels a much greater proportion of HOD than the latter does); it also allows the absence of appreciable

signals for D_2O elimination from any of the labelled analogues of **1** to be understood. However, the incorporation of a hydrogen atom from the methyl group of the two-carbon entity of **1** cannot be interpreted by Model H.

Model I allows for the possibility that 25% of ions formed as **4** undergo skeletal isomerization to **4'** prior to the second hydrogen transfer. This refinement opens a route for transfer of a hydrogen atom from the methyl group which was not originally part of the propyl substituent to oxygen. Model I provides a good approximation to the observed ratios of H_2O, HCD and D_2O that are lost from labelled analogues of **1**. Its only significant deficiency is that it slightly, but systematically, underestimates the proportion of H_2O elimination. This inaccuracy may arise merely because model I makes no allowance for the possibility of primary isotope effects discriminating against deuterium atom transfer to oxygen. Any such primary isotope effects should be small since the rate-limiting step in both H_2O and C_3H_6 loss from **1** is construed to be **1a** → **2a**.

The proportion of ions which participate in the steps which convert **4** into **4'** is greater (25%) for ions that lose water than that (10%) for those which eliminate propene. This apparent anomaly reflects two differences in the alternative fragmentations. First, both the skeletal rearrangement(s) and water loss should be favoured at lower internal energies; consequently, low energy ions which expel water also show an enhanced tendency to participate in isomerizations such as **4** → **4'**. Secondly, when **3** is formed from **1**, *via* **1a** and **2a**, any ions which eliminate water *must* undergo recombination to **4** before the second hydrogen transfer can occur. These ions *always* have the opportunity to rearrange to **4'**. In contrast, propene elimination need not (and probably normally does not) entail recombination of **3** to **4**. Therefore, most of the ions which expel propene do so by simple separation of the

components of **3**, without ever isomerizing to **4**, thus reducing their tendency to participate in the process(es) which isomerize **4** to **4'**. As a result, **4** → **4'** occurs more often for the ions which eventually eliminate water.

Comparison of the Chemistry of $CH_3CH{=}O^+CH_2CH_2CH_3$ *and* $CH_2{=}O^+CH_2CH_2CH_3$

The observed site-selectivities for the hydrogen transfer steps in the reactions of **1** differ markedly from those found in the fragmentation of its lower homologue, $CH_2{=}O^+CH_2CH_2CH_3$, **11**. The contrast in the reactivity of **1** and **11** is most clearly seen by considering how they lose H_2O. As was shown in the previous section, expulsion of water from labelled analogues of **1** mainly proceeds by selection of one hydrogen atom each from the α-methylene and γ-methyl group of the initial propyl substituent. On the other hand, loss of water from labelled analogues of **11** involves almost random participation of the seven hydrogen atoms of the corresponding propyl substituent. Whereas no labelled analogue of **1** eliminates D_2O to a significant extent, $CH_2{=}O^+CD_2CH_2CH_3$, $CH_2{=}O^+CH_2CD_2CH_3$ and $CH_2{=}O^+CH_2CH_2CD_3$ all lose appreciable (3, 3 and 10%, respectively) amounts of D_2O [20]. This contrast apparently reflects the nature of the rearrangement which converts the developing propyl cation into its stable isopropyl isomer. This step is unidirectional in the case of **1a** → **2a**. On the other hand, the corresponding step { $CH_2{=}O{\cdots}{+}CH_2CH_2CH_3$, **11a**, → $[CH_2{=}O\ {+}CH(CH_3)_2]$, **12a**} is at least partly reversible starting from **11**. Indeed, the reactions of **11a** and **12a** are explicable by INC-mediated mechanisms which allow **11a** and **12a** to interconvert with one another or rearrange to a common structure before dissociating.

However, this explanation poses another question: why should **1a**→**2a** be unidirectional when **11a**→**12a** is not? The stabilization energies of **1a**, **2a**, **11a** and **12a** should be fairly similar. In fact, **1a** and **2a** ought to be slightly more effectively

stabilized than **11a** and **12a**, with respect to their separated components, by ion-dipole attractions and related forces because $CH_3CH{=}O$ has a greater dipole moment (μ) and is a larger and more polarizable molecule than $CH_2{=}O$ (μ=2.7 and 2.4 D [34], respectively). It would appear plausible on this basis to suppose that interconversion of **1a** and **2a** should be at least as facile as that of **11a** and **12a**.

This apparent difficulty is resolved when the energetic analysis is extended to include steps which occur after isomerization of the incipient cation. The stabilization energies of **1a**, **2a**, **11a** and **12a** certainly exert an important influence on the relative rates and reversibility of **1a**→**2a** and **11a**→**12a**, but the energetics of proton transfer between the components of **2a** and **12a** must also be considered. This step is energetically favourable for **2a** because the proton affinity E_{pa} of $CH_3CH{=}O$ exceeds that of $CH_3CH{=}CH_2$ by 30 kJ/mol [35,36]. In contrast, proton transfer between the components of **12a** is energetically unfavourable by 33 kJ/mol [35,36]. This possibility of exothermic proton transfer, which is open to **2a** but not **12a**, is much more significant than the marginally superior stabilization of **2a** compared with **12a**. In both systems, the magnitudes of the stabilization energies of **2a** and **12a** are comparable to or greater than the energy (65-80 kJ/mol) released by isomerization of $^+CH_2CH_2CH_3$ to $^+CH(CH_3)_2$ [37,38]. However, reversion of **2a** to **1a** requires more energy than proton transfer followed by dissociation to give $CH_3CH{=}OH^+$ and C_3H_6; therefore, rearrangement of **2a** to **1a** is unidirectional. In contrast, the critical energy for reversion of **12a** to **11a** is lower than that for formation of $CH_2{=}OH^+$ and C_3H_6 *via* proton transfer between the components of **12a** and comparable to that for fragmentation to form $^+CH(CH_3)_2$ and CH_2O.

The contrasts between the reactions of **1** and **11** can be understood by comparing the relevant portions of the PEPs for isomerization and dissociation of these $C_4H_9O^+$ and $C_5H_{11}O^+$ ions, Fig. 8.2. These PEPs were constructed using known [35-42] and

estimated [23,43-48] enthalpies of formation. There are some uncertainties concerning the enthalpies of certain intermediates or transition states and also the depth of the energy wells (if any) occupied by one or two species. Nevertheless, the following points deserve emphasis.

Firstly, the energies of the products of C_3H_6 and CH_2O or CH_3CHO loss are known with confidence [35-37]. There is no doubt about which combination of products is energetically preferable in each system. Moreover, there are good reasons for placing the estimated energies of **11a** and **12a** *ca.* 70 kJ/mol below the total energy of the separated products [23]. Similarly, **1a** and **2a** should lie *ca.* 80 kJ/mol lower than the total energy of CH_3CHO and the appropriate $C_3H_7^+$ cation [23]. Consequently, the view that isomerization of the developing cation in **1a** becomes rate-limiting because of the changes in the PEP induced by the possibility of exothermic proton transfer leading to C_3H_6 loss seems secure.

Secondly, there is more uncertainty about the geometries and energies of **3** and the analogous species [CH_2=OH^+ CH_3CH=CH_2], **13**. If assessed as INCs stabilized purely by ion-dipole attractions, these species would exist in very shallow energy wells *ca.* 10 kJ/mol deep because C_3H_6 has only a small permanent dipole moment (μ=0.37 D). It is likely that the depth of these wells could be increased by ion-induced dipole attractions and other ionic forces, but it may be more accurate to regard these species as proton-bridged complexes in which C_3H_6 and CH_2O or CH_3CHO are coordinated to a common proton. This complication does not, however, affect the essential conclusion of the previous paragraph, provided that **3** and **13** are appreciably bound relative to the separated products, as is certainly the case. It is in fact not strictly necessary for **3** and **13** to lie in energy wells because it is the changes in the relative energies of **1a** or **11a** and the products of C_3H_6 loss that causes the isomerization of **1a** to be unidirectional and rate-limiting even though that of **11a** is not.

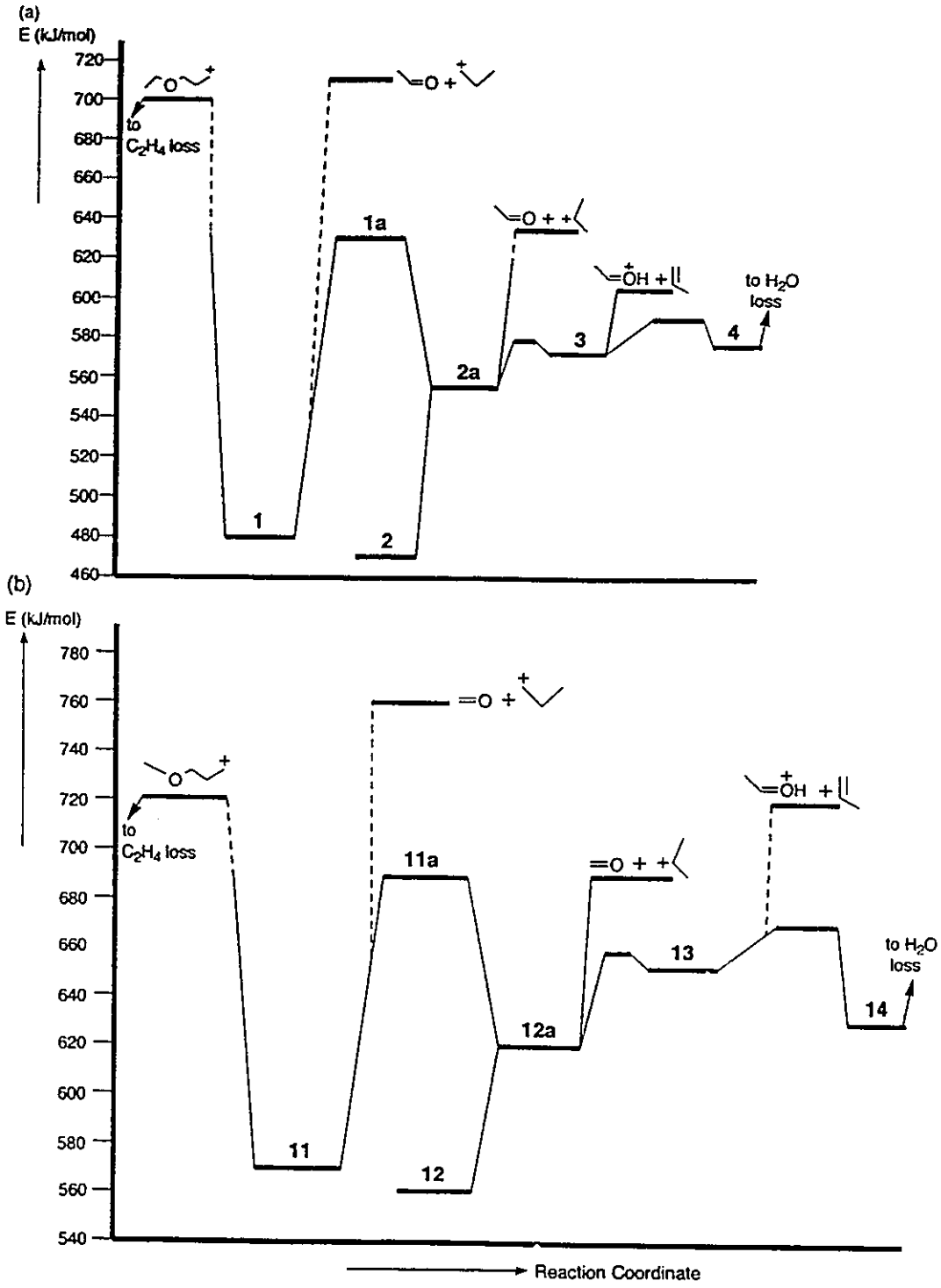

Figure 8.2 Partial potential energy profiles for isomerization and dissociation of $CH_3CH{=}O^+CH_2CH_2CH_3$ and $CH_2{=}O^+CH_2CH_2CH_3$.

Thirdly, experimental values for the enthalpies of formation of **1**, **2**, **11** and **12** { $CH_2O^+CH(CH_3)_2$} are not known. The energies of these ions can be estimated from those [39] of their lower homologues either by means of a group equivalent approach [43,44] or from an algorithm [47] derived from trends in the enthalpies of formation of oxonium ions and the corresponding carbonium ions. Any errors in the estimated energies of **1**, **2**, **11** and **12** are of little consequence in the present context: there is no doubt that these oxonium ions are stable species existing in substantial energy wells.

The enthalpies of formation of the open-chain cations, $CH_3CH^+CH_2CHROH$, formed by recombination of the components of [$CH_3CH{=}CH_2$ $RCHOH^+$], are estimated from known hydride abstraction energies [40]. It is necessary to include a correction of 10 kJ/mol to allow for the destabilizing influence of the electron-withdrawing γ-hydroxy group on the nearby cationic site [45,46]. Experimental values for the energies of **10** (R=CH_3) and **14** (R=H) are very difficult to obtain because formation of such species is usually pre-empted by ring-closure at threshold to give thermodynamically more stable structures. Despite the uncertainty surrounding the energies of **10** and **14**, it is clear that these species lie below the total enthalpies of formation of the products of C_3H_6 loss. As a result, it is plausible to suppose that formation of these intermediates or transition states will compete with C_3H_6 elimination in the dissociation of metastable ions. It is not necessary that **10** and **14** correspond to energy minima, but merely that they should lie at a lower energy level than those of the products of C_3H_6 elimination. In actual fact, there is strong evidence [49] that the open-chain cation, $CH_3CH^+CH_2CH_2OCH_3$, corresponding to **14** does exist in an energy well, though this need not necessarily imply that the homologous ions containing a hydroxy group are also stable species.

Finally, the combined energies of the probable products of H_2O expulsion are still lower than those of **10** and **14**. Thus, the combined experimental enthalpies of formation of H_2O and the 1-methylallyl cation ($CH_3CH^+CH{=}CH_2$) (845 [50] and -240 [41,42] kJ/mol, respectively) formed from **11** and **12** amount to 605 kJ/mol. A mechanism for H_2O elimination from **1** and **2** involving direct cleavage of **10a** gives the 1-methylhomoallyl cation, $CH_3CH^+CH_2CH{=}CH_2$; the enthalpy of this species is estimated to be 800 kJ/mol on the assumption that the E_{pa} of penta-1,4-diene is *ca.* 830 kJ/mol, giving a total energy for these products of 560 kJ/mol. If, as is very likely, rearrangement of the developing $C_5H_9^+$ cation precedes H_2O loss, even more favourable products become accessible (e.g. the 1,3-dimethylallyl cation, $CH_3CH^+CH{=}CHCH_3$, having an enthalpy [51] of 765 kJ/mol). In the present context, details of the later stages of the mechanism for H_2O elimination from **11** and **12** or **1** and **2** are not of primary importance, but it is clear that recombination of the components of **11a** or **1a** to form $CH_3CH^+CH_2CHROH$ with eventual expulsion of H_2O is more favourable than C_3H_6 loss in either system (R=CH_3 or H, respectively). Therefore, the occurrence of H_2O elimination from both $RCH{=}O^+CH_2CH_2CH_3$ ions is explained, even though this process entails far more extensive rearrangement than RCH=O or C_3H_6 expulsion. When R=CH_3, rate-limiting isomerization of **1a** to **2a** yields a dissociating population of $C_5H_{11}O^+$ ions with a higher average internal energy than is the case when **2a** is formed directly from **2**. The higher energy ions show an enhanced tendency to fragment *via* the channel involving the least rearrangement [52]. Consequently, the ratio of C_3H_6:H_2O loss from **1** exceeds that found for **2** [22]; indeed, **2** loses almost exclusively (97%) H_2O, whereas **1** expels H_2O and C_3H_6 in comparable abundances (Table 8.1). Furthermore, the $T_{0.5}$ value for H_2O elimination from **1** exceeds that for **2** [23]. In contrast, no such rate-limiting isomerization occurs when R=H. Therefore, **11** and **12** eliminate CH_2O and H_2O in similar ratios [21], with identical KE releases [23] and there is a common preference for H_2O loss.

Conclusions

The reactions of metastable oxonium ions generated as $CH_3CH{=}O^+CH_2CH_2CH_3$ are intelligible in detail by means of INC-mediated mechanisms. Both propene and water elimination occur after rate-limiting rearrangement of the incipient $^+CH_2CH_2CH_3$ cation to $^+CH(CH_3)_2$ has taken place. The site-selectivity in the hydrogen transfer step(s) reflects the unidirectional nature of the cation isomerization. The hydrogen transfer that precedes propene loss occurs predominantly from the α- and γ-positions of the initial propyl substituent. This dissociation of $CH_3CH{=}O^+CH_2CH_2CH_3$ shows many similarities with the corresponding fragmentation of immonium ions and protonated amines containing a propyl group. In particular, the hydrogen transfer is influenced by an unusual inverse isotope effect, as has been reported in analogous immonium ion systems. This isotope effect may be a diagnostic characteristic in INC-mediated alkene eliminations following rate-limiting cation isomerizations. Water loss from $CH_3CH{=}O^+CH_2CH_2CH_3$ exhibits a similar selectivity, with the additional preference for eventually transferring the second hydrogen from the methyl group of the incipient $^+CH(CH_3)_2$ which is not affected when $[CH_3CH{=}O\ ^+CH(CH_3)_2]$ rearranges to $[\ CH_3CH{=}OH^+\ CH_2{=}CHCH_3]$. This site-selectivity contrasts sharply with that found for water loss from $CH_2{=}O^+CH_2CH_2CH_3$. The selectivity in the hydrogen transfers that precede water expulsion from oxonium ions depends strongly on whether the cation rearrangement is reversible. The reversibility of this isomerization is influenced not only by the extent to which the $RCH{=}O\cdots{}^+CH_2CH_2CH_3$ and $[RCH{=}O\ ^+CH(CH_3)_2]$ species are stabilized with respect to their separated components, but also the energetics of proton transfer to give $[RCH{=}OH^+\ CH_2{=}CHCH_3]$. When proton transfer is energetically favourable (e.g. $R{=}CH_3$), reversion of $[RCH{=}O\ ^+CH(CH_3)_2]$ to $RCH{=}O\cdots{}^+CH_2CH_2CH_3$ can be pre-empted by dissociation, even when the species containing incipient propyl cations are extensively stabilized.

Rererences

1. R.G. Cooks, J.H. Beynon, R.M. Caprioli and G.R. Lester, Metastable Ions, Elsevier, Amsterdam (1973).
2. For reviews, see: D.H. Williams, *Acc. Chem. Res.*, **10**, 280 (1977); D.H. Williams, *Philos. Trans. R. Soc., London Ser. A*, **293**, 117 (1977); R.D. Bowen, D.H. Williams and H. Schwarz, *Angew. Chem. Int. Ed. Engl.*, **18**, 451 (1979); R.D. Bowen and D.H. Williams Rearrangements in Ground and Excited States, Ed., P. DeMayo, Academic Press, New York, Vol. 1, Chapter 2 (1980).
3. The term 'critical energy' corresponds conceptually to the expression 'activation energy', see A. Maccoll, *Org. Mass Spectrom.*, **15**, 109 (1980).
4. R.D. Bowen, B.J. Stapleton and D.H. Williams, *J. Chem. Scc. Chem. Commun.*, 24 (1978).
5. T.H. Morton, *J. Am. Chem. Soc.*, **102**, 1596 (1980).
6. P. Longevialle and R. Botter, *J. Chem. Soc. Chem. Commun.*, 823 (1980).
7. T.H. Morton, *Tetrahedron*, **38**, 3195 (1982).
8. B.L.M. van Baar, J.K. Terlouw, S. Akkok, W. Zummack and H. Schwarz, *Int. J. Mass Spectrom. Ion Processes*, **81**, 217 (1987); N. Heinrich and H. Schwarz, Ion and Cluster Ion Spectroscopy, Ed., J.P. Maier, Elsevier, Amsterdam, 329 (1989).
9. D.J. McAdoo, *Mass Spectrom. Rev.*, **7**, 363 (1988).
10. S. Hammerum, Fundamentals of Gas-Phase Ion Chemistry, Ed., K.R. Jennings, Kluwer, Dordrecht, 379 (1990).
11. R.D. Bowen, *Acc. Chem. Res.*, **24**, 364 (1991).
12. P. Longevialle, *Mass Spectrom. Rev.*, **11**, 157 (1992).
13. D.J. McAdoo and T.H. Morton, *Acc. Chem. Res.*, **26**, 295 (1993).
14. P.C. Burgers and J.K. Terlouw, Specialist Periodical Reports: Mass Spectrometry, Ed., M.E. Rose, Royal Society of Chemistry, Cambridge, Vol. 10, Chapter 2 (1989).
15. For a review of the importance of INCs in the reactions of onium ions and related species, see R.D. Bowen, *Org. Mass Spectrom.*, **28**, 1577 (1993).
16. H.J. Veith and J.H. Gross, *Org. Mass Spectrom.*, **26**, 1097 (1991).
17. R.D. Bowen, A.W. Colburn and P.J. Derrick, *J. Chem. Soc. Perkin Trans. 2*, 285 (1993); 1405; 2363.
18. H.E. Audier and T.H. Morton, *Org. Mass Spectrom.*, **28**, 1218 (1993).
19. For a review of the reactions of immonium ions, see R.D. Bowen, *Mass Spectrom. Rev.*, **10**, 225 (1991).
20. R.D. Bowen, A.W. Colburn and P.J. Derrick, *J. Chem. Soc. Perkin Trans. 2*, 147 (1991).
21. T.J. Mead and D.H. Williams, *J. Chem. Soc. Perkin Trans. 2*, 876 (1972).

22. G.A. Smith and D.H. Williams, *J. Am. Chem. Soc.*, **91**, 5254 (1969).
23. R.D. Bowen and D.H. Williams, *Int. J. Mass Spectrom. Ion Phys.*, **29**, 47 (1979).
24. P.C. Burgers, J.K. Terlouw and J.L. Holmes, *Org. Mass Spectrom.*, **17**, 369 (1982).
25. For earlier work on CA spectra, see: K. Levsen and F.W. McLafferty, *J. Am. Chem. Soc.*, **96**, 139 (1974); F.W. McLafferty, R. Kornfeld, F.W. Haddon, K. Levsen, I. Sakai, P.F. Bente III, Shih-Chuantsai and H.D.R. Schuddemage, *J. Am. Chem. Soc.*, **95**, 3886 (1973); K. Levsen and F.W. McLafferty, *J. Am. Chem. Soc.*, **96**, 139 (1974).
26. M. George, C.A. Kingsmill, D. Suh, J.K. Terlouw and J.L. Holmes, *J. Am. Chem. Soc.*, **116**, 7807 (1994).
27. C. Djerassi and C. Fenselau, *J. Am. Chem. Soc.*, **87**, 5754; 5752 (1965); S. Sample and C. Djerassi, *J. Am. Chem. Soc.*, **88**, 1937 (1966).
28. H.E. Audier, R. Flammang, A. Maquestiau and A. Milliet, *Nouv. J. Chem.*, **4**, 531 (1980).
29. J.V. Headley and A.G. Harrison, *Can. J. Chem.*, **63**, 609 (1985).
30. R.D. Bowen, unpublished results.
31. J.L. Holmes, R.T.B. Rye and J.K. Terlouw, *Org. Mass Spectrom.*, **14**, 606 (1979).
32. D.J. McAdoo and C.E. Hudson, *Int. J. Mass Spectrom. Ion Processes*, **88**, 133 (1989).
33. R.D. Bowen and D.H. Williams, *J. Am. Chem. Soc.*, **100**, 7454 (1978).
34. D.R. Lide and A.A. Maryott, Selected Values of Electric Dipole Moments for Molecules in the Gas-Phase, NSRDS-NBS 10, National Bureau of Standards, Washington, D.C. (1967).
35. S.G. Lias, J.F. Liebman and R.D. Levin, *J. Phys. Chem. Ref. Data*, **13**, 695 (1984).
36. S.G. Lias, J.E. Bartmess, J.F. Liebman, J.L. Holmes, R.D. Levin and W.G. Mallard, *J. Phys. Chem. Ref. Data*, Suppl. 1, **17** (1988).
37. F.P. Lossing and G.P. Semeluk, *Can. J. Chem.*, **48**, 955 (1970).
38. W. Koch, B. Liu and P.v.R. Schleyer, *J. Am. Chem. Soc.*, **111**, 3479 (1989).
39. F.P. Lossing, *J. Am. Chem. Soc.*, **99**, 7526 (1977).
40. F.P. Lossing and J.L. Holmes, *J. Am. Chem. Soc.*, **106**, 6917 (1984), and references cited therein.
41. J.D. Cox and G. Pilcher, Thermochemistry of Organic and Organometallic Compounds, Academic Press, New York (1970).
42. J.B. Pedley, R.D. Naylor and S.P. Kirby, Thermochemical Data of Organic Compounds, Chapman and Hall, London, 2nd Ed. (1986).
43. J.L. Franklin, *Ind. Eng. Chem.*, **41**, 1070 (1949); *J. Chem. Phys.*, **21**, 2029 (1953).
44. S.W. Benson, Thermochemical Kinetics, Wiley, New York, 2nd Ed. (1986).
45. L. Radom, J.A. Pople and P.v.R. Schleyer, *J. Am. Chem. Soc.*, **94**, 5935 (1972).
46. R.D. Bowen and D.H. Williams, *Org. Mass Spectrom.*, **12**, 475 (1977).
47. A. Maccoll, *Org. Mass Spectrom.*, **20**, 715 (1985).

48. J.L. Holmes, M. Fingas and F.P. Lossing, *Can. J. Chem.*, **59**, 80 (1981); **60**, 2365 (1982).

49. R.D. Bowen, A.W. Colburn and P.J. Derrick, *J. Chem. Soc. Chem. Commun.*, 1274 (1989); R.D. Bowen and P.J. Derrick, *Org. Mass Spectrom.*, **28**, 1197 (1993).

50. F.P. Lossing, *Can. J. Chem.*, **50**, 3973 (1972).

51. F.P. Lossing and J.C. Traeger, *Int. J. Mass Spectrom. Ion Phys.*, **19**, 9 (1976).

52. G. Hvistendahl and D.H. Williams, *J. Am. Chem. Soc.*, **97**, 3097 (1975).

CHAPTER 9

The mechanism of alkene elimination from the oxonium ions $(CH_3CH_2)_2C{=}OH^+$, $CH_3CH_2CH_2(CH_3)C{=}OH^+$ and $(CH_3CH_2CH_2)_2C{=}OH^+$

Introduction

Many members of the important homologous series of oxonium ions, $C_nH_{2n+1}O^+$, have been extensively investigated, especially at low internal energies, thus giving considerable mechanistic insight into their interesting chemistry [1]. A major class of fragmentation is alkene loss, which often may be described by several reasonable mechanisms involving conventional steps and classical intermediates. Thus, metastable $(CH_3)_2C{=}OH^+$, **1**, and $CH_3CH_2CH{=}OH^+$, **2**, eliminate C_2H_4 [2,3].

An early study [4] found that the carbon atoms of the eliminated molecule of ethylene were selected at random in fast fragmentations of ^{13}C-labelled analogues of **1**. However, two subsequent investigations showed that $(CH_3)_2{}^{13}C{=}OH^+$ lost C_2H_4 with high selectivities in both fast fragmentations in the ion source (89%) [5] and slow

The work presented here was appeared in an article having the same title:

R.D. Bowen, D. Suh and J.K. Terlouw, *Eur. Mass Spectrom.*, **1**, 33 (1995).

dissociations in the field-free regions (99% and 89%) [5,6]. Consequently, the C-O bond usually remains unbroken when C_2H_4 is eliminated from **1** [5,6].

The frist study [6] of ^{13}C-labelled analogues of **2** reported that $CH_3CH_2{}^{13}CH{=}OH^+$ eliminated C_2H_4 and $C^{13}CH_4$ at almost equal rates (in the ratio 49:51). This unexpected result was interpreted by supposing that after two consecutive 1,2-H shifts starting from $CH_3CH_2{}^{13}CH{=}OH^+$, ring closure of the resultant open-chain cation, $^+CH_2CH_2{}^{13}CH_2OH$, gives a protonated labelled oxetane, $\overline{CH_2CH_2{}^{13}CH_2OH}^+$, in which the original α- and γ-carbon atoms are equivalent [6]. Consequently, when this protonated oxetane reopens and ethylene loss occurs by fission of the central C-C bond, C_2H_4 and $C^{13}CH_4$ are eliminated with equal probabilities by cleavage of $^+CH_2CH_2{}^{13}CH_2OH$ and $^{+13}CH_2CH_2CH_2OH$, respectively. Supporting evidence for this proposal was found in the loss of $C^{13}CH_4$ with high selectivity (99%) from $CH_3{}^{13}CH_2CH{=}OH^+$ [6]. However, a later investigation [7] of $CH_3CH_2{}^{13}CH{=}OH^+$ was at variance with the formation of protonated oxetane because it indicated that $C^{13}CH_4$ elimination was of negligible importance compared to C_2H_4 loss. A third study [8] extended the analysis to include $^{13}CH_3CH_2CH{=}OH^+$, which was found to expel $C^{13}CH_4$ with high selectivity, thus confirming that the initial C-O bond in **2** is normally not broken in ethylene elimination. The erroneous early report [6] of $C^{13}CH_4$ loss from $CH_3CH_2{}^{13}CH{=}OH^+$ probably arose from confusion caused by an overlapping signal corresponding to C_2H_4 elimination from $CH_3CH_2CH{=}OH^+$ generated from residual $CH_3CH_2CH_2OH$ in the sample of $CH_3CH_2{}^{13}CH_2OH$ in which the level of ^{13}C-incorporation was only ~50%.

The most consistent overview of these data is that C_2H_4 loss from **2** takes place after two consecutive 1,2-H shifts, followed by σ-cleavage of $^+CH_2CH_2CH_2OH$, **3**, without ring closure to $\overline{CH_2CH_2CH_2OH}^+$. The rates of these 1,2-H shifts are faster than that of σ-cleavage, thus explaining why the carbon-bound hydrogens of ^2H-labelled analogues of **2** become statistically distributed prior to ethylene loss [9]. Similarly,

fragmentation of **1** proceeds by unidirectional rearrangement to **2** [10], via a 1,2-H shift to $^{+}CH_2CH(CH_3)OH$, followed by a 1,2-methyl shift, rather than by a route involving formation and subsequent ring opening of the protonated oxirane, $CH_3\overline{CHCH_2O}H^+$ [4]. The latter alternative [$^{+}CH_2CH(CH_3)OH \rightarrow CH_3\overline{CHCH_2O}H^+ \rightarrow CH_3CH^+CH_2OH$] is excluded by the ^{13}C-labelling results because migration of the oxygen function would break the original C-O bond. This overall interpretation is consistent with the results of detailed collisional and neutralization-reionization studies of $C_3H_7O^+$ ions [11,12], which reveal that **2** and $CH_3\overline{CHCH_2O}H^+$ readily isomerize to form a common structure or mixture of structures that are distinct from **1** and $\overline{CH_2CH_2CH_2O}H^+$, both of which are discrete stable species. These results suggest strongly that $CH_3\overline{CHCH_2O}H^+$ is accessible to **2** via $CH_3CH^+CH_2OH$, probably on a reversible basis, and that ring-opening of the protonated oxirane at low internal energies always occurs to give the more stable secondary cation, $CH_3CH^+CH_2OH$, thus conserving the C-O bond in **2**.

A further investigation of the generality of these mechanistic conclusions concerning the mechanism of alkene loss from oxonium ions is now timely. This objective can be achieved by examining the behaviour of the homologous $C_5H_{11}O^+$ ions, which are known to expel C_3H_6 in slow dissociations [13,14].

Results and discussion

The oxonium ions $(CH_3CH_2)_2C{=}OH^+$, **4**, and $CH_3CH_2CH_2(CH_3)C{=}OH^+$, **5**, display closely similar reactions that resemble those of $CH_3CH_2(CH_3)CHCH{=}OH^+$, **6**, Table 9.1. Skeletal isomerization must precede C_3H_6 elimination from **4** and **6**; moreover, the loss of an appreciable amount of C_3H_6 as well as the expected $C_3H_3D_3$ from $CD_3CH_2CH_2(CH_3)C{=}OH^+$ shows that propene expulsion cannot be explained unless the initial heavy atom framework of **5** is sometimes reorganized [13,14].

Table 9.1. Reactions of metastable $C_5H_{11}O^+$ ions

Ion structure	Neutral species lost: H_2O RA[a]	H_2O T[b]	C_3H_6 RA	C_3H_6 T
$(CH_3CH_2)_2C{=}OH^+$	35[c]	2.2	65[c]	1.7
	44[d]	2.5	56[d]	
	51[e]		49[e]	
	43[f]		57[f]	
$CH_3CH_2CH_2C(CH_3){=}OH^+$	24[c]	2.2	76[c]	1.7
	38[d]	2.5	62[d]	
	39[e]		61[e]	
	32[f]		68[f]	
$CH_3CH_2CH(CH_3)CH{=}OH^+$	49[c]	1.6	51[c]	1.7
	70[d]	1.8	30[d]	
	71[e]		29[e]	
	58[f]		42[f]	

[a] RA = Relative abundance normalized to a total of 100 units. [b] T = Kinetic energy release (in kJ/mol) estimated from the width at half-height of the associated metastable peak. [c] Measured by metastable peak areas arising from dissociation in the second field-free region of the VG Analytical ZAB-R mass spectrometer of ions generated by dissociative ionization of the appropriate alcohol. [d] Measured by metastable peak heights arising from dissociation in the second field-free region of an AEI MS 902 mass spectrometer of ions generated by dissociative ionization of the appropriate alcohol. [e] Data from reference 13 (ions generated by dissociative ionization of alcohols). [f] Data from reference 14 (ions generated by protonation under chemical ionization conditions of the appropriate ketone or aldehyde).

Various routes for these skeletal rearrangements have been considered, including migration of the hydroxy function via formation of protonated oxiranes [13], Scheme 9.1, or protonated oxetanes [14], Scheme 9.2. Both these routes involve rupture of the original C-O bond. Alternatively, a series of 1,2-H and 1,2-alkyl shifts could allow **4**

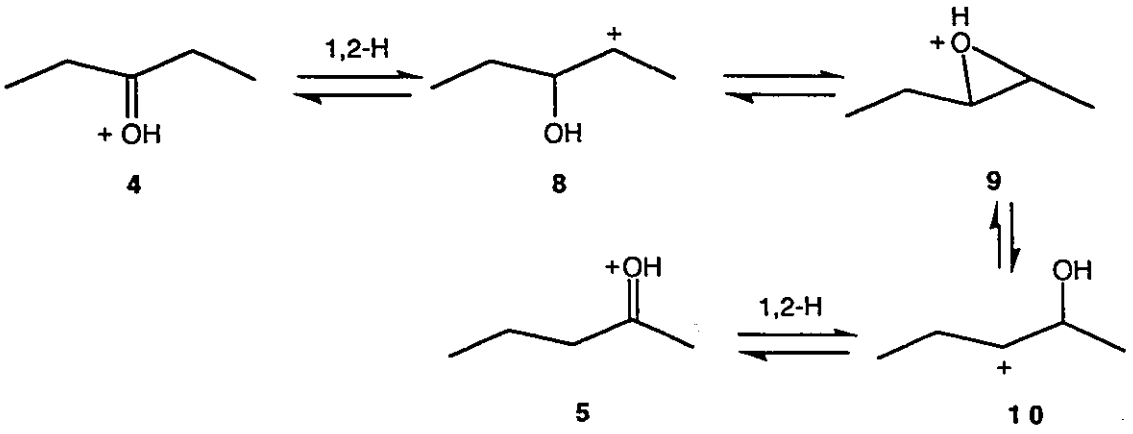

Scheme 9.1

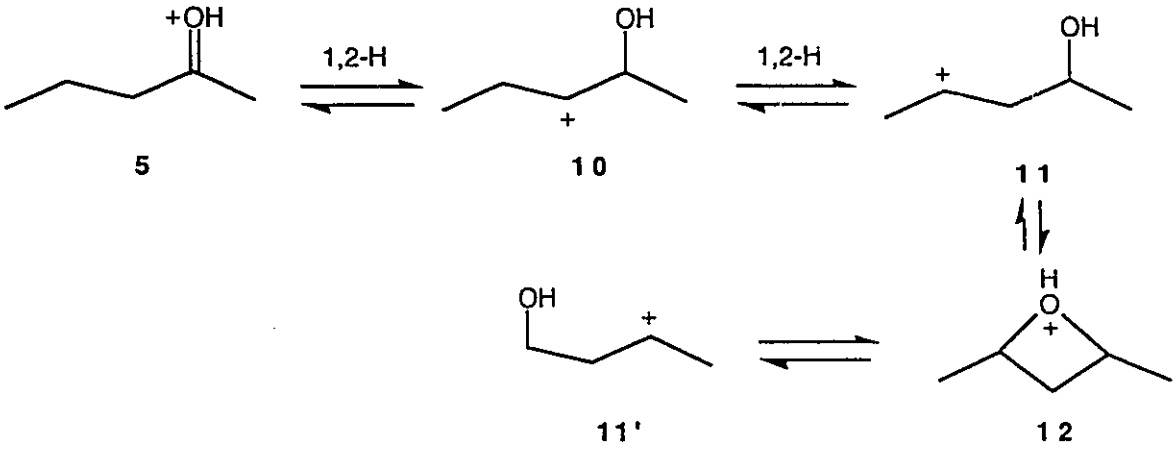

Scheme 9.2

and **5** to reach common intermediates accessible to **6**, while maintaining the initial C-O linkage [14], Scheme 9.3. The behaviour of ^{13}C-labelled analogues of **4** and **5** unequivocally excludes the first possibility, Table 9.2. Thus, $(CH_3CH_2)_2{}^{13}C{=}OH^+$ expels C_3H_6 with high selectivity (~88%), but exclusive $C_2{}^{13}CH_6$ elimination would be predicted on the basis of transfer of the oxygen function from C-3 to C-2 or C-4. Consequently, reorganization of the carbon skeleton of **4** must precede C_3H_6 loss.

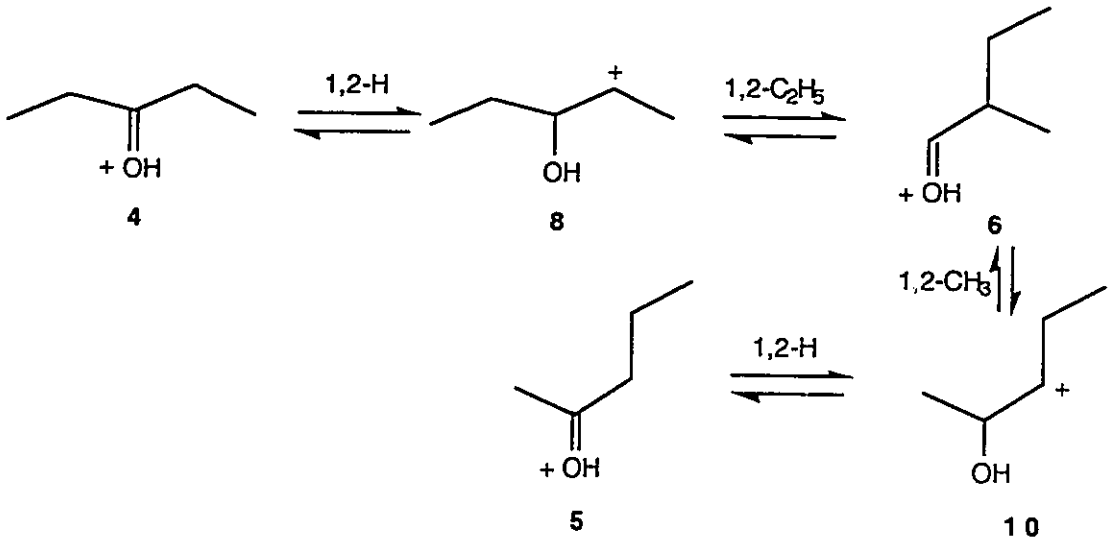

Scheme 9.3

Table 9.2. Reactions of metastable $C_4{}^{13}CH_{11}O^+$ ions

Ion structure	Neutral species lost: H_2O RA[a]	T[b]	C_3H_6 RA	T	$C_2{}^{13}CH_6$ RA	T
$(CH_3CH_2)_2{}^{13}C{=}OH^+$	33[c]	2.2	59.1[c]	1.7	8.2[c]	1.6
$CH_3CH_2CH_2{}^{13}C(CH_3){=}OH^+$	25[c]	2.3	66.9[c]	1.7	8.4[c]	1.5
$CH_3CH_2CH(^{13}CH_3)CH{=}OH^+$	26[c]	2.3	58.5[c]	1.7	15.7[c]	1.5

[a,b,c] See footnotes to Table 9.1; RA values for propene losses are quoted to one decimal place simply in order to avoid introducing rounding errors.

The occurrence of almost identical minor amounts (12% and 11%, respectively) of $C_2{}^{13}CH_6$ expulsion from $(CH_3CH_2)_2{}^{13}C{=}OH^+$ and $CH_3CH_2CH_2(CH_3){}^{13}C{=}OH^+$ points to a common chemistry for these ions in which the C-O bond is occasionally broken prior to propene loss. Therefore, a small proportion of the ions which reach the probable

reacting configuration for propene elimination, $CH_3CH^+CH_2(CH_3)CHOH$, **11**, undergo ring closure to the protonated oxetane, $CH_3\overline{CHCH_2(CH_3)CHOH^+}$, **12**, followed by ring opening in the opposite sense to give $CH_3CH(OH)CH_2CH^+CH_3$, **11'**, thus opening a channel for $C_2{}^{13}CH_6$ expulsion from $(CH_3CH_2)_2{}^{13}C{=}OH^+$ and $CH_3CH_2CH_2(CH_3){}^{13}C{=}OH^+$.

The loss of a greater proportion (~21%) of $C_2{}^{13}CH_6$ from $CH_3CH_2CH_2({}^{13}CH_3)C{=}OH^+$ suggests strongly that a route other than cyclization to the protonated oxetane allows the methyl group originally attached to the carbon atom carrying the oxygen function to be transferred to a position from which it can be expelled in the eliminated propene. If rearrangement via the protonated oxetane was the only route for this process, the same percentages of C_3H_6 and $C_2{}^{13}CH_6$ would be lost from $CH_3CH_2CH_2(CH_3){}^{13}C{=}OH^+$ and $CH_3CH_2CH_2({}^{13}CH_3)C{=}OH^+$. A likely explanation is that a small proportion of ions generated as **5** isomerize to **4**, so allowing the two methyl groups to become equivalent, before dissociation via **11** or **11'** occurs. All the data can be accommodated by Scheme 9.4: one quarter of the ions which reach structure **11** rearrange to **12**, thus, allowing one eighth to expel C_3H_6 after attaining **11'**; similarly, one quarter of ions generated as **5** isomerize via **8** to **4**, so allowing exchange of the two methyl groups to precede formation of **11**.

Scheme 9.4 also explains some interesting general features of the reactions of **4**, **5** and **6**. Elimination of H_2O competes with C_3H_6 loss more effectively starting from **6** than from **4** or **5**; furthermore, the kinetic energy (KE) release associated with H_2O expulsion from **6** is smaller than those for the corresponding dissociation of **4** and **5**. Thermochemical data [15] indicate that the products given by H_2O loss are ~50 kJ/mol more stable than those formed by C_3H_6 expulsion.

These trends reveal that H_2O loss has a lower critical [16] energy than C_3H_6 elimination and that the population of dissociating metastable ions formed as **6** has a lower average [2,17] internal energy than those generated as **4** or **5**. Isomerization of

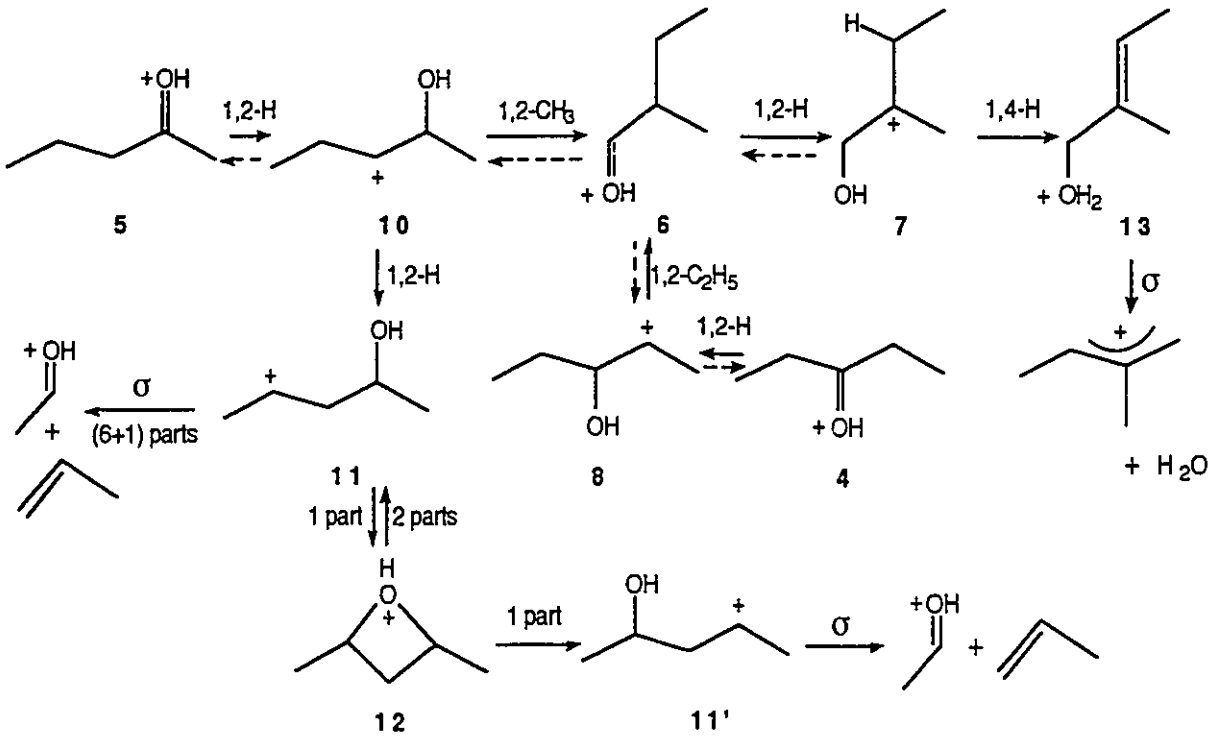

Scheme 9.4

4 and **5** to **7** and other structures accessible to **6** is normally irreversible: these rearranged ions tend to dissociate faster than they revert to **4** or **5**. This finding is in accord with the labelling data. The highest energy species en route to $CH_3CH{=}OH^+$ and C_3H_6 are probably the secondary cations $CH_3CH_2CH^+CH(CH_3)OH$, **10**, and $CH_3CH^+CH(OH)CH_2CH_3$, **8**. These open-chain cations should have appreciably higher enthalpies of formation than the isomeric secondary cation, **11**, because the unfavourable interaction between the electron-withdrawing β-hydroxy group and the nearby charage site will be greater for **8** and **10** than is the case for **11**, which contains a more distant γ-hydroxy substituent [18,19]. It is significant that the KE releases associated with C_3H_6 loss from **4**, **5** and **6** are the same within experimental error, whereas in H_2O elimination dissociation of **6** has an appreciably lower KE release than those associated with fragmentation of **4** and **5**. This distinction arises

because C_3H_6 loss from **4**, **5** and **6** necessarily entails rearrangement to **11** via **10**. However, although **4** and **5** must also isomerize to **8** and/or **10** before expelling H_2O, **6** can undergo this reaction via the more stable tertiary cation $CH_3CH_2C^+(CH_3)CH_2OH$, **7**, without rearranging to either **8** or **10**.

There are clear contrasts between the behaviour of **2** and those of its higher homologues **4**, **5** and **6**. Even at very low internal energies, **2** apparently interconverts freely with the protonated oxirane, $CH_3\overline{CHCH_2O}H^+$, via $CH_3CH^+CH_2OH$, as is shown by the close similarity of the collision-induced dissociation (CID) spectra of $C_3H_7O^+$ ions generated by direct protonation of propionaldehyde and methyloxirane, respectively [11,12]. However, **2** does not rearrange to the protonated oxetane, $\overline{CH_2CH_2CH_2O}H^+$, via $^+CH_2CH_2CH_2OH$, even at the slightly higher internal energies needed to induce C_2H_4 loss [7,8]. On the other hand, the ^{13}C-labelling results reported in this study establish that **4** and **5** do not interconvert rapidly via the corresponding protonated oxirane, **9**, prior to elimination of C_3H_6. This finding is consistent with collisional studies [14,20] of $C_5H_{11}O^+$ ions generated by fragmentation of ionized alcohols or by protonation of the appropriate $C_5H_{10}O$ precursors: although the reactions of metastable **4** and **5** are essentially identical and similar to those of **6** [13,14], each of these three ions displays a distinctive CID spectrum, all of which differ from that of **9**. These results indicate that **4**, **5** and **6** (and probably **9**) exist in discrete potential energy wells, such that there are sizeable barriers for rearrangement of each to any of the others. Nevertheless, at internal energies sufficient to induce dissociation of metastable ions, **4** and **5** are able to reach common intermediates and transition states which are also accessible to **6**. Moreover, the main route for isomerization of **4** to **5** involves formation of **6**, rather than **9**, because the C-O linkage of **4** is conserved with a selectivity of almost 90% in propene loss. However, both the new ^{13}C-labelling experiments and earlier

^{2}H-labelling data [14] indicate that a small percentage of ions generated as **5** are able to rearrange to the protonated oxetane, **12**, thus allowing the initial C-O bond to be eventually broken before C_3H_6 is lost.

The greatly reduced degree of interconversion of **4** with **9** can be partly attributed to differences in the energetics of the isomeric $C_5H_{11}O^+$ ions compared to those of the lower homologues in the $C_3H_7O^+$ system. Construction of a potential energy profile (PEP) [21] for $C_3H_7O^+$ ions reveals that the energies of both $CH_3\overline{CHCH_2O}H^+$ and $CH_3CH^+CH_2OH$ are much lower (by 86 and 108 kJ/mol, respectively [22]) than the combined enthalpies of formation of $CH_2{=}OH^+$ and C_2H_4.

Furthermore, the postulated reacting configuration for C_2H_4 loss ($^+CH_2CH_2CH_2OH$) lies at an appreciably higher energy than **2**, $CH_3\overline{CHCH_2O}H^+$ and $CH_3CH^+CH_2OH$. Consequently, the rate of interconversion of **2** with $CH_3\overline{CHCH_2O}H^+$ and $CH_3CH^+CH_2OH$ becomes quite rapid even at energies close to or slightly below those needed to promote C_2H_4 expulsion. In contrast, when the PEP for the analogous $C_5H_{11}O^+$ ions is constructed from known [15,23-29] or estimated [18,19,30-32] thermochemical data, Figure 9.1, it is evident that the corresponding open-chain cations, **8** and **10**, do not lie appreciably below the threshold for C_3H_6 elimination. Moreover, the postulated reacting configuration for C_3H_6 loss (**11**) is lower in energy than **8** and **10**. As a result, the energy needed to promote rearrangement of **4** and **5** to **10** and **8** is comparable to that required to induce C_3H_6 loss. In other words, once **10** has been formed from **5** (or from **4** via isomerization involving **6**), further rearrangement via the favourable 1,2-H shift to **11** followed by C_3H_6 elimination requires almost no additional energy. Consequently, interconversion of **4** and **5** via any route involving **10** is reduced in efficiency because it must occur in competition with exoergic formation of **11** which leads C_3H_6 loss.

However, even after due allowance for these energetic differences has been made, it appears that another factor must discriminate against ring closure of the α-hydroxy

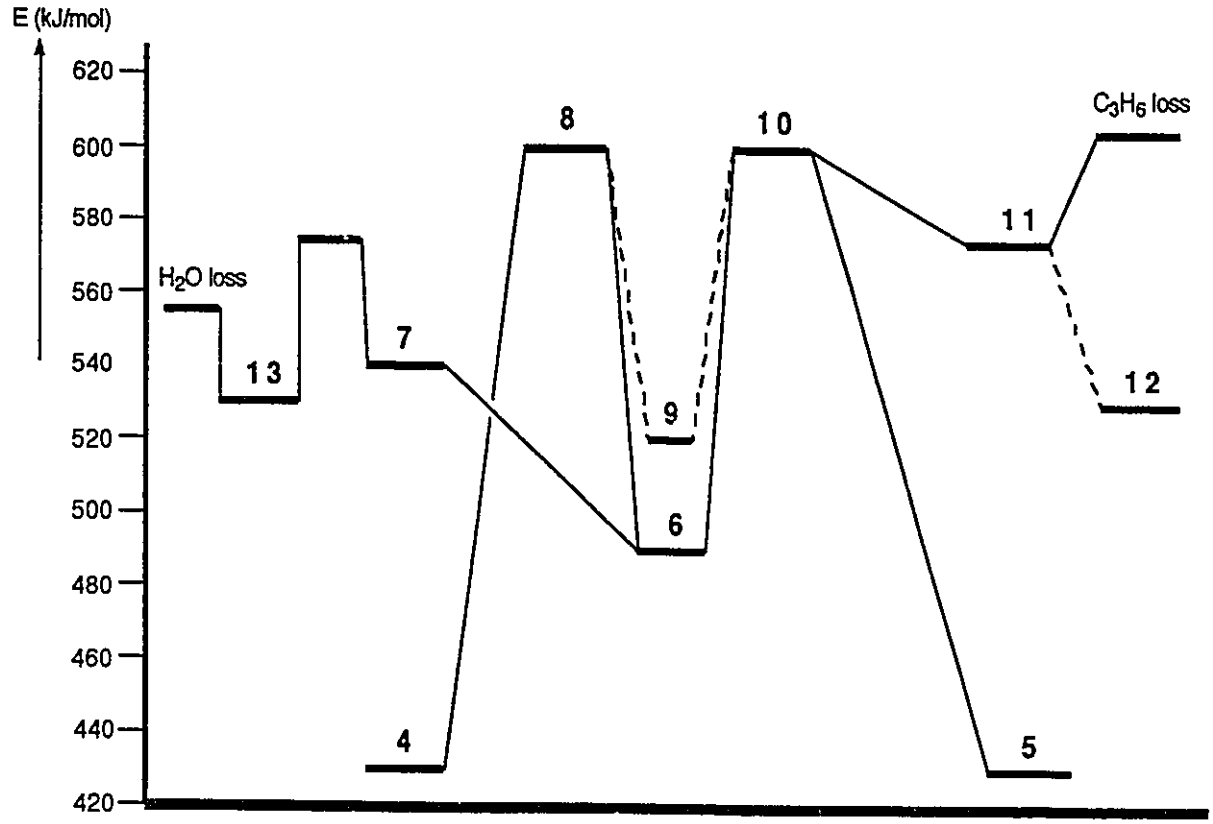

Figure 9.1 Potential energy profile for isomerization and dissociation of **4**, **5** and **6**.

cations to protonated oxiranes. Elimination of C_3H_6 from **4** via either the proposed dominant route (**4→8→6→10→11**) or the pathway (**4→8→9→5→10→11**) involving the protonated oxirane necessarily entails initial formation of the same open-chain cation, **8**. Therefore, the 1,2-C_2H_5 shift which converts **8** into **6** must occur more rapidly than the apparently favourable cyclization to **9**. A similar argument suggests strongly that the 1,2-H shift by which **8** may revert to **4** must also take place more readily than ring closure to **9**. These trends may reflect the energetics of the relevant steps: both the 1,2-C_2H_5 and the 1,2-H shift in **8** lead to species (**6** and **4**, respectively) that are lower in energy than **9**. However, there may also be an additional effect discriminating against formation of **9** because the conformation of **8** that is best suited

to cyclization to **9** is one in which the C-O bond and the unoccupied p-orbital lie in a common plane. This conformation is one which maximizes the unfavourable interaction between the hydroxyl substituent and the unoccupied p-orbital [18]. In contrast, the conformations appropriate for the 1,2-C_2H_5 or the 1,2-H shifts bring the substituent that is about to migrate, rather than the C-O bond, into a common plane with the unoccupied p-orbital. Moreover, it is one of these rotamers which should be initially formed by the 1,2-H shift which converts **4** into **8**. These conformational considerations may also favour the 1,2-C_2H_5 or the 1,2-H shifts over cyclization to form protonated oxiranes.

The major conclusions concerning the mechanism of C_3H_6 loss from **4** and **5** are reinforced by the behaviour of the higher homologue $(CH_3CH_2CH_2)_2C{=}OH^+$, **14**. This species is known [33] to lose predominantly H_2O and C_3H_6, together with smaller amounts of C_4H_8 and "C_3H_8O" (actually sequential elimination [34] of H_2O and C_3H_6). Expulsion of C_4H_8 entails skeletal rearrangement and could occur via reorganization of the carbon framework or by migration of the oxygen function. The loss of C_3H_6 and C_4H_8 with high selectivities (>99% and >95%, respectively), Table 9.3, establishes that the former is the case, Scheme 9.5. Any migration of the oxygen function from C-4 to C-3 or C-5 via protonated oxiranes would result in $C_3{}^{13}CH_8$ elimination from $(CH_3CH_2CH_2)_2{}^{13}C{=}OH^+$. Similarly, any involvement of protonated oxetanes would lead to C_5H_{10} loss from $(CH_3CH_2CH_2)_2C{=}OH^+$ and $C_4{}^{13}CH_{10}$ elimination from $(CH_3CH_2CH_2)_2{}^{13}C{=}OH^+$. However, none of these precesses is observed to a measurable extent.

Table 9.3. Reactions of metastable $C_7H_{15}O^+$ and $C_6{}^{13}CH_{15}O^+$ ions

	Neutral species lost											
	H_2O		C_3H_6		$C_2{}^{13}CH_6$		C_4H_8		$C_3{}^{13}CH_8$		C_3H_8O	
Ion structure	RA[a]	T[b]	RA	T	RA	T	RA	T	RA	T	RA	T
$(CH_3CH_2CH_2)_2C{=}OH^+$	59[c]	3.1	31.0[c]	2.4			8.0[c]	2.2			2[c]	~3
$(CH_3CH_2CH_2)_2{}^{13}C{=}OH^+$	60[c]	3.2	32.1[c]	2.4	< 0.5		7.5[c]	2.5	< 0.5		~2[c]	

[a,b,c] See footnotes to Table 9.1; RA values for propene losses are quoted to one decimal place simply in order to avoid introducing rounding errors.

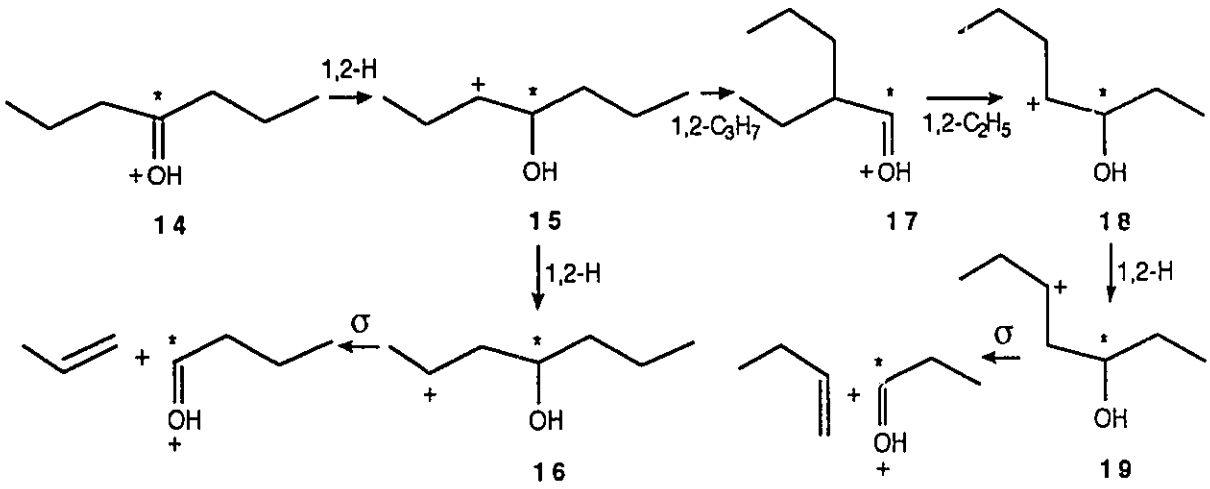

[* Denotes ^{13}C]

Scheme 9.5

Conclusions

The skeletal isomerizations which often precede alkene expulsion from oxonium ions of general structure $R_1R_2C{=}OH^+$ normally involve reorganization of the carbon

framework via 1,2-H and 1,2-alkyl shifts. Migration of the oxygen function rarely, if ever, occurs via protonated oxiranes and only occasionally via protonated oxetanes. The 1,2-alkyl shifts in the α-hydroxy cations occur more rapidly than cyclization to the protonated oxiranes, even though formation of such three-membered rings is often considered to be a kinetically facile process. Since the enthalpies of formation of protonated oxiranes are lower than those of the relevant α-hydroxy cations, this finding suggests strongly that 1,2-H and 1,2-alkyl shifts are kinetically preferable to cyclization in these systems.

References

1. R.D. Bowen, A.W. Colburn and P.J. Derrick, *Org. Mass Spectrom.* **25**, 509 (1990), and references therein.
2. A.N.H. Yeo and D.H. Williams, *J. Am. Chem. Soc.* **93**, 395 (1971).
3. C.W. Tsang and A.G. Harrison, *Org. Mass Spectrom.* **7**, 1377 (1973).
4. A.W. Seigel, *Org. Mass Spectrom.* **3**, 1417 (1970).
5. C.W. Tsang and A.G. Harrison, *Org. Mass Spectrom.* **5**, 877 (1971).
6. R.D. Bowen, J.R. Kalman and D.H. Williams, *J. Am. Chem. Soc.* **99**, 5481 (1977).
7. J.L. Holmes, R.T.B. Rye and J.K. Terlouw, *Org. Mass Spectrom.* **14**, 606 (1979).
8. D.J. McAdoo and C.E. Hudson, *Int. J. Mass Spectrom. Ion Processes* **88**, 133 (1989).
9. R.D. Bowen, D.H. Williams, G. Hvistendahl and J.R. Kalman, *Org. Mass Spectrom.* **12**, 721 (1978).
10. G. Hvistendahl, R.D. Bowen and D.H. Williams, *J. Chem. Soc., Chem. Commun.* 29, (1976).
11. A.G. Harrison, T. Gaumann and D. Stahl, *Org. Mass Spectrom.* **18**, 517 (1983).
12. S.J.A. Curtis and A.G. Harrison, *J. Am. Soc. Mass Spectrom.* 1, 310 (1990).
13. H.E. Audier, R. Flammang, A. Maquestiau and A. Milliet, *Nouv. J. Chem.* **4**, 531, (1980).
14. J.V. Headley and A.G. Harrison, *Can. J. Chem.* **63**, 609 (1985).
15. S.G. Lias, J.E. Bartmess, J.F. Liebman, J.L. Holmes, R.D. Levin and W.G. Mallard, *J. Phys. Chem. Ref. Data* **17**, Suppl. 1 (1988).

16. The term "critical energy" corresponds conceptually to the expression "activation energy", see: A. Maccoll, *Org. Mass Spectrom.* **15**, 109 (1980).
17. R.G. Cooks, J.H. Beynon, R.M. Caprioli and G.R. Lester, *Metastable Ions*. Elsevier, Amsterdam (1973).
18. L. Radom, J.A. Pople and P.V.R. Schleyer, *J. Am. Chem. Soc.* **94**, 5935 (1972).
19. R.D. Bowen and D.H. Williams, *Org. Mass Spectrom.* **12**, 475 (1977).
20. F.W. McLafferty and I. Sakai, *Org. Mass Spectrom.* **7**, 971 (1973).
21. For reviews of the PEP approach, see: D.H. Williams, *Acc. Chem. Res.* **10**, 280 (1977); D.H. Williams, *Philos. Trans. R. Soc. London Ser. A* **293**, 117 (1977); R.D. Bowen, D.H. Williams and H. Schwarz, *Angew. Chem. Int. Edn Eng.* **18**, 451 (1979); R.D. Bowen and D.H. Williams, in *Rearrangements in Ground and Excited States*, Ed. by P. Demayo. Academic Press, New York, Volume 1, Chapter 2 (1980).
22. R.D. Bowen and A.G. Harrison, *Org. Mass Spectrom.* **16**, 159 (1981).
23. F.P. Lossing and G.P. Semeluk, *Can. J. Chem.* **48**, 955 (1970).
24. F.P. Lossing and J.C. Traeger, *Int. J. Mass Spectrom. Ion. Phys.* **19**, 9 (1976).
25. F.P. Losssing, *J. Am. Chem. Soc.* **99**, 7526 (1977).
26. F.P. Lossing and J.L. Holmes, *J. Am. Chem. Soc.* **106**, 6917 (1984), and references cited therein.
27. S.G. Lias, J.F. Liebman and R.D. Levin, *J. Phys. Chem. Ref. Data* **13**, 695 (1988).
28. J.D. Cox and G. Pilcher, *Thermochemistry of Organic and Organometallic Compounds*. Academic Press, New York (1970).
29. J.B. Pedley, R.D. Naylor and S.P. Kirby, *Thermochemical Data of Organic Compounds*, 2nd Edition. Chapman and Hall, London (1986).
30. J.L. Franklin, *Ind. Eng. Chem.* **41**, 1070 (1949); *J. Chem. Phys.* **21**, 2029 (1953).
31. S.W. Benson, *Thermochemical Kinetics*, 2nd Edition. Wiley, New York (1986).
32. J.L. Holmes, M. Fingas and F.P. Lossing, *Can. J. Chem.* **59**, 80 (1981); **60**, 2365 (1982).
33. U.I. Zahorszky, *Org. Mass Spectrom.* **17**, 253 (1982).
34. S. Chowdhury and A.G. Harrison, *Org. Mass Spectrom.* **23**, 79 (1988).

CHAPTER 10

Isomerization and Dissociation Processes of Protonated β-Propiolactone and Related $C_3H_5O_2^+$ Isomers : A Combined Experimental and Theoretical Study

Introduction

Carbenium ions stabilized by electron-donating groups have been extensively studied in solution and in the gas phase [1]. Such species are readily generated in the rarefied gas phase of a mass spectrometer [1b,c] where one-electron oxidation of solitary organic molecules may yield stabilized carbenium ions as dissociation products either directly or following (extensive) isomerization. For example, the m/z 87

This work has been published under the above title:

D. Suh, C.A. Kingsmill and J.K. Terlouw, *Org. Mass Spectrom.*, **28**, 1270 (1993).

$C_4H_7O_2^+$ ion formed by the loss of an alkyl group R$^\bullet$ from ionized aliphatic esters $CH_3CH(R)COOCH_3$ [1b] does not have the structure $CH_3CHCOOCH_3^+$ expected from a direct bond cleavage but rather $CH_2{=}CHC(OH)OCH_3^+$ [1b]:

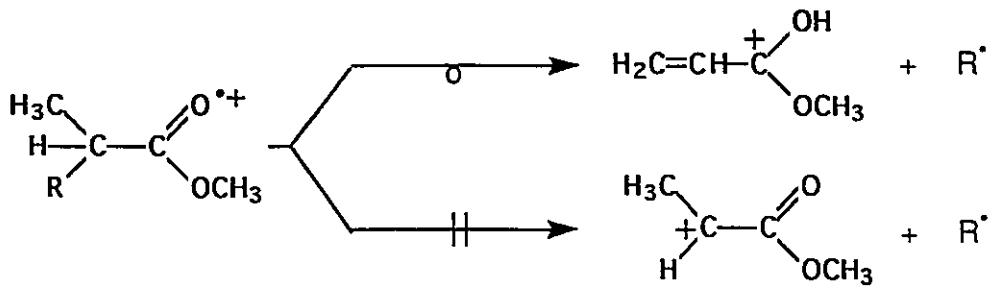

The stabilization brought about by three electron-donating groups in $CH_2{=}CHC(OH)OCH_3^+$ is the major driving force. The concept of carbenium ion stabilization by charge dispersal has a proven reputation in organic chemistry: for example, it neatly rationalizes the observation that amides protonate at oxygen, not at nitrogen [2].

In recent years [1], there has been considerable interest in carbenium ions substituted by an electron-withdrawing group, such as in $CH_3CHCOOCH_3^+$, and despite their elevated enthalpies [1d] and high reactivities, a wide variety of such ions (also referred to as "destabilized" [1d,3] carbenium ions) have been generated and even used in organic syntheses [1d]. Creary [1d], in a review on electronegatively substituted carbocations, indicated that such species are attractive intermediates in organic reactions and that they may lie unsuspected. It is noted that the lone pair of the α-carbonyl oxygen atom in ions such as $CH_3CHCOOCH_3^+$ may form a bond with the putative carbenium centre leading to a three-membered ring isomer, $CH_3(H)\overline{C\text{-}O\text{-}C}OCH_3^+$, if the stabilization by charge dispersal can outweigh the destabilizing ring strain energy.Theoretical calculations indicate that this is the case

for the prototype species $^{+}CH_2COOH$, a "capto" carbenium ion which collapses [1d,4] to $\overline{CH_2\text{-}O\text{-}COH}^{+}$, a "dative" carbenium ion. Species such as $CH_3CHCOOCH_3^{+}$, a carbenium ion substituted by an electron-donating and an electronegative substituent, have therefore been referred to as "captodative" carbenium ions [5].

As mentioned above, "destabilized" carbenium ions are not readily generated in the mass spectrometer because rearrangement processes lead to more stable isomers. However, it has been shown [3-6] that substitution of the alkyl group R by iodine can lead to the desired "destabilized" carbenium ion by oxidative C-I bond cleavage. Two explanations have been given for this observation: the barrier for the rearrangement reactions leading to a more stable isomer may be raised by iodine substitution [3b] or the C-I bond may be weaker than the C-C bond, thus favouring direct C-I cleavage [6].

Using this method, the carboxypropylium ions $CH_3CH_2CHCOOH^{+}$ and $CH_3CHCH_2COOH^{+}$ has been previously generated [5] and it has been found, inter alia, that they are key intermediates in the breakdown of protonated β-butyrolactone to $CH_3C{=}O^{+} + CH_3CHO$ and to $CH_3CHOH^{+} + CH_2CO$ via the complex $[CH_3CH{=}O\cdots H\cdots CH_2{=}C{=}O]^{+}$.

In a recent thermolytic study [7], it was concluded that, in solution, protonation of β-propiolactone (and acrylic acid) does not lead to fragmentation but to the equilibrium

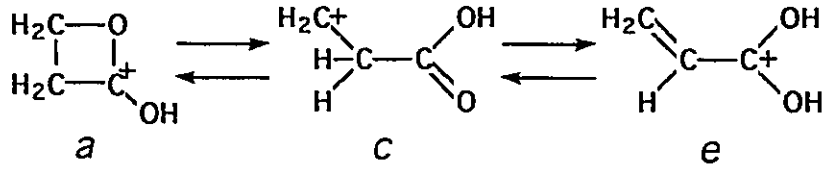

a *c* *e*

It was further noted in this study that in the mass spectrometer and under conditions of chemical ionization ions *a* do dissociate, namely to m/z 55 (by dehydration) and to m/z 45 and 43. The structures $HOC{=}O^{+}$ and $CH_2{=}COH^{+}$ were assigned to the latter products

for no apparent reason other than that they can be generated from *a* by [2+2] cycloreversions. However, it had been established [5] that the methyl homologue of *a*, $CH_3\overline{CHCH_2OC}OH^+$, does not spontaneously undergo cycloreversions: by combining results from a variety of mass spectrometry-based techniques it was established that under collision free conditions ions $CH_3\overline{CHCH_2OC}OH^+$ do not produce $HOCO^+$ but the isobaric species CH_3CHOH^+ and that they do not generate $CH_2{=}COH^+$ but its more stable isomer CH_3CO^+. This raises the question of whether the products from *a* are indeed $HOCO^+$ and $CH_2{=}COH^+$ and thus, it was decided to examine in detail the unimolecular (spontaneous and activated) chemistry of protonated β-propiolactone by mass spectrometry-based experiments and *ab initio* molecular orbital calculations. It will be shown that in the rarefied gas-phase ions *a* and *e* do not interconvert and that therefore the equilibrium observed in solution does not proceed as shown. Moreover, metastable ions *a* do not undergo cycloreversions but instead they spontaneously dissociate into $CH_3C{=}O^+ + CH_2O$, $CH_3CHOH^+ + CO$, $CH_2{=}CH\text{-}C{=}O^+ + H_2O$ and $C_2H_5^+ + CO_2$. These dissociations are preceded by extensive isomerization reactions which involve ions akin to the carboxy ethylium ions $^+CH_2CH_2COOH$,*c*, and $CH_3CHCOOH^+$,*d*, and the carbonyl cation $HOCH_2CH_2\text{-}C{=}O^+$,*f*.

Results and discussion

Formation of $C_3H_5O_2^+$ ions

Scheme 10.1 shows the $C_3H_5O_2^+$ ions which were considered in the context of the isomerization *(b-f)* and dissociation *(g-l)* behaviour of protonated β-propiolactone, *a*, in the gas-phase. Also given are the precursor molecules which were used to generate the various $C_3H_5O_2^+$ isomeric ions. The geometries of the $C_3H_5O_2^+$ isomers and transition states are shown in Figure 10.1.

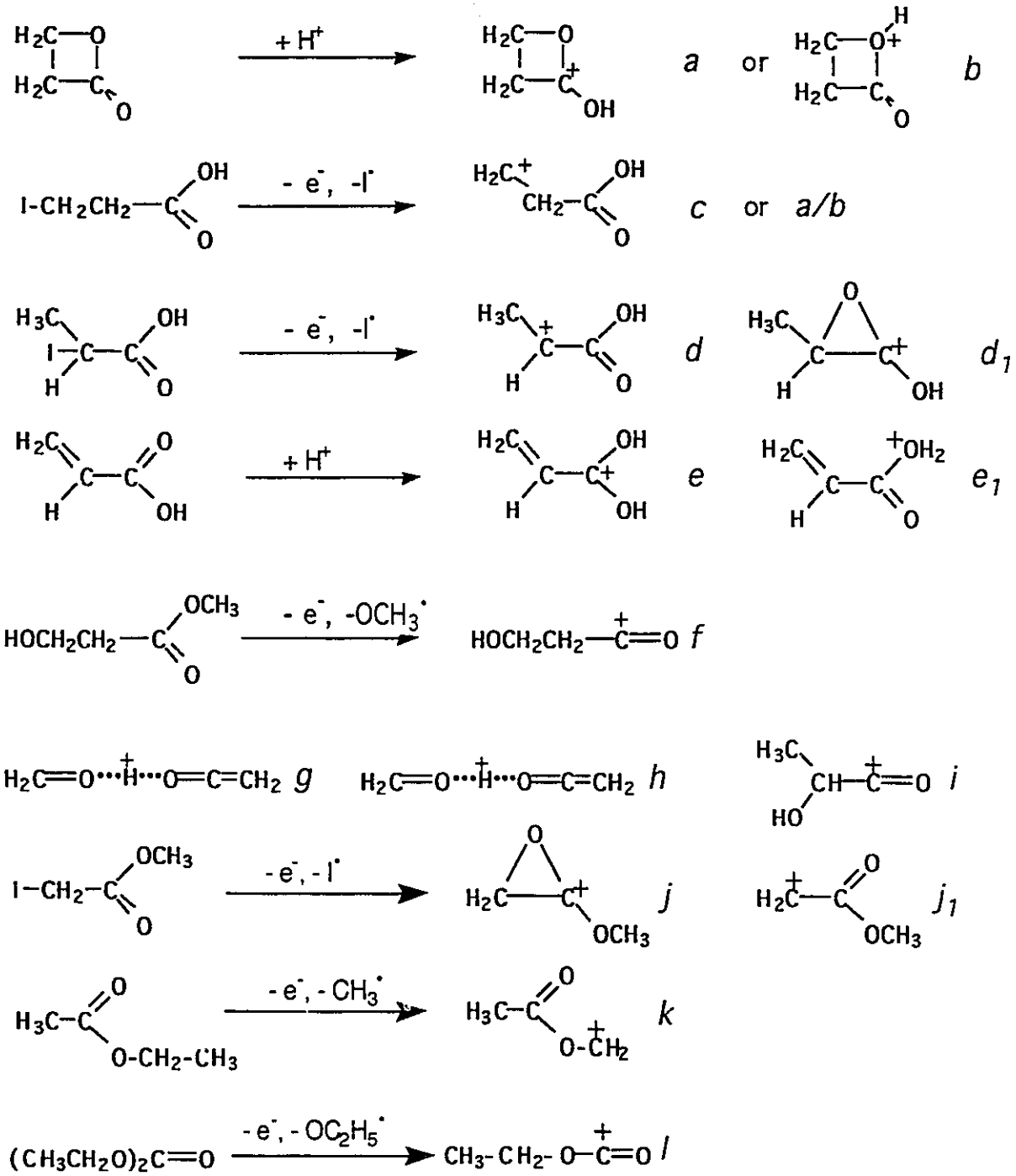

Scheme 10.1

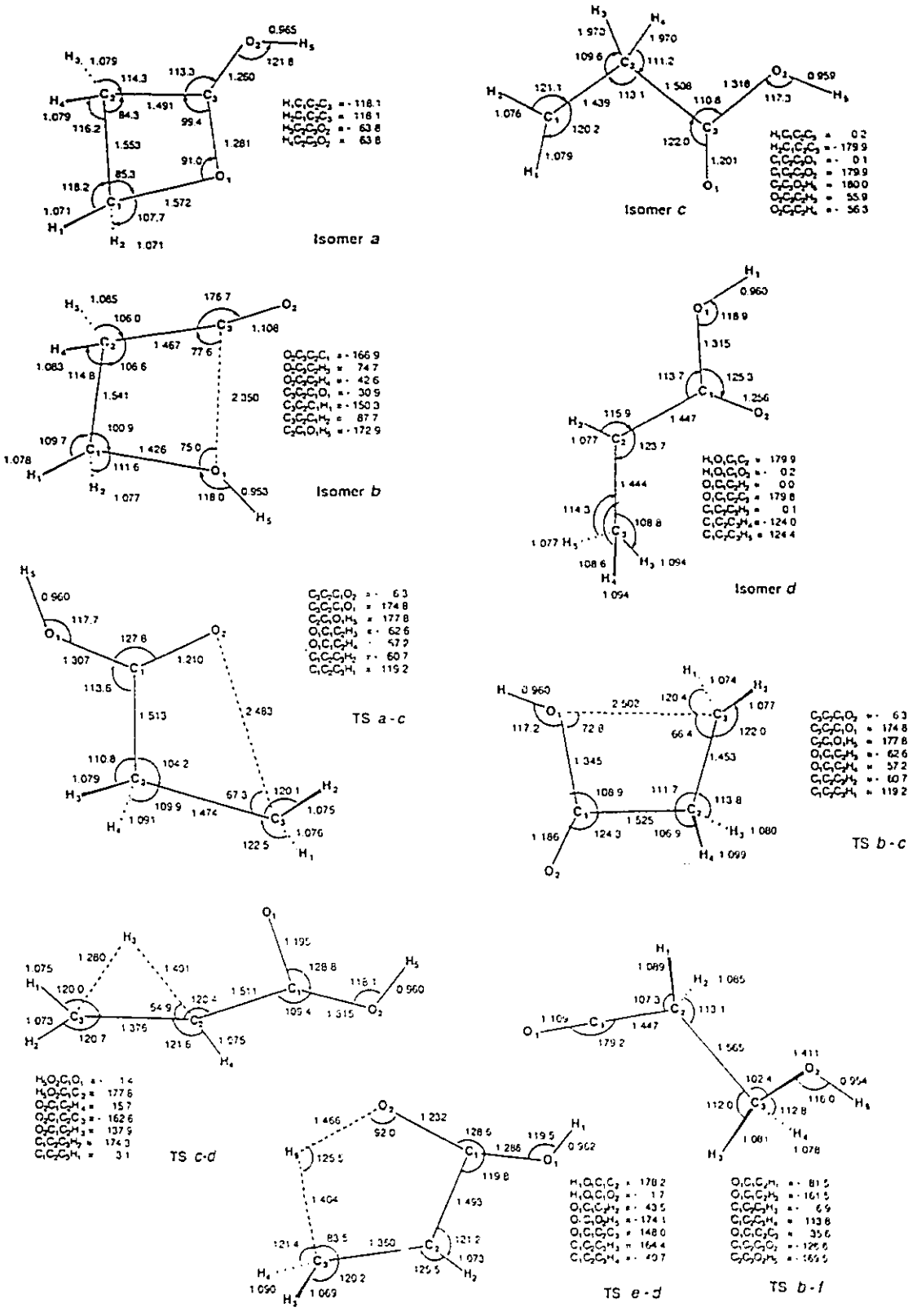

Figure 10.1. Geometries of $C_3H_5O_2^+$ isomeric ions and some transition states of the MP3/6-31G*//4-31G level of theory.

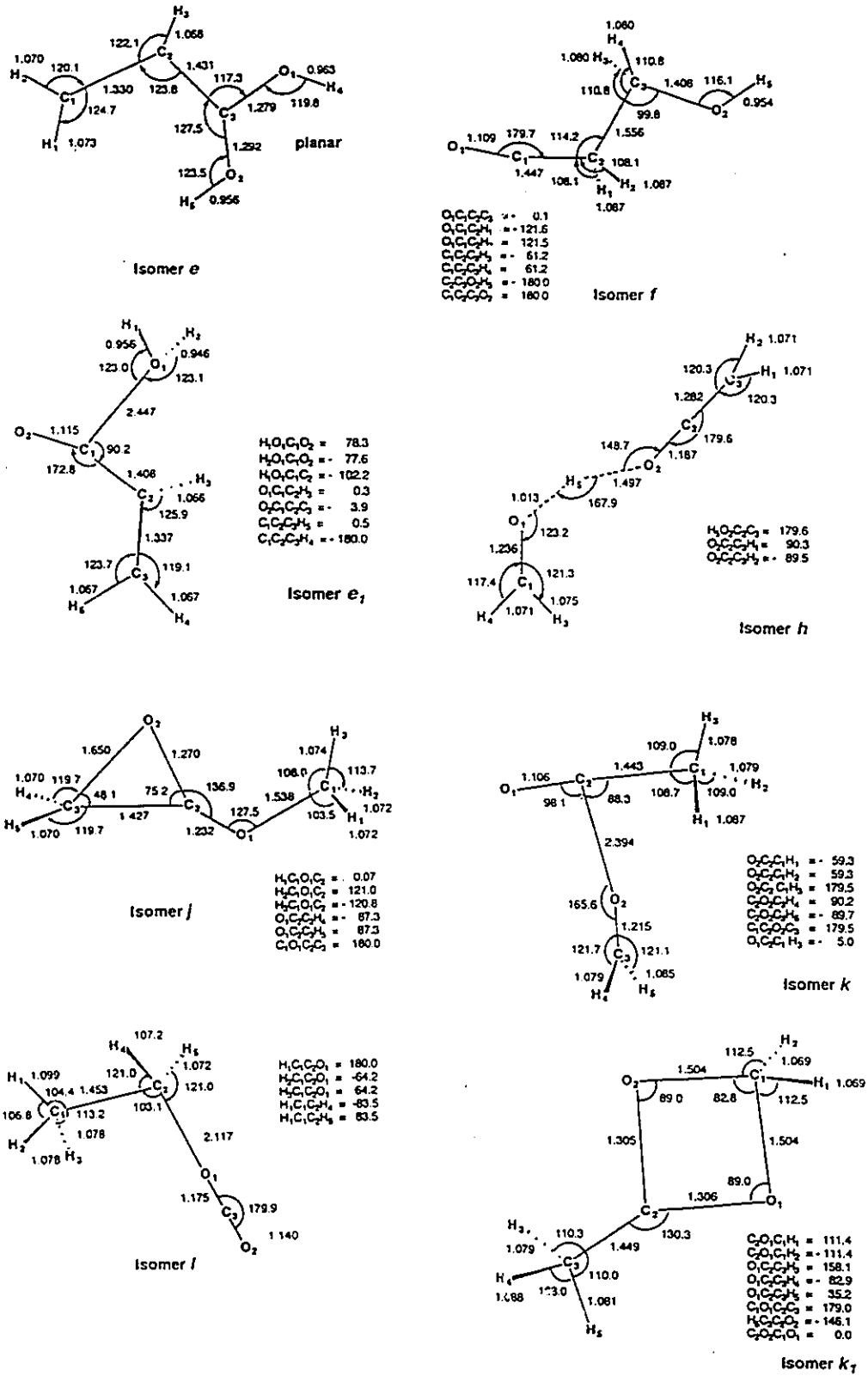

Figure 10.1. Continued.

There are no literature data available on the proton affinities or the site of protonation of lactones in the gas-phase. Considering that in solution the keto group is the favoured site for protonation [8], it seems likely that the gas-phase protonation of β-propiolactone yields ions *a* rather than *b* . In the next section, this question will be examined and evidence that this is indeed the case will be presented.

The carboxyethylium ions *c* and *d* (or d_1) might be generated by simple bond fission in 3- and 2-iodopropionic acid, respectively. However, if the loss of I$^{\bullet}$ from 2-iodopropionic acid involves anchimeric assistance [6] of either the keto or the hydroxyl group the resulting product ions will be *a* or *b* .

Protonation of acrylic acid in the gas phase [9] (and in solution [10]) occurs at the keto group, resulting in the exclusive generation of ions *e* ,not e_1 . The $C_3H_5O_2^+$ ions generated by loss of Cl$^{\bullet}$ and Br$^{\bullet}$ from 3-chloro- and 3-bromopropionic acid respectively (this work), yield metastable ion (MI) , CA and NR spectra which are indistinguishable from those of protonated acrylic acid and thus these precursor molecules can also be used as a convenient source for the formation of ions *e*. Loss of $C_2H_3^{\bullet}$ from CH_2=CH-$COOC_2H_5^{\bullet+}$, ionized ethyl acrylate, also cleanly yields ions *e* and not *l*. The latter ion can, however, be generated from diethyl carbonate, as is indicated in the Scheme 10.1.

The proton-bound species *g* and *h* were only considered computationally. Attempts to generate ion *i*, CH_3-C(H)(OH)-C=O$^+$, a likely intermediate in the loss of CO (see below), were not successful. One of the precursor molecules examined, 2-hydroxyhexan-3-one, could yield the desired ion by loss of $C_3H_7^{\bullet}$, but unfortunately the molecular ions appear to lose $CH_3C{=}O^{\bullet}$ instead to produce $C_4H_9O^+$.

MI, CA and NR spectra of ions a-f

Table 10.1 and Fig. 10.2 give the MI, CA and NR spectra of ions *a-f*. MI and CA spectra of the other isomers, *j-l*, were also obtained but since these ions are not immediately related to the isomerization chemistry of ion *a*, these data will be discussed later. It follows even from a cursory inspection of the CA and NR spectra

Table 10.1. Metastable Ion [MI] Spectra of the $C_3H_5O_2^+$ isomers of the proposed structures *a-f* and *j-l* generated by the reactions shown in Scheme 10.1.

Proposed Ion structure	m/z 55 (-H_2O)		m/z 45 (-CO)		m/z 43 (-CH_2O)		m/z 29 (-CO_2)	
	I (%)	$T_{0.5}$ (meV)[a]	I (%)	$T_{0.5}$ (meV)[b]	I (%)	$T_{0.5}$ (meV)	I (%)	$T_{0.5}$ (meV)
a	**30**	590	**100**	170	**35**	35	**20**	150
c	**90**	520	**100**	120	**60**	30	**60**	110
d	**100**	520	**80**	130	**45**	30	**35**	110
e	**100**	140						
f	**65**	530	**100**	140	**35**	30	**20**	110
j			**15**	870	**100**	890		
k					**100**	0.5		
l	**5**[c]		**100**	15			**10**	≤ 0.5

[a] The metastable peaks of ions *a*, *c*, *d* and *f* contain a minor narrow component of varying intensity (≤ 5 %, by area) which probably results from collision induced dissociations. The KER values given refer to the major broad component. [b] The metastable peaks of ions *a*, *c*, *d* and *f* consist of two unresolved components of comparable abundance. [c] This signal ($T_{0.5}$ = 35 meV) is probably due to a $C_4H_9O^+$ impurity [11].

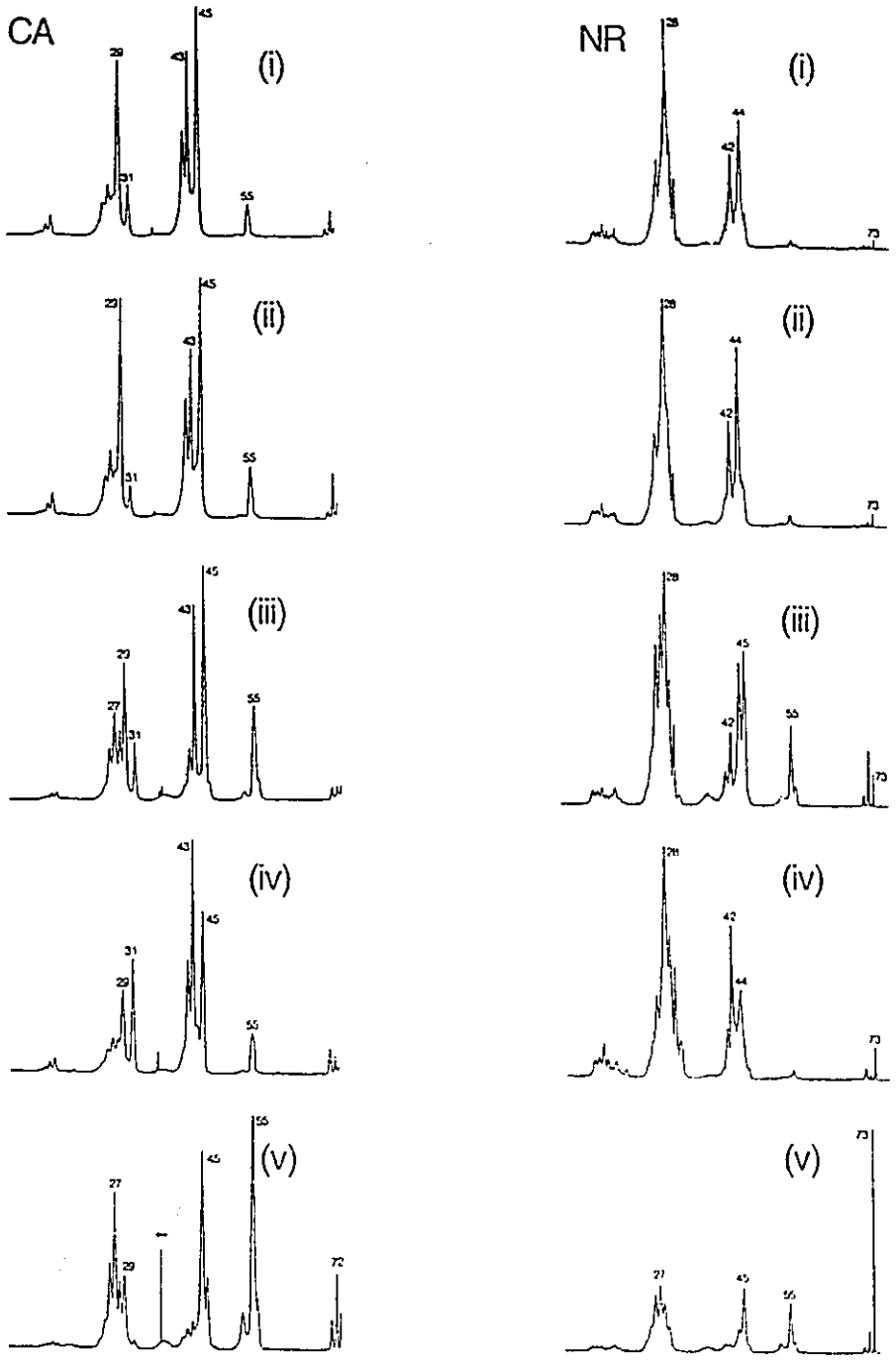

Figure 10.2. Collisional activation (CA) spectra (left) and neutralization-reionization (NR) spectra (right) of the $C_3H_5O_2^{+\bullet}$ ions (see Scheme 11.1) generated from (i) β-propiolactone; (ii) ICH_2CH_2COOH; (iii) $CH_3CH(I)(COOH$; (iv) $HOCH_2CH_2COOCH_3$ and (v) CH_2=CHCOOH + H^+.

shown in Fig. 10.2 that the spectra of ion *e* are distinctly different from those of the other (proposed) isomers. Protonation of β-propiolactone (either self-protonation or protonation with $CH_3OH_2^+$) produces CA and NR spectra which are very close to those of the product ion generated by loss of I$^\bullet$ from 3-iodopropionic acid, which indicates that ions of the same structure are generated. The spectra of ions proposed to have the structures *d* (*d*$_1$) and *f* are clearly different from these.

The MI spectrum of ion *e* is unique in that it shows one dissociation only, *viz.*, loss of H_2O, which is characterized by a kinetic energy release (KER), $T_{0.5}$, of 140 meV. The other isomers also lose H_2O but with much larger KERs, $T_{0.5}$ = 520-590 meV (see Table 10.1) and, moreover, they undergo three other competing processes leading to ions at m/z 45, 43 and m/z 29, respectively. From double collision experiments, it follows that these ions are CH_3CHOH^+, $CH_3C{=}O^+$ and $C_2H_5^+$, respectively. These observations indicate that the dissociation chemistry of ion *a* is not related to that of ion *e* and that ion *a* may interconvert with *b, c, d* and *f* prior to its spontaneous unimolecular dissociations. Thus, these spectra are analysed in more detail in conjunction with the results of *ab initio* calculations and appearance energy (AE) measurements.

Theoretical results: relative energies for various $C_3H_5O_2^+$ ions and the principal features of the potential energy surface for ions a-f

Table 10.2 lists the calculated UMP3/6-31G*// 4-31G energies, the ZPVEs and the total relative energies of the various $C_3H_5O_2^+$ isomers studied and the transition states associated with the isomerization processes between ions *a* - *f*. The anchor point is $\Delta H_f(e)$ = 385 kJ/mol.

Table 10.2 Total energies (Hartrees), zero-point vibrational energies [ZPVE] and relative calculated E[rel][a] energies (kJ/mol) for isomers and components of the $C_3H_5O_2^+$ system.

Species	UHF/4-31G	6-31G*//4-31G	UMP3/6-31G*// 4-31G	ZPVE	E[rel][a]	E[exp][b]
Ion						
a	-265.54210	-265.95708	-266.69440	227	23	
b	-265.55223	-265.95206	-266.68718	223	39	
c	-265.52018	-265.91701	-266.63994	215	166	(88)[c]
d	-265.51436	-265.90478	-266.63942	211	153	145[d]
e	-265.57886	-265.97065	-266.70263	224	0	0
e_1	-265.55909	-265.94541	-266.67936	213	50	
f	-265.53902	-265.94312	-266.67784	221	62	74[e]
h	-265.52018	-265.90866	-266.63803	208	154	157[f]
j	-265.47516	-265.89822	-266.63616	218	169	174[g]
k	-265.54679	-265.95300	-266.68105	209	42	48[h]
k_1	-265.50726	-265.94060	-266.68060	222	55	
l	-265.54945	-265.95978	-266.67725	210	53	
Isomerization TS						
a-c	-265.51305	-265.91301	-266.63385	216	173	
b-c	-265.51477	-265.90964	-266.63446	215	171	
b-f	-265.53619	-265.94021	-266.67543	221	68	
c-d	-265.50054	-265.90987	-266.64491	210	139	
e-d	-265.46549	-265.86718	-266.61779	206	205	
Dissociation products						
CH_2=CH-C=O$^+$ + H_2O	-265.52542	-265.09992	-266.64910	203	121	124

[a]The relative calculated energies include scaled (0.9) zero-point vibrational contributions. [b] Relative to ion *e*, ΔH_f = 385+10 kJ/mol [9,12a], energies for dissociation products from Ref. 12. [c] See text, AE (m/z 73) ICH_2CH_2COOH = 9.92 eV; ΔH_f (acid) = -378 kJ/mol [12b]; ΔH_f (I•) = 107 kJ/mol [12a]; [d] AE (m/z 73) $CH_3C(H)(I)COOH$ = 10.40 eV, ΔH_f (acid) = -368 kJ/mol [est. +10 kJ/mol, from ΔH_f (CH_3COCH_3) - ΔH_f (ICH_2COCH_3) + ΔH_f (CH_3CH_2COOH): (-131) - (-217) + (-454) = -368 kJ/mol [12c]], ΔH_f (I•) = 107 kJ/mol [12a].[e] AE (m/z 73) $CH_3CO(CH_2)_2OH$ =10.34 eV, ΔH_f (ketone) = -389 kJ/mol [12b], ΔH_f (CH_3•) = 146 kJ/mol [12a].[f] Estimate, see text, based on the relationship given in Ref. 9. [g] AE (m/z 73) ICH_2COOCH_3 = 10.30 eV, ΔH_f (ester) = - 328 kJ/mol [12c], ΔH_f (I•) = 107 kJ/mol [12a]. [h] AE (m/z 73) $CH_3COOC_2H_5$ =10.60 eV, ΔH_f (ester) = - 444 kJ/mol [12a], ΔH_f (CH_3•) = 146 kJ/mol [12a].

It is shown by the calculations show that the preferred site of protonation of β-propiolactone is the carbonyl group, albeit that protonation at the ether oxygen is only slightly more energy demanding. From $\Delta H_f(a)$ and the known ΔH_f of β-propiolactone, - 283 kJ/mol [12a], this strained lactone is predicted to have a proton affinty (PA) of 840 kJ/mol. This value seems reasonable considering that the experimental PA of cyclopentanone is 832 kJ/mol [12a]. Comparison of the computed energies with the available experimental values (Table 10.2) shows that agreement between experiment and theory is generally good, except for the ΔH_f for ion *c*. The AE value for m/z 73 in ICH_2CH_2COOH, 9.92 eV, leads to ΔH_f ('*c* ') = 473 kJ/mol, whereas theory predicts a much higher value, 551 kJ/mol. Note that the derived experimental ΔH_f value does not correspond with any of the investigated isomeric structures and that the CA spectrum of the ion is very close to that of protonated β-propiolactone. The 3rd ffr CA mass spectrum of the m/z 73 ions generated by either the metastable or the collision induced loss of I$^\bullet$ from $ICH_2CH_2COOH^{\bullet+}$ appears to be very close to that of 4 keV source-generated ions. This indicates that mostly ions of a single structure are generated.

Therefore, it is proposed that the measured AE of the m/z 73 ion from ICH_2CH_2COOH does not correspond with the threshold generation of a stable $C_3H_5O_2^+$ isomer. Rather, it is proposed that loss of I$^\bullet$ from $I\text{-}CH_2CH_2COOH^{\bullet+}$ (largely) yields ions *a* and that the observed AE reflects the height of the barrier for the rearrangement reaction leading to *a*. In this context it is relevant to note that the measured AE (m/z 73) from $Br\text{-}CH_2CH_2COOH$, 10.52 eV, leads to the same ΔH_f (m/z 73) = 477 kJ/mol for the product ion as that found with the iodo compound. In this case, however, the CA mass spectrum leaves no doubt that the daughter ions are "pure" *e* (see Ref. 6 for a rationale), since it is indistinguishable from that of protonated acrylic acid. Again, the AE may reflect the height of the barrier for the rearrangement reaction (leading to *e*) rather than the enthalpy for the treshold generation of a stable ion.

Theory and experiment are in agreement with the proposal that loss of I$^{\bullet}$ from $CH_3C(H)ICOOH^{\bullet+}$ produces ions of structure *d*. As already mentioned, in post-Hartree-Fock (HF)-type calculations [4] the lower homologue of this ion, $^{+}CH_2COOH$, is not a minimum on the potential energy surface, but it collapses to the ring-closed isomer $\overline{CH_2OCO}H^{+}$, a resonance-stabilized, but strained, carbenium ion. The same conclusion is arrived at the (HF) level of theory. Similarly, it is indicated that the carbenium ion $^{+}CH_2C(=O)OCH_3$, ion j_1, generated by loss of I$^{\bullet}$ from $ICH_2C(=O)OCH_3$, is not a minimum but that it collapses to $\overline{CH_2OCO}COCH_3^{+}$, *j*. On the other hand, at this level of theory ion *d* is stable, whereas its ring-closed isomer d_1 is not a minimum. It could be argued (but see the last section) that stabilization by electron donation of the additional methyl group in *d* (a 'captodative' ion) prevents it from adopting the cyclic structure.

Figure 10.3 shows the principal features of the potential energy surface for ions *a-f*. The energy levels for the dissociation products are experimental values and the barriers for the observed dissociations of the metastable ions marked as ≡≡≡ are estimates from metastable peak observations: it was observed (see Table 10.1) that metastable ions *a*, *c*, *d* and *f* undergo four dissociations, viz. loss of H_2O, CO, CH_2O and CO_2, whereas ions *e* show only loss of H_2O with a relatively small kinetic energy release. In Table 10.3 are shown the minimum thermochemical energy levels for the above processes and for reactions not observed in the MI spectra.

Since the direct bond cleavage reaction $i \rightarrow CH_2OH^{+}$ (m/z 31) + CH_2CO is *not* observed, the metastable window must lie below 653 kJ/mol. Also, the mere observation that the above four reactions occur competitively indicates that these reactions have similar TS energies. Since the metastable dissociation leading to the products of highest enthalpies, CH_3CO^{+} + CH_2O, has a $T_{0.5}$ value of only 3 kJ/mol (see Table 10.1), its TS cannot lie far above 544 kJ/mol. In fact, the results are compatible

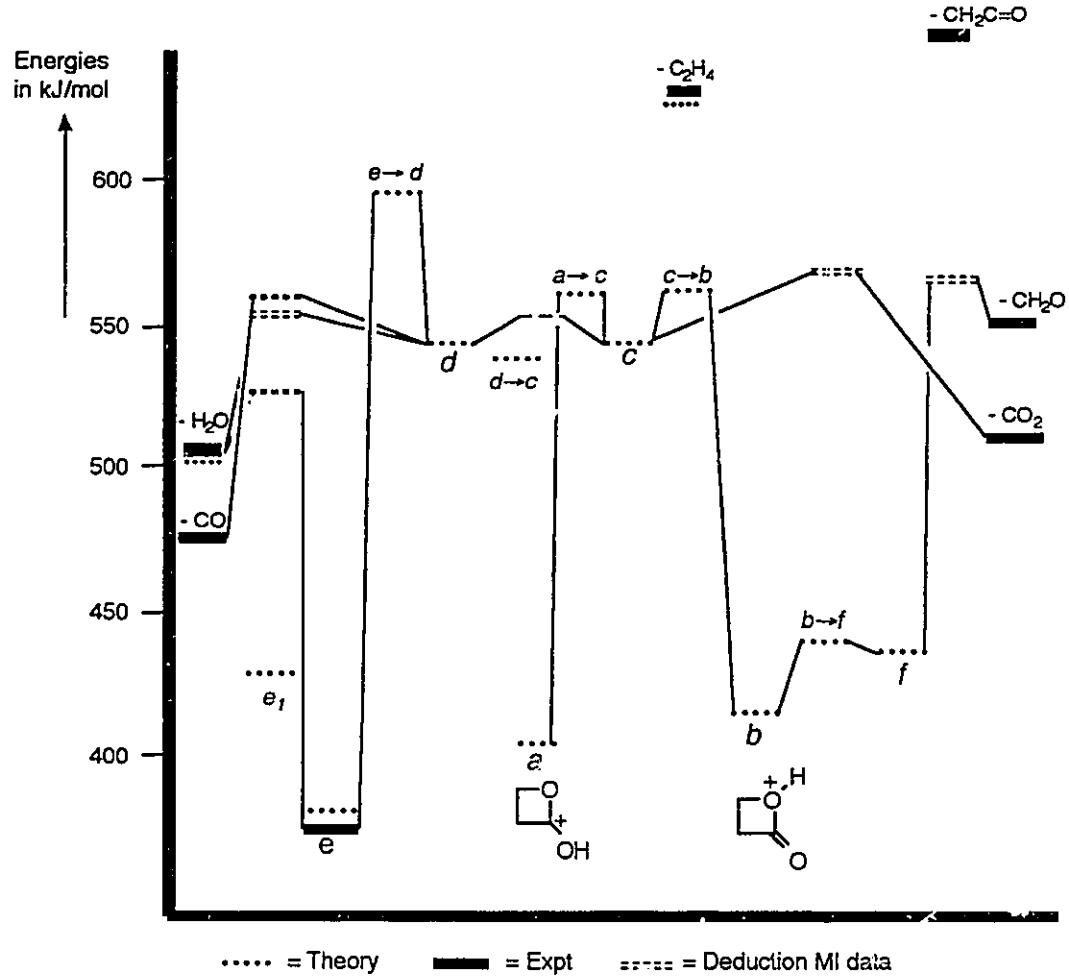

Figure 10.3. Potential energy diagram for the interconversion and dissociation of the $C_3H_5O_2^+$ ions *a-f* (UMP3/6-31G*//4-31G level of theory).

with all dissociation transition states lying close to TS *a*→*c* and TS *b*→*c*, i.e. at ~ 555 kJ/mol, as indicated in Figure 10.3. Since ions *e* do not communicate with the other isomers and since the T value for loss of H_2O therefrom is much smaller than that for the other isomers, the TS for loss of H_2O from *e* must lie below that for the other isomers (see Figure 10.3).

The 4-31G calculations indicate that the electronic energy of TS *c-d* lies 52 kJ/mol above isomer *c* and 36 kJ/mol above isomer *d*. However, when single-point correlation is taken into account, TS *c-d* lies below both isomers. The use of a larger basis set does not solve this problem: the UMP3/6-31G* //6-31G* results show a TS

Table 10.3 Minimum energy requirements[a] for possible dissociation products of the $C_3H_5O_2^+$ ions *a - l*

m/z	Products			$\Sigma\Delta H_f$ (kJ/mol)
55	CH_2=CHCO$^+$	+	H_2O	506
45	HOCO$^+$	+	C_2H_4	644
	CH_3CHOH^+	+	CO	473
	$CH_3OCH_2^+$	+	CO	000
	$CH_2CH_2OH^+$	+	CO	688[b]
	Oxirane + H$^+$	+	CO	581
	CH_2=CH-OH_2^+	+	CO	510
43	CH_3CO^+	+	CH_2O	544
	CH_2=COH$^+$	+	CH_2O	695
29	HCO$^+$	+	CH_3CHO	657
	$C_2H_5^+$	+	CO_2	510
31	CH_2OH^+	+	CH_2CO	653

[a] Values from Ref. [12]. [b] Value from [Ref. 13].

which is still lower in energy than the products when correlation is employed. This problem was further addressed (and satisfactorily solved) by performing MP2/6-31G* geometry optimizations followed by single-point MP3/6-31G* calculations which, in view of the size of the system, were limited to isomers *c*, *d* and *e* (the anchor point) and the transition states *c* → *d* and *d* → *e*. The results will be discussed in detail in the last section, where the question of the 'destabilizing' effect of the α-COOH functionality on the positively charged carbon atom in ion *d* is also addressed.

Finally, it should be noted that the low barrier for the interconversion *b*→*f* predicted by theory and the observation that the CA mass spectrum of *f* shows an intense structure diagnostic peak at m/z 31 (CH_2OH^+) confirms the proposal that the protonation of β-propiolactone (largely) produces ions *a* rather than *b*.

Isomerization and dissociation processes of protonated β-propiolactone

The most apparent conclusion from the metastable ion data (Table 10.1) is that ions *e* having internal energies of at least 124 kJ/mol (the dissociation limit for H_2O loss) do not communicate with any of the ions *a*, *c*, *d* or *f*, in sharp contrast to conclusions drawn from the solution experiments. It is therefore proposed that the observed equilibrium in solution is actually and perhaps not surprisingly an intermolecular process and that it does not involve the high energy isomer *c*. According to the calculations, ions *e* are trapped by the barrier $e \rightarrow d$; indeed, this provides an explanation for an otherwise disconcerting observation, namely that the isotopologue [14] $CH_2{=}CHC(OD)_2^+$ specifically loses D_2O; this had already indicated that the 1,3-hydrogen shift $e \rightarrow e_1$ followed by loss of H_2O has a lower barrier than the 1,4-hydrogen shift $e \rightarrow d$. This high barrier $e \rightarrow d$ is now associated with the elevated ΔH_f of *d* (see Figure 10.3).

The MI data indicate that metastable ions *a*, *c*, *d* and *f* freely interconvert prior to dissociation, i.e.:

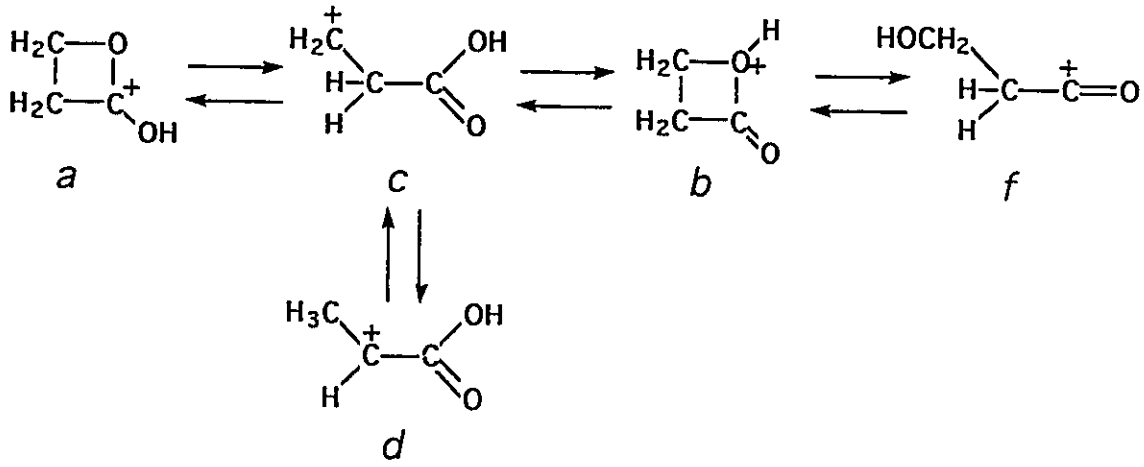

The CA mass spectra of these ions (Fig. 10.2) are dominated by the low-energy processes, but some structure characteristic features are present. The spectrum of ion *d* shows a telltale peak at m/z 56 : loss of $OH^{\bullet}$ to produce $CH_3CH=C=O^{\bullet+}$. This ionized ketene is 35 kJ/mol more stable than its distonic isomer $CH_2CH_2C=O^{\bullet+}$ [15], a possible direct bond-cleavage product of *f*. However, *f* does not undergo loss of $OH^{\bullet}$ but rather dissociates directly by cleavage of the C-C bond to produce CH_2OH^+ (m/z 31) + $CH_2C=O$ (this direct bond cleavage requires 180 kJ/mol less energy than loss of $OH^{\bullet}$ [12a]). The CA spectrum of isomer *e* is unique in that *e* dissociates directly to m/z 46, $^+C(OH)_2$ [16]. Moreover, 3rd ffr collision experiments on the m/z 45 ions in the CA spectrum of *e*-$(OD)_2$ show that these ions are exclusively $HOCO^+$ and $DOCO^+$, respectively, not $C_2H_5O^+$ or $C_2H_4DO^+$ ions.

Evidence that the neutral counterparts of ions *d*, $CH_3CHCOOH^{\bullet}$, and *e*, $CH_2=C(OH)_2^{\bullet}$ are stable species in the gas-phase comes from their NR spectra [(iii) and (v) in Fig. 10.2] which show an intense survivor signal and fragment ions characteristic of the proposed structure. That $CH_3CHCOOH^{\bullet}$ is stable parallels results from ESR spectroscopy, where this radical along with $^{\bullet}CH_2CH_2COOH$ has been detected as a product from the reaction of the peroxomonosulphate anion and Ti(III) with propionic acid [17].

As already mentioned, metastable ions *a*, *d* and *f* dissociate to ions of m/z 55, 45, 43 and 29. The elemental composition and atom connectivity of these product ions were established by CA mass spectrometry of the metastably generated ions : m/z 55 is $CH_2=CH-C=O^+$ [18], m/z 43 is $CH_3C=O^+$ and m/z 29 is $C_2H_5^+$.

As far as the loss of H_2O is concerned, the isotopomers [14] *a*-OD (from the deuteronation of β-propiolactone and loss of $I^{\bullet}$ from $ICH_2CH_2COOD^{\bullet+}$), *d*-OD and *f*-OD almost exclusively (~ 95%) lose HDO (and CH_2O), indicating that hardly any H/D exchange reactions take place, in agreement with the high barrier for *d*→*e*. It is

proposed that loss of water proceeds from e_1 formed from *e* via a 1,3-hydrogen shift or from *d* via a 1,4-hydrogen shift :

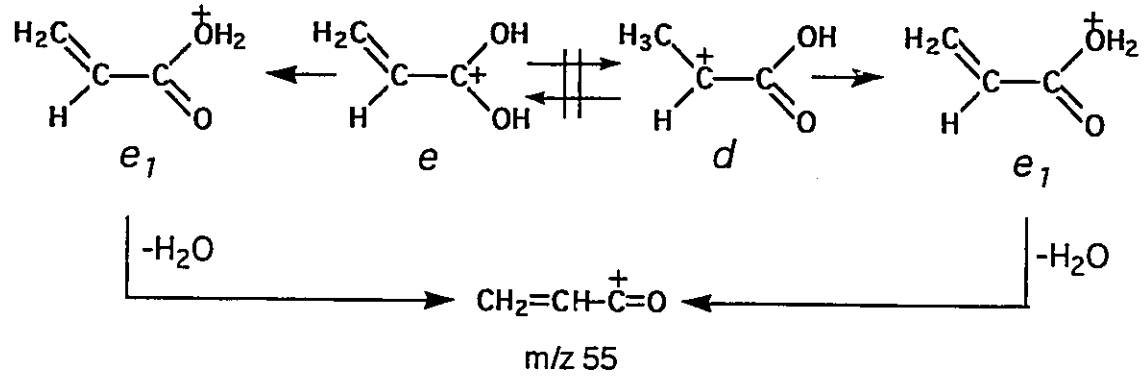

The difference in the transition state energies is reflected in the different $T_{0.5}$ values (see Table 10.1). Considering the geometry of e_1 shown in Fig. 10.1, this ion is best viewed as an ion-dipole complex. The calculated ion-dipole attraction, 288 μ/r^2 kJ/mol (μ in D, r in Å), is 89 kJ/mol, close to the C-OH_2 bond strength,71 kJ/mol, derived from the appropriate data in Table 10.2.

Loss of CO (m/z 45) from *a*, *c*, *d* and *f* is associated with a metastable peak consisting of two unresolved components of comparable abundance. The CA mass spectrum of the metastable peak m/z 73 → m/z 45 from *d* is shown in Figure 10.4(a). The spectrum is compatible with the formation of CH_3CHOH^+, not $CH_2=CHOH_2^+$, but the weak peaks at m/z 17 and m/z 28 indicate that some $HOCO^+$ is cogenerated (by loss of C_2H_4). When collision gas was admitted to the metastable region, relatively more $HOCO^+$ was produced (see Figure 10.4(c)) and so it is concluded that the higher energy loss of C_2H_4 is collision induced. In Figure 10.4(b) is shown the CA mass spectrum of the metastably formed m/z 45 ions from *f*. It can be seen that even less $HOCO^+$ is produced and moreover this spectrum did not change when collision gas

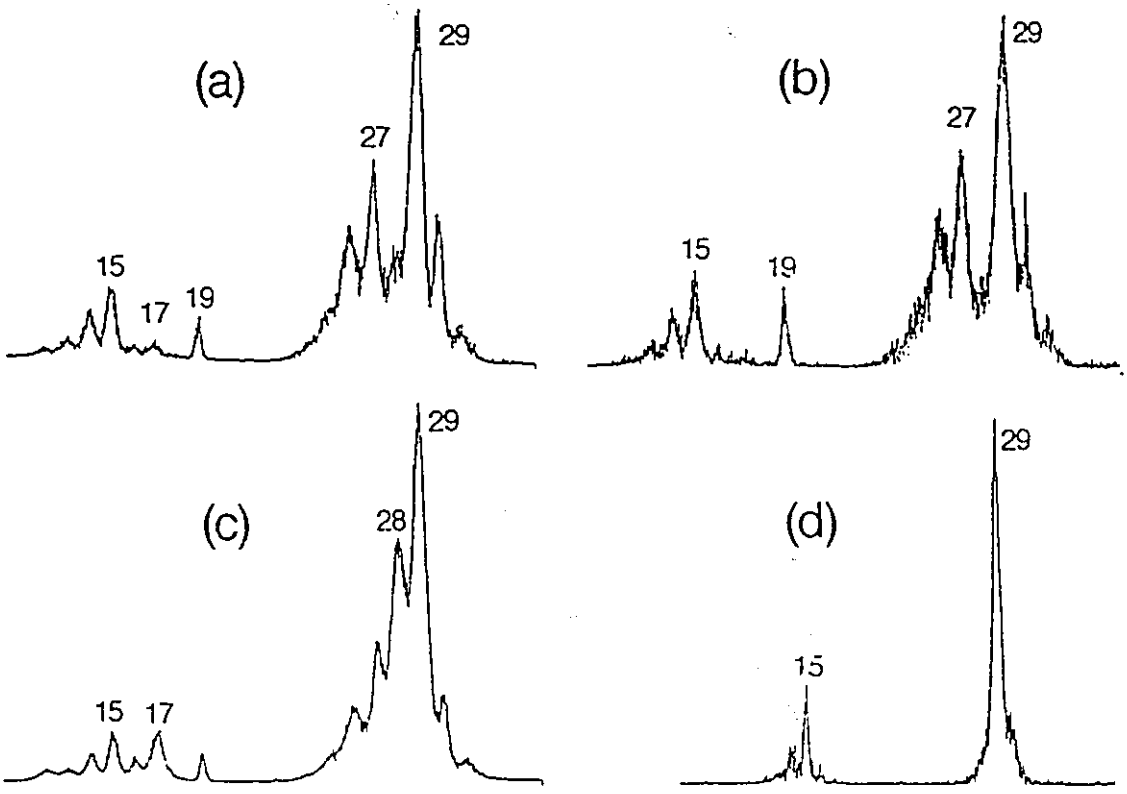

Figure 10.4. CA mass spectra (3rd ffr) of the metastable peak m/z 73 → m/z 45 (2nd ffr) for (a) ions *d* from $CH_3CHICOOH$; (b) ions *f* from $HOCH_2CH_2COOCH_3$; (c) as (a), but collision gas added to the metastable region; (d) ions *j* from ICH_2COOCH_3. For reference spectra of $C_2H_5O^+$ and CHO_2^+, see ref. 30.

was added (Fig. 10.4(b)). The associated metastable peak is nevertheless composite and most likely comprises the same components as those for *a* (generated from either protonation of β-propiolactone or loss of I• from 3-iodopropionic acid) and *d*. Hence the spontaneous loss of CO occurs via two mechanisms: analogous to reactions observed for related α-acylcarbenium ions [3], the reaction leading to the larger T value can be viewed as a 1,2-OH shift followed by C-C cleavage:

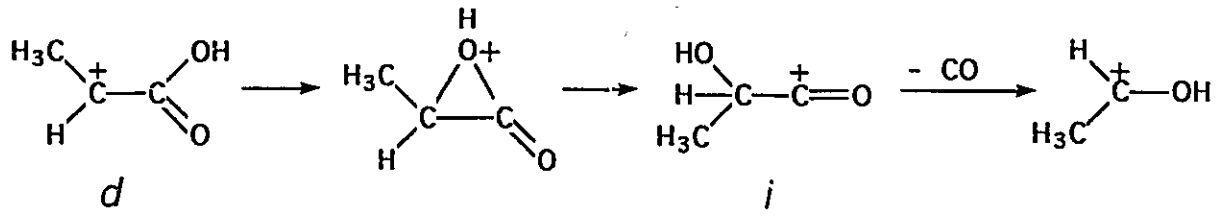

The mechanism associated with the smaller T value is not known. Note that the direct CO loss from *f* producing ions of initial structure $CH_2CH_2OH^+$ has a minimum energy requirement (see Table 10.3) which is far too high for competition. As far as the magnitude of the KER is concerned, the reaction may occur from the ion $CH_3CH_2O\text{-}C{=}O^+$, *l* (see below), but it is difficult to see how this ion can be generated from *a*-*d* or *f*.

The loss of CH_2O (m/z 43) is associated with a Gaussian-shaped metastable peak whose $T_{0.5}$ value is relatively small, 30 meV. This loss is proposed to occur via a mechanism analogous to the loss of CH_3CHO from the $C_4H_7O_2^+$ homologues, i.e. from ions *f* via a formaldehyde-acetylium complex :

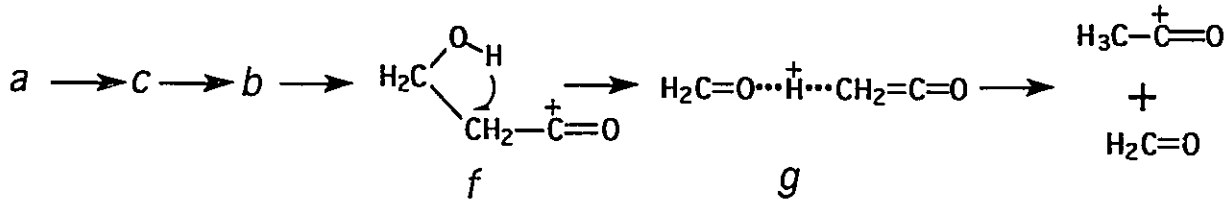

All computational attempts to identify *g* as a viable species failed and hence its participation in the above proposal remains speculative. It is noted,however, that the analogue $[H_2C{=}N(H)\cdots H\cdots CH_2{=}C{=}O]^+$ was calculated to be a minimum and that in this species the ketene dipole vector also points away from the charge [19]. Ketene ion complexes have also been invoked in the dissociation of $CH_3C(=O)CH_2C{=}O^+$[20].

The related proton-bound species $[CH_2{=}O\cdots H\cdots O{=}C{=}CH_2]^+$, *h*, was found to be a minimum lying 154 kJ/mol above *e* (see Table 10.2 and Figure 10.1). Although this isomer is energetically accessible, it is probably not involved in the loss of CH_2O since it would yield $CH_2{=}CCH^+$ rather than CH_3CO^+. The $CH_2{=}O\cdots H$ distance in *h* is short, 1.013 Å, with a corresponding high lone pair directionality; the $CH_2{=}C{=}O\cdots H$ distance is 1.497 Å, with a concomitantly smaller lone pair directionality. Using the empirical relationship for the estimation of the stabilization energy (SE) in $O\cdots H\cdots O$ bridged species [21], the estimated ΔH_f of ion *h* is 542 kJ/mol, compared with theory, which predicts 539 kJ/mol.

In the context of the loss of CH_2O from *f*, it is also considered the possible participation of ion *k*, $CH_3C(=O)OCH_2^+$. Ionized ethyl acetate, $CH_3COOCH_2CH_3^{\bullet+}$, loses $CH_3^\bullet$ and since deuterium labelling shows that the methyl lost originates exclusively from the ethyl group, the resulting $C_3H_5O_2^+$ product ion could indeed be $CH_3C(=O)\text{-}OCH_2^+$, *k*. This species undergoes only one dissociation in the micro second time-frame, namely to $CH_3C{=}O^+ + CH_2O$ with an exceedingly small kinetic energy release, 50 J/mol, indicative of cleavage of an ion-dipole bond [22], $CH_3\text{-}C{=}O^+\cdots\cdots O{=}CH_2$ (*k*) $\rightarrow CH_3\text{-}C{=}O^+ + O{=}CH_2$. The theoretical calculations show that the ion-dipole species *k* is indeed stable: it has a C•••O distance of 2.394 Å (which is smaller than the sum of the C and O van der Waals radii) and a calculated ΔH_f of 427 kJ/mol, which is close to the experimentally obtained ΔH_f, 435 kJ/mol (see Table 10.2). The C•••O bond strength (from $\Delta H_f[CH_3CO^+] = \Delta H_f[CH_2O] - \Delta H_f[k]$) is 109 kJ/mol, close to the

value calculated for an ion-dipole interactions, 117 kJ/mol (from 288 μ/r^2 kJ/mol (μ in D, r in Å)). Ion *k* could be involved in the dissociation of *a*, *c*, *d* and *f*, but experiments with the OD-labelled isotopomers dictate (see above) that it should not undergo any hydrogen-exchange reactions, i.e. it ought not to interconvert with *j* :

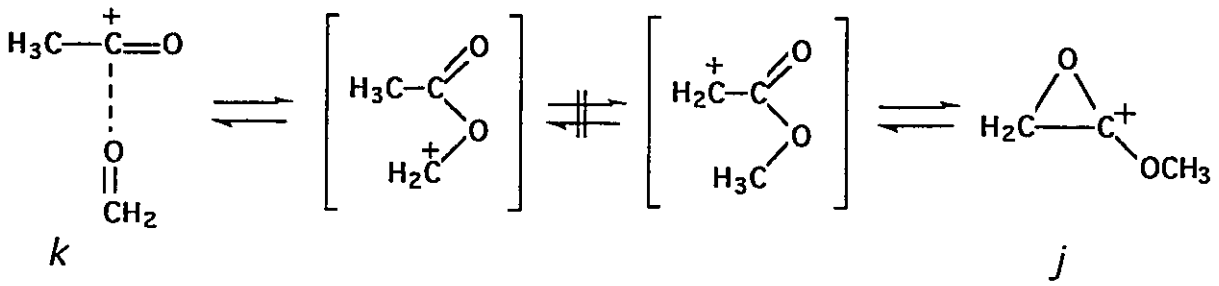

k *j*

Ion *j* was generated by I$^{\bullet}$ loss from $ICH_2COOCH_3^{\bullet+}$ (see Scheme 10.1) and it is unique in its dissociation behaviour: its MI spectrum displays (dish-shaped) metastable peaks at m/z 45 and 43, corresponding with loss of CO (T_H = 0.87 eV) and CH_2O (T_H = 0.89 eV). Moverover, as can be seen from Figure 10.4(d), decarbonylation leads to $CH_3OCH_2^+$, not CH_3CHOH^+. As shown in Fig. 10.5, the barrier for the 1,4-shift *j* → *k* lies at least 80 kJ/mol above the minimum energy requirement for the loss of CH_2O from *k* and hence it is concluded that ion *j* does not communicate with *k*. Therefore, ion *k* may be an intermediate in the loss of CH_2O from *a*-*d* and *f*.

Although a structure akin to the ion-dipole species *k*, viz. the four-membered ring structure k_1 (see Fig. 10.1), is also found to be a minimum, it does not seem to be generated from ethyl acetate ions. This is because the ^{18}O-labelled ester $CH_3(=^{16}O)^{18}OC_2H_5^{\bullet+}$ generates $C_3H_5{}^{16}O^{18}O$ ions $CH_3(=^{16}O)^{18}OCH_2^+$, which, in the metastable time-frame, lose $CH_2=^{18}O$ exclusively. Considering the geometry of ion k_1, this isomer may reasonably be expected to lose $CH_2=^{18}O$ and $CH_2=^{16}O$ to (about) the same extent.

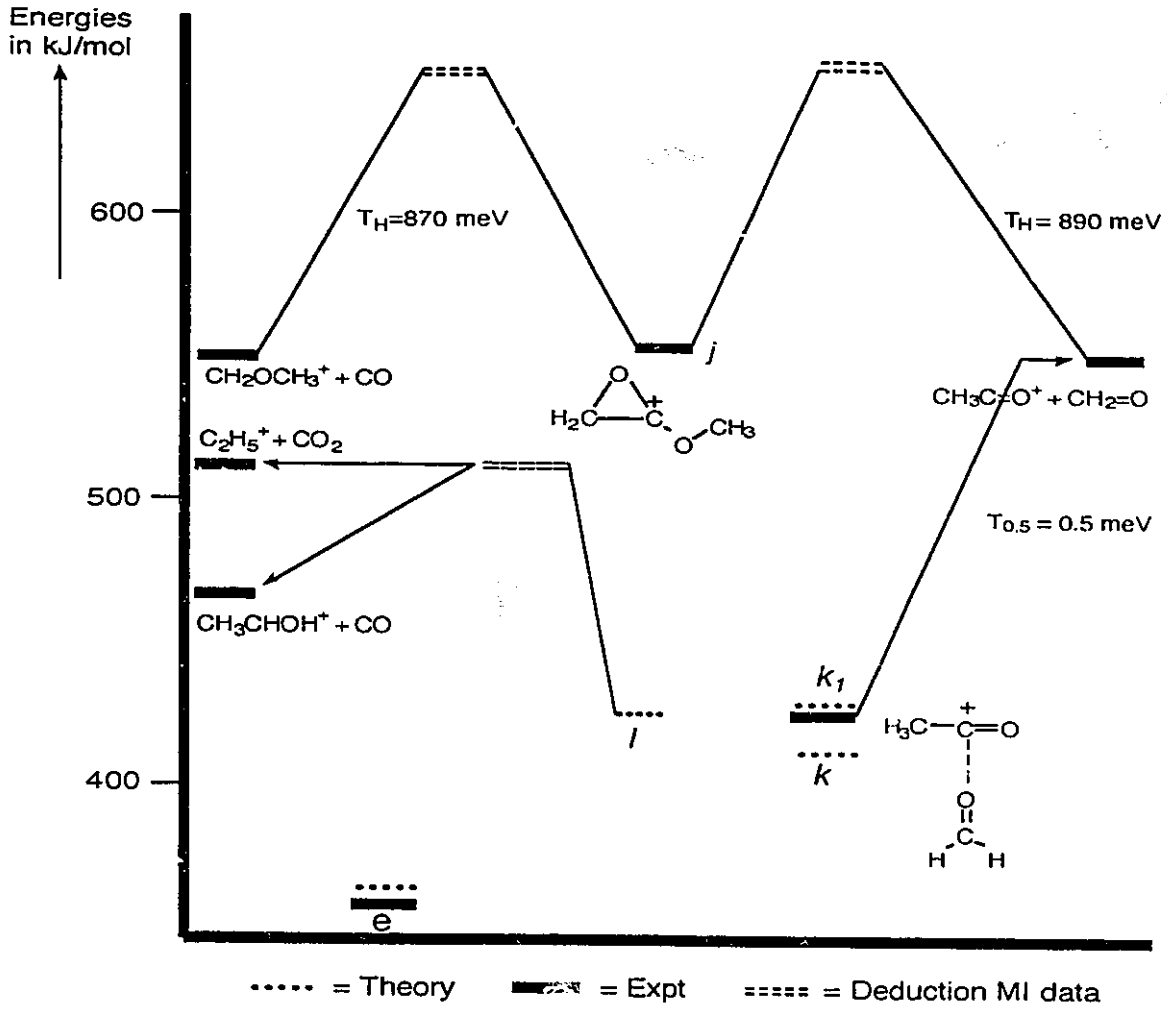

Figure 10.5. Potential energy diagram for the dissociation of the isomeric ions *j*, *k* and *l* (UMP3/6-31G*//4-31G level of theory).

The loss of CO_2 from *a-d* and f is proposed to occur from ion *c* via a 1,4-hydrogen shift, possibly via $CH_3CH_2CO_2^+$. This intermediate most likely lies higher in energy than its isomer $CH_3CH_2O\text{-}C{=}O^+$, *l* , as does its lower homologue HCO_2^+, which lies ~ 400 kJ/mol above $HOCO^+$ [23]. Ion *l* was made by loss of $C_2H_5O^\bullet$ from diethyl carbonate and it shows an interesting unimolecular chemistry. As shown in Table 10.1, the metastable ions predominantly lose CO (Gaussian-type metastable peak, $T_{0.5}$ = 15 meV), whereas the direct loss of CO_2 is only a minor process. In the CA mass

spectrum the two reactions become of equal importance. The KER associated with the loss of CO_2 (Table 10.1) is very small, parallelling the behaviour of the lower homologue, CH_3O-C=O$^+$ [4]. Thus (see Table 10.3 and Fig. 10.5), metastable ions *l* dissociate at, or just above, 510 kJ/mol and hence loss of CH_2O is absent. The $T_{0.5}$ value for loss of CO from ions *a-d* and *f* is much larger (by a factor 100) than that for loss of CO from ion *l* , which indicates that a large barrier exists for interconversion. This makes it highly unlikely that the mechanism for loss of CO from *l*, CH_3CH_2O-C=O$^+ \overset{1,2\text{-H}}{\rightarrow}$ CH_3CHOH^+ + CO, is associated with the narrow component of the metastable peaks for loss of CO from ions *a-d* and *f*.

Structure and energy of ion c and the putatively destabilized carbenium ion d: bridged and closed vs. open structures

As noted above, at the HF (MP3/6-31G*//4-31G and MP3/6-31G*//6-31G*) level of theory the electronic energy of TS *c-d* is lower than either that of *c* or *d*. To address this problem and to establish whether *d* can collapse to a three-membered ring structure (as was the case for the lower homologue, $^+CH_2COOH \rightarrow \overline{CH_2O\dot{C}OH}^+$, [4]), electron correlation at the MP2 level of theory was included in the geometry optimization using the 6-31G* basis set followed by MP3/6-31G* single-point calculations. The geometries of the derived structures are shown in Fig. 10.6 and the corresponding energies are given in Table 10.4. It is seen by comparing structures d_1 (Fig. 10.6) and *d* (Fig. 10.1) that on inclusion of electron correlation the carbonyl oxygen atom moves towards the charged carbon atom until a situation is reached (geometry d_1) where the gain in energy by charge dispersal is counterbalanced by the loss in energy due to ring strain, resulting in a structure in between that of *d* and an

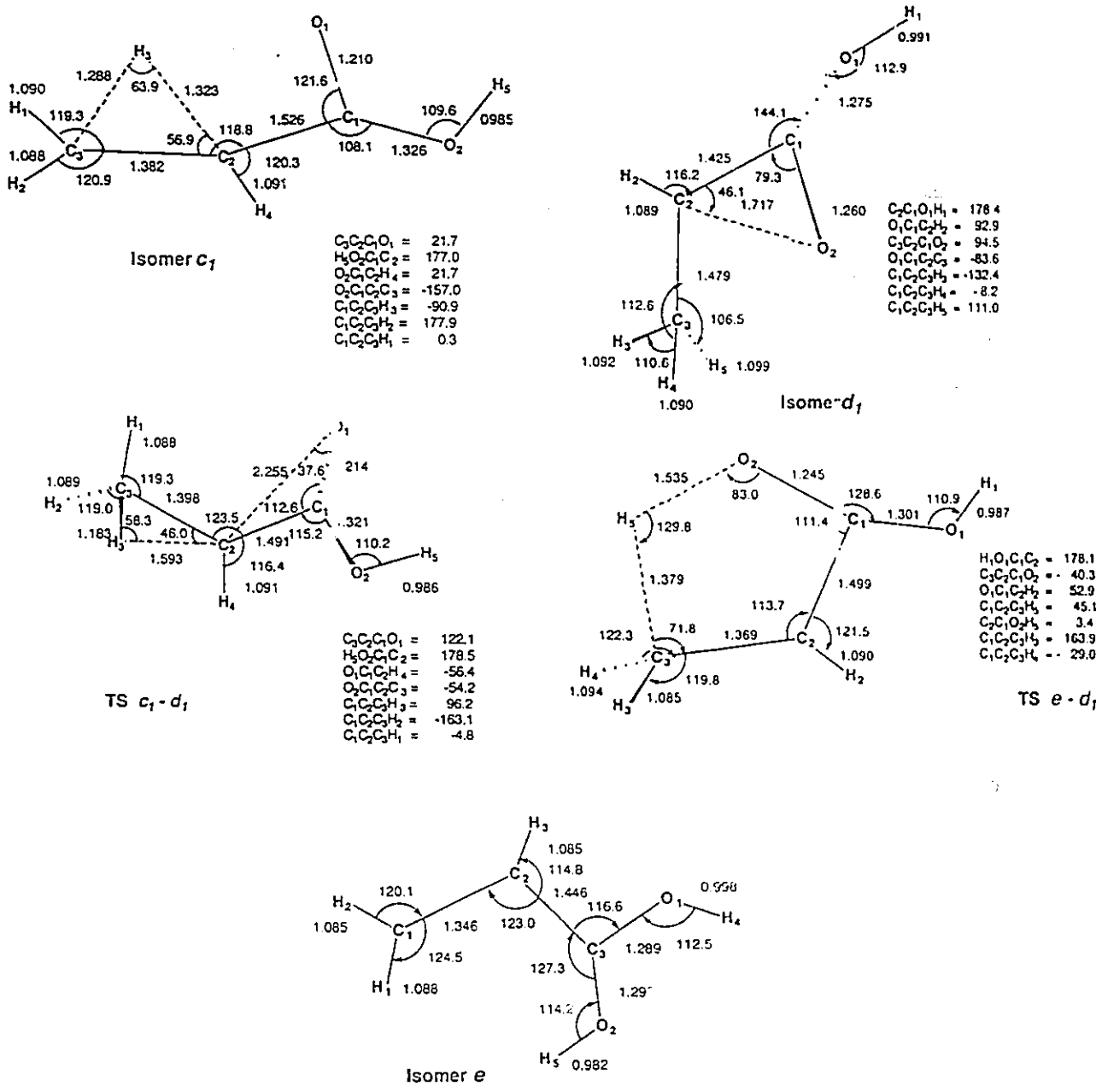

Figure 10.6. Geometries of the $C_3H_5O_2^+$ isomeric ions c_1, d_1 and e and the transition states TS $c_1 \rightarrow d_1$ and TS $d_1 \rightarrow e$ at the MP3/6-31G*//MP2/6-31G* level of theory.

Table 10.4 Total energies (Hartrees), zero-point vibrational energies [ZPVE] and relative calculated E[rel][a] energies (kJ/mol) for isomers c_1, d_1, *e* and transition states (basis set 6-31G*)

Species	MP2	MP3//MP2	ZPVE	E[rel][a]	E[exp][a]
Ion c_1	-266.63312	-266.64822	205	148	
Ion d_1	-266.64644	-266.65553	210	135	145+10
TS c_1-d_1	-266.63081	-266.64486	200	153	
Ion *e*	-265.68774	-266.70719	212	0	0
TS d_1-*e*	-265.51436	-265.90478	195	211	

[a] The relative calculated energies include scaled (0.96) zero-point vibrational contributions. This scaling factor was calculated as follows: for ion *e*, for which the HF and MP2 geometries are very similar, geometry optimizations and ZPVE calculations were performed with both methods. The calculated ZPVEs are 226 kJ/mol for HF and 212 kJ/mol for MP2. The electronic correlation effects in the MP2 calculation are therefore responsible for a reduction in the ZPVE of 6.2%. In order to compensate for the remaining errors in the ZPVE calculation, a scaling factor of 0.9/0.938% = 0.96 was used for calculating the relative energies.

isosceles geometry [although, considering the C(H)C=O angle in d_1 (79.2 °), resembling more the latter]. On inclusion of electron correlation, ion *c* is found to adopt a bridged structure c_1, where the bridging hydrogen is situated near the mid-point above the carbon atoms (see Fig. 10.6). A transition state (TS $c_1 \rightarrow d_1$) was located connecting c_1 and d_1 whose electronic and total energies are higher than those of c_1 and d_1; however, the total energies of c_1, d_1 and TS $c_1 \rightarrow d_1$ are very close and any of them may in fact correspond to the experimentally derived ΔH_f given in Table 10.4. Hence, in agreement with the experimental observations, loss of I• from $CH_3C(H)ICOOH$ may well yield an equilibrating mixture of c_1 and d_1.

The atom arrangement is structure c_1 is very close to that of the ethyl cation itself [24,25], which in ground state also adopts a bridged structure. Hence it appears that substituting α-COOH group by a hydrogen atom has virtually no influence on the structure. Similarly, from the estimated stabilization energy (SE) discussed below, it appears that α-COOH functionality behaves as a hydrogen substituent. When comparing the bridged structures for R = H [4] and R = CH_3 [this work], it is seen that for R = CH_3 the $C_1C_2O_3$ angle is larger (79.3 *vs.* 75.2 °) with a concomitantly larger C(1)-O(3) bond (1.717 *vs.* 1.619 Å), reflecting the stabilizing influence of a CH_3 group on a positive charge. Finally, as discussed above, at the HF level of theory (MP3/6-31G*//4-31G and MP3/6-31G*//6-31G*), ions *c* and *d* do correspond to minima and their calculated total energies (see Table 10.2) can be used to estimate the magnitude of the 'destabilization' energy of an α-COOH substituent on a positively charged carbon atom.

One useful way of quantifying the stabilization energy (SE) invoves the change in the heterolytic bond dissociation energy or hydride affinity, $D[R^+–H^-]$, with respect to the reference value $D[CH_3^+–H^-]$: SE = $D[CH_3^+– H^-] – D[R^+– H^-]$ [26]. This same SE can also be derived from the change in total energies of the species in the isodesmic reaction [27]:

$CH_3^+ + RH \rightarrow CH_4 + R^+ + SE$:

$$CH_3^+ + CH_3COOH \rightarrow CH_4 + CH_2COOH^+ + SE_1$$

$$CH_3CH_2^+ + CH_3CH_2COOH \rightarrow CH_3CH_3 + CH_3CHCOOH^+ + SE_2$$

Using $\Delta H_f[CH_2COOH^+]$ = 724 kJ/mol (from $\Delta H_f[\overline{CH_2\text{-}C\text{-}OH}^+]$ (exp.) = 586 kJ/mol [4] and the computed difference $\Delta H_f[CH_2COOH^+] - \Delta H_f[\overline{CH_2\text{-}C\text{-}OH}^+]$ =138 kJ/mol [28]), $\Delta H_f[CH_3CHCOOH^+]$ = 538 kJ/mol (see Table 10.2) and the established values for the other

components [12a], the following results are arrived: $SE_1 = +12$ kJ/mol and $SE_2 = +2$ kJ/mol. The values obtained are small (compare the SEs in Ref. 29), which indicates, in agreement with the above computational results at a higher level of theory, that the destabilizing inductive effect of α-COOH functionality is counterbalanced by electron donation and as a result these ions cannot really be viewed as "destabilized". It is therefore not surprising that α-carbonyl cations can, in solution, be formed at rates comparable to the unsubstituted analogues [1d,f].

References

1. For selected reviews see: (a) P. Vogel, Carbocation Chemistry, Elsevier, Amsterdam, (1985); (b)P.C. Burgers and J.K. Terlouw, in *Specialist Periodical Reports: Mass Spectrometry*, ed. by M.E. Rose, Chapt.2, Vol. 10. Royal Society of Chemistry, London (1989); (c) Th.T. Tidwell, *Angew. Chem.*, **96**, 16 (1984); (d) X. Creary, *Chem. Rev.*, **91**, 1625 (1991); (e) P.K. Das, *Chem. Rev.*, **93** 119 (1993); (f) L.J. Johnston, P. Kvong, A. Shelemay and E. Lee-Raft, *J. Am. Chem. Soc.*, **115**, 1664 (1993).
2. A. Bagno, C. Comuzzi and G. Scorrano, *J. Am. Soc., Perkin Trans. 2.*, 283 (1993).
3. (a) A.-M. Dommrose and H-Fr. Grützmacher, *Int. J. Mass Spectrom.*, **22**, 26 (1987); (b) A.-M. Dommrose and H.-Fr. Grützmacher, *Org. Mass Spectrom.*, **22**, 437 (1987); (c) R. Wolf, A.-M. Dommrose and H.-Fr. Grüzmacher, *Org. Mass Spectrom.*, **23**, 26 (1980).
4. M.C. Blanchette, J.L. Holmes, C.E.C.A. Hop, F.P. Lossing, R.Postma, P.J.A. Ruttink and J.K. Terlouw, *J. Am. Chem. Soc.*, **108**, 7589 (1986).
5. P.C. Burgers, K.J. van den Berg, H. Visser and J.K. Terlouw, *Int. J. Mass Spectrom. Ion Proc.*, **101**,83 (1990).
6. P.C. Burgers, J.L. Holmes, F.P. Lossing, F.R. Povel and J.K. Terlouw, *Org. Mass Spectrom.*, **18**, 335 (1983).
7. G. Asensio, M.A. Miranda, J. Perez-Prieto, M.J. Sabater and A. Simon-Fuentes, *Angew. Chem.*, **102**, 1187 (1990).
8. G.A. Olah, A.M. White and D.H. O'Brien, *Chem. Rev.*, **70**, 56 (1970).
9. G. Bouchoux, F. Djazi, R. Houriet and E. Rolli, *J. Org. Chem.*, **53**, 3498 (1988).
10. A.M. Amat, G. Asensio, M.J. Castello, M.A. Miranda and A. Simon-Fuentes, *J. Org. Chem.*, **52**, 4790 (1988).

11. A. Maquestiau, D. Beugnies, R. Flammang, R. Houriet and G. Bouchoux, *Rapid Commun. Mass Spectrom.*, **2**, 177 (1988)
12. (a) S. Lias, J.E. Bartmess, J.F. Liebman, J.L. Holmes, R.D. Levin and W.G. Mallard, *J. Phys. Chem. Ref. Data*, **17**, Suppl 1 (1988); (b)S.W. Benson, *Thermochemical Kinetics*, Wiley-Interscience, New York (1976); and (c) J.L. Holmes and M. Dakubu, *Org. Mass Spectrom.*, **24**, 461 (1989).
13. R.H. Nobes, W.R. Rodwell, W.J. Bouma and L. Radom, *J. Am. Chem. Soc.*, **103**, 1913 (1981).
14. (a) J.I. Seeman, H.V. Secor, R. Disselkamp and F.R. Bernstein, *J. Chem. Soc., Chem. Commun.* 713 (1992); (b) J.I. Seeman and J.B. Paine III, *Chem. Eng. News* Dec. 7, 2 (1992).
15. J.C. Traeger, C.E. Hudson and D.J. McAdoo, *Org. Mass Spectrom.*, **24**, 230 (1989).
16. P.C. Burgers, A.A. Mommers and J.L. Holmes, *J. Am. Chem. Soc.*, **105**, 5976 (1983).
17. B.G. Gilbert and J.K. Slell, *J. Chem. Soc., Perkin Trans 2*, 1201 (1990).
18. J.L. Holmes, J.K. Terlouw and P.C. Burgers, *Org. Mass Spectrom.*, **15**, 140 (1980).
19. P.C. Burgers, C.A. Kingsmill, G.A. McGibbon and J.K. Terlouw, *Org. Mass Spectrom.*, **27**, 398 (1992).
20. J. Torlajuda, D. Berthomieu, J.-P. Morizur and H.-E. Audier, *J. Am. Chem. Soc.*, **114**, 10874 (1992).
21. (a) U. Seeger, R. Seeger, J.A. Pople and P.v.R. Schleyer, *Chem. Phys. Lett.*, **55**, 399 (1978); (b) M.J. Frisch, H.F. Schaefer III and J.S. Brinkley, *J. Phys. Chem.*, **89**, 2192 (1985); (c) J.G. Yu, X.Y. Fu, R.Z. Liu, K. Yamashita, N. Koga and K. Morokuma, *Chem. Phys. Lett.*, **125**, 438 (1986); and (d) J.K. Terlouw, P.J.A. Ruttink and P.C. Burgers, in preparation.
22. P.J.A. Ruttink, *J. Phys. Chem.*, **91**, 703 (1987).
23. (a) U. Seeger, R. Seeger, J.A. Pople and P. V. R. Schleyer, *Chem. Phys. Lett.*, **55**, 399 (1978); (b) M.J. Frisch, H.F. Schaefer III and J.S. Brinkley, *J. Phys. Chem.*, **89**, 2192 (1985); (c) J.G. Yu, X.Y. Fu, R.Z. Liu, K. Yamashita, N. Koga and K. Morokuma, *Chem. Phys. Lett.*, **125**, 438 (1986); (d) J.K. Terlouw, P.J.A. Ruttink and P.C. Burgers, in preparation.
24. M.W. Wong, J. Baker, R. Nobes and L. Radom, *J. Am. Chem. Soc.*, **109**, 2245 (1987), and references cited therein.
25. L. Radom, *Org. Mass Spectrom.*, **26**, 359 (1991), and references cited therein.
26. F.P. Lossing and J.L. Holmes, *J. Am. Chem. Soc.*, **106**, 6917 (1984).
27. (a) W.J. Hehre, R. Ditchfield, L. Radom and J.A. Pople, *J. Am. Chem. Soc.*, **92**, 4796 (1970); (b) Y. Apeloig and M. Karni, *J. Chem. Soc., Perkin Trans. 2*, 625 (1988); (c) D. J. Pasto, *J. Am. Chem. Soc.*, **110**, 8164 (1980).
28. (a) M.H. Lien and A.C. Hopkinson, *J. Am. Chem. Soc.*, **110**, 3788 (1988); (b) C.F. Rodriguez and A.C. Hopkinson, *Org. Mass Spectrom.*, **20**, 691 (1985).
29. S. Hoz and J.L. Wolk, *Tetrahedron Lett.*, 4085 (1990).

30. P.C. Burgers, J.K. Terlouw and J.L. Holmes, *Org. Mass Spectrom.*, **17**, 369 (1982); P.C. Burgers, J.L. Holmes and J.E. Szuleijko, *Int. J. Mass Spectrom. Ion Processes*, **57**, 159 (1984), and references cited therein.

Addendum to Chapter 10.

In a recent publication (J. Am. Chem. Soc., **115**, 7396 (1993)), it was concluded that β-propiolactone, contrary to larger ketones, is less basic (25 kJ/mol) than the corresponding aliphatic ester. Also at the MP2/6-31G*//MP2-6-31G* level of theory, the proton affinity for the ether oxygen was found to be only 4.6 kJ/mol lower than that for the keto atom, in good agreement with the results obtained in this study (Table 10.2 and Fig. 10.3). From a topologica analysis it was concluded that protonation of the ether oxygen atom is accompanied by significant activation of the acyl C-O linkage; this also follows from the work described in Chapter 10: not only lies TS *b* - *f* only 29 kJ/mol above *b*, but also structure *b* has a stretched C-O bond, it being only *ca.* 0.4 Å shorter than the sum of the van der Walls radii.

SUMMARY

This thesis discusses tandem mass spectrometry based experiments in conjunction with high-level *ab initio* molecular orbital calculations for the elucidation of ion structures and decomposition mechanisms in the study of gas-phase ion chemistry. Spectial attention is given for the determination of stable ions with unexpected structures (eg. distonc ions, ion-neutral complexes and H-bridged radical cations) and their role in the unimolecular decomposition of organic ions in the gas-phase is emphasized.

To begin with, Chapter 1 gives a brief discussion of the Quasi-Equilibrium Theory (QET) whose basic principles are essential in understanding and interpreting a mass spectrum. Also included in this Chapter are the tandem mass spectrometry-based techniques together with experimental methods to measure appropriate ionization and/or appearance energies from which heat of formation (ΔH_f) values for ions and neutral species can be obtained. The combined information obtained from the above in conjunction with *ab initio* calculations can be used to confidently assign ion structures. Ions having unconventional structures such as distonic ions, ion/neutral complexes and hydrogen-bridged ions, their characteristics and their role in the studies of unimolecular rearrangement reactions in the gas-phase are illustrated.

Chapter 2 describes the remarkable unimolecular chemistry of the acetol radical cation, $CH_3C(=O)CH_2OH^{\bullet+}$, *viz.* the loss of $HCO^{\bullet}$ to form CH_3CHOH^+ ions. A detailed analysis of multiple collision experiments on ^2H-labelled acetol ions shows that the O···H···O hydrogen-bridged ion $[CH_3C=O\cdots H\cdots O=CH_2]^{\bullet+}$, a key intermediate on the

(related) methyl acetate hypersurface, is not directly involved in the dissociation chemistry of metastable acetol ions. Integration of the experimental information with the results of *ab initio* molecular orbital calculations provides evidence that the loss of $HCO^{\bullet}$ from ionized acetol involves isomerization into the ion-dipole complexes $CH_3C(=O)^+\cdots O(H)\text{-}CH_2^{\bullet}$ and $CH_3C(=O)H^{\bullet+}\cdots O{=}CH_2$. The combined informations show that another stable O···H···O hydrogen-bridged isomer, $[CH_2C(H){=}O\cdots H\cdots O{=}CH_2]^{\bullet+}$, does not communicate with either the acetol or the methyl acetate hypersurface.

Chapters 3 and 4 further present experimentally established cases of oxygen containing radical cations of the type $[HOCH(R^1)C(=O)R^2]^{\bullet+}$ which may dissociate via intramolecular C-H···O bonding, *viz.* methyl glycolate (R^1=H, R^2=OCH_3), methyl lactate (R^1=CH_3, R^2=OCH_3) and acetoin (R^1=R^2=CH_3). These species all undergo major unimolecular decomposition reactions, *viz.* loss of $R^1CO^{\bullet}$ by double hydrogen transfer. Tandem mass spectrometry based experiments on ^2H-, ^{13}C- and ^{18}O-labelled isotopologues in conjunction with *ab initio* calculations show that the loss of $R^1CO^{\bullet}$ proceeds via the C-H···O bonded intermediate $R^1C(H){=}O\cdots H\text{-}C(=O)R^{2\,\bullet+}$. It is further proposed that this C-H···O bonded intermediate does not lose $R^1CO^{\bullet}$ via a hydrogen atom shift from neutral $R^1C(H)$= ionized $H\text{-}C(=O)R^{2\,\bullet+}$. Instead, charge transfer takes place from ionized $H\text{-}C(=O)R^{2\,\bullet+}$ to neutral $R^1C(H){=}O$ which thus becomes charged. Now, the ionized $R^1C(H){=}O^{\bullet+}$ can rotate and donate a *proton* to neutral $H\text{-}C(=O)R^2$ after which dissociation follows.

In Chapter 5, the unimolecular chemistry of the enol form of ionized methyl glycolate, $HOCH{=}C(OH)OCH_3^{\bullet+}$ is investigated by a variety of tandem mass spectrometry based techniques using ^2H-, ^{13}C- and ^{18}O-labelled precursor molecules. It is shown that the keto-enol tautomeric equilibrium does not occur in ionized methyl glycolate in contrast to the behaviour of ionized methyl acetate, in which the latter ions readily interconvert with their enol isomers prior to dissociation. This is because the HO-CH

functionality opens up facile rearrangement/dissociation pathways in both ionized methyl glycolate and its enol isomer whose energy requirements lie below the keto-enol tautomerization barrier. Also, the experimentally inaccessible H-bridged radical cation $[CH_3\text{-}O(H)\cdots H\cdots O{=}CH]^{\bullet+}$, one of the most stable isomers on the $C_2H_6O_2^{\bullet+}$ potential energy surface, is identified.

Chapter 6 discusses the unimolecular chemistry of ionized ethyl glycolate, $HOCH_2CO_2C_2H_5^{\bullet+}$, and its enol isomer, $HOCH{=}C(OH)OC_2H_5^{\bullet+}$. From a variety of techniques, including ^2H-, ^{13}C- and ^{18}O-labelling experiments, kinetic energy release information, analysis of collisional activation and neutralization-reionization mass spectra and thermochemical measurements, it is shown that the ionized ethyl glycolate undergoes unidirectional tautomerism to its enol isomer, prior to C_2H_4 loss, via two 1,5-H shifts. This contrasts sharply with the behaviour of the lower homologues, ionized methyl glycolate and its enol isomer, for which the analogous tautomerism via 1,4-H shift does not occur.

Chapters 7 and 8 illustrate that ion-neutral complex (INC)-mediated mechanisms permitting cation rearrangements, hydrogen transfers and skeletal rearrangements often offer a means of understanding previously inexplicable phenomena.

From the integration of experimental information, it is shown that ionized di-*n*-butyl ethers undergo unidirectional skeletal isomerization to ionized *n*-butyl *sec*-butyl ether, prior to loss of $C_2H_5^{\bullet}$, via an ion-neutral complex comprising neutal *n*-butanol and ionized methyl cyclopropane. Moreover, the initial 1,4-H shift is influenced by a significant isotope effect, as would be expected if this step is rate limiting in ethyl radical loss, which occurs by α-cleavage of the *sec*-butyl group in the isomerized ionized ether.

Also, the site selectivity in the hydrogen transfer step(s) observed in propene and water loss from metastable oxonium ions generated as $CH_3CH{=}O^+CH_2CH_2CH_3$ is interpreted by means of INC-mediated mechanisms involving an unidirectional rate-limiting rearrangement of the incipient $^+CH_2CH_2CH_3$ cation to $^+CH(CH_3)_2$.

In Chapter 9, the reactions of metastable oxonium ions $(CH_3CH_2)_2C{=}OH^+$, $CH_3CH_2CH_2(CH_3)C{=}OH^+$ and $(CH_3CH_2CH_2)_2C{=}OH^+$ are studied by ^{13}C-labelling experiments. Alkene elimination from these oxonium ions is proposed to occur after rearrangement of the carbon skeleton by a combination of 1,2-H and 1,2-alkyl shifts, without disrupting the C-O bond.

In Chapter 10, part of the $C_3H_5O_2^+$ potential energy surface is investigated by *ab initio* molecular orbital calculations together with mass spectrometric experiments. From these studies, it is concluded that protonated acrylic acid ions, $CH_2{=}CH(OH)_2^+$, do not communicate with carbonyl-protonated β-propiolactone ions, $CH_2CH_2OCOH^+$ and that the observed equilibrium between these two ions in solution is due to an intermolecular process. Analysis of appropriate isodesmic reactions indicates that the α-COOH group in ion $CH_3CHCOOH^+$ behaves as a hydrogen atom and therefore this group cannot be said to destabilize the adjacent positive charge.

Contrary to earlier suggestions, ions $CH_2CH_2OCOH^+$ do not undergo cycloreversions to $HOCO^+ + C_2H_4$ and $CH_2{=}COH^+ + CH_2O$, but rather they spontaneously dissociate $CH_3CHOH^+ + CO$, $CH_3CO^+ + CH_2O$, $CH_2{=}CHCO^+ + H_2O$ and $CH_3CH_2^+ + CO_2$. The product ions of these dissociations are characterized by double collision experiments and mechanisms for their formation are proposed.

EXPERIMENTAL

All tandem-mass spectrometry-based experiments were performed with the McMaster University VG Analytical ZAB-R instrument of $BE_1(Q)E_2$ geometry (B, magnet; Q, quadrupole; E, electric sector) using an accelerating voltage of 8 or 10 keV. The custom built ZAB-R mass spectrometer is a three sector BEE type instrument whose design is based on the standard, non-extended geometry of the ZAB-2f mass spectrometer [1].

The ion source having 160/700 Diffstak pumping is equipped with four inlet systems for sample introduction to the source: i) the septum inlet is used for compounds having very high vapour pressures; ii) an all glass heated inlet system (AGHIS), which can also be used as a very low vapour pressure (VLVP) inlet, is used for volatile compounds. It is often necessary to cool the sample with ice/water bath to control the sample vapour pressure; iii) an all quartz direct insertion probe is used for less volatile compounds. For liquid samples having very low vapour pressures, it is useful to smear the sample on the tip of the probe so as to obtain good sensitivity; and iv) a direct solid insertion probe is used for solids which have very low vapour pressure. The VLVP pyrolysis unit has been described elsewhere [2]. Briefly, the pyrolysis oven is constructed of silica and has a high temperature zone of *ca.* 25 mm length. The exit of the oven into the ion source was situated *ca.* 10 mm from the ionizing electron beam. The samples were introduced into the pyrolysis unit by evaporation from a small glass bulb kept at room temperature.

An Autospec magnet (B) precedes the second field-free region (ffr) housing which has the form of a rectangular box. This box [79 x 23 x 23 cm] has an easily removable top lid and side panels. The box may be quickly isolated from its two 160/700 Diffstaks and the other sectors by using four valves. This enables rapid access to the collision chambers and the lens assemblies which are mounted on its "optical bench" type of internal base. The box contains three collision gas chambers 1, 2 and 3 whose locations are shown in Fig. C-2: i) cell 1 [30(l) x 3(w) x 14(h) mm] is a home-built chamber used for neutralization experiments with organic vapours (eg. trimethylamine and N,N- dimethylaniline); ii) cell 2 [20(l) x 1(w) x 10(h) mm], which is electrically isolated to 5 kV and is preceded by a (de)-accelerating lens, is used for neutralization experiments with permanent gases (eg. xenon and cyclopropane); and iii) cell 3 [20(l) x 1(w) x 10(h) mm], which is also electrically isolated and is equipped with a y-focus/deflection lens assemblies, is used for "standard" reionization and collision-induced dissociation (CID) experiments. These collision chambers are situated at distances of 270, 44 and 10 mm, respectively, from the focal point at the intermediate slit located next to the glass window which is situated on the top of the box.

After the first electrostatic analyser (E_1), there is a box type collector housing in which the third ffr collision gas chamber is located in front of a small Autospec ESA (E_2, 5" radius, 72.5 ^{o}). This housing contains two photomultiplier type detectors and a fifth 160/700 Diffstak is used to pump this region.

A Quadrupole mass analyzer (200 amu), with a channeltron electron multiplier detector, is mounted on one side of cell 2 - perpendicular to the flight path of the fast moving ion beam. The QUAD is used to acquire spectra of ionized target (T) molecules and their dissociation products resulting from the neutralization process of a

mass selected ion beam [3]. This technique was not used in the work described in this thesis.

The ZAB-R has a mass range of 1200 daltons at 8 kV accelerating voltage and a mass resolution of up to 40,000.

The metastable ion (MI) spectra were obtained by the mass-analyzed ion kinetic energy (MIKE) technique [4]. The quoted spectra are integrated data, compiled from 2-5 individual scans. Typical operating conditions were 70 eV ionizing electron energy and 7910 V accelerating voltage. The kinetic energy release (KER) values were estimated from the width at half-height of the appropriate metastable peak, by means of the standard one-line equation [4,5], after applying the usual correction [6] for the width at half-height of the main beam.

The collision-induced dissociation (CID) and neutralization-reionization (NR) mass spectra of 8 keV ions were obtained in the second ffr using O_2 to effect collision-induced dissociation or reionization (main beam transmission, 80 %) and cyclopropane and/or N,N-dimethylaniline vapour for neutralization. The structure of the product ions of spontaneous or collision-induced dissociations in the second ffr was probed by obtaining their CID mass spectra in the third ffr using He and/or O_2 as the collision gas and mass-selected precursor ions of 10 keV translational energy.

All spectra were recorded using a small PC-based data system with ZABCAT software developed by Mommers Technologies Inc. (Ottawa, Canada).

Appearance energy (AE) values were measured by Dr. F.P. Lossing, using the procedure described in ref. 7. Metastable AE measurements were performed as described in ref. 8.

All compounds used in this thesis, unless otherwise indicated, were commercially available (Aldrich, Milwaukee, USA) and purified where necessary.

Deuteration was achieved by dissolving a small amount of sample in CH_3OD after which methanol was removed; this was repeated three times. Deuteronation was achieved by dissolving the compound in D_2O and introducing the solution into a chemical ionization source.

For the experiments described in Chapter 2, $CH_3C(=O)CD_2OH$ was synthesized by reducing the thioketal of methyl pyruvate [9] with $LiAlD_4$ and decomposing the product by the method of Corey et al. [10]. The solid, recrystallized HgCl adduct was admitted to the ion source via the solids probe.

For the experiments of Chapter 3, the OCH_3-labelled methyl glycolates were prepared on a small scale by conventional methods using CD_3OH, $^{13}CH_3OH$, $CH_3{}^{18}OH$ and $^{13}CH_3{}^{18}OH$. The isotopomer $HOCD_2C(=O)OCH_3$ was prepared as a 1:1 mixture with the unlabelled compound, by the reaction of methyl bromoacetate-d_2 (from bromoacetic acid-d_2 [11]) with sodium glycolate in methanol. The dimethyl carbonate isotopomers $CH_3OC(=O)OCD_3$ and $CH_3OC(=O)O^{13}CD_3$ were prepared by esterification of methyl chloroformate with CD_3OD and $^{13}CD_3OH$ using catalytic amount of Ag_2O. The methyl lactate isotopomer $HOCD(CH_3)C(=O)OCH_3$ was prepared by esterification of 2-*d*-lactic acid, which was synthesized according to ref. 12.

In Chapters 4 and 5, acetoin-$(C=O^{18})$ and dimethyl tartrate-$(C=O^{18})_2$ were obtained by exchange of the unlabelled compounds with $H_2{}^{18}O$ in acidic medium at room temperature. The labelled compounds $(CH_3)_2CHCH(OH)C(=O)OCD_3$ and $(CH_3)_2CHCH(OD)$-$C(=O)OCH_3$ were made by esterification of the acid with CD_3OD and CH_3OD exchange of the ester, respectively.

The CD_2-labelled ethyl glycolate, $HOCD_2C(=O)OCH_2CH_3$, used in Chapter 6 was prepared as described above for the methyl analogue in ethanol. The OCH_2CH_3-labelled esters were obtained on a small scale by esterification of the appropriate acids with CH_3CD_2OH, CD_3CH_2OH and $CH_3CH_2{}^{18}OH$.

The ions studied in Chapter 7 and 8 were generated by electron-impact induced ionization of dibutyl ethers and by dissociative ionization of propyl isopropyl ethers, respectively. Details of experimental procedures for the synthesis of these ethers are described, respectively, in ref. [13] and [14].

The oxonium ions investigated in Chapter 9 were generated by dissociative ionization of the appropriate secondary or tertiary alcohols. The experimental details for the preparation of these alcohols are given in ref. 15.

Iodomethyl acetate and 3- and 2-iodopropionic acids investigated in Chapter 10 were synthesized as described in ref. 16. Oxygen-18-labelled ethyl acetate, $CH_3C(=^{16}O)^{18}OC_2H_5$, was prepared by esterification of acetic acid with $CH_3CH_2{}^{18}OH$.

References

1. R.P. Morgan, J.H. Beynon, R.H. Bateman and B.N. Green, *Int. J. Mass Spectrom. Ion Phys.*,**28**, 171 (1978).
2. J.K. Terlouw, J.L. Holmes and F.P. Lossing, *Can. J. Chem.*, **61**, 1722 (1983).
3. T. Wong, J.K. Terlouw, T. Weiske and H. Schwarz, *Int. J. Mass Spectrom. Ion Processes*, **113**, R23 (1992).
4. R.G. Cooks, J.H. Beynon, R.M. Caprioli and G.R. Lester, Metastable Ions, Elsevier, Amsterdam (1973).
5. K. Levsen, Fundamental Aspects of Organic Mass Spectrometry, Verlag-Chemie, Weinheim (1978).
6. M.A. Baldwin, P.J. Derrick and R.P. Morgan, *Org. Mass Spectrom.*, **11**, 440 (1976).
7. F.P. Lossing and J.C. Traeger, *Int. J. Mass Spectrom. Ion Phys.*, **19**, 9 (1976).
8. P.C. Burgers and J.L. Holmes, *Org. Mass Spectrom.*, **17**, 123 (1982).
9. L.F. Fieser, *J. Am. Chem. Soc.*, **76**, 1945 (1954).
10. E.J. Corey, D. Seebach and K. Freedman, *J. Am. Chem. Soc.*, **89**, 434 (1967).
11. C.F. [illegible]ard, *J. Chem. Soc.*, 1161 (1922).
12. O.A. Mamer, *Biomed. Environ. Mass Spectrom.*, **15**, 57 (1988).
13. R.D. Bowen, D. Suh and J.K. Terlouw, *Org. Mass Spectrom.*, **29**, 791 (1994).
14. R.D. Bowen, D. Suh and J.K. Terlouw, *J. Chem. Soc. Perkin Trans. 2*, 119 (1995).

15. R.D. Bowen, D. Suh and J.K. Terlouw, *Eur. Mass Spectrom.*, **1**, 33 (1995).

16. a) R. Fitgh, *Justus Liebigs Ann. Chem.*, **42**, 188 (1877); b) F.L.M. Patterson, J.B. Strothers and R.G. Woolford, *J. Am. Chem. Soc.*, **78**, 2255 (1976).